Changements cellulaires et moléculaires précoces au site d'injection des vaccins : Caractérisation de la réponse innée et adaptative à l'injection d'un MVA recombinant

Pierre Rosenbaum

NNT : 2016SACLS373

THESE DE DOCTORAT
DE
L'UNIVERSITE PARIS-SACLAY
PREPAREE AU
CEA FONTENAY-AUX-ROSES

ECOLE DOCTORALE N°569

Innovation thérapeutique : Du fondamental à l'appliqué

Immunologie

Par

Mr Pierre Rosenbaum

Changements cellulaires et moléculaires précoces au site d'injection des vaccins : Caractérisation de la réponse innée et adaptative A l'injection d'un MVA recombinant

Thèse présentée et soutenue à Fontenay-aux-Roses, le 17 Novembre 2016 :

Composition du Jury :

Mme, Autran, Brigitte	Professeur-praticien hospitalier à la Pitié Salpêtrière (Paris)	Présidente
Mr, Sutter, Gerd	Professeur à Ludwig-Maximilians-Universität (München)	Rapporteur
Mme, Seddiki, Nabila	Maitre de conférences à université Paris Est (Créteil)	Rapportrice
Mme, Schwartz-Cornil, Isabelle	Directeur de recherche à l'INRA (Jouy-En-Josas)	Examinatrice
Mme, Rittner, Karola	Docteur à Transgène SA® (Illkirch Graffenstaden)	Examinatrice
Mr, Le Grand, Roger	Directeur de recherche au CEA (Fontenay-aux-Roses)	Directeur de thèse
Mr, Martinon, Frédéric	Chargé de recherche au CEA (Fontenay-aux-Roses)	Co-directeur de thèse

Remerciements

Je tiens à remercier le Pr. Gerd Sutter pour avoir très gentiment accepté de rapporter cette thèse et de partager son expertise du MVA. Un grand merci au Dr. Isabelle Schwartz pour son évaluation méticuleuse de ma thèse malgré les délais serrés et les complications administratives.
Je remercie chaleureusement le Dr. Nabila Seddiki de sa bienveillance et son adaptabilité qui m'ont permis de soutenir à la date initialement prévue. Merci au Pr. Brigitte Autran d'avoir aimablement accepté d'endosser pleinement le rôle de présidente ainsi qu'au Dr. Karola Rittner pour ses remarques pertinentes sur mon travail en qualité d'examinatrice.
Cette thèse a été pour moi un voyage personnel et professionnel que je n'oublierai jamais. J'ai tant appris à vos côtés qu'il faudrait plus que ces quelques lignes de dithyrambes pour vous en rendre un juste échantillon.
Un grand merci à Frédéric Martinon ; tu as su me donner l'autonomie nécessaire à mon épanouissement tout en m'accordant une oreille attentive pour me soutenir dans les moments difficiles.
A Roger Le Grand, vous m'avez fait confiance pour me prendre en thèse, vous vous êtes rendu disponible pour évaluer avec discernement et objectivité mon travail et le faire avancer. Vous avez été remarquable et bienveillant jusqu'au bout. Merci.

A tout le labo, vous me manquez déjà☹, je n'aurai strictement rien pu faire sans votre bonne humeur et votre humour ravageur quotidien. Décidasse spéciale à Lulu « my master », Bibi la bisounours, Laminou aka « El Bogossito » aka « El Chapo », Candy « pharma44 en force », Guga Do Brasil, Kwanito « Calé Barré », Adrien « Le Zizou portugais », Ernesto « Le Mc Gyver de Cuba », André « Chico les astuces», Samuel « les bon tuyaux », Nicolas « On lâche Rien », Brayce de Nayce, Sab « Chanteuse étoile », Pascal C. et Frédéric « Les chambreurs fous », Anne-Sophie « les bon conseils », Seb « On s'fait un terra », Benoit « Obi Chuck », Jean-Marie « Pa'ni Pwoblem' », Cyril Filou, David « Fromage », Mo « 555 », Mélis, Benoit « La bonne humeur du PACA », 16, Inana, Simon, Nadia, Jean-Louis, Mélanie, Candice, Rahima, Karen, Céline G., Julien, Céline M., Sabine, Romain, Marie-Thérèse, Malvina, Manu, Jamila, Joseph, Christine, Martin, Christophe, Antonio, Néla, Fanny, Thomas, Timothée, Sibylleet tout le monde !

Merci à mon adorable famille : Ma maman et mon papa, vous êtes toujours derrière moi pour m'encourager et êtes prêts à tout pour m'aider, même quand ce n'est pas raisonnable. Mes Frérots, vous m'avez permis de donner le coup de collier quand il le fallait, mais m'avez aussi aidé à décompresser notamment grâce à la Pierre Lecomte academy. A la petite Tiphaine la merveille des merveilles. Je remercie énormément ma petite fleur, tu m'as supporté au quotidien dans tous les sens du terme pendant cette période riche en rebondissements. Avec tes sourires, ton empathie et ton amour, tout m'a été rendu plus facile. Je t'aime petit chou. Merci à tous mes amis qui m'ont tous soutenu/aidé/fait rigoler par leur gentillesse pendant cette période de thèse. Je pense aux potes de Vannes ou assimilé : Youny, Nilsous, Simono, Jopin, Drichon, Samolo… ainsi qu'aux potos de mon crew pharma de Rennes : Antho, Panpan, Vice, Patnol, Mursiche, Cécile, Vincenzo, Bairai, Olier, Modé, Kami, Morgane …
Un merci tout particulier à ceux qui m'ont fait l'honneur de leur présence pour la soutenance.

Table des matières

Table des figures

Table des tableaux

Liste des abréviations

ADCC : Cytotoxicité médiée par les cellules anticorps-dépendante (« Antibody-dependent cell-mediated cytotoxicity »)

APC :Cellules présentatrices d'antigènes (« Antigen presenting cells »)

BCl : « B-cell lymphoma »

BTLA : « B and T lymphocytes attenuator »

CD : Cluster de différenciation

CEA : Commissariat aux énergies atomiques et alternatives

CMH : Complexe majeur d'histocompatibilité

cGAS : « Cyclic GMP-AMP synthase »

DC : Cellule dendritique (« dendritic cell »)

EEV : Virus extracellulaire enveloppé (virion du MVA)

G-CSF : Facteur de stimulation des colonies de granulocytes **(«** Granulocyte-colony stimulating factor »)

GM-CSF : Facteur de stimulation des colonies de granulocytes et macrophages **(«** Granulocyte-macrophages colony stimulating factor »)

HIV : Virus de l'immunodéficience humaine (« Human immunodeficiency virus »)

ICOS : « Inducible T cells costimulator »

ID : Intradermique

IFN : Interféron

IRF : « Interferon regulatory factors »

Ig : Immunoglobuline

IL : Interleukine

ILC : Cellules innées lymphoïdes (« innate lymphoïd cells »)

IM : Intramusculaire

IMV : Virus intracellulaire mature (virion du MVA)

LPS : Lipopolysaccharide

MDS : Analyse à échelle multidimensionnelle (« Multidimensionnal scale analysis »)

MDSC : Dérivé de cellule myéloide suppressive (« myeloid derived suppressive cell »)

MIP : Protéine inflammatoire des macrophages (« macrophage inflammatory protein »)

MPL : Monophosphoryl lipide A

MVA : Virus de la vaccine modifié de souche Ankara (« Modified vaccinia virus Ankara »)

NHP : Primate non-humain (« non-human primate)

OMS : Organisation mondiale de la santé

PAMP : Motif moléculaire associé au pathogène (« Pathogen associated molecular pattern »)

PBMC : Cellules du sang périphérique mononuclées(« péripheral blood mononuclear cells »)

PD : « Programmed cell death »

Poly(I:C) : Acide polyinosinique-polycytidiyique

PRR : Recepteur de reconnaissance d'un motif du pathogène (« pattern recognition receptor »)

rMVA : Virus de la vaccine modifié de souche Ankara recombinant

ROS : Espèces activées de l'oxygène (« reactive oxygen species »)

SAP : « SLAM-associated protein »

SC : Sous-cutané

SLAM :«signaling lymphocytic activation molecule»

SPADE :« spanning tree progression analysis of density normalized events»

STING :«stimulator of interferon genes»

Tfh : lymphocytes T folliculaires auxiliaires («T follicular helper»)

Th : lymphocytes T auxiliaires («T helper»)

TLR : Toll-like récepteur

TNF : Facteur de nécrose tumorale (« Tumor necrosis factor »)

Treg : Lymphocytes T régulateurs

TRIF : «TIR domain-containing adaptor protein inducing interferon beta »

SIDA : Syndrôme de l'immunodéficience acquise

SIV : Virus de l'immunodéficience simienne (« Simian immunodeficiency virus »)

VV : Virus de la vaccine (« Vaccinia virus »)

Introduction

A. Vaccins

I. Histoire de la vaccination

a. La découverte de la vaccination

(Paragraphes inspirés de ma thèse de pharmacie[1])

La variole était une maladie endémique et mortelle existant depuis l'antiquité. Hugues Capet, Louis XV, mais aussi Huayna Capac, grand empereur Inca du XVe siècle ou encore Ramsès V seraient des victimes de la variole. Elle se manifestait par l'apparition d'éruptions cutanées sous forme de pustules qui pouvaient couvrir jusqu'à l'ensemble du corps de l'hôte contaminé. Pour y lutter, les chinois, à une époque estimée autour du XVIe siècle effectuaient un processus dit de variolisation, qui consistait en l'inoculation de la substance contenue dans les pustules d'une personne infectée à une personne saine. Bien que ce procédé ne fût pas sans risques (mortels), il présentait toutefois une certaine efficacité mise en évidence par Daniel Bernoulli, le mathématicien, en 1760. Mais c'est le médecin Anglais Edward Jenner qui fit naître la vaccination. Il est parvenu à effectuer le constat suivant : les personnes traitant les vaches à la ferme et atteintes de « Cow Pox » ou « variole des vaches » semblent immunisées contre la variole humaine. Par la suite, E. Jenner est parvenu à mettre au point en 1796 le premier vaccin permettant de lutter contre la variole. Cette première étape fut la première pierre à l'édifice menant à l'éradication de cette maladie du globe en 1980. Le scientifique Anglais a ainsi ouvert le champ à une arme des plus redoutables contre les maladies infectieuses.

Louis Pasteur a ensuite développé une autre technique de vaccination. Il a montré qu'en mettant dans des conditions extrêmes un agent infectieux, il était possible de diminuer la pathogénicité de ce dernier. Il parvint ainsi, aidé par les travaux de Robert Koch sur le bacille du charbon, à développer les premiers vaccins atténués.

Il réussit notamment -en suspendant une moelle épinière de chien infecté par le virus de la rage à l'air asséché- à mettre au point un vaccin contre cette pathologie en 1885.

De nombreuses victoires contre les maladies infectieuses ont par la suite pu être remportées en utilisant des souches virales atténuées. Le vaccin contre la tuberculose développé par Calmette et Guérin en 1921 ou le vaccin contre la poliomyélite développé par Jonas Salk en 1952 en sont de bonnes illustrations. Des vaccins à partir de virus tués ont également rapidement vu le jour, à l'image de ceux contre la peste et le choléra.

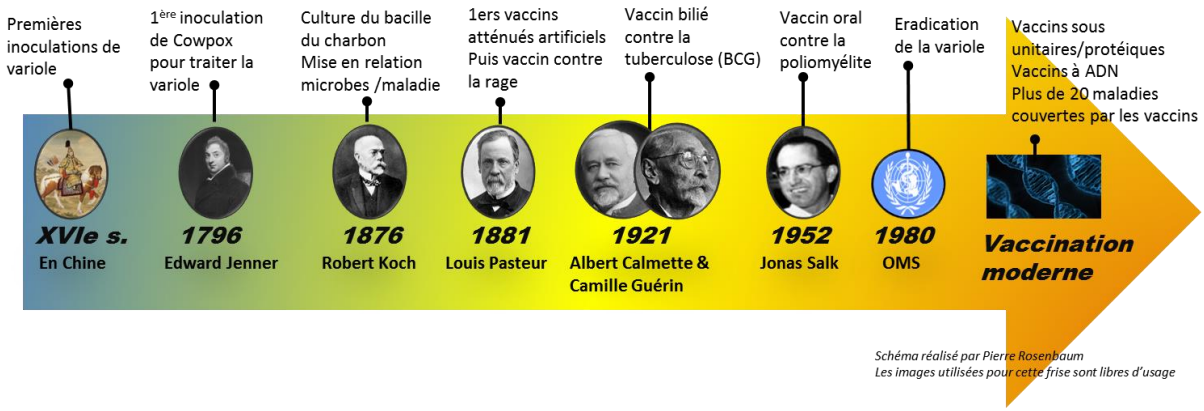

Figure 1: Quelques dates clés de l'histoire de la vaccination
Schéma réalisé dans le cadre de cette thèse

b. *La vaccination aujourd'hui*

La vaccination est considérée comme l'une des mesures de santé publique les plus importantes du XXe siècle. Ce procédé a aujourd'hui démontré toute son efficacité, et permettrait d'éviter 2 à 3 millions de décès par an selon l'OMS (Source : http://www.who.int/topics/immunization/fr/). Il s'agit de l'unique moyen connu à ce jour d'éradiquer une maladie infectieuse de la surface du globe, comme ce fut le cas avec la variole, une pathologie autrefois endémique et mortelle. De surcroit, l'essor de la vaccination a permis la réduction drastique d'un nombre conséquent de pathologies infectieuses, qui incluent la diphtérie, la poliomyélite, les hépatites A et B, la varicelle, la coqueluche , et bien d'autres encore (exemples en**Fig.1**).

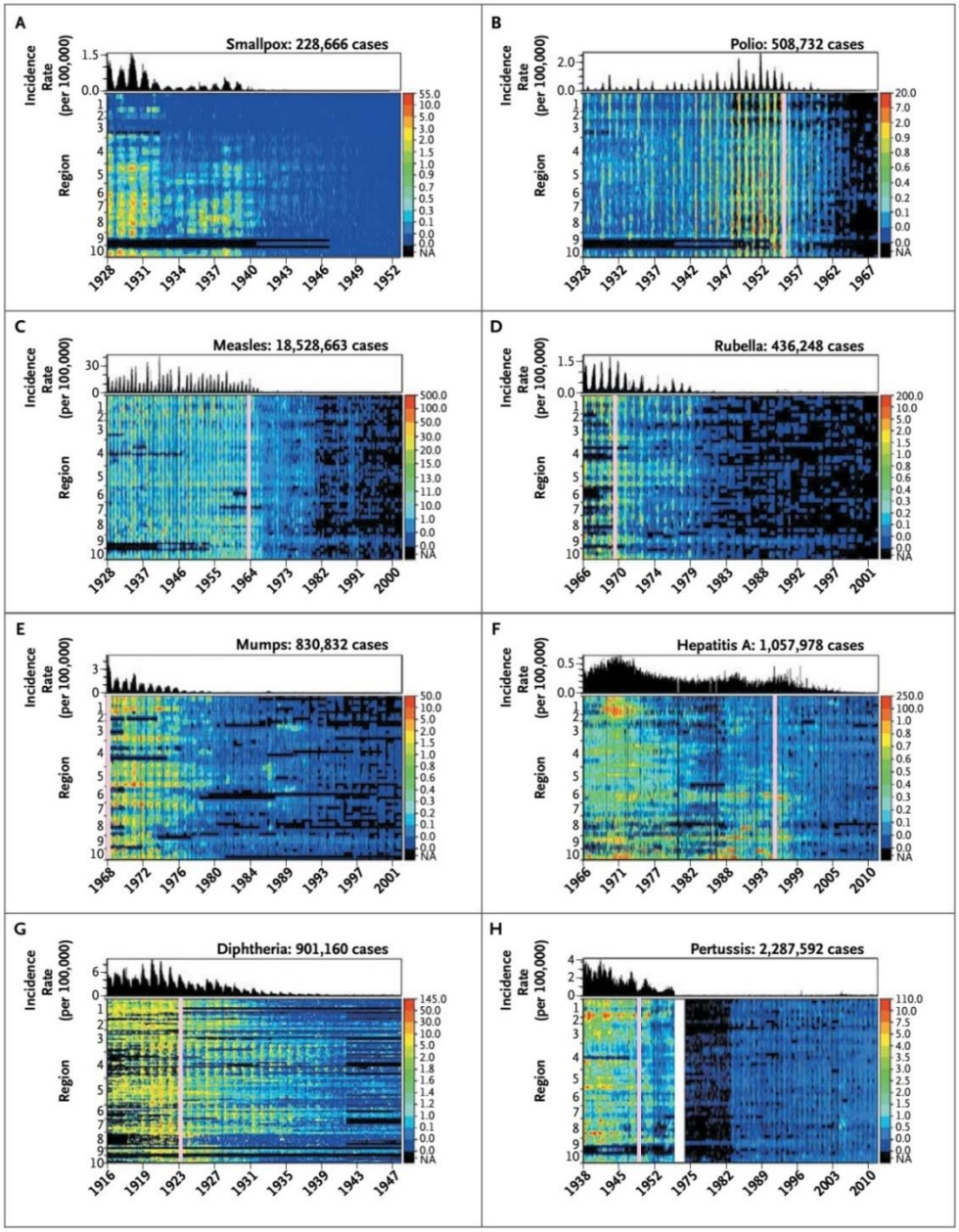

Figure 2: Quelques victoires de la vaccination

Extrait d'une étude intégrant quelques 87 950 807 rapports de cas individuels de maladie. L'ordonnée représente les différentes régions des Etats-Unis. La ligne verticale rose représente l'arrivée du vaccin sur le marché américain. Plus la coloration est bleue, plus l'incidence de la maladie est faible dans la région. On y constate que l'arrivée du vaccin entraine une importante diminution de la maladie quelques années plus tard.Image extraite de Van Penhuis et al.[2]

II. Généralités sur les vaccins

a. *Définition*

Le Larousse (http://www.larousse.fr/dictionnaires/francais/vaccin/80859) définit le vaccin de la manière suivante :« *Substance d'origine microbienne (microbes vivants atténués ou tués, substances solubles) qui, administrée à un individu ou à un animal, lui confère l'immunité à l'égard de l'infection déterminée par les microbes mêmes dont elle provient et parfois à l'égard d'autres infections*. »

L'OMS (http://www.who.int/topics/immunization/fr/) considère que « […] *les vaccins, qui stimulent le système immunitaire, prémunissent la personne d'une infection ou d'une maladie*. »

La vaccination a donc pour effet d'activer le système immunitaire du sujet, et notamment d'induire des cellules lymphocytaires dites « mémoires » qui persistent dans l'organisme. De ce fait, lorsque l'infection « naturelle » par le pathogène contre lequel l'individu a été préalablement vacciné se présente, le système immunitaire reconnaîtra -par l'intermédiaire de ces cellules mémoires- le pathogène et l'éliminera avant que ce dernier ne devienne nocif. En d'autres termes, un vaccin mime l'infection contre laquelle il protège, agissant en quelque sorte comme un leurre pour le système immunitaire, mais qui lui permettra de « mémoriser » l'infection comme dans le cas d'un « vrai » pathogène.

b. *Propriétés du vaccin*

En conséquence, pour qu'un vaccin soit intéressant, il lui faut trois propriétés principales :

1. *Induire une réponse immunitaire forte.*

En effet, si les vaccins composés de bactéries ou virus entiers sont susceptibles d'induire une immunité pouvant dans certains cas perdurer le temps d'une vie, d'autres, composés de sous unités protéiques ou d'ADN, présentent des capacités plus réduites à stimuler le système immunitaire et doivent être suppléés par des adjuvants pour être efficaces.

2. *Induire une réponse immunitaire adaptée.*

Il ne suffit pas d'obtenir une réponse forte, il faut aussi qu'elle soit adaptée. En effet, le système immunitaire est -comme nous le détaillerons par la suite dans ce manuscrit- un processus complexe qui peut réagir de différentes manières en fonction du type d'infection ou de lésion. Malheureusement, ce dernier peut commettre certaines erreurs. Par ailleurs, au cours de leur évolution, la plupart des microorganismes ont développé de nombreux outils pour contourner le système immunitaire des hôtes qu'ils infectent. Dans le cadre de la vaccination, certains adjuvants permettent d'aider le système immunitaire à réagir de manière plus appropriée contre certaines infections.

3. *Être inoffensif.*

La réponse du système immunitaire contre le vaccin doit être maîtrisée. Ainsi ils doivent être très bien tolérés par l'ensemble de la population. De ce fait, avant sa mise sur le marché, l'innocuité de chaque vaccin est surveillée de près. Et même après sa distribution, un suivi rigoureux des effets secondaires engendrés par le vaccin est mis en place.

Il peut être dans certains cas difficile de concilier l'efficacité avec l'innocuité. En effet, un vaccin très immunogène est susceptible d'induire une importante inflammation. Cependant, une forte réaction inflammatoire peut être également douloureuse pour l'individu vacciné, et constitue de ce fait un effet secondaire délétère.

Il s'agira donc de soigneusement évaluer la balance bénéfice/risque et également de choisir judicieusement les ingrédients qui composent le vaccin. C'est pourquoi, les mécanismes d'action des différents composants d'un vaccin doivent être connus le mieux possible, afin de pouvoir trouver la meilleure association.

a. *Les types de vaccins*

Pour ôter les risques que représentent l'utilisation directe d'une bactérie ou d'un virus pathogène, il est possible le « tuer » avec des composés chimiques ou à la chaleur pour ainsi produire un vaccin dit **inactivé**. Ces vaccins présentent l'avantage de ne pas être dangereux pour l'organisme hôte. En revanche, ils risquent d'induire une réponse immunitaire plus limitée. Une autre stratégie consiste à rendre le pathogène moins virulent en le soumettant à des conditions particulières pour en faire un vaccin dit **atténué**. Par la suite, un procédé consistant à forcer le virus ou la bactérie à se multiplier un très grand nombre de fois *in vitro* a été utilisé. En effet, à chaque multiplication, à cause des rares imperfections du matériel cellulaire de la cellule hôte exploitée par le microorganisme, ce dernier perd une (infime) partie de son génome. Ces mutations ont un effet négligeable après seulement quelques cycles de multiplication, en revanche sur du plus long terme, ce procédé devient incroyablement efficace pour obtenir une version du microorganisme d'origine appauvrie de nombreuses de ses propriétés.

Par exemple :

- **Le Bacille de Calmette et Guérin** (BCG) constitue le seul vaccin disponible contre la tuberculose. Il a été mis au point à partir d'une souche de *Mycobacterium bovis* -un cousin proche du *Mycobacterium tuberculosis* responsable de la tuberculose- initialement virulente mais qui a subi 13 années de passages *in vitro* pour donner le jour à une version très atténuée[3].
- **Le Modified Vaccinia-virus Ankara** (MVA) constitue un autre exemple. Il s'agit cette fois ci d'une version atténuée du virus de la vaccine qui a subi 530 passages consécutifs *in vitro* sur des fibroblastes d'embryons de poulet[4]. Ce vaccin sera l'objet d'une attention particulière, puisqu'il s'agit du principal modèle d'étude utilisé dans cette thèse. Il constitue également un vecteur viral d'intérêt dans le développement de futurs vaccins.

Outre le temps et la patience que cette stratégie nécessite, une autre interrogation réside dans notre méconnaissance des sites précis qui ont été sujets à des modifications lors des passages. Les effets

sont donc évalués uniquement de manière empirique : on peut tout à fait rendre le produit créé moins immunogène, c'est-à-dire qu'il stimule trop peu le système immunitaire, ou encore lui faire conserver certaines capacités délétères.

C'est pourquoi avec les progrès du génie génétique et moléculaire, on cherche aujourd'hui à affaiblir le microorganisme d'une manière plus rationnelle, en supprimant spécifiquement les gènes codants des facteurs de virulence du microorganisme. Cependant on s'expose toujours à obtenir une trop faible immunogénicité ou à la persistance de certains effets secondaires.

b. Les composants du vaccin

Les vaccins modernes sont composés de trois ingrédients principaux: L'antigène, le vecteur et l'adjuvant. (Paragraphes inspirés de ma thèse d'exercice de pharmacie[1])

1. L'antigène

Il correspond à la spécificité contre laquelle on souhaite induire une réponse mémoire. Il s'agit du pathogène en entier dans le cas des vaccins inactivés ou atténués, de fragments ou de sous unités dans le cas de vaccins sous-unitaires ou de recombinants.

2. Le Vecteur

Le vecteur sert de mode de transport et d'expression de l'antigène. Il peut s'agir d'un micro-organisme (adénovirus, poxvirus…). Il est en effet possible de modifier génétiquement des virus peu pathogènes déjà existants pour qu'ils expriment à leur surface des antigènes provenant d'un autre micro-organisme. On fait ainsi un usage bénéfique du vecteur viral en utilisant ses propriétés naturelles à infecter des cellules. Une alternative consiste en l'utilisation d'une enveloppe synthétique (liposomes, Nanoparticules, Virus-like-particules…).

3. L'adjuvant

Les réponses induites par les vaccins vivants sont généralement suffisamment intenses pour induire une immunité à long terme, mais ce n'est pas toujours le cas des vaccins inactivés ou des vaccins sous unitaires[5]. Les adjuvants sont des molécules permettant de stimuler voire de moduler la réponse immunitaire en synergie avec l'antigène de façon à exacerber la réponse spécifique dirigée

contre cet antigène. Ils permettent donc d'améliorer la réponse spécifique du système immunitaire et la mémoire qui en résulte. Actuellement, seuls l'alum[6]puis plus récemment le MF59[7], et le MPL (associé à l'alum, donnant l'AS04[8]**)** possèdent une licence leur permettant d'être utilisés comme adjuvants vaccinaux chez l'homme. L'alum permet de stimuler la réponse immunitaire par deux principaux effets. D'une part, il permet un « effet dépôt » lors de l'administration de l'antigène. Cela signifie que l'antigène est libéré lentement et progressivement dans l'organisme. D'autre part, il stimule également de manière non spécifique le sujet en tant que corps étranger entrant dans un organisme. Ces deux phénomènes occasionnent une augmentation locale des populations cellulaires de l'immunité innée (macrophages, granulocytes, cellules dendritiques…). Il faut noter que tout excipient présent dans une préparation vaccinale peut avoir un effet « adjuvant » sur le vaccin en stimulant le système immunitaire de manière aspécifique.

Aujourd'hui, de nombreux adjuvants sont en développement, parmi lesquels figurent des molécules dérivées de composants bactériens (MPL et autre dérivés du LPS), des saponines d'origine végétale (Quil-A), mais aussi des stimulants ciblant spécifiquement certain composants de la réponse

Immunitaire innée, comprenant les adjuvants agonistes ligands des TLR.

III. Avantages et limites de la vaccination

a. ***Avantages***

1. *Bénéfice sanitaire*

La vaccination est une intervention préventive, effectuée avant d'être infecté par le pathogène. Elle prévient donc de tous les effets délétères de la maladie, qui peuvent se traduire par de graves séquelles jusqu'au décès.

2. *Bénéfice économique*

Le coût d'un vaccin est en effet souvent dérisoire par rapport au coût des soins nécessaires pour guérir d'une maladie infectieuse. De surcroit, la personne malade ne travaillera pas, ce qui est également préjudiciable sur un plan économique et social.

3. *Immunité de groupe*

Une personne vaccinée participe également à la non-propagation de la maladie. En effet, lorsque le nombre de sujets vaccinés atteint un certain seuil, toute la population bénéficiera d'une immunité dite « de groupe ». En pratique, l'épidémie sera contenue du fait que l'environnement d'un sujet malade et contagieux sera constitué de sujets immunisés. Le virus n'aura ainsi pas la capacité d'infecter un nouvel hôte et n'aura donc pas d'échappatoire. Cela permet aux sujets sains et non immunisés de ne pas être malades.

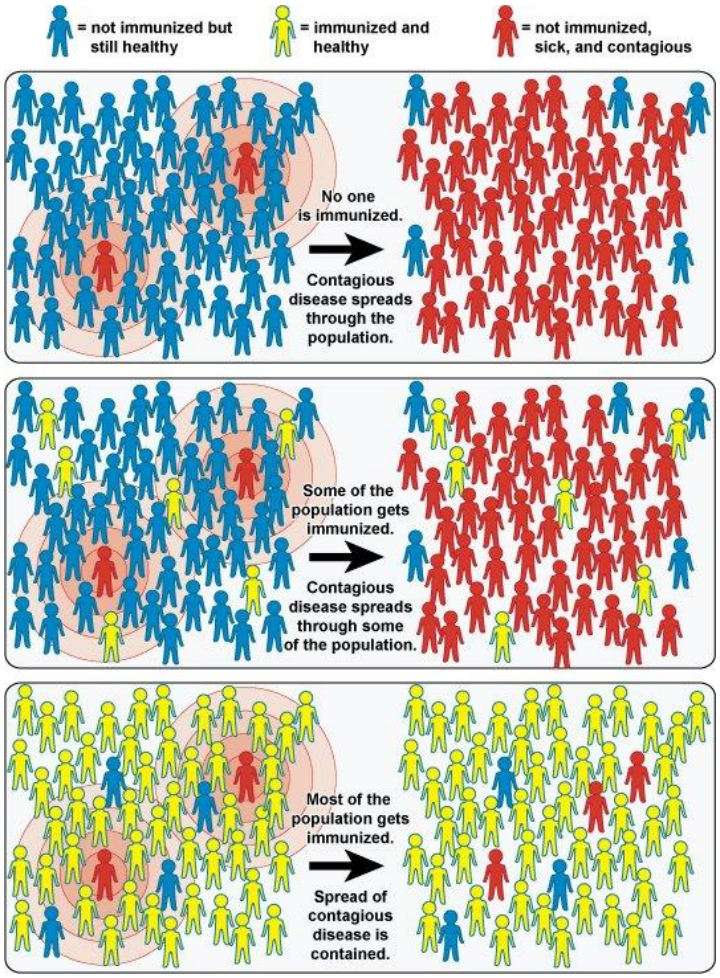

Figure 3: Immunité de groupe
(https://commons.wikimedia.org/wiki/File:Community_Immunity.jpg)

b. *Limites*

1. *L'amélioration de vaccins existants*

Cependant, de nombreux vaccins nécessitent d'être améliorés. Pour la plupart d'entre eux, nous manquons notamment d'indicateurs fiables de leur efficacité. La recherche de ces corrélats de protection –ces mesures biologiques (souvent sérologiques) indiquant (indirectement) si une personne est immunisée à la maladie ou non- revêt donc une importance primordiale pour évaluer la qualité d'un vaccin et trouver des axes d'amélioration. Cela nécessite de mieux connaître les mécanismes immunologiques impliqués dans le processus vaccinal.

On peut citer le cas du vaccin contre la coqueluche. Il s'agissait à l'origine d'un vaccin inactivé contenant une suspension de *Bordetella pertussis,* la bactérie vectrice de la maladie. Puis un nouveau vaccin acellulaire –contenant uniquement quelques composés protéiques du *Bordetella pertussis*- a

progressivement été utilisé à la place de l'ancien car il induisait moins d'effets secondaires. Si l'on estimait au départ que l'efficacité des deux vaccins était comparable, le vaccin acellulaire s'est finalement avéré moins bien protéger que son ainé[9]. De surcroit, le vaccin acellulaire, n'empêcherait pas la personne immunisée d'être infectée par la bactérie, même si cette dernière ne présente pas de symptômes cliniques[10]. Cela rend donc possible la persistance du microorganisme ainsi que sa transmission dans la population, mais aussi de mère à enfant. Cela fait des nourrissons des cibles particulièrement vulnérables. Le cas de la grippe est également sensible. Le vaccin doit en effet être administré chaque année pour protéger contre les souches à l'origine des épidémies saisonnières du fait des capacités de mutation du virus influenza.

2. *Des vaccins contre certaines pathologies difficiles à mettre au point*

Pour d'autres pathologies comme le SIDA, l'hépatite C ou le paludisme, la situation est encore plus préoccupante : nous ne sommes toujours pas parvenus à mettre au point de vaccin efficace. Par exemple, le virus de l'immunodéficience humaine (HIV) dispose de propriétés très particulières : en plus d'être très instable et de beaucoup muter, il s'attaque directement à des cellules du système immunitaire, les lymphocytes T CD4 et les macrophages. Les stratégies vaccinales sont donc pour l'instant en échec, comme ce fut le cas de l'étude « STEP » en 2005[11]. Si en 2009, l'essai RV144 réalisé en partie en Thaïlande a donné des résultats modestes mais prometteurs[12], il reste encore beaucoup de chemin à parcourir.

c. ***Perspectives***

Au niveau scientifique, de nombreux axes de recherche sont évoqués. L'un d'entre eux consiste en une meilleure compréhension des mécanismes de la réponse immunitaire. Avec une parfaite connaissance de ces procédés, il serait en effet possible de développer de nouveaux vaccins plus efficaces. L'utilisation de vaccins de référence (du fait de leur efficacité) comme celui contre la fièvre jaune et certains dérivés de la vaccine comme le MVA sont donc investigués en profondeur dans de nombreux laboratoires d'immunologie comme celui du CEA de Fontenay-aux-Roses.

B. Le système immunitaire

Le système immunitaire est un réseau complexe qui englobe des entités très diverses s'échelonnant de la plus insignifiante des molécules à des organes entiers concourant tous à la défense de l'organisme. Ces éléments interagissent entre eux de manière permanente et continue dans l'objectif de protéger l'individu des menaces qui pourraient nuire à son intégrité. Ce système biologique coordonné « apprend » à discriminer les éléments appartement au « soi » des éléments du « non-soi » et établit une réponse dite « immunitaire » adaptée à la menace. Cette dernière pourra tolérer l'élément étranger ou au contraire tenter de l'éliminer.

I. Les cellules non professionnelles de l'immunité : des maillons essentiels à la défense de l'organisme

A l'instar des cellules de l'organisme qui assurent des fonctions métaboliques particulières comme le stockage d'énergie ou la dégradation de composés chimiques, d'autres sont spécialistes de l'immunité. Cependant, même les cellules non-immunitaires jouent un rôle crucial. En effet, la plupart des cellules sont capables de présenter des peptides -produits de dégradation des protéines suite à l'utilisation de la machinerie cellulaire -à leur surface via leur complexe majeur d'histocompatibilité (CMH) de classe I[13]. De ce fait, si la cellule est infectée par un pathogène ou présente certains dysfonctionnements, des cellules immunitaires (les lymphocytes T CD8) pourront reconnaitre ce peptide comme étant non conforme et agir en conséquence. Dans le cadre d'une infection HIV par exemple, ce processus sera largement mise en jeu, et la réponse immunitaire dépendra largement du profil de CMH de l'individu infecté[14].

Les cellules non-immunitaires sont non seulement capables de détecter certains pathogènes,mais peuvent également produire certaines cytokines –de petites protéines permettant de communiquer à distance avec d'autres cellules- émettant un signal de danger pouvant attirer des cellules spécialisées sur le site d'une éventuelle lésion[15,16], voire même de les activer [17]. De surcroît, certaines

cellules non-immunitaires comme les cellules épithéliales peuvent produire des protéines nommées défensines, qui protègent également l'organisme de certains microbes[18]. Certaines fonctions cellulaires sont quant à elles connexes à la fonction immunitaire. Ainsi, par exemple, les cellules endothéliales, pourtant non-immunitaires, seront prépondérantes car elles permettent l'adhérence puis le passage des cellules immunitaires en provenance de la circulation sanguine vers un foyer infectieux par exemple[19].

II. Organisation des cellules immunitaires

Le système immunitaire s'articule autour d'un réseau complexe de cellules dites « immunitaires ».

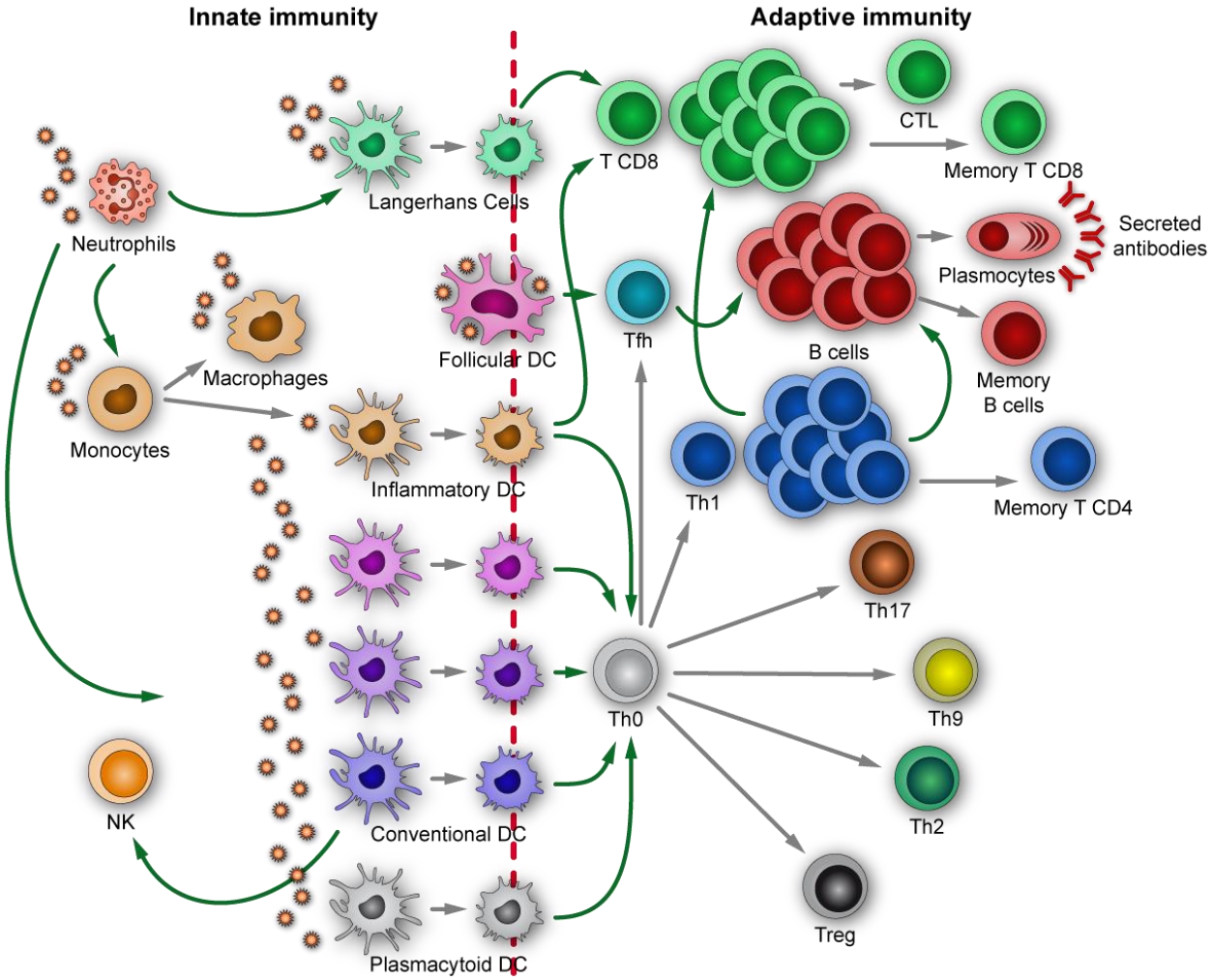

Figure 4: L'arsenal des cellules immunitaires

Organisation générale des principales cellules de l'immunité. La réponse acquise ("adaptive immunity") est fortement influencée par l'origine et la nature des cellules présentant l'antigène.

a. *Cellules myéloïdes*

Les cellules myéloïdes comprennent les granulocytes, les macrophages, les monocytes ou encore les cellules dendritiques (DCs). Ces cellules sont présentes dans différents organes, mais circulent également dans le sang et les vaisseaux lymphatiques, de manière à rapidement migrer sur les sites de lésion. Les monocytes sont des cellules circulant dans le sang. Elles sont capables de migrer dans un tissu en réponse à un stimulus moléculaire. Une de leurs particularités est notamment d'être pourvues d'une importante plasticité cellulaire leur permettant -une fois arrivées sur le site de la

lésion- de s'activer, puis de se différencier en macrophages ou en cellules dendritiques en fonction du stimulus reçu[20]. Plus généralement, chaque type de cellule immunitaire dispose de certaines spécificités. Ainsi les granulocytes sont plutôt spécialisés dans la production de facteurs et médiateurs pro-inflammatoires, mais sont aussi dotées de certaines fonctions d'endocytose. Les macrophages, eux, excellent dans la phagocytose de cellules endommagées ou apoptotiques, alors que les cellules dendritiques jouent un rôle clé dans la présentation antigénique (plus de précisions chapitre B.III.c).

b. Cellules lymphoïdes

Les cellules lymphoïdes comprennent principalement les lymphocytes et les cellules NK. Les lymphocytes B et T sont notamment mis à contribution dans le cadre d'une réponse immunitaire spécifique du pathogène ciblé. Les lymphocytes T CD4 possèdent la capacité d'interagir avec les cellules présentatrices d'antigène puis d'induire l'activation d'autres populations cellulaires comme les lymphocytes B –sécréteurs d'anticorps- ou les lymphocytes T CD8 cytotoxiques.

c. Cytokines

Ces glycoprotéines solubles sont synthétisées et excrétées en majorité par les cellules immunitaires. Elles occupent une place prépondérante dans la communication entre les effecteurs cellulaires dans l'élaboration de la réponse immunitaire. Ces cytokines activent des récepteurs de cellules situés à distance pour y exercer diverses fonctions.

1. Chémokines

Les chémokines, ou cytokines chimiotactiques, ont pour rôle d'attirer les leucocytes vers un foyer d'inflammation. Ces protéines de 8 à 10 kilodaltons se divisent en deux grandes catégories. Les α chémokines présentent le motif cystéine-acide aminé-cystéine (CXC). Son représentant le plus connu, le CXCL8, (ou interleukine(IL) 8), influence le recrutement des neutrophiles. Les β chémokines, comme le CCL3 (MIP1α) et CCL4 (MIP1β)[21], présentent un motif cystéine-cystéine (CC) et sont impliquées dans le recrutement d'autres populations cellulaires comme les monocytes.

2. Activité antivirale

Les interférons (IFN) de type I, comprenant l'IFNα et l'IFNβ, ont la capacité d'interférer sur la multiplication virale en induisant l'activation de protéines kinases inhibant la synthèse protéique des cellules infectées[22]. La synthèse d'interférons de type I est principalement induite suite aux interactions entre les « pattern recognition receptors » et leurs ligands. Il s'ensuit une cascade de signalisation mettant en jeu de nombreuses molécules, notamment de la famille des TRIFs (« TIR-domain-containing adapter-inducing interferon-β ») et des IRFs (« interféron regulating factors »)[23]. Cependant, les voies d'activation seront différentes en ce qui concerne le MVA, notre vaccin d'étude. En effet, la production d'interféron de type I sera dans ce cas déclenchée par une détection de l'ADN cytosoliquepar cGAS (« Cyclic AMP-GMP synthase »), qui activera un récepteur du réticulum endoplasmique nommé STING (« Stimulator of interferon genes »).Ce dernier induira notamment l'IRF3 et l'IRF7, à l'origine de la production d'interférons[24]. En outre, cette voie de signalisation récemment décrite permet d'induire les cellules voisines indépendamment de la sécrétion de cytokines, par l'entremise de jonctions communicantes[25].

3. Activation et différenciation cellulaire

Les cytokines sont principalement produites en quantité par les cellules de l'immunité innée, et jouent un rôle majeur dans la réponse inflammatoire. Ainsi certaines cytokines dites pro-inflammatoires comprenant l'IL1, l'IL6 et le TNFα permettent l'activation et l'entretien du recrutement de granulocytes et des macrophages au niveau du foyer inflammatoire, alors que d'autres cytokines auront un effet plutôt opposé, comme l'IL10, ou l'IL1ra. Ce dernier entre en compétition avec l'IL1 en se fixant au même récepteur cellulaire, limitant ainsi son effet. D'autres cytokines, comme l'IFNγ, l'IL12, l'IL4 ou l'IL5 jouent un rôle clé dans la différentiation des lymphocytes T CD4.

d. *La détection des pathogènes*

Pour répondre efficacement à une menace, les cellules de l'immunité innée notamment, sont capables d'identifier les signaux dangereux provenant de pathogènes extérieurs. Pour cela elles reconnaissent des motifs moléculaires associés aux pathogènes (PAMPs). Ces PAMPs sont détectés par l'intermédiaire de récepteurs nommés « pattern recognition receptors » (PRRs) dont les principales familles sont les « Toll-like receptors » (TLRs) », les « NOD-like receptors » (NLRs) ou les « RIG-I like receptors » (RLRs).

Microorganismes	PAMPs	TLR	Autres PRRs
Bactéries, mycobactéries	lipopolysaccharide (LPS)	TLR4	NOD1, NOD2
	lipoprotéines	TLR2/1, TLR2/6	
	flagelline	TLR5	
	ADN	TLR9	
	ARN	TLR7	
Virus	ADN	TLR9	RIG-I
	ARN	TLR3,TLR7,TLR8	
	Protéines de structure	TLR2, TLR4	
Champignons	bêta-glucane, zymosan	TLR2,TLR6	
	mannanes	TLR2, TLR4	
	ADN	TLR9	
	ARN	TLR7	
Parasites	tGPI-mutine(*Trypanosoma*)	TLR2	
	phosphatidylglycoinositol (*Trypanosoma*)	TLR4	
	ADN	TLR9	
	hemozoine (*Plasmodium*)	TLR9	
	profiline-like molecule (*Toxoplasma*)	TLR11	

Tableau 1 : Liste non-exhaustive des PAMPs et de leur PRRs associés
Inspiré du travail de Taro Kawai et Shizuo Akira, 2011[26]

Une interaction entre un PAMP et son récepteur initie une cascade de phosphorylation/déphosphorylation aboutissant au recrutement ainsi qu'à l'activation d'effecteurs de la réponse immunitaire innée. Un aperçu de cette complexité, ainsi que les voies de signalisation engagées et le type de réponse induite peut être visualisé sur la figure 7.

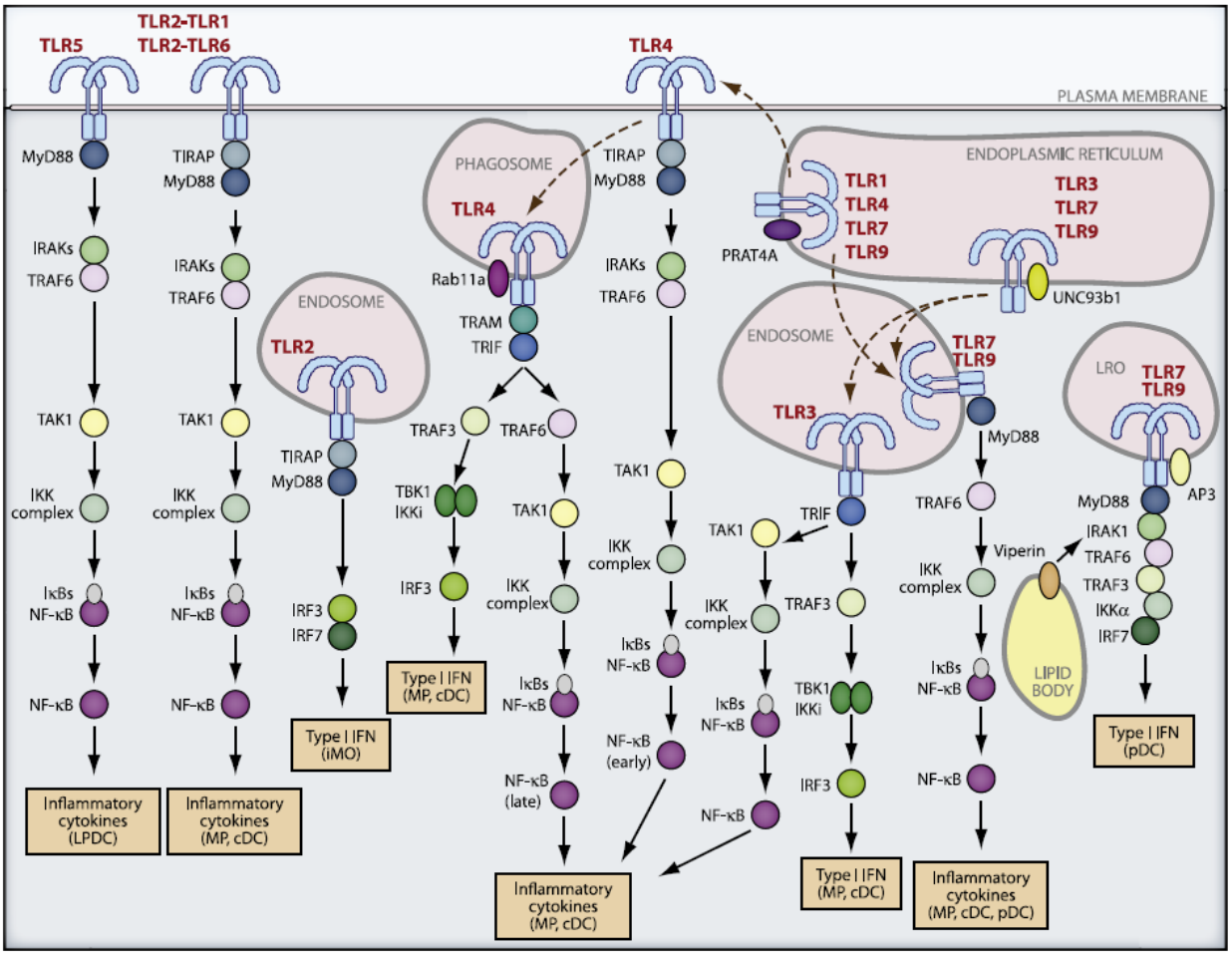

Figure 5: Voies de signalisation engagées et réponse induite par l'activation de TLRs[26]

e. *Le processus inflammatoire*

L'inflammation correspond à un processus biologique faisant partie intégrante de l'immunité innée. Cornelius Celsus, un médecin Romain de l'antiquité, fut le premier à décrire cette inflammation au travers de quatre manifestations cliniques bien identifiées[27] :

- *calor* (chaleur)
- *dolor* (douleur)
- *tumor* (gonflement/oedème)
- *rubor* (rougeur)

Ces signes physiologiques sont en fait associés à une cascade de réactions immunitaires en réponse à une lésion, à la suite de la détection d'un pathogène grâce à leur PRR. En premier lieu, les cellules

présentes sur le site de la lésion sécrètent des médiateurs de l'inflammation, comme les prostaglandines. Ces dernières induisent le recrutement de cellules dites « inflammatoires », à savoir les granulocytes et les macrophages[28]. Il s'ensuit une amplification de la réponse inflammatoire par l'intermédiaire de ces cellules. En effet, elles synthétiseront à leur tour des médiateurs inflammatoires ainsi que des cytokines pro-inflammatoires comme l'IL6[27]. Ces cellules s'accumuleront ainsi sur le site de la lésion et contribueront activement à l'élimination du pathogène.

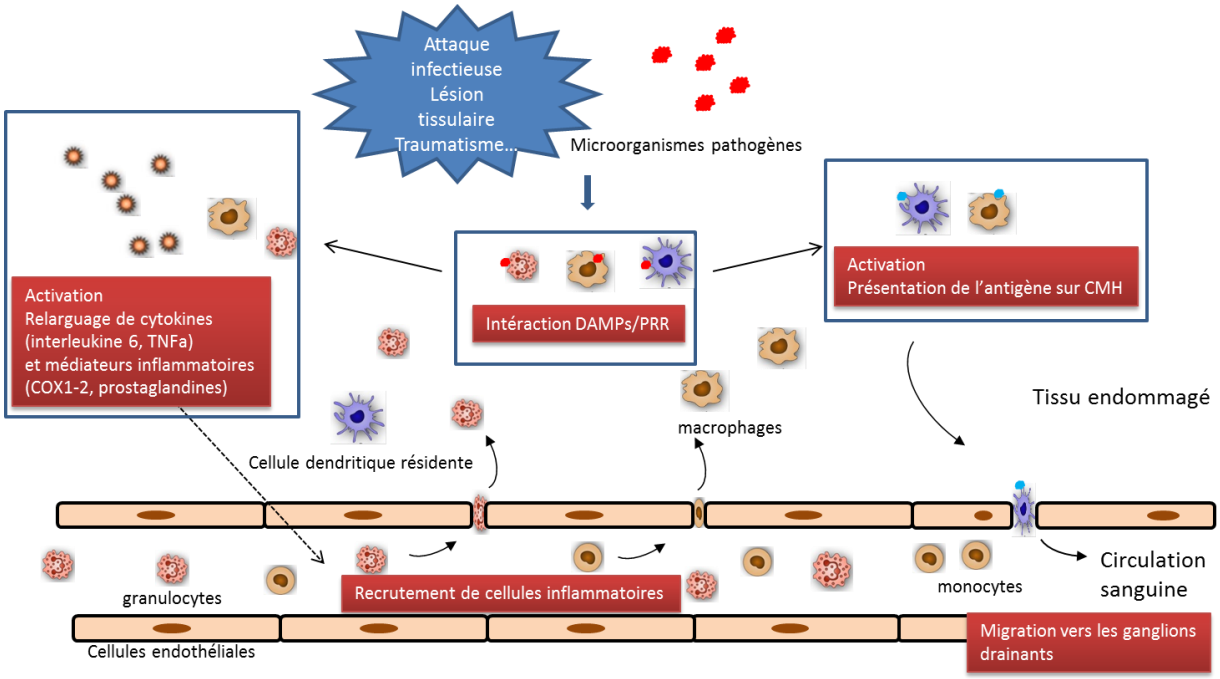

Figure 6 : Version simplifiée des premières étapes de la réponse inflammatoire
Inspiré du travail de Charles N. Seran et John Savill[29]

f. Les cellules présentatrices d'antigène

Les cellules présentatrices d'antigène (APCs) constituent un maillon essentiel dans l'élaboration de la réponse immunitaire. Leur rôle principal est en effet de détecter, d'endocyter, puis de présenter l'antigène à leur surface par l'intermédiaire des molécules de classe II du complexe majeur d'histocompatibilité (CMH) pour activer les lymphocytes T CD4 naïfs. La synapse immunologique ainsi formée entre les deux cellules constitue une étape charnière de la réponse immunitaire puisqu'elle influe largement sur la maturation et la différenciation des ces lymphocytes T CD4, qui sont les chefs d'orchestre de la réponse adaptative. Les principales APCs sont les cellules dendritiques, une sous-population rare de cellule myéloïdes[30]. Certaines cellules dendritiques disposent d'une capacité

unique nommée cross-présentation. Cette propriété leur permet de présenter un antigène d'origine extracellulaire sur leur CMH I (au lieu du CMH II classiquement), leur permettant d'activer directement les lymphocytes T CD8. Les cellules dendritiques comportent plusieurs sous-populations, dont les cellules de Langerhans –caractérisées par leur localisation dans l'épiderme et la présence de formations particulières nommées granules de Birbeck- et les cellules dendritiques plasmacytoïdes ayant des propriétés antivirales accrues via leur capacité à produire de grandes quantités d'interféron de type I[31]. En tant qu'APCs, ces cellules expriment de nombreux TLRs et autres PRRs différents de manière à pouvoir appréhender de nombreux pathogènes différents[32]. Il est à noter que d'autres cellules possèdent cette capacité de présentation d'antigène, comme les macrophages et les lymphocytes B[33,34].

III. Immunité adaptative

La réponse immunitaire adaptative (ou acquise) correspond à une réponse plus tardive mais spécifique du pathogène ciblé. Cette dernière implique principalement les lymphocytes B et T. Une des grandes propriétés de cette réponse adaptative est sa capacité à induire des lymphocytes B et T dits « mémoires », qui perdurent dans l'organisme après l'épisode infectieux. C'est cette fonction qui explique l'efficacité des vaccins. En effet, ces cellules protègeront l'hôte d'attaques ultérieures en s'activant immédiatement après une nouvelle rencontre du pathogène et permettent de développer une réponse spécifique immédiate, alors que cette dernière avait nécessité beaucoup plus de temps lors du premier contact[35].

Suite à la présentation antigénique, les lymphocytes T helper, ou auxiliaires (Th) 0 naïfs se différencient et orientent la réponse immunitaire. Le profil de la réponse immunitaire dépendra ainsi en partie de la réponse immunitaire innée dont les APCs sont issues[36].

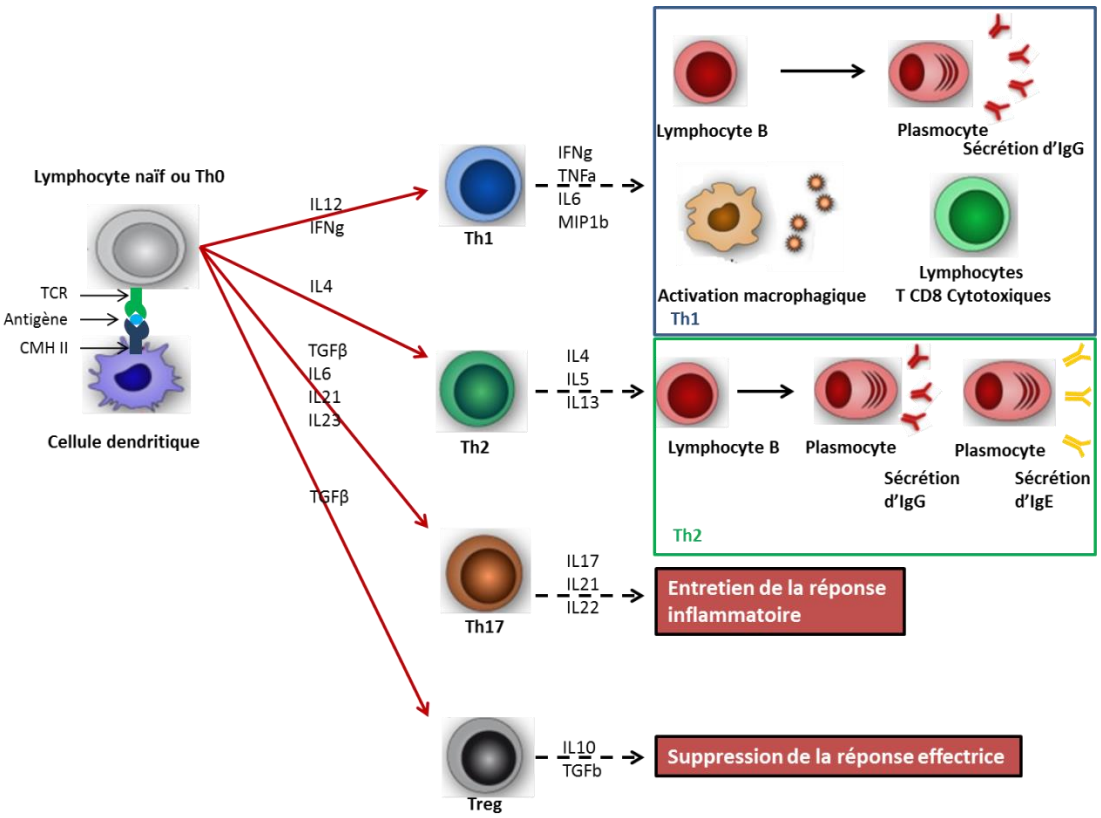

Figure 7: Les profils de réponse lymphocytaire
Inspiré du travail d'Idris Khodja et al.,complété par d'autre références[37–39]

a. *Les lymphocytes T CD4 auxiliaires*

Les lymphocytes Th1 sont caractérisés par la production d'IFNγ. Ces cellules produisent un panel relativement varié de cytokines, dont la plupart sont à connotation pro-inflammatoire, comme le MIP1β, le TNFα ou l'IL6. Elles induisent une immunité dite « cellulaire » car elles entrainent l'activation des macrophages, mais également la prolifération de cellules NKT et CD8 cytotoxiques[40]. Ces lymphocytes Th1 sont également capables d'induire une immunité humorale en induisant la prolifération des lymphocytes B, puis leur différenciation en plasmocytes. Ces derniers peuvent sécréter d'importantes quantités d'immunoglobuline G (IgG). Ces anticorps exercent différents effets sur le pathogène comme la formation de complexes immuns neutralisants facilitant la phagocytose et l'opsonisation du pathogène ou encore une cytotoxicité cellulaire dépendante des anticorps (ADCC).

Les lymphocytes Th2 sont caractérisés par la production d'IL4, et IL5. Ils vont notamment favoriser la production d'anticorps IgE par les lymphocytes B[41]. Ces anticorps sont particulièrement efficaces pour lutter contre les infections parasitaires.

D'autres profils de réponse T existent également. Ainsi, les lymphocytes T régulateurs (Treg) sont caractérisés par l'expression de CD25 et de FoxP3. Ils induisent des effets immunosuppressifs sur la mise en place de la réponse. Les lymphocytes T helper 17, caractérisés par leur sécrétion abondante d'IL17, entretiennent quant à eux la réponse inflammatoire.

b. *Les lymphocytes Tfh « follicular helper »*

Cette sous population de lymphocytes T CD4 n'a été identifiée qu'assez récemment, au cours des années 2000. Cette dernière est notamment caractérisée par une expression importante d'un récepteur aux chémokines particulier, le CXCR5[42,43]. Ce récepteur va leur permettre de migrer au niveau des centres germinatifs des organes lymphoïdes secondaires, riches en lymphocytes B activés. Les lymphocytes Tfh jouent un rôle prépondérant dans le développement et le maintien de ces structures spécialisées, en induisant l'activation des lymphocytes B. Ils sont également fortement

impliqués dans leur prolifération, leur survie, ainsi que dans leur différenciation. Pour cela, les Tfh produisent notamment deux cytokines clés :

- **L'IL21** : Elle est Impliquée dans l'expression du Bcl6 activant les lymphocytes B[44]. Paradoxalement, elle favorise également dans certains cas la différenciation de ces lymphocytes B en plasmocytes, par l'uprégulation du facteur Blimp1[45]. Les facteurs en cause dans l'induction de l'une ou l'autre de ces voies n'ont cependant pas encore été clairement déterminés. Par ailleurs, l'IL21 induit aussi des changements de classe des immunoglobulines (IgG et IgA)[46].
- **L'IL4** : Elle exerce dans ce cadre un rôle anti-apototique en induisant l'expression de Bcl2[47]. Cette fonction est essentielle au maintien des centres germinatifs. Elle permet le changement de classe des immunoglobulines, notamment IgE de manière indépendante des lymphocytes Th2 par l'entremise de protéines SAP et SLAM[48].

L'interaction entre Tfh et lymphocytes B demeure néanmoins un processus complexe mettant en jeu la synthèse de nombreux effecteurs (CD40L, ICOS, BTLA, PD-1…) dont tous les mécanismes n'ont pas pas encore été élucidés[49] .

Dans l'ensemble, les lymphocytes Tfhrevêtent un intérêt grandissant en infectiologie. Ainsi, au cours d'une infection par le HIV, ces cellules ont été décrites comme cibles du virus. L'étude des réservoirs viraux a ainsi permis de mettre en évidence une nouvelle population nommée lymphocytes T folliculaires cytotoxiques capables d'éliminer les cellules B et Tfh infectées dans les follicules[50].Les lymphocytes Tfh attisent par ailleurs également l'intérêt des vaccinologues. Il a en effet été montré que la quantité de lymphocytes Tfh était directement corrélée à la production d'anticorps spécifiques[51–53]. Cibler ces cellules avec un vaccin pourrait ainsi impacter d'une manière majeure la réponse humorale.

c. *Lymphocytes T Cytotoxiques*

Les lymphocytes T CD8 sont les principales cellules exerçant des fonctions cytotoxiques spécifiques de l'antigène. Le lymphocyte T CD8 détecte dans un premier temps un antigène non conforme par l'entremise d'une interaction entre récepteur T et CMH I. Cela entraîne une cascade de signalisation chez les lymphocytes induisant l'excrétion de perforine. Cette dernière est un maillon essentiel à la cytotoxité cellulaire[54]. Elle créé des pores dans la membrane de la cellule cible. Ces pores sont formés par l'agrégation de monomères de perforine sur des fractions membranaires de phosphorylcholine en présence de calcium[55]. Dans un second temps, des molécules incluant le granzyme B passent par ces pores. Il s'agit d'un important inducteur d'apoptose (de suicide) cellulaire[56]. Il contribue en effet à activer les voies de mort cellulaire (caspase) et exerce entre autres une activité protéolytique sur certaines cibles clé de la membrane nucléaire et du cytosquelette[56].

d. *Lymphocytes B*

Les lymphocytes B présentent de multiples fonctions. Elles peuvent jouer le rôle d'APC. Cependant, elles échouent à induire la prolifération de cellules T CD4. Les lymphocytes B ne stimulent également pas suffisamment les lymphocytes T CD4 naïfs pour les différencier en Th1 ou Th2[57,58]. En revanche, elles pourraient être impliquées dans la mise en place d'une réponse anergique ou tolérogénique dans certaines conditions[59,60]. Une fois stimulées, ces cellules sont également capables de proliférer et de se différencier en plasmocytes. Ces dernières sont les cellules spécialisées dans la synthèse d'anticorps solubles. Ces anticorps sont à l'origine de la réponse humorale. Il existe différentes classes d'immunoglobulines (Ig) :

- IgG : La forme la plus abondante d'immunoglobulines
- IgM : Peu matures, il s'agit des premières Ig à être présentes dans le sang après une infection
- IgA : Principalement localisées au niveau des muqueuses
- IgD : Fonctionnalités anti-microbiennes
- IgE : Impliquées dans les réactions allergiques et parasitaires

Par ailleurs il existe également des lymphocytes B mémoires. Ils permettent la synthèse d'anticorps différenciés et spécifiques du pathogène de manière rapide en cas de nouvelle rencontre avec ce dernier.

e. Capacité migratoire des lymphocytes

Les lymphocytes possèdent à leur surface divers récepteurs de chémokines. Ces récepteurs dirigent les déplacements de ces cellules dans l'organisme, qui peuvent ainsi sortir de la circulation sanguine et migrer vers des tissus d'intérêt. L'expression de ces récepteurs permet ausside discriminer les lymphocytes Th1 (qui expriment CXCR3 et CCR5)[61] des Th2, (qui expriment CCR4)[62]. Deux autres récepteurs ont fait l'objet d'un intérêt soutenu au cours de cette thèse :

Le CCR7 : Ses ligands sont le CCL19 and CCL21. Il participe à la migration des cellules immunitaires vers les ganglions lymphatiques[63]. Il est exprimé par diverses des sous populations de lymphocytes T, mais également des APCs. Il est également utilisé pour discriminer certaines sous populations de lymphocytes T en association avec d'autres marqueurs comme le CD27[64].

Le CD62L : Il ne s'agit pas d'un récepteur de chémokine, mais d'une L-selectine impliquée dans les phénomènes d'adhérence cellulaire et de migration vers les organes lymphatiques[65]. Il est exprimé chez les lymphocytes T naifs, mais aussi par certaines sous populations de T mémoires[66].

f. A propos de l'efficacité de la réponse spécifique

Ainsi, la capacité de l'organisme à éliminer un pathogène dépendra du type de réponse T développée. Or, il se peut que cette réponse ne soit pas adaptée à la menace. C'est par exemple le cas de lors d'une allergie, où elle est disproportionnée à la menace. Au contraire, dans le cadre de tumeurs, le système immunitaire réagit souvent de manière limitée, car il doit lutter contre des cellules « du soi » dérégulées, qu'il ne perçoit pas nécessairement comme un danger. On peut aussi citer le cas les maladies auto-immunes qui ne sont autres qu'un dysfonctionnement du système immunitaire qui attaque les cellules de son propre organisme. Dans le cadre des maladies infectieuses également, on rencontre des cas où la réponse immunitaire développée n'est pas la

réponse adéquate. Par exemple, une tuberculose, peut induire une importante production d'anticorps, mais ces derniers n'auront qu'une efficacité limitée du fait de l'épaisseur de la paroi cellulaire du *Mycobactérium tuberculosis* ainsi que sa localisation intracellulaire[67]. Ainsi, le spectre des pathologies associées au système immunitaire est extrêmement large. C'est pourquoi, il est fondamental d'étudier et de comprendre les voies d'induction et de régulation du système immunitaire au niveau tissulaire, cellulaire et moléculaire, le but ultime étant de réguler et diriger ses réponses aux antigènes.

C. Les compartiments de l'immunité importants pour la vaccination

I. Généralités

La réponse immunitaire se joue à différents niveaux dans l'organisme. Les organes lymphoïdes primaires et secondaires sont constitués d'organes dédiés à l'immunité. Le réseau lymphatique, est quant à lui, un réseau parallèle à la circulation sanguine permettant l'élimination de protéines insolubles, mais également la circulation de cellules de l'immunité. Il communique avec les tissus ainsi que de nombreux organes lymphoïdes, notamment les ganglions lymphatiques.

Les organes lymphoïdes primaires permettent la fabrication et la différenciation de cellules du système immunitaire. Ils comprennent :

- La moelle osseuse

Il s'agit du lieu de production de la quasi-totalité des cellules immunitaires. C'est également ici que résident les plasmocytes à longue durée de vie, qui sont responsables de la production massive d'anticorps.

- Le thymus

Il assure la maturation des lymphocytes T. Cette étape cruciale les sélectionne pour ne conserver que les cellules aptes à distinguer efficacement les peptides du « soi » des peptides du « non soi ».

Les organes lymphoïdes secondaires, quant à eux, comprennent :

- Les ganglions lymphatiques

Il s'agit de zones très riches en lymphocytes naïfs, au niveau de laquelle s'effectue la présentation d'antigènes par les APCs.

- La rate

Elle est la zone d'épuration sanguine de l'organisme. Son rôle principal est l'élimination des éléments figurés du sang. Elle est toutefois considérée également comme un organe lymphoïde ayant un rôle

dans l'immunité. En effet, elle constitue également un lieu privilégié de rencontre entre antigène et lymphocytes, dont elle est abondamment pourvue.

- Formations lymphoïdes associées aux muqueuses

Il s'agit de zones riches en lymphocytes, réparties au sein des muqueuses respiratoires, du digestif (plaques de Peyer, amygdales), et urogénitales. Ces zones jouent un rôle important dans les processus immunitaires locaux, comme l'induction d'une tolérance à la flore intestinale.

Au-delà des organes lymphoïdes primaires et secondaires, le système immunitaire surveille l'intégralité de l'organisme. Il existe donc des "sentinelles" partout, d'où la possibilité d'administrer des vaccins par différentes voies.

II. Le site d'injection

Le site d'injection d'un vaccin occupe une place importante dans la mise en place de la réponse immunitaire, puisque les cellules exposées seront les premières à détecter l'antigène et à émettre un signal de danger. Cette réponse pourrait varier en fonction de la nature des cellules résidentes. En effet, les cellules immunitaires, notamment les APCs, ne sont pas réparties uniformément dans l'organisme. Ainsi certains tissus comme la peau ou les muqueuses, qui constituent des interfaces entre l'environnement extérieur et l'organisme, en sont fortement pourvues, au contraire d'autres tissus dédiés à d'autres fonction comme le muscle squelettique[68] et, dans une moindre mesure, le tissu sous-cutané. Pourtant, les voies intramusculaire (IM) et sous cutanée (SC) constituent les deux principales voies d'administration de vaccins. Cela s'explique principalement par des raisons pratiques, car les injections y sont simples à effectuer, tout en étant efficaces. Pourtant, aujourd'hui, divers essais vaccinaux mettent en évidence un effet « dose-sparing » au bénéfice de la voie d'administration intradermique (ID). En effet il suffirait dans certains cas d'une dose jusqu'à 10 fois inférieure injectée par voie ID pour induire une réponse équivalente à une vaccination classique par voie IM ou SC[69]. Malgré des intérêts économiques évidents, la voie ID est pourtant peu utilisée à ce

jour du fait d'un geste technique plus difficile à réaliser et donc moins reproductible. Ainsi, de nombreux systèmes comme patch à micro-aiguille sont en cours de développement pour tenter de pallier à ce problème[70].

a. *Voie intramusculaire*

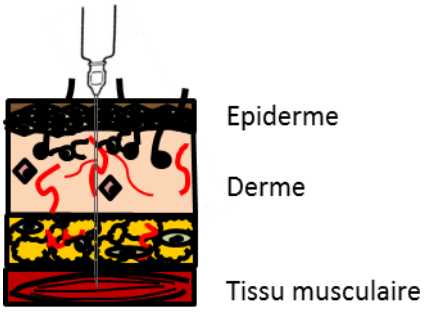

Figure 8: Voie d'administration intramusculaire

L'administration intramusculaire d'un vaccin est généralement effectuée chez l'homme au niveau du muscle deltoïde. Dans certains cas, une injection sur le muscle fessier ou le muscle vaste externe peuvent être effectuées. Comme indiqué sur le schéma, l'injection s'y effectue avec un angle de 90° entre la peau et le muscle visé. Il s'agit de la voie classiquement utilisée pour la quasi-totalité des vaccins.

Le muscle est principalement composé de fibres musculaires dédiées à la motricité de l'individu. Etant vascularisé et supporté par du tissu conjonctif, quelques cellules immunitaires comme quelque rares cellules dendritiques et des macrophages y résident à l'état basal[71]. Peu d'études se sont intéressées à la réponse immunitaire locale à un vaccin dans le tissu musculaire. Les recherches effectuées à ce sujet concernent surtout l'effet local d'adjuvants vaccinaux comme l'Alum ou le MF59, mais aussi des vaccins vivants atténués comme le MVA[72] sur des modèles murins[73,74]. Ces publications s'attardent sur la cinétique de recrutement des cellules inflammatoire dans le tissu et constituent une base de réflexion intéressante pour l'article complémentaire présenté dans cette thèse, dédiée à la réponse précoce induite au niveau du tissu musculaire.

b. *Voie sous-cutanée*

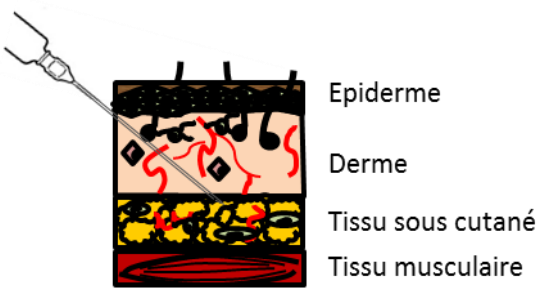

Figure 9: Voie d'administration sous cutanée

L'administration par voie sous cutanée s'effectue chez l'homme préférentiellement au niveau du bras ou au niveau de la cuisse. Pour effectuer cette injection, il faut effectuer un pli avec la peau et introduire l'aiguille de la seringue d'environ 1 cm avec un angle de 45° par rapport à la surface. Des vaccins comme ceux de la grippe, la rubéole ou la varicelle peuvent être administrés par voie sous cutanée. Ce sont généralement des vaccins de type "vivants atténués".

Le tissu sous cutané, qui correspond à du tissu adipeux, est dédié principalement au stockage de triglycérides, qui s'effectue par l'entremise des adipocytes largement représentés dans ce tissu. Cependant, ce tissu richement vascularisé est abondamment pourvu de macrophages. Il a été également décrit pour avoir certaines fonctions immunitaires avec une aptitude à produire des protéines inflammatoires et à être mis en relation avec les nœuds lymphatiques proximaux[75,76]. Il n'a cependant que très peu été étudié dans le contexte de la vaccination. Néanmoins, il s'agit d'un site d'intérêt dans les processus infectieux. En effet, il constitue entre autres un potentiel réservoir viral lors d'une infection SIV chez le primate non humain[77].

c. *Voie intradermique*

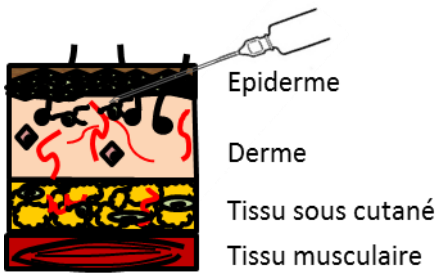

Figure 10 : Voie d'administration intradermique

La voie d'administration intradermique s'effectue classiquement par l'intermédiaire de la technique de Mantoux. Cette dernière consiste à étirer la peau puis à insérer une seringue de faible calibre en la positionnant de façon presque tangentielle à la surface de la peau de manière à administrer le liquide juste sous la couche épidermique[78]. L'apparition d'une papule blanche sous la peau est un indicateur d'une bonne administration. Cette technique nécessite une bonne expertise technique pour être bien reproductible, ce qui limite son utilisation. Le bacille de Calmette et Guérin (BCG), vaccin contre la tuberculose, est néanmoins administré par cette voie. Le premier vaccin de l'histoire, celui contre la variole, s'effectuait par scarification, une voie proche de l'intradermique bien que plus invasive[79].

La peau représente aujourd'hui un organe d'intérêt pour les immunologistes de par sa grande diversité en cellules immunitaires. Certains immunologistes n'hésitent pas à parler d'immunité cutanée[80] tant les populations immunitaires y sont riches. On y trouve ainsi à l'état basal chez l'homme des populations très hétérogènes de lymphocytes comprenant des T CD4+, des T CD8+, des T mémoires, mais également des lymphocytes plus impliqués dans l'immunité innée comme des NKT ou des Tγδ[81]. La plupart des populations lymphocytaires sont localisées dans le derme, mais la présence de lymphocytes T dans l'épiderme, notamment des T résidentes mémoires, est désormais également établie[82]. Les cellules T CD4+ sont susceptibles d'être activées localement vers un profil Th1, Th2, ou encore Th17 pour induire une réponse locale rapide[81]. Des macrophages résident également dans la peau, et dans le derme plus particulièrement. Ces derniers jouent notamment un rôle important dans l'homéostasie, la production de cytokines, ainsi que la phagocytose de cellules sénescentes[83].

Les cellules dendritiques de la peau

Chez l'homme, on dénombre de nombreuses populations de DCs. Les cellules de Langerhans sont les seules cellules dendritiques présentes dans l'épiderme à l'état basal. Elles sont caractérisées par la présence de granules de Birbeck dans leur cytoplasme, ainsi que l'expression de langerine[84]. Leur dendrites leur confèrent la capacité unique de détecter les pathogènes à la surface de la peau[85]. De ce fait, ces dernières sont confrontées à la flore cutanée, et seraient plus tolérogènes que les autres DC du derme[86]. Elles possèdent des capacités de cross-présentation[87], dont l'efficacité pourrait toutefois être discutée selon le modèle d'étude[88,89]. Comme toutes les DCs, elles possèdent également des capacités de présentation de l'antigène. Ces dernières induiraient plutôt un profil Th2[89], mais peuvent également être à l'origine d'autres type de réponse lymphocytaire selon les circonstances, comme Th17 ou Th22[90,91]. Dans le derme, on distingue au moins trois sous-populations de DCs en fonction des marqueurs exprimés à leur surface : les CD14+ DCs , CD141+ DCs, ainsi que le les CD1a+ DCs[90,92]. Ces cellules se distinguent principalement par l'expression de leurs récepteurs membranaires, mais aussi au niveau fonctionnel. Ainsi, les CD14+ DCs possèdent des caractéristiques proches des macrophages de la peau, et sont capables de produire un large panel de cytokines, notamment pro-inflammatoires[92]. Les CD14+ DCs sont également les seules DCs de la peau capables d'activer dans les ganglions des lymphocytes T follicular helper (Tfh) qui permettent la différenciation des lymphocytes B en cellules productrices d'anticorps[89]. Les CD141+ DCs sont quant à elles d'excellentes cellules cross-présentatrices d'antigène[93]. Les CD1a+ présentent des fonctions intermédiaires et ne se distinguent pas dans l'induction d'un profil lymphocytaire particulier[89].

III. Les ganglions lymphatiques drainants

Les ganglions lymphatiques sont distribués tout le long du réseau de vaisseaux lymphatiques dédié à la circulation et la patrouille de cellules immunitaires, jalonnant l'ensemble de l'organisme. C'est notamment par ces vaisseaux lymphatiques que les APCs en provenance du foyer d'infection migrent versle ganglion lymphatique drainant. Ces ganglions sont extrêmement riches en lymphocytes B et T. Et c'est au niveau de ce même ganglion qu'ont lieu la plupart des interactions APCs/lymphocytes. Durant cet échange de nombreux marqueurs membranaires sont engagés, constituant ainsi une synapse immunologique. Au cours de cette interaction, de nombreux signaux moléculaires sont également transmis entre les cellules. Ces derniers induisent la maturation des lymphocytes T et la production, à leur tour, les cytokines caractéristiques du type de la réponse immunitaire adaptative engendrée.Les ganglions constituent de ce fait des organes clés pour l'étude de la réponse immunitaire. Dans le cadre de cette thèse, on y cherchera notamment l'arrivée d'APC en provenance d'un site d'infection.

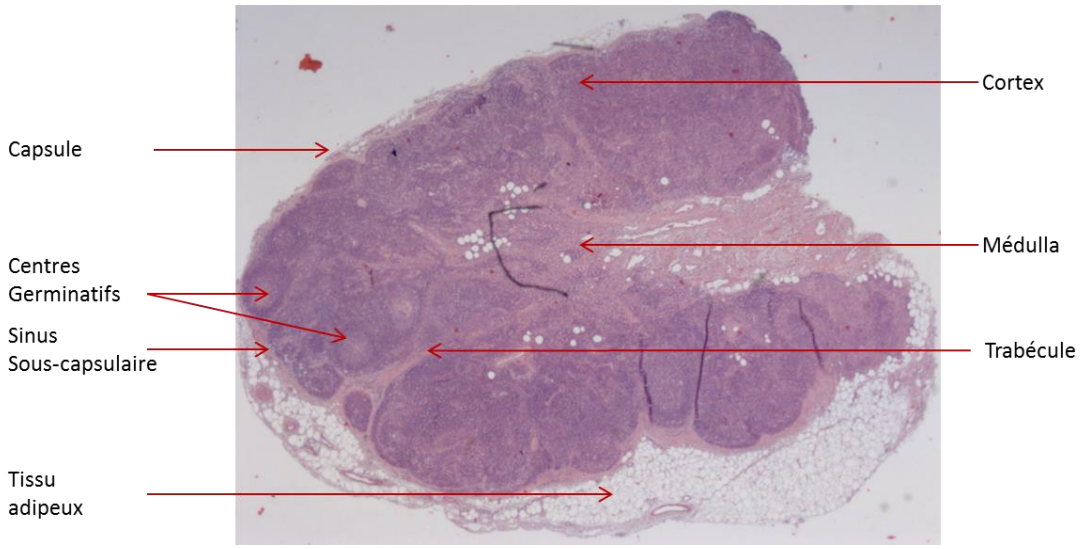

Figure 11 : Coupe transversale d'un ganglion lymphatique inguinal de primate-non-humain
Coloration hemalun, eosine

IV. Le sang périphérique

Le compartiment sanguin dispose de nombreux intérêts dans le cadre de l'évaluation d'une réponse immunitaire. Il constitue du compartiment d'étude privilégié pour évaluer si la réaction immunitaire est non pas uniquement locale, mais généralisée à tout l'organisme (systémique).

Ce compartiment représente une voie majeure de passage de cellules immunitaires. De ce fait, en cas de processus immunitaire en cours, de nombreux marqueurs de la réponse sont localisés dans le sang. C'est le cas par exemple des anticorps, mais également de certaines sous populations cellulaires particulières comme les sous populations de monocytes. On peut également considérer le sang périphérique comme un reflet de la réponse immunitaire (et mémoire) de l'organisme. Son étude donnera ainsi des indications sur les réactions immunitaires en cours dans l'organisme. Il faut cependant garder à l'esprit que ce reflet peut s'avérer imparfait et donner des informations incomplètes.

Un avantage clé du compartiment sanguin demeure son accessibilité. En effet, que ce soit pour des études pour des modèles animaux et surtout chez l'homme, il est possible d'y faire des prélèvements de sang réguliers ou en quantité suffisante pour y effectuer des analyses poussées. Du fait de cette simplicité d'utilisation, le sang périphérique constitue probablement le compartiment le plus étudié en immunologie.

D. Approche d'étude du projet de recherche

I. Objectifs de la thèse

Ces recherches ont pour but d'améliorer nos connaissances sur le fonctionnement du système immunitaire, et plus particulièrement sur l'influence des étapes précoces de la réponse à un vaccin sur la mémoire à long terme induite par cette vaccination. L'étude est réalisée dans un modèle de vaccination du macaque cynomolgus (ou *Macaca fascicularis*) par le MVA. Le macaque cynomolgus a été choisi pour sa proximité phylogénétique avec l'homme. Le MVA a été choisi d'une part comme modèle de vaccin vivant atténué et d'autre part comme modèle de vecteur recombinant. Le travail a été divisé en plusieurs étapes :

1) Caractérisation de la cinétique d'infection locale par le rMVA
2) Caractérisation de la réponse immunitaire précoce au niveau du site d'injection, des ganglions drainants et du compartiment systémique
3) Caractérisation de la réponse adaptative dans le sang
4) Associer les éléments de la réponse adaptative et ceux de la réponse innée dans le but d'identifier des biomarqueurs prédictifs de la réponse immunitaire

Cette étude s'inscrit dans une démarche globale d'acquisition de données et de construction d'algorithmes dont le but ultime est la modélisation des réponses aux vaccins chez l'homme.

II. Modèle d'étude

a. *Un modèle animal particulier, le Macaque Cynomolgus*

1. *Le modèle murin*

La plupart des grandes avancées en immunologie fondamentale ont été effectuées grâce au modèle murin. Ce modèle dispose en effet de nombreux points forts :

- Des possibilités de monitoring développées (possibilité de prélever des organes, d'effectuer des prélèvements réguliers….)

- Utilisation d'un même fond génétique, limitant la variabilité intra-espèce et augmentant la reproductibilité de l'expérimentation
- Un coût raisonnable, permettant l'utilisation d'effectifs (relativement) importants
- Une abondance d'appareils et de réactifs développés pour ce modèle
- Possibilité d' « éteindre » un gène dans des modèles de souris KO pour faire des études fonctionnelles

Il s'agit de ce fait d'un modèle d'étude indispensable. Cependant, il ne doit pas être unique pour autant. En effet, Mark M. Davis, dans une publication de 2008[94], signifie avec un brin d'humour que les chercheurs ont peut-être trop tendance à s'appuyer sur le modèle murin, à tel point d'en oublier les limites. Ainsi, de nombreux essais précliniques effectués sur des modèles murins se sont avérés peu prédictifs des réponses chez l'homme[95–97]. Une des raisons invoquées est le côté artificiel des protocoles expérimentaux pour faire développer la maladie à l'animal -souvent à l'occasion d'une ou plusieurs injection du virus/bactérie à très forte dose-, qui ne mime en aucun cas une infection naturelle[98]. De plus, les 65 millions d'années d'évolution qui séparent la souris de l'homme[99] influencent indéniablement et de manière importante le système immunitaire des deux organismes qui présentent de nombreuses hétérogénéités à tous les niveaux : expression des TLR, récepteurs exprimés par les leucocytes, types de défensines… Des tentatives sont néanmoins en cours pour permettre de corriger ces limitations. En effet, des modèles de souris dites « humanisées » se développent. Il s'agit de souris immunocompétentes dont le système immunitaire est reconstitué avec des cellules souches humaines. Cependant, certaines cellules peinent encore à être totalement immunocompétentes dans ce contexte chimérique, même si des progrès sont à noter[100,101].

2. Le modèle primate non-humain(NHP)

Le primate non-humain constitue un modèle d'étude plus adapté lorsqu'il s'agit de caractériser la réponse immunitaire à un vaccin. En effet, sa forte proximité phylogénétique avec l'homme[102] lui octroie une meilleure fiabilité. Il est de ce fait régulièrement utilisé dans le cadre d'études précliniques[97]. Il constitue en outre un excellent modèle pour étudier de nombreuses maladies

infectieuses. Outre le virus de l'immunodéficience simienne (SIV), qui infecte certains macaques comme le *macaca fascicularis* (ou macaque cynomolgus) d'une manière très similaire au HIV chez l'homme, de nombreuses similarités avec l'homme pour plusieurs pathologies incluant la coqueluche (avec le babouin notamment), Ebola, la tuberculose et bien d'autres encore ont été mises en évidence [103–106].

L'utilisation du modèle NHP permet également de nombreuses possibilités concernant le suivi de la réponse immunitaire, comme prélever un site d'injection, des ganglions lymphatiques drainants ou d'autre organes d'intérêt, ce qu'il est impossible de faire dans le cadre d'études cliniques chez l'homme. Par ailleurs du fait de leur proximité phylogénétique, de nombreux outils conçus pour fonctionner chez l'homme fonctionnent également chez le NHP par une réaction croisée. Cependant ce modèle aura certaines limitations, comme la nécessité d'avoir des techniciens experts pour maîtriser ce modèle particulier, un coût important, nécessitant souvent de travailler avec des effectifs plus modestes, ou une grande variabilité intra-espèce lié à un important polymorphisme génétique. Le NHP, et plus particulièrement le macaque cynomolgus est le modèle retenu pour cette thèse de par sa fiabilité pour l'étude des interactions immunitaires complexes et les possibilités de suivi immunologique qu'il propose.

Paramètres	*In silico*	*In vitro*	Murin	Primate non-humain	Homme
Coût	**++**	**++**	+	**-**	**+/-**
Variabilité liée au modèle	**++**	**+**	**+**	**-**	**-**
Proximité avec l'homme	**--**	**-**	**+/-**	**+**	**++**
Facilité d'utilisation	**+/-**	**+**	**+**	**+/-**	**+**
Possibilités d'immunomonitoring	**X**	**X**	**++**	**+**	**+/-**

++	Très bon
+	Bon
+/-	Moyen
-	Mauvais
--	Très mauvais
X	Non relevant

Tableau 2 : Tableau récapitulatif des avantages et inconvénients de plusieurs modèles

Il est à noter qu'il existe de nombreux autres modèles d'études que ceux cités ci-dessus qui peuvent être tout à fait valide en fonction de la question posée. Ainsi, on évoquera le cochon, par exemple, qui présente beaucoup de similarités physiologiques avec l'homme[107]. Il s'agira donc d'évaluer soigneusement les avantages et inconvénients de chacun d'entre eux pour répondre de la manière la plus adéquate possible à la problématique posée.

b. MVA : Un virus atténué dérivé de la vaccine

1. *Caractéristique générales du Vaccinia virus* (VV)

Le virus de la vaccine (VV) est un large virus enveloppé de la famille des poxviridae, du genre Orthopoxvirus. Son génome à ADN double brin linéaire, d'environ 190 kilobases (kb)codant environ 200 gènes,le classe dans le groupe I de la classification de Baltimore. Bien que son génome soit composé d'ADN, le virus de la vaccine possède la particularité de se multiplier non pas dans le noyau, mais dans le cytoplasme des cellules qu'il infecte. Par ailleurs, il a la particularité de former deux types de virions. Les premiers produits sont des virus intracellulaires matures (IMV) qui resteront dans la cellule hôte jusqu'à sa lyse, alors que les seconds, les virus extracellulaires enveloppés (EEV), sont appelés à rapidement quitter la cellule. Ces deux types de virions disposent de propriétés biologiques différentes[108].

2. *Entrée du VV dans la cellule hôte*

Peu de choses sont connues de l'entrée de l'EEV dans la cellule du fait de sa structure complexe et de sa rareté par rapport à l'IMV. On sait en revanche que la membrane des IMVs fusionne avec celle de la cellule hôte. Ce procédé met en jeu de très diverses protéines (telles que D8, A27, H3, H2 ou encore L5…) qui se lient à des glycosaminoglycanes membranaires (héparane sulfate ou chondroïtine sulfate notamment) de la cellule hôte. Certains polysaccharides faciliteraient l'entrée du virus, qui pourrait également s'effectuer via des radeaux lipidiques à la surface de la cellule[109]. Contrairement à des virus comme les HIV ou influenza, il n'y a donc pas de récepteurs spécifiques nécessaires à l'entrée des poxvirus dans la cellule.

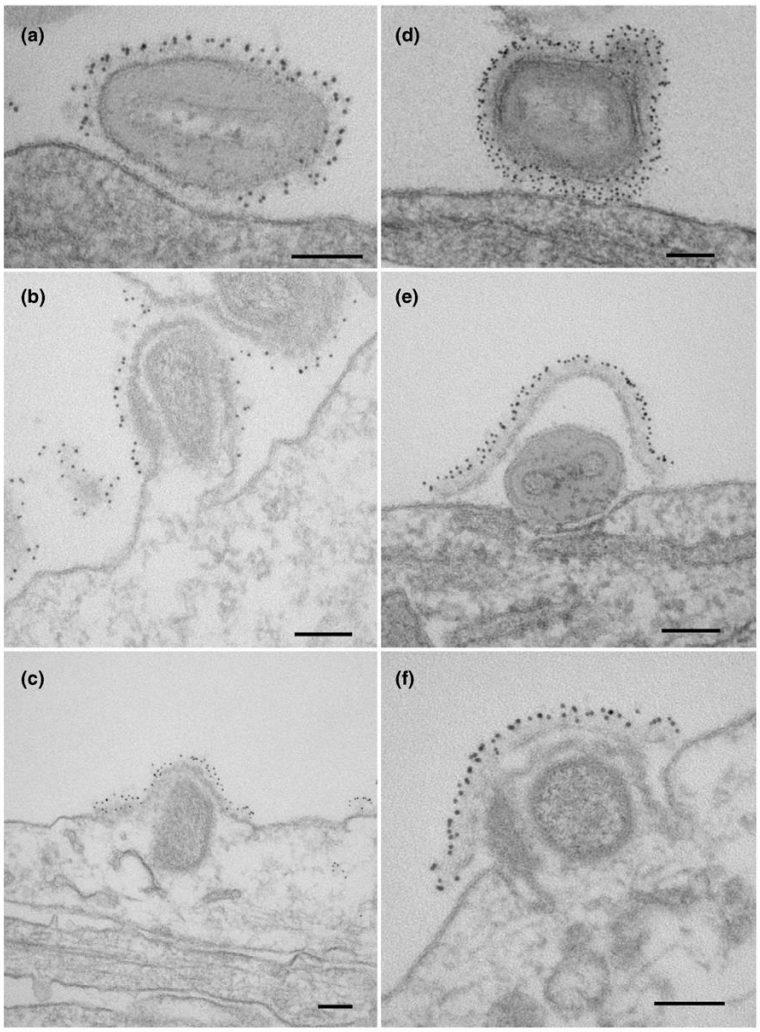

Figure 12 : Schéma d'entrée d'un vaccinia virus IMV dans une cellule hôte en microscopie électronique[108]

3. Le VV dispose de nombreux outils pour échapper au système immunitaire de l'hôte

A l'instar de nombreux autres virus, le *vaccinia virus* est particulièrement bien équipé pour échapper au système immunitaire de l'hôte. Les EEV, de par leur constitution membranaire particulière résistent par exemple mieux aux anticorps neutralisants que les IMV[110]. Ils restent également infectieux malgré l'opsonisation. Le *vaccinia virus* exprime également des protéines nommées serpines qui limitent l'activité des lymphocytes cytotoxiques en altérant la présentation antigénique à la surface du CMH I. Un large pool de protéines très diverses permet au virus de s'opposer également à de nombreuses autres production de cytokines et chémokines, ou encore en limitant l'action de la voie du complément[111].

4. *Intérêt du VV en vaccination*

Le virus de la vaccine a permis l'éradication de la variole en induisant une protection efficace durant une vie entière chez les sujets vaccinés. De plus, il possède certaines propriétés d'innocuité chez l'homme. De ce fait, le premier vaccin recombinant, développé il y a plus de trente ans, associait également le *vaccinia virus* avec un antigène de surface de l'hépatite B[112]. Ces vaccins recombinants ont dans un premier temps été développés à partir de virus entiers. Mais par la suite, de nombreuses versions atténuées - notamment des poxvirus- ont vu le jour. On y trouve des versions atténuées du virus de la vaccine comme le MVA ou le NYVAC®.

5. *Le MVA, un vecteur viral prometteur*

Le MVA est un virus vivant atténué du virus de la vaccine. Il résulte de 530 passages sur des fibroblastes d'embryons de poulet[4] de la souche Ankara du virus de la vaccine. Cela a induit une dysfonction aléatoire d'un certain nombre de gènes du virus, occasionnant six délétions majeures à l'origine d'une perte de virulence[113]. Certains gènes impliqués dans la régulation de la réponse innée nommés K1L, N1L et A52L ont également été tronqués[24]. Cela a induit des modifications concernant la réponse interféron de type I. En effet, contrairement au virus de la vaccine, le MVA n'est pas capable de contrecarrer la production d'interféron de type I de l'hôte grâce à la synthèse d'un récepteur soluble[111,114,115]. Ces réponses interféron emprunteront en revanche des voies de signalisation alternatives originales (III.c.2.).En outre, il a perdu sa capacité à se multiplier dans la plupart des cellules de mammifères[116]. Cette propriété est précieuse en vaccinologie, puisqu'elle assure que le virus ne persistera pas dans l'organisme et ne se réactivera pas. Malgré ces délétions, le MVA a conservé la plupart de ses propriétés d'immunogénicité. Mieux encore, il s'avère dans de nombreux cas encore plus immunogène que le *vaccinia virus*[117]. Il est également très bien toléré chez l'homme[118,119].

Il a également été utilisé en Allemagne comme vaccin antivariolique avec succès lors de la campagne d'éradication initiée par l'OMS[120].

Le MVA est génétiquement stable, ce qui permet sa production à grande échelle tout en conservant ses propriétés d'immunogénicité. Par ailleurs, l'importance des délétions dans son génome (31kb[113]) rend possible l'insertion de gènes de grande taille. Tous ces atouts en font un candidat idéal pour le développement de vaccins recombinants, d'autant plus qu'il n'y a pas de brevet restreignant son utilisation (contrairement au NYVAC® par exemple). De ce fait, le MVA est aujourd'hui largement utilisé dans de nombreux essais cliniques pour des vaccins contre influenza, tuberculose, Ebola, ou encore HIV[119,121–123].

6. Le choix du MVA pour cette thèse

Nous avons utilisé deux constructions différentes dans cette thèse. D'une part un MVA recombinant (TG15938) exprimant un gène codant la GFP exprimé sur le promoteur p11k7.5 (GenBank Accession Number CS054492). D'autre part un MVA recombinant exprimant les gènes codant les protéines gag, pol, et nef du HIV-B. Cette construction est utilisé conjointement par l'ensemble du Labex Vaccine Research Institute et est de ce fait actuellement utilisé dans un essai clinique de phase 1[124,125]. Ce vaccin recombinant a consisté en la fusion d'un MVA (TG17401) et une cassette d'expression sous promoteur p5HR codant un polypeptide Gag fusionné à des épitopes de protéines virales Pol et Nef du HIV-1. Ces deux constructions ont été aimablement fournies par la société Transgène®.

III. Biologie des systèmes

a. *Généralités*

La biologie des systèmes décrit les interactions, la structure, la dynamique entre toutes les parties d'un système biologique entier, dans le but de prédire son comportement[126]. Cette approche s'est développée de manière concomitante avec les progrès exponentiels des techniques de séquençage haut débit. La biologie des systèmes trouve un champ d'application important dans le domaine du vaccin, et prendra le nom de vaccinologie des systèmes. Il s'agit d'une approche interdisciplinaire alliant notamment biologie et informatique[127]. Au-delà des analyses de séquences et d'expression des gènes, cette méthode intègre et combine toutes les techniques générant dans leur ensemble un grand nombre de données. L'usage d'une telle approche, en ce qui concerne le travail présenté ici, a pour but l'indentification de biomarqueurs prédictifs de la réponse immunitaire[128] et la compréhension du fonctionnement de certains mécanismes l'immunitaires[129] induits par la réponse aux vaccins.

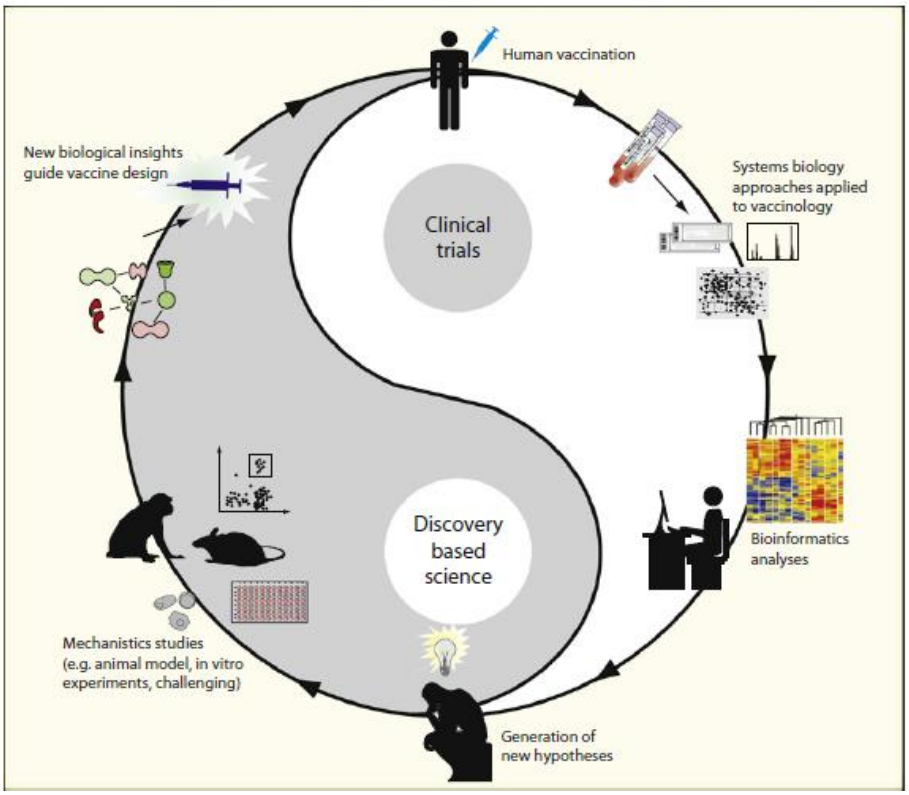

Figure 13 : Les différentes étapes d'une approche type « vaccinologie des systèmes »[130]

b. La vaccinologie des systèmes appliquée à notre problématique

Ainsi, cette thèse, qui adopte également une approche holistique, aura pour particularité de décrire tous les événements cellulaires et moléculaires induits par l'injection de notre MVA recombinant, puis d'établir les relations entre ces effecteurs afin d'évaluer leur influence sur la réponse immunitaire. En outre, évaluer dans sa globalité une réponse immunitaire *in vivo* présente l'avantage de ne négliger à priori aucune signature qui pourrait s'avérer importante dans la mise en place de l'immunité.

1. Ressources technologiques

En contrepartie, cela passe par l'utilisation de technologies avancées permettant de générer un jeu de données important souvent difficiles à appréhender dans leur ensemble. Dans notre cas il s'agira de combiner les outils suivants :

- **Histologie/Imagerie** : pour évaluer la localisation et la dynamique des cellules à l'échelle du tissu et les éventuelles lésions induites par le vaccin
- **Cytométrie en flux** : pour caractériser l'évolution des populations cellulaires dans différents compartiments
- **Cytométrie de masse** : pour caractériser finement la réponse vaccinale. Elle permet, par rapport à la cytométrie en flux, d'utiliser davantage de marqueurs
- **Luminex** : pour évaluer les principales cytokines produites dans les places fortes de l'immunité (site d'injection, ganglion drainant, sang)
- **Analyse du transcriptome** : pour mettre en évidence les principaux effecteurs moléculaires ainsi que les voies de signalisations majeures engagées dans la réponse.

2. Ressources bioinformatiques

Une bonne analyse de la réponse nécessite des ressources informatiques permettant de :

a. Développer les outils adéquats pour effectuer une première analyse des données

L'analyse des données générées par une étude transcriptomiques est ainsi grandement facilitée par l'utilisation de scripts permettant de :

- Standardiser les données
- Générer la liste des gènes différemment exprimés entre deux conditions
- Créer des figures permettant d'évaluer rapidement les similarités et dissimilarités entre deux conditions (multidimensional scale analysis[131] (MDS))

Des ressources bioinformatiques sont également indispensables pour effectuer des analyses de données de cytométrie de masse. Du fait de l'important nombre de marqueurs utilisés simultanément, ces dernières génèrent en effet trop de données pour pouvoir être exploitées pleinement avec des outils de cytométrie classique. Ainsi, on a recours à des algorithmes comme SPADE (« Spanning tree progression of density »), permettant de trier les cellules en fonction des différents marqueurs qu'elles expriment.

b. Intégrer l'ensemble des données

Cette étape complexe permet de mieux comprendre comment les effecteurs interagissent entre eux, mais également d'identifier des signatures biologiques. Elle consiste en la mise en relation des données obtenues à la fois au niveau du tissu, des cellules et des gènes. Dans le cadre de cette thèse, nous nous sommes basés sur les corrélations entre l'ensemble des marqueurs analysés pour proposer un réseau de co-expression.

Résultats

A. Article 1

Kinetics and magnitude of the inflammatory response directly drives the early steps of the adaptive responseafter MVA ID injection of the modified vaccinia virus Ankara.

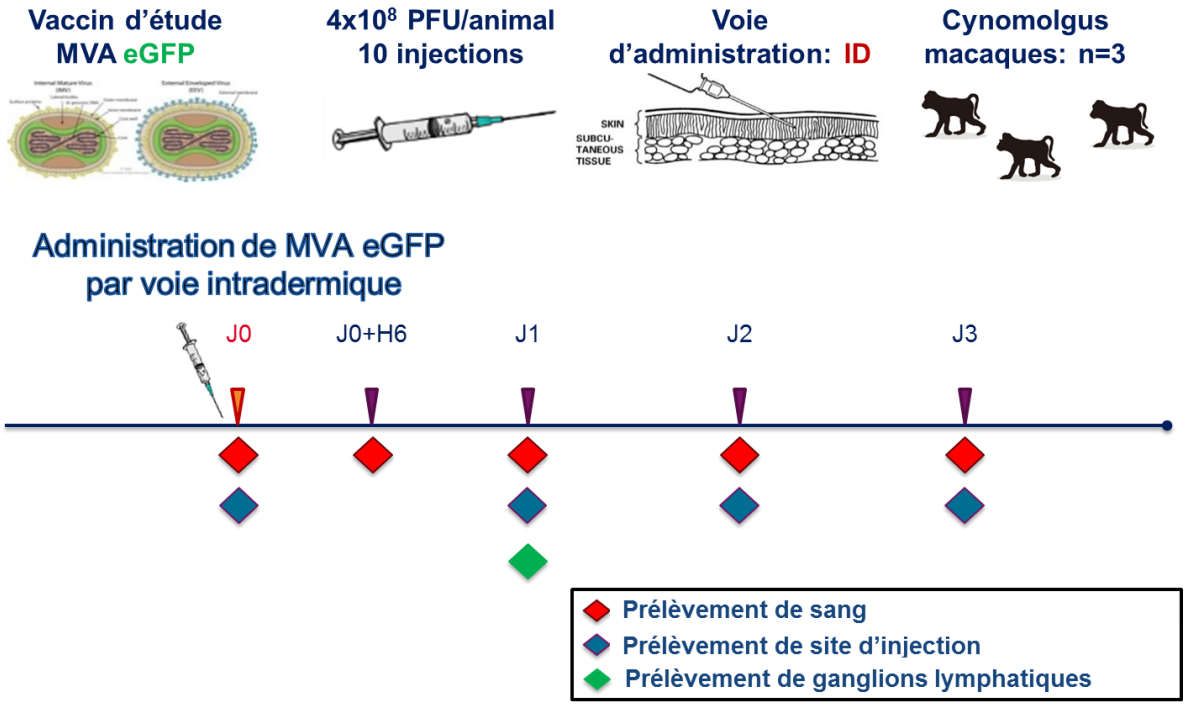

Figure 14 : Schéma expérimental du suivi de la réponse innée induite par le MVA par voie intradermique

En nous appuyant sur le schéma expérimental indiqué en **figure 14**, nous avons évalué la réponse innée induite par une MVA eGFP administré par voie intradermique sur une cinétique de 3 jours sur un groupe de trois animaux.

Dans cet article, nous étudions les cinétiques d'inflammation et d'infection induites par le MVA recombinant. Nous y montrons que le MVA est capable d'infecter la plupart des cellules de la peau, et que cette infection a lieu entre 14h et 72h post injection. Entre 24 et 48 heures, nous observons une franche réaction inflammatoire, caractérisée par un recrutement massif et transitoire de granulocytes, de macrophages ainsi que de cellules présentant un phénotype de monocytes, associée

à des signatures de cytokines pro-inflammatoires (G-CSF, IL6, IL1β, MIP1α, MIP1β, TNFα). Après 48 heures, les cytokines produites dans le microenvironnement cutané apparaissent plus diversifiées, avec l'apparition d'IL15, d'IL17 ou de TGFα. Cette réaction locale se répercute également au niveau systémique où de nombreux flux de cellules immunitaires sont observés. En effet, outre le recrutement très précoce et fugace de granulocytes, diverses sous-populations monocytaires apparaissent recrutées un peu plus tardivement (phénotypes pro-inflammatoire CD14+CD16+, mais également suppresseurs CD33+CD11b+HLADR-). En parallèle, les lymphocytes T et B ainsi que certaines cellules NK quittent transitoirement ce compartiment. L'étude des signatures moléculaires s'est inscrite en cohérence avec les observations effectuées au niveau cellulaire, en plus de mettre en évidence d'autres voies de signalisation et de régulation moins attendues (interactions cellules NK-DCs, interféron γ, IL2). La réponse innée au niveau des ganglions drainants s'est avérée moins marquée du fait d'une importante hétérogénéité. Nous proposons ensuite un réseau de co-expression illustrant l'ensemble des corrélations positives entre les effecteurs analysés et caractérisés dans le temps. Il en ressort que de nombreux effecteurs de la réponse semblent liés entre eux, parmi lesquels l'IL18 (dans les ganglions), le TNFα, le TGFα, et les CD14+MDSCs jouent un rôle central. L'ensemble de ces effecteurs semblent diriger, dès les premières heures, l'orientation de la réponse immunitaire dans le ganglion drainant.

Cette étude propose ainsi une analyse particulièrement poussée des dynamiques d'inflammation et d'infection induites par le MVA dans un modèle *in vivo* pertinent. En effet, la multiplicité des compartiments d'études (peau, sang et ganglions lymphatiques), à différents échelles (tissu, cellules, cytokines, signatures moléculaires) suivant une cinétique permet d'atteindre un niveau de détail jusqu'ici rarement atteint. L'utilisation d'une approche intégrative originale a permis en outre de tirer parti de cette analyse fine afin de non seulement illustrer la complexité de la réponse innée, mais également de générer des hypothèses sur le rôle de certains effecteurs potentiellement cruciaux susceptibles d'impacter l'élaboration des premières étapes de la réponse acquise au niveau du ganglion drainant.

Multiple cellular and molecular entitiesof the early inflammatory response are involved in the modulation of the first steps of the adaptive response after a recombinant MVA vaccine injection

Pierre Rosenbaum[1,4], Nicolas Tchitchek[1,4], Mélanie Rathaux[1,4], Lev Stimmer[2,3], Hakim Hocini[4,5], Yves Levy[4,5], Catherine Chapon[1,4], Roger Le Grand[1,4], and Frédéric Martinon[1,4,†]

[1]CEA – Université Paris Sud 11 – INSERM U1184, Immunology of viral infections and autoimmune diseases, 92265 Fontenay-aux-Roses, France

[2]CEA – INSERM, MIRCen, UMS27, 92265 Fontenay-aux-Roses, France

[3]INSERM, U1169, 94270 Kremlin-Bicêtre, France

[4]Vaccine Research Institute, Henri Mondor Hospital, 94010 Créteil, France

[5]INSERM, U955, Team 16, Clinical and Infectious Diseases Department, Hospital Henri Mondor, University of Paris East, 94010 Créteil, France

[†]**Corresponding author**

Correspondence should be addressed to: Frédéric Martinon, CEA, 18 Route du Panorama, 92265 Fontenay-aux-Roses, France (frederic.martinon@cea.fr).

Short title: Early response to rMVA vaccine

Abstract

The early immune response induced by a vaccine may be crucial for its efficacy. To better understand it, we deciphered dynamics of infection and kinetics of inflammation from 0h to 72h induced after intradermal administration of a modified vaccinia virus Ankara (MVA) based vaccine in a non-human primate (NHP) model. We investigated three key localizations: the site of injection, the blood and the draining lymph node. Inspired by system vaccinology approaches, a wide set of techniques involving histology, *ex vivo* and *in vivo* imaging, flow cytometry, Luminex and transcriptomic assay covering macroscopic to molecular immune events. Using this rich and heterogenic dataset, we then designed a coexpression network -based on significant correlations over the time between studied effectors- dedicated to identify major interactions and key effectors of this immune response.

MVA was able to infect a wide set of skin cells from 14h to 72h post intradermal injection. The vaccine also induced a strong local inflammatory response. Indeed, we highlighted an important granulocytes and macrophages recruitment associated with pro-inflammatory cytokines releasing such as GM-CSF, IL6, IL1β, MIP1α, MIP1βor TNFα between 24h and 48h p.i, but more diverse at 72h (IL2, TGFα, IL15 but also G-CSF). MVA injection also impacted the systemic compartment, withan early increase of$CD66^{high}$granulocytes, CD14+CD16+ monocytes and possibly CD14+MDSCs-like cellsassociated with IL6 and IL1ra releasing. Draining lymph node activation appeared however less clearly. Finally, the coexpression network highlighted a hub of correlation between local and lymph node cytokine productions. Altogether, this study provided some insights to better understand the innate immune response process triggered by MVA, characterizing the innate response in the deep details. Then, the use of an innovative integrative approach highlighted the complexity and the multiplicity of this response, but also several key innate effectors –such as TNFα, TGFα, or CD14+MDSCs- susceptible to interfere in the first steps of the adaptive response in the draining lymph node.

Introduction

Vaccination is one of the most efficient strategy to fight against infectious diseases, but nowadays, it faces a lot of hurdles. Indeed, no vaccine is available for major threats like AIDS, tuberculosis or Ebola. In addition, many existing vaccines may benefit from improvement in duration, breadth of efficacy, reactogenicity or delivery. Vaccines innovation would be favored by an increased understanding of basic immune mechanisms associated with vaccination immune processes. Recently, improvements have been made in pathogen sensing of key cell effectors such as dendritic cells through pattern recognition receptors (PRR)[126,127], and also at the characterization of the interplay between innate and adaptive immunity using molecular signatures obtained through emergent omic technologies which may contribute to the elaboration of predictive models of vaccines' efficacy and safety [121,122,128]. However, most of this knowledge have been generated using *in vitro* and rodent models [129–131] and little is known on the very early events driving the vaccine response *in vivo* in humans and its relevant animal models like non-human primate models [67,132–136].

Early molecular and cellular changes at site of vaccine injection largely contribute to the quality of vaccine response. Deciphering the associated mechanisms may help the identification of novel approaches to better modulate the type, breadth and duration of induced immunity. Skin represents a promising target for vaccine injection due to the diversity of resident and recruited immune cells, including macrophages, epidermal Langerhans cellsmultiple subsets of dermal dendritic cells (DCs) [84,86] expressing a wide set ofPRRs[26,137] which can be used to tune vaccine immune profiles [138]. In addition, as the results of the efficiency of local antigen presenting cells, intradermal route vaccination may contribute to dose sparing, which could represent a decisive advantage for products with scale up production constrains [63,66,139,140].

Here we aimed at the characterization of the immune response induced by intradermal injection of the modified vaccinia virus Ankara (MVA) [141]. This attenuated vaccinia virus was safely used as a Smallpox vaccine in humans [142] and represents today a promising vector for recombinant vaccines

expressing HIV, malaria, hepatitis C virus, mycobacteria or Ebola antigens [143–146]. The use of NHP model was guided here by the phylogenetic proximity withhumans resulting in similarities in their immune system and highly predicting vaccine response in humans [96,147]. We studied in NHP the dynamics of responses to skin injection of a recombinant MVA (rMVA) combining *in vivo* imaging technologies with detailed analysis of cell recruitment and circulation, cytokine production changes at site of vaccine injection as well as in blood and draining lymph node, in addition to transcriptome changes in the blood and draining lymph nodes

Materials and Methods

Ethics statement

Adult males cynomolgus macaques (*Macaca fascicularis*), each weighing between 4 to 6 kg, and imported from Mauritius, were housed in the CEA animal facilities of Fontenay-aux-Roses (France). Macaques were handled in accordance with national regulations (Alternatives Permit Number A 92-32-02), in compliance with Standards for Human Care and Use of Laboratory of the Office for Laboratory Animal Welfare under Office for Laboratory Animal Welfare Assurance number A5826-01, and the European Directive (2010/63, recommendation N°9). This project received the government authorization Number 12-013.

Regular follow-up of the animals (clinical examination, temperature, weight) was performed during the duration of the study. Interventions were performed by veterinarians and staff of the "Animal Science and Welfare" core facility of IDMIT infrastructure at CEA (http://www.idmitcenter.fr/fr/). Vaccine injections, confocal endomicroscopy *in vivo* imaging, tissue biopsies and blood samples were performed after sedation with chlorhydrate ketamin (10 mg/kg, Imalgen®, Rhone-Mérieux, Lyon, France).

Intradermal immunization

Prior to injection, the skin was shaved and cleaned with ethanol 70%. Sites of injection dedicated to imaging were tape stripped. Each animal received simultaneously a total of 10 intradermal injections containing each $4x10^7$ PFU in 200µL of a rMVA expressing eGFP (MVATGN33.1 Transgene SA, Illkirch-Graffenstaden, France) equally divided into two areas: (i) 5 to 10 cm from the left inguinal lymph node area; and (ii) on the top left of the back. A dotted line was drawn around the site with a felt pen in order to later identify the site of injection at biopsy.

Tissue and blood samples

Prior to biopsies, the skin and inguinal area were cleaned with povidone iodate solution (Vetedine®, Vetoquinol SA, Lure, France). Biopsies sized 8mm in diameter and were processed in untreated skin as control or in treated skin at 24h, 48h and 72h after the injections. The inguinal lymph node directly draining the rMVA injected skin was gathered 24h p.i.. Inguinal lymph node of the contralateral site also collected at 24 p.i. was sampled and used to compare to the vaccine site draining lymph node. Blood was collected into K3-EDTA tubes (Greiner Bio-One, Frickenhausen, Germany) for cell blood counting (HmX;Beckman Coulter), plasma collection and flow cytometry. Plasma for cytokine analysis was collected after 10 minutes and 2,000g centrifugation. A volume of 500µL of blood collected in lithium heparin (Vacutainer BD) was mixed with 1mL tempus RNA tube (Thermofischer Scientific, Waltham,MA, USA), for transcriptomic analysis. Tissue biopsies dedicated to transcriptomics were preserved in 1 mL RNA later solution (Qiagen, Hilden, Germany) at 4°C overnight and then stored at -20°C.

Extraction of cells from tissue biopsies

Tissues were cleaned with 70% ethanol solution and fat tissue was removed. Total skin (epidermis and dermis) and lymph node biopsies were then washed with PBS, weighed, cut in small pieces and finally digested at 37°C under agitation (80rpm) during 60 and 15 minutes respectively using 2mL of a solution containing DMEM (Thermofischer Scientific), 5% FCS (Lonza, Basel, Switzerland), 1% Penicillin Streptomycin Neomycin (Thermofischer Scientific), 10mM Hepes (Thermofischer Scientific), 2mg/mL collagenase D (Roche) and 0.02 mg/mL DNAse I (Roche, Basel, Switzerland). Tissue was then filtered using 70µm cell strainer and centrifuged. The supernatant was collected for the tissue cytokine analysis. Tissue leftover was shredded with GentleMACs® dissociator (Miltenyi Biotec, Paris, France). The cell suspension was then washed with PBS and then stained for flow cytometry analysis. Flow cytometry was performed on cells extracted from one single skin biopsy or one single lymph node.

Flow cytometry in tissue cells

All the steps of the staining were processed at 4°C. Cell suspensions were first stained with viability dye LiveDead® (Thermofischer Scientific) for 15 minutes, then washed with PBS. Fc receptors were blocked by using PBS supplemented with 5% macaque serum during 20 minutes. Skin cell suspensions were stained during 30 minutes with 90µL of mix of antibodies diluted in BD Horizon Brilliant® Stain Buffer (BD) containing CD1a (DAKO, Glostrup, Denmark, Clone O10) extemporaneously coupled with Zenon IgG1 AF700 (Thermofischer Scientific), HLA-DR (BD Biosciences, Franklin Lakes, NJ, USA, clone G46-6), CD163 (BD, clone GHI/61), CD11c (Biolegend, San Diego CA, USA clone 3.9), CD45(BD, clone DO58-1283), CD66 (Miltenyi Biotec, clone TET2), CD3 (BD, clone SP34-2), CD20 (BD, clone 2H7), CD11b (Beckman Coulter, Brea, CA,USA, clone Bear 1), CD16 (Beckman Coulter, 3G8) and NKG2a (Beckman Coulter, clone Z199). Cells were then washed twice using PBS and fixed using 150µL BD Cellfix® (BD). Lymph node cell suspensions were stained during 30 minutes with 90µL of mix of antibodies diluted in BD Horizon Brilliant® Stain Buffer (BD) HLA-DR (BD Biosciences, Franklin Lakes, NJ, USA, clone G46-6), CD163 (BD, clone GHI/61), CD11c (Biolegend, San Diega, CA, USA clone 3.9), CD123 (BD, Clone 7G3), CD66 (Miltenyi Biotec, clone TET2), CD3 (BD, clone SP34-2),CD20 (BD, clone 2H7), CD11b (Beckman Coulter, Brea, CA,USA, clone Bear 1), CD16 (Beckman Coulter, 3G8) and NKG2a (Beckman Coulter, clone Z199). Cells were then washed twice using PBS and fixed in 150µL of BD Cellfix® (BD).

Flow cytometry on whole blood cells

100µL of blood was immediately stained for 30 minutes with 90µL of antibodies mix diluted in BD Horizon® stained buffer (BD) containing anti-CD123 (BD, Clone 7G3), anti-HLA-DR (BD Biosciences,Franklin Lakes, NJ, USA, clone G46-6), anti-CD163 (BD, clone GHI/61), anti-CD11c (Biolegend, San Diego, CA, USA clone 3.9), anti-CD45 (BD, clone DO58-1283), anti-CD66 (Miltenyi Biotec, clone TET2), anti-CD3 (BD, clone SP34-2), anti-CD20 (BD, clone 2H7), anti-CD8 (BD, clone RPA-T8), anti-CD11b (Beckman Coulter, Brea, CA,USA, clone Bear 1), anti-CD14 (BD, Clone M5E2), anti-

CD33 (Miltenyi, Clone AC104.3E3), anti-CD16 (Beckman Coulter, 3G8) and anti-NKG2a (Beckman Coulter, clone Z199), and cells were then fixed and red blood cells removed with 1 mL of BD FACs Lysing® (BD) during 10 minutes at room temperature and washed twice using PBS. The design of cytometry panel and rational for gating strategies were mostly based upon our previous work [148]. For the analysis of skin and lymph node cell suspensions, we divided the number of events in each cell population by the initial weigh of the digested biopsy. This choice was done in order not to miss minor cell movement that could have been outshined by the massive inflammatory cell recruitments. Similarly, to keep absolute values in the blood, we reported our flow cytometry data to complete blood counts to obtaining a number of cells per mL or liter.

Flow cytometry gating strategy for skin cells

The flow cytometry gating strategy of skincells is shown in Supplementary Figure 1.A. After doublet and debris exclusion, living cells were selected, and then CD45+ leukocytes discriminated from non-leukocytes. Among CD45+ cells, granulocytes were first discriminated using CD66+ and SSC-A+ markers. Among CD45+ CD66- cells, lymphocytes were regrouped as lineage CD3+ of CD20+ cells (LinCD3CD20). Macrophages were identified as CD45+, LinCD3CD20-, CD66-, CD11b+ and CD163+ cells. The CD45+, Lin (CD3, CD20)-, CD163-, CD66-, HLADR+, CD11b+ cells were considered as cells coming from blood monocytes due to their close phenotype and were thus called monocytoid cells. Natural killer (NK) cells were defined as expressing the following phenotype: CD45+, CD66-, LinCD3CD20-, CD11b-, NKG2a+. Cells expressing CD45+, CD66-, LinCD3CD20-, CD11b-, NKG2a-, HLADR+ and CD11c+ were considered as dendritic cells. Cells showing no expression in our markers panel but CD45 were named “other leukocytes”.

Gating strategy of blood cells by flow cytometry

The flow cytometry gating strategy of bloodcells is shown in Supplementary Figure 1.B. To optimize this panel, we used both NKG2a and CD33 markers on the same fluorophore. We showed on

histograms that those markers are not staining the same cell populations and are thus exclusive (**Fig.1D**). We confirmed indeed that NKG2a but not CD33 is expressed on cells gated as NK cells. Some CD16- NK cells also express NKG2A. Similarly, we showed that CD33 but not NKG2a is expressed on cells defined as myeloid dendritic suppressor cells (MDSC) derived from monocyte and dendritic cell subsets. As a result, we discriminated cell populations described below accordingly. Likewise, the skin analysis, doublets and debris were excluded. Then, SSC-A+CD66+ cells were considered as granulocytes. We surmised that most of them were polymorphonyclear neutrophils (PMN) as their recruitment kinetic fits with PMN complete blood count. However, we cannot rule out the presence of subpar populations of eosinophils and basophils. Lymphocytes were gated as LinCD3CD20+ cells; CD16+NKG2a+ NK cells as LinCD3CD20-, CD16+ and NKG2a+. Three main subtypes of monocytes were discriminated using CD14 and CD16 markers [149] as follows: CD14+CD16- monocytes, classical monocytes as LinCD3CD20-, CD14+ and CD16- and HLADR+ cells. CD14-CD16+ as LinCD3CD20-, CD14- and CD16+ cells; CD14+CD16+ monocytes as LinCD3CD20-, CD14+ and CD16+. pDCs were gated on their LinCD3CD20-, CD14-, CD16-, HLADR+ and CD123+ expression. Cells showing LinCD3CD20-, CD14-, CD16-, $HLADR^{mid}$ and CD123+ expression were considered as remaining basophils. The use of the CD33 marker led us to discriminate other dendritic cell subsets as follows: LinCD3CD20-, CD14-, CD16-, HLADR+, CD123- and CD33- cells are showing unique phenotype and were thus considered as CD33- DCs; The LinCD3, CD20-, CD14-, CD16-, HLADR+, CD123- and CD33+ were identified as conventional CD33+DCs; and LinCD3CD20-, CD14-, CD16-, HLADR+, CD123-, CD11b+ and CD33+ were identified as CD14low monocytes with similar phenotypes as classical monocytes with the only difference in the low expression of CD14. In accordance with literature[150], MDSCs were also identified as follows: LinCD3CD20-, CD14-, CD16-, HLADR-, CD123-, $CD66^{low}$, CD11b+, and most likely CD33+ for granulocytes derived MDSCs and LinCD3CD20-, CD14-, HLADR-, CD11b+, CD33+ for monocytes derived MDSCs. Other remaining HLADR- subpopulations were then discriminated as follows: LinCD3CD20-, CD14-, CD16-, HLADR-, CD123-, $CD11b^{low}$, $CD66^{low}$ as $CD66^{low}$ granulocytes escaping from the initial gating of granulocytes; LinCD3CD20-, CD14-, CD16-, HLADR-,

CD123-, CD66-, (CD33, NKG2a)+, considered as CD16-NKG2a+ NK cells; and cells expressing no markers in our panel were named “other cells”.

Gating strategy of lymph node cells by flow cytometry

The flow cytometry gating strategy of lymph node cells is shown in Supplementary Figure 1.C. After excluding doublets, debris and selecting living cells, lymphocytes were gated on their LinCD3CD20+ expression and then gated between B and T subtype using HLADR , being positive for B lymphocytes and negative for T lymphocytes. Then granulocytes were gated on LinCD3CD20-, CD11b+ and CD66+ expression; classical NK cells were identified as LinCD3CD20-, CD66-, CD16+ and NKG2a+, whereas another subpopulation considered as CD16- NK cells were identified as LinCD3CD20-, CD66-, CD16- and NKG2a+. Macrophages were distinguished with their expression of LinCD3CD20-, CD66-, NKG2a-, CD11b+ and CD163+. Three dendritic cell populations were then identified as follows: pDCs as linCD3CD20-, CD66-, NKG2a-,CD11b-, CD163- HLADR+ and CD123+; CD1a+ dendritic cells as CD66-, NKG2a-, CD11b-, CD163-, HLADR+, CD123-, CD1a+; and finally CD11c+ dendritic cells as linCD3CD20-, NKG2a-, CD66-, CD11b-, CD163-, HLADR+, CD123-, CD1a- and CD11c+; Remaining cells expressing no markers in our panel were called “other cells”.

Time-lapse confocal videomicroscopy of early kinetics of MVA infection in the skin

Simultaneously to rMVA-eGFP injection, 10µg of HLADR AF700 (Bioloegend) diluted in PBS was injected through intradermal route 4h prior biopsies at each site of injection dedicated to confocal videomicroscopy. After fat tissue removal, skin biopsies were imaged during 18h accordingly with our previously reported work [151]. Numbers of GFP+ cells and HLADR+ cells were calculated using Volocity software® (PerkinElmer, Coventry, England), after applying a fine filter and then excluding objects below 200µm^3 and above 4,000µm^3.

Confocal endomicroscopy for rMVA visualization in the skin of living animals

In vivo confocal endomicroscopy was performed with a fibered confocal fluorescence microscope (Cellvizio®, Mauna Kea Technologies®, Paris, France). A probe recording green fluorescence signal sweeping the site of interest was applied two times during approximately 30 seconds. GFP+ objects were counted in each frame (size>20µm²) using ImageJ software®[152]. For each observed site, the analysis was performed on the 50 frames containing the highest number of GFP+ objects. For each timepoints, the number of fluorescent cells of up to three sites of injection was measured. The mean±SD of GFP+ cells was calculated taking into account all the sites analyzed.

Histopathology

Skin or lymph node samples were fixed at 4°C using 4% paraformaldehyde during 24h. Samples were preserved in PBS condition at 4°C. Paraffin inclusion was made using an automaton successively replacing PBS with alcohol, xylene and paraffin. Tissue was cut afterward using microtome and set on slides. Hemalun Eosin coloration was then made using an automaton Microm HMS740 (Thermofischer Scientific), alternating xylene, alcohol, Hematoxylin (Labonord, Templemars, France), Eosin (VWR international, Fontenay-sous-Bois, France) baths.

Immunohistochemistry

Prior to staining, 3µm slides were incubated at 37°C overnight. Paraffine was removed by washing slides with increasing concentrations of xylene (VWR), then ethanol (VWR), and water using an automaton Microm HMS740. Unmask procedure was performed using citrate tempus (Diagnostic Biosystems, Pleasanton, CA, USA) in a 95°C bath during 20 minutes. Peroxidase blocking was then performed using 3 % dihydrogenated water 10 minutes (Sigma Aldrich, Saint-Louis, MO, USA). Saturation using normal horse serum (Vectorlaboratories, Burlingame, CA, USA) 10%, BSA (Sigma Aldrich) 5%, PBS was performed during 30 minutes. Primary staining with anti-GFP antibody (7.5µg per slide) in saturation solution, (Abcam, Cambridge, UK) were then performed for 1 hour 30

minutes. Secondary antibody staining using biotinylated anti chicken IgG (Abcam) 1/200 in PBS was then applied for 30 minutes. Then an ABC Complex using Vectastain ABC Kit standard Elite (Vector) and then diaminobenzidin (Vector) were performed following manufacturer's recommendations for respectively 30 minutes and 5 minutes. Then slides were put in water bath to be colored using HMS740 automaton with successive bath hematoxylin**,** water, increasing concentrations of ethanol and xylene. Washing using bath of PBS three times five minute were performed between each step of the procedure.

Local and systemic cytokine releasing analysis

Supernatant of digestion medium of lymph node and skin and plasma recuperated were conservedat -80°C prior to their use. These samples were then titrated with a 23-plex MAP NHP Immunoassay kit PCYTMG-40K-PX23® (Millipore, Billerica, MA, USA) according to supplier instructionsand measuring the concentrations of following cytokines: G-CSF, GM-CSF, IFN-Y, IL-1ra, IL-1b, IL-2, IL-4, IL-5, IL-6, IL-8, IL10, IL-12/23(p40); IL-13, IL-15, IL-17, IL-18, MCP-1, MIP-1α, MIP-1β, sCD40L, TGFα, TNFα and VEGF.

RNA isolation and microarray profiles

Biopsies were immediately immersed into RLT-beta-mercaptoethanol 1/100 lysis buffer (Qiagen, Courtaboeuf Cedex, France). Samples were then disrupted and homogenized using a TissueLyser LT (Qiagen, Courtaboeuf Cedex, France) and RNA purified on Qiagen RNeasy Micro Kit. Whole blood RNA was recovered in tempus tubes (ThermoFisher scientific) and RNA purified using *Tempus*™ Spin RNA Isolation*Kit* (ThermoFisher scientific). For both purifications, contaminant DNA was removed using RNA Cleanup step of RNeasy Micro Kit. Purified RNA was then quantified using a ND-8000 spectrophotometer (NanoDrop Technologies, Fisher Scientific, Illkirch Cedex, France) before being checked for integrity on a 2100 BioAnalyzer (Agilent Technologies, Massy Cedex, France). cDNA was synthesized and biotin-labelled using Ambion Illumina TotalPrep RNA Amplification Kits (Applied

Biosystem/Ambion, Saint-Aubin, France). Labeled cRNA were hybridized on Illumina Human HT-12V4 BeadChips. All steps were done following the manufacturers' protocols. Raw and normalized microarray data have been deposited in the ArrayExpress database [153] under an accession number XXX.

Statistical analysis and graphical representations

Cytometry, Luminex and transcriptomic data were analyzed using R [154]. Hierarchical clustering was performed based on the Euclidean metric and using the Ward linkage method. Flow cytometry and Luminex measurements have been scaled in the heatmaps representations in order to have the same minimal and maximal expression values. Differentially expressed genes were identified using paired Student t-test (q-value<0.01) and based on a fold-change threshold of 1.2. Multidimensional scaling representations were generated using the SVD-MDS algorithm [125]. Multidimensional scaling methods aim to represent the similarities between high-dimensional objects, generally in a 2- or 3-dimensions. The Kruskal Stress [155] indicated at the bottom of the representation quantifies the quality of the MDS as the fraction of information lost during the dimensionality reduction process. Functional enrichment analysis of the different lists of differentially expressed genes was performed using Ingenuity Pathway Analysis software (IPA®, Qiagen, http://www.qiagen.com/ingenuity). Upstream regulators having a q-value<10^{-3} and belonging to cytokine signaling, humoral immune response or pathogen influenced signaling categories were represented at the exception of FSH, LH and prolactin regulators. Canonical pathways having a q-value<10^{-3} and belonging to cellular immune response, cytokine signaling, humoral immune response and pathogen influenced signaling categories were represented. Statistical analysis for flow cytometry and Luminex data were performed using Prism 6.0® (Graphpad Software Inc., La Jolla, CA, USA). Two-sided Friedman tests followed by a Dunn's post-test comparing each timepoint with the baseline were performed. This significance calculated using Friedman's test highlights a cell population or cytokine movement over the kinetics, but the precise timepoint of recruitment could only have been assessed or partially

evaluated using Dunn's post-test to the limited sample size. Significant correlations between Luminex, and cytometry variables were identified using the Pearson coefficient of correlation based on a correlation threshold of 0.80 and a q-value threshold of 0.05. Representation of the co-expression network was performed using Cytoscape® [156].

Results

Kinetics of skin cells rMVA infection

Mantoux intradermal injection of $4x10^7$ PFU in 200µL of eGFP-rMVA induce a local inflammatory lesion limited to the site of injection, detected as early as 24h (**Fig. 1A**),and progressively turning into a blister 72h post injection (p.i.)**.** Epidermis thickness increases by 24h p.i., with limited parakeratosis followed by mild parakeratosis 48h p.i. and epidermal cells necrosis at 72h p.i. (**Fig. 1B**). In the dermis, edema associated to moderate perivascular neutrophilic and macrophage infiltration is observed from 24h to 72h p.i.. The interface between the lower dermis and the hypodermis is the siege of a severe and massive neutrophilic and macrophage infiltration associated with necrosis. The rMVA expressed eGFP was tracked in skin cells by repeatedly *in vivo* imaging (**Fig.2A**) using non-invasive Cellvizio® confocal endomicroscopy. This technology allows both, detection of infected cells expressing the eGFP and detection of cells capturing eGFP produced in the skin. Data at early time points shows that the injected viral particles do not contain eGFP, at least in sufficient amount to be detected by our microscopy approach, demonstrating that an *in vivo* infection step is required. Expression of eGFP was detected as for 24h p.i., peaking at 48h (mean±SD, 56.2±59.3 cells.mm^{-2}) and persisted at high level until day 3 (22.8±24.7 cells.mm^{-2}). Signal disappeared by day 7 (**Fig. 2B**). Time-lapse confocal microscopy performed on a skin biopsy collected 4h after *in vivo* injection of the rMVA and maintained in culture until 22h p.i. (**Fig. 2C**), confirms this kinetics, with first eGFP signal detected by 13-15h p.i. and reaching maximum by 18-22h (**Fig. 2D**). Interestingly, some but not all eGFP+ cells also express HLA-DR indicating that both, antigen presenting cells (APC) and non-APC have been targeted by the vaccine. *In situ* analysis reveals the heterogeneous morphology of eGFP+ cells which include dendritic cells, macrophages, adipocytes and granulocytes (**Fig. 3**). The majority of these cells are localized in vascularized areas, such as the papillary-reticular dermis interface and the hypodermis layer. Interestingly, no eGFP producing cells were detected in the epidermis. Altogether, we evaluated the kinetics of local infection of rMVA after an intradermal immunization in NHP between 13-15h to 72h p.i.

Diversity of skin cells containing vaccine antigens

To further characterize the phenotype of skin cells positive for eGFP, flow cytometry was performed on cell suspensions obtained from whole injection site of one single biopsy, including epidermis and dermis, and collected at different time points following eGFP-rMVA injection (**Fig. 4-5 & Fig. S1**). Locally recruited cells mainly includes inflammatory myeloid cells with values peaking at 24-48h p.i. (**Fig. 4A**) with statistically significant increased numbersof macrophages, granulocytes and monocytoid cells (Friedman test;*p-value*<0.05). Confirming above observations using *in vivo* and *ex vivo* microscopy, cells containing locally produced eGFP reached a peak between 24h (25.8±4.95% of total living cells) and 48h (19.5±3.1%) post injection, and persist at 72h (6.4±5.9%), to completely disappear by 168h (**Fig. S1**). The rMVA exhibits an important pleiotropism (**Fig. 5A & Fig.5B**) confirming *in vivo* in the primate model, previously reported observations [157,158]. Leukocytes, granulocytes, monocyte/macrophages and lymphocytes represent the major targeted population with proportions of infected cells in the considered population ranging from 6% to more than 40%. Infection of myeloid cells (granulocytes, monocyte/macrophages and dendritic cells) seems to occur at early time points (24h p.i.) whereas lymphocytes and other non-leukocyte stroma cells appeared to reach a maximum at 72h and 48h, respectively. Interestingly, since granulocytes and PMN in particular, represent the vast majority of locally recruited cells, it also represents by far the predominant population containing eGFP antigen when reported to number of cells per gram of tissue (**Fig. 5C**). We may therefore surmise that this population will significantly impact on the mechanisms of vaccine specific response installation. Interestingly, DC which are major resident sentinels in the skin are not highly positive for eGFP in proportion and do not represent a major eGFP+ population in number questioning their respective role in rMVA vaccination process. In addition to infect almost all cell types we identified on the skin, rMVA has been shown being very immunogenic, significantly recruiting monocytoid cells, granulocytes and macrophages to the site of injection. Likewise all this study, the significance was calculated using Friedman's test highlights a cell

population movement over the kinetics, but the precise timepoint of recruitment could only have been assessed or partially evaluated using Dunn's post-test to the limited sample size.

Skin rMVA injection induces strong local production of innate and adaptive mediators

As expected, recruitment of inflammatory cells at site on injection is associated with local release of inflammatory related cytokines and chemokines we measured in supernatant of digested biopsies (**Fig. 4B**). A first group of pro-inflammatory molecules, including GM-CSF, IL1-β, IL-6, MIP1α, MIP1β and TNFα, is significantly increased (Friedman test;*p-value*<0.05) as early as 24h p.i. (no earlier time points were tested), but then rapidly decrease to baselines levels by 72h. This early increase is associated to second group of inflammatory cytokines clustering together and which includes MCP1, IL-12/23(p40), IL-8, IL-18 and G-CSF, which however persist a high levels at 72h (no later time points were tested). These molecules certainly reflect macrophages and PMN activity mainly. As part as the inflammation process, we also observed in these groups an increase of angiogenic factors TGFα and VEGF. Also this cluster includes anti-inflammatory mediators like IL-10 and IL-1ra which prolonged expression is expected. Finally, cytokines related to adaptive response, including IL-2 and IL-13 are also detected in this cluster as early as 24h p.i. indicating that although no T and B cell massive recruitment was observed, local resident cells or cells with limited recruitment to undetectable level are contributing to the installation of the vaccine response. Also we cannot exclude here transudation of cytokines from blood vessels or that we are simply measuring the content of the limited blood vessels volume in the biopsy. Interestingly, adaptive response mediators are also present in a third cluster of cytokines which include IFNY, IL-5, IL-4, IL1-5 and IL17α, which are detectable as early as 24h p.i. and which appeared to consistently increase until 72h p.i.. This group also includes soluble CD40L. Overall, we observed at site of vaccine injection several waves of immune mediators production that recapitulates innate (GM-CSF, IL1β, MIP1α, MIP1β, IL6, TNFα) and adaptive processes (IL2) and suggesting very early local interactions between the different compartments involved in immune response installation.

From site of injection to systemic vaccine response

Cellular and molecular changes occurring at the site of vaccine injection have regional and systemic impacts we try to connect by exploring subsequent changes in draining lymph nodes and blood. $CD66^{high}$Granulocytes are among the first population to significantly increase ($p<0.05$) very early (6h) following vaccine injection, probably as a result of rapid bone marrow release (**Fig.6A**). These cell numbers peaked 6h-24h then rapidly decrease to reach base line levels by 72h p.i.. Interestingly PMN which were also abundant in the skin, showed however a slightly delayed kinetics. Classical monocytes (CD14+CD16-) also increase in blood by 6h p.i., but then rapidly decrease by 24h p.i. probably as a result of its differentiation into proinflammatory(CD14+CD16+) and non classical(CD14-CD16+) which indeed increased by 24h and 72h, respectively. As for granulocytes, classical monocytes increase seems to precede the recruitment of monocyte/macrophages in the skin. By contrast to the above myeloid populations, T & B lymphocytes, NK cells and pDC tend to disappear from blood early following vaccine injection (6h), then to reappear at later time points reflecting probably its circulation to tissues and lymphoid tissues in particular.

Interestingly, 24h following vaccine injection we observed an increase (Friedman test ;p-value = 0.0559) of myeloid-derived suppressor cells (MDSCs) of the CD14+HLADR-CD33+ monocytic phenotype (M)-MDSC. This population is preceded by a transient increase, between 6 and 24h of early-stage Lineage negative MDSCs considered to be immature MDSC precursors[159] . No clear change in PMN-MDSC (CD14-HLADR-CD11b+CD66+) was observed although this represents a small population in peripheral blood (**Fig.S2B**). Although M-MDSC are generally considered as pathogenic cells associated with chronic inflammation in cancer, HIV infection or autoimmune diseases, very little is known on its physiological role. Recently the induction of this population has been observed in macaques following booster immunizations with rMVA expressing SIV antigens, which increased levels correlate with reduced vaccine efficacy [150]. Whether this is an MVA specifically induced mechanism remains to be demonstrated, but as many suppressive factors, it may not be surprising to

observe such suppressive cells delayed increase as a mechanisms to control vaccine induced acute inflammation [160].

Cytokines levels in blood follow a distinct kinetics profile to that observed in the skin**(Fig.6B)**. Although IL-6 is transiently increased at 6h-24h in blood and skin, as well as associated acute inflammation molecules like IL-1β and MIP-1α/β and MCP-1, its persist at high levels by 72h in blood whereas detection is transient in skin. Interestingly, TNF-α is a cytokine with clear distinct pattern between skin and blood compartments suggesting a specific role in the two compartments. Similar differences could be observed for factors like IL-12 and TGF-α. In addition, cytokines associated to adaptive T & B cell response, including IL-2, IL-4, IL-17α, IL-15, IL-5 have a progressive increase with strong levels detected at late time points (72h) which do not strictly match kinetics in the skin. Transcriptomics profiles in blood cells confirm changes associated with inflammation and adaptive response installation with peaking changes at 24-48h (around 350 down- or up- regulated genes). Indeed, acute phase, IL-6 and TNF-α related genes are increase by 6h post rMVA injection. Genes related to Th1/Th17 response also transiently increase by 24h. However, most of the genes related to T cell responses significantly decreased by 24h-48h, certainly reflecting the decrease of T cells in blood migrating to lymphoid tissues during the process of adaptive response installation, rather than a gene expression down regulation. Also the important granulocytes recruitment in the blood might dilute gene detection in other cell populations.

To better visualize similarities and dissimilarities in transcriptomics generated data we used the multidimensional scaling (MDS) multivariate statistical analysis which has superior fidelity in representing the distance between different instances when analyzing high-dimensional geometric objects, as compared to more classical singular value decomposition (SVD) based methods such as principal component analysis (40). MDS restricted to our set of differentially expressed genes in blood reveals a good segregation between time points (**Fig.8A**). The 24h p.i time point is the most distant compared to the baseline. Genes regulated 6h and 48h p.i show intermediate distance to base line and have close gene expression profiles. The 72h p.i profile is coming back, close to the

baseline values. The functional enrichment analysis reveals that genes associated with several upstream regulators and canonical pathways were significantly modified (p-value<10^{-3}) in blood cells. Not surprisingly and in accordance to cell changes in blood and cytokine levels in plasma, up-regulation of genes associated with inflammatory response is observed at early timepoints (TNFα, IL-6, IL-32 and acute phase response signaling). At the opposite and in coherence of T cells migration out of the circulation, canonical pathways and regulators contributing to mediate lymphocyte response such as IL-2, CD28 signaling or iCOS-iCOSL signaling are reduced over the kinetics. Transcripts regulating important innate canonical pathways, like antigen presentation pathways, CCR5 signaling in macrophages, IL-10 signaling or NK-DCs crosstalk, showed some activity without however any overall clear up- or down- regulation (**Fig. 8*C***).

To sum up, local immune reaction observed after rMVA intradermal immunization has important repercussions in the systemic compartiment. We indeed observed a significant increase over the time of numerous immune cell subsets in the blood (CD66high granulocytes, CD14+ CD16- monocytes, CD14+CD16+ monocytes) with inflammatory cytokine releasing at early timepoints (IL1ra, IL6). Significantly recruited cytokines become more heterogenic and mor rich at 48h and 72h p.i. This inflammatory response is also imprinted in the molecular signature, where groups of gene related with acute inflammation are upregulated (IFNγ, IL6, TNF, acute response signaling) between 6h and 24h.

rMVA induces a variable activation of the dLNs after intradermal injection

To approach the tissue interactions dynamics during the process of anti-rMVA response installation we also collected lymph nodes draining the vaccine injection site by 24h p.i.. We have limited access to peripheral lymph nodes in macaques and to reduce the interference between biopsies induced inflammation and sealing we avoid collection of lymph nodes at base line for comparison.

The inguinal area was selected for vaccine injection, approximately at 4 cm above the inguinal draining lymph nodes because the easy access to this area with minimal surgery. Our previous

experience demonstrated that all distant peripheral lymph nodes are not equal in terms of cells composition and transcriptomic profiles, we there made the decision to use for comparison the contralateral inguinal lymph node collected at the same time point. This control tissue is also influenced by changes at the systemic levels occurring in the same animal by 24h post vaccine injection, we however surmise that our decision may favor the identification of specific changes associated with the injection site. Because only three animals per group have been included, significant differences between lymph nodes were not observed, although a tendency to increased macrophage and granulocyte levels was detected by flow cytometry (**Fig.7A**). These cells recruitment are concordant to changes occurring concomitantly in the injected skin for these same populations; Although more diverse between animals, increased levels of APC such as CD1a+DC as well as T lymphocytes could be observed. Cytokines measured in total tissue extracts confirms the increase of inflammatory cytokines like IL-6, TNFα and particularly MCP-1 and G-CSF/IL-8 for macrophages and PMN, respectively (**Fig.7B**). Additional cytokines related to the adaptive response also tend to be measured at high levels in the draining lymph node including IL-4, INFY, IL-2 and IL-13. Finally, there is a trend to an increased expression of genes associated with the beginning of an immune reaction in the lymph node draining the vaccine injection site. In spite of the limited number of regulated genes, transcriptomic signatures remained well segregated in MDS analysis (**Fig.8B**). In addition, we also have one significantly enriched upstream regulator, ATF3, which can be related to immune functions such as TLR4 signaling [161]. In spite of a mild activation, some markers of activation still appear to be upregulated in the draining lymph node, without however reaching a significativity threshold due to the limited sample size.

Co-expression network representation of the early response highlight the key role of the inflammatory local effectors

So far, our study has described the nature of the immune process separately in all key compartment. But, in order to provide a better overview of the innate immune reaction, and better understand the

interaction and the role of each effector, we needed to integrate our data in a global analysis. As represented in the Figure 9A, we obtained different kinetic profiles depending on the localization and the biological variable, such as macrophages, granulocytes, IL6 or TNFα. Intra-individual heterogeneity was also noticed for several parameters such as granulocytes on the skin. To establish links between our parameters, we calculated Pearson's correlation between all of them (**Fig.9B**). We then extended this approach to the integrality of our dataset (**Supplementary table 1**). For the lymph nodes, non-draining lymph node was considered as an untreated condition to allow the possibility of establishing correlation. For the transcriptomics, we separated in gene clusters differentially expressed markers having the same kinetic profile to obtain one single value to simplify the representation. We only considered correlation with R>0.8 and q-value<0.05.This led us to the building of a co-expression network where nodes correspond to the biological variables and edges correspond to a significant correlation between two variables.(**Fig. 10A**). Parameters were organized accordingly to their type (cell, cytokine or gene cluster) and their localization (skin, blood or lymph nodes) To evaluate the role of each compartment and biological samples in the early immune response, number of correlations (or degree of connectivity)was assessed.

Important polarities are unraveled by this complex co-expression network. Cytokines measured in the skin are strongly correlated with cytokines in draining lymph nodes (48 connections) with major molecules including inflammatory mediators like TNFα, MIP-1β, IL-6 and IL-1β as well as factors associated with monocyte/macrophage and PMN recruitment like TGFα, G-CSF and GM-CSF. Also IL-2 significant linked these two tissues. Also, gene clusters of the lymph node were strongly associated with cytokine produced on the skin (41 connections). Those gene cluster were however not associated with any particular immune pathway. To a lesser extent (35 connections), cytokine levels are also correlated between blood and skin with TNFα and TGFα on one hand, again emphasizing a role for PMN and monocyte macrophages, and on the other hand Th1/Th17 and Th2 cytokines like IL-17α, IL-15, IL-5 and IL-12/23 certainly reflecting the impact of injection site on adaptive response installation. Surprisingly, a degree of connectivity of 8 only was found between blood and lymph

nodes, involving mainly inflammatory cytokines. This may be due to lower quantities of cytokines related to adaptive response which therefore weight less in the co-expression network or because these events are measured too early in our study. Indeed, we might expect the predominance adaptive response mediators a bit later following rMVA injection. For that purpose, later time points for lymph node biopsies may have been more appropriated. Not surprisingly, connection of PMN and monocyte/macrophages cells are predominant between the skin and blood, whereas lymphocytes are more connected in the lymph nodes compared to myeloid cells. Looking at the number of significant correlation built by biological variables individually (**Supplementary table 2**) highlights a pivotal role of several expected mediators, such as down- and up-regulated gene clusters, and skin produced TNFα and TGFα, and others more surprising like lymph node IL18 or blood monocyte derived MDSCs.

Overall, this global visualization emphasizes the strong impact of local reaction at injection site in the skin in the very early changes occurring in blood and lymph nodes and the predominant role we may hypothesize for monocyte/macrophages and PMN in relation to the associated soluble mediators, and most particularly TNFα and TGFα. Interestingly, we tried also to organize these connections accordingly to evaluated time points following vaccine injection (**Fig.10B**). Again, the peak of inflammatory response associated the blood, the skin and the lymph nodes by 24h p.i. with monocyte/macrophages, PMN and related cytokines as major actors. However, the kinetics visualization also unraveled a bit later impact of inflammatory monocytes and monocyte derived MDSCs which is compatible with activation and differentiation kinetics of myeloid cells and a role of suppressor factors in the control of acute inflammation. As expected, adaptive response related factors predominate at later time points (72p.i.).

Discussion

Unraveling early immune processes and establishing precisely how it interferes with adaptive response could open new possibilities in vaccine development. In this study, using an MVA vaccinated NHP study model with a specific kinetic, we highlight *in vivo* the central role of several inflammatory markers on the elaboration of the very first steps of the vaccine-specific response.

First, we characterized dynamics of MVA infection on the skin, beginning around 15 h post-injection and persisting until 3 days p.i. We established that MVA infected equally several types of cells. The local innate response is characterized by massive early recruitment of granulocytes, macrophages and monocytoid cells associated with local GM-CSF, IL1b, MIP1β, MIP1α and TNFα releasing. MVA also elicited an innate response, at a systemic level, initiated by a rapid and transient granulocytes recruitment and IL6, IL1ra release between 6h and 24h post-MVA injection followed by a persistent cell trafficking involving inflammatory monocytes. This systemic inflammation was confirmed by molecular signatures such as genes upregulating IL6 and TNF pathways, but also acute phase response signaling. A possible but limited activation of the draining lymph node was also shown. Finally, our study highlighted the correlations between local and draining lymph node cytokine releasing.

The strength of this study relies on his study model. Indeed, non-human primate has been found to be very relevant in basic immunology research and can provide unique insights of the understanding of complex immune reaction after vaccine immunization. In addition, the large set of technique used combined with an original approached allowed us to have a good overview of this particular immune response, emphasizing the role of important mediators such as proinflammatory cytokine produced or granulocytes locally recruited. Unfortunately, this *in vivo* model does not allow investigating specific cell functionalities that could provide us to go further in the analysis.

As a modified form of the vaccinia virus, MVA can infect a cell through two forms, the intracellular mature virus (IMV) and the extra cellular enveloped virus (EEV). Both of these forms bind and fuse with the host cell membrane but are not associated with specific cell receptors [158]. For instance,

some particular scavenger receptors called MARCO has been shown to be involved in the entry of the vaccinia virus in keratinocytes [162]. This particular viral entry could have a large influence after MVA intradermal injection, since it can lead to an increase of its immunogenicity. In addition, to infect a large diversity of cells, MVA is widely sensed by a large set of pattern recognition receptors (PRR) such as TLR2, TLR6, MDA5 or NALP3 inflammasome pathways [163]. Those PRR are expressed in several resident cells of the skin, including most of the immune cells, but also keratinocytes which express TLR2 and TLR6 [75]. As a result, the recruitment of granulocytes, monocytoidcells and macrophages mostly originating from the blood was expected as a part of the early inflammatory response to the vaccine [164]. It is also in accordance with previous studies using vaccine adjuvants in the same model[140]. We observed no clear-cut dendritic cell migration in this study, which is possibly outshined by the magnitude of the inflammatory response. This important cellular trafficking and pathogen sensing, especially 24h p.i. can be associated with the microenvironment modifications observed with the local cytokine releasing, particularly with G-CSF, GM-CSF, IL1b, IL6, MIP1β and TNFα which contribute to the recruitment of granulocytes and macrophages, increase their cytotoxic activity and their chemoattraction in the tissue. After 24h p.i., this cytokine storm conjugated with the local apoptosis of granulocytes lead to a microenvironment modification probably mainly driven by macrophages [29] inducing inflammation resolution as well as the progressive of other cytokines such as IL2 or IL15, opening the way to a potential local T_specific lymphocyte response. These data show that rMVA intradermal administration does not only induce a local immune response, but also an important systemic inflammation occurring even before the appearance of the first signs of rMVA infected cells within the skin. We can hypothesize that the first immune signal is delivered by the resident skin cells through inflammatory eicosanoid mediators right after rMVA administration[29], leading to rapid granulocyte releasing in the bone marrow migrating to the site of injection through the blood. The level of IL6 and IL1ra and the upregulation of acute response pathways 6h to 24h post-MVA injectioncould be associated with the increase of granulocytes in the blood. Similarly to the site of injection, this first wave of cellular recruitment leads to a more diverse systemic response,

possibly involving a broad variety of immune cells types such as monocytes subsets. Inversely, the downregulation of numerous pathways involving lymphocyte response could be linked with a decrease of lymphocytes in the blood. In addition to lymphocytes, CD33+ DCs and CD16- NK cells leave the systemic compartment, and are also not found on the site and thus might migrate directly to lymph nodes at the later time point.

The correlations between our biological parameters suggest that the magnitude of the inflammatory response directly drives the early steps of the adaptive response. Among those early major effectors, we also observe very early correlations built with IL2 in the lymph node. In addition to TNFα[140] this cytokine is also driving Th1 response, which is in accordance with the main T response profile induced by MVA [157,165]. Nevertheless, an in-depth analysis reveals also a part of the complexity of the integrated immune response, with the presence of effectors of Th2 response profile such as IL6, IL10 in the lymph node, simultaneously. Moreover, IL18, which is a cytokine from IL1 family and thus with Th1 profile [166] is anti-correlated with several recruited cells and cytokine as their number fall down after MVA immunization (Supplementary table1). It could however also be a signature of a previous inflammasome activation and is thus consistent with MVA induced response observed in mice models[167]. The co-expression network also teaches us about the interaction between the innate effectors.Notably, it allowed identifying major hubs that are correlated with critical immune parameters such as TNFα or monocytes derived MDSCs. TNFα, as a central cytokine of the inflammatory response, can be described as an expected key factor of the innate response. This cytokine is indeed produced and released by granulocytes and macrophages and act as a strong pro-inflammatory signal leading to tissue necrosis. But in particular contexts, TNFα can also induce TLR expression, and even activate DCs and inducing T responses[168]. In a vaccination context in the skin, it has been shown to induce *in vivo* Langerhans cells migration to the draining lymph node to elicit Th1 response[140]. Our correlation network also highlights blood monocytes derived MDSCs as a dominant effector of this response. This cell population may also be recruited after MVA injection (Friedman's test p-value = 0.0553; Supplementary table I). This recruitment was unexpected, since these cells are

associated with immunosuppressive processes such as tumor immune evasion and lymphocyte suppression through the production of reactive oxygen species[169,170]. However, in a vaccine study involving prime-boost strategy using MVA in a context of SIV immunization, similar MDSCs were also recruited in the blood and were found to exert T CD8 suppression in vitro[150]. In addition, those MDSCs could also play a role in the microenvironment switch from a transient pro-inflammatory to a persisting and a more heterogenic and anti-inflammatory profile observed in the skin tissue[160]. These cells could therefore act at early phase downregulating inflammatory response.

This longitudinal study reveals concrete insights about the elaboration of the immune response to MVA. Our original approach combining flow cytometry, Luminex, transcriptomic analysis but also tools derived from systems biology such has correlation networks indeed illustrates here that the settling of the immune response can be depicted as a continuum of a cellular and cytokine trafficking that are influencing and synergizing each other to lead to the vaccine induced response. Those synergies correspond to a cascade of reactions depending on the original stimulus. In this context, we show that the magnitude of the early effectors, particularly those triggering at the site of injection such as local granulocyte, or TNFα releasing are directly associated with the first steps of the adaptive response orientation, as it is related with draining lymph nodes dendritic cell recruitment and cytokines releasing. In addition, other markers such as monocytes derived MDSCs, which are building many correlations, should be considered as a potential signature of the response. Identification of such signatures is extremely valuable to understand how to effectively orientate immune response profiles, and could contribute to a rational-based vaccine development.

Acknowledgements

This work was supported by French government “Programme d’Investissements d’Avenir” (PIA) under Grant ANR-11-INBS-0008 funding the Infectious Disease Models and Innovative Therapies (IDMIT, Fontenay-aux-Roses, France) infrastructure and PIA grants ANR-10-LABX-77 and ANR-10-

EQPX-02-01 funding the Vaccine Research Institute (VRI, Créteil, France), the FlowCyTech facility, respectively. The European Commission Advanced Immunization Technologies (ADITEC) Grant FP7-HEALTH-2011-280873 also contributes to this research.

References

1. Rosenbaum, P. Etude de la réponse immunitaire induite par des adjuvants agonistes des TLR sur la peau de macaque. (These de pharmacie, Rennes, 2012). at <http://www.sudoc.fr/167282689>
2. van Panhuis, W. G. *et al.*Contagious Diseases in the United States from 1888 to the Present. *N. Engl. J. Med.***369,** 2152–2158 (2013).
3. Andersen, P. & Doherty, T. M. The success and failure of BCG - implications for a novel tuberculosis vaccine. *Nat. Rev. Microbiol.***3,** 656–662 (2005).
4. Mayr, A., Hochstein-Mintzel, V. & Stickl, H. Abstammung, Eigenschaften und Verwendung des attenuierten Vaccinia-Stammes MVA. *Infection***3,** 6–14 (1975).
5. Kim, J., Rerks-Ngarm, S. & Excler, J. HIV Vaccines-Lessons learned and the way forward. *Curr. Opin. HIV***5,** 428–434 (2010).
6. Ahmed, S. S., Plotkin, S. a, Black, S. & Coffman, R. L. Assessing the safety of adjuvanted vaccines. *Sci. Transl. Med.***3,** 93rv2 (2011).
7. Cristiani, C. *et al.* Safety of MF-59 adjuvanted vaccine for pandemic influenza: Results of the vaccination campaign in an Italian health district. *Vaccine***29,** 3443–3448 (2011).
8. Paavonen, J. *et al.* Efficacy of a prophylactic adjuvanted bivalent L1 virus-like-particle vaccine against infection with human papillomavirus types 16 and 18 in young women: an interim analysis of a phase III double-blind, randomised controlled trial. *Lancet***369,** 2161–2170 (2007).
9. Liko, J., Robison, S. G. & Cieslak, P. R. Priming with Whole-Cell versus Acellular Pertussis Vaccine. *N. Engl. J. Med.***368,** 581–2 (2013).
10. Warfel, J. M., Zimmerman, L. I. & Merkel, T. J. Acellular pertussis vaccines protect against disease but fail to prevent infection and transmission in a nonhuman primate model. *Proc. Natl. Acad. Sci. U. S. A.***111,** 787–92 (2014).
11. Buchbinder, S. P. *et al.* Efficacy assessment of a cell-mediated immunity HIV-1 vaccine (the

Step Study): a double-blind, randomised, placebo-controlled, test-of-concept trial. *Lancet***372,** 1881–1893 (2008).

12. Rerks-Ngarm, S. *et al.* Vaccination with ALVAC and AIDSVAX to Prevent HIV-1 Infection in Thailand. *N. Engl. J. Med.***361,** 2209–2220 (2009).
13. Hewitt, E. W. The MHC class I antigen presentation pathway: Strategies for viral immune evasion. *Immunology***110,** 163–169 (2003).
14. Goulder, P. J. R. & Watkins, D. I. Impact of MHC class I diversity on immune control of immunodeficiency virus replication. *Nat. Rev. Immunol.***8,** 619–30 (2008).
15. Silzle, T., Randolph, G. J., Kreutz, M. & Kunz-Schughart, L. A. The fibroblast: Sentinel cell and local immune modulator in tumor tissue. *Int. J. Cancer***108,** 173–180 (2004).
16. Kupper, T. S. *et al.* Production of IL-6 by Keratinocytes. *Ann. N. Y. Acad. Sci.***557,** 454–465 (2008).
17. Saalbach, A. *et al.* Dermal fibroblasts induce maturation of dendritic cells. *J Immunol***178,** 4966–4974 (2007).
18. Tecle, T., Tripathi, S. & Hartshorn, K. L. Review: Defensins and cathelicidins in lung immunity. *Innate Immun.***16,** 151–159 (2010).
19. Danese, S., Dejana, E. & Fiocchi, C. Immune Regulation by Microvascular Endothelial Cells: Directing Innate and Adaptive Immunity, Coagulation, and Inflammation. *J. Immunol.***178,** 6017–6022 (2007).
20. Guilliams, M. *et al.* Dendritic cells, monocytes and macrophages: a unified nomenclature based on ontogeny TL - 14. *Nat. Rev. Immunol.***14 VN - r,** 571–578 (2014).
21. Epstein, F. H. & Luster, A. D. Chemokines — Chemotactic Cytokines That Mediate Inflammation. *N. Engl. J. Med.***338,** 436–445 (1998).
22. Biron, C. a. Role of early cytokines, including alpha and beta interferons (IFN-alpha/beta), in innate and adaptive immune responses to viral infections. *Semin. Immunol.***10,** 383–390 (1998).

23. Leroy, M. & Desmecht, D. Les interférons de type I et leur fonction antivirale. *Ann. médecine vétérinaire***150,** 73–107 (2006).

24. Dai, P. *et al.* Modified Vaccinia Virus Ankara Triggers Type I IFN Production in Murine Conventional Dendritic Cells via a cGAS/STING-Mediated Cytosolic DNA-Sensing Pathway. *PLoS Pathog.***10,** (2014).

25. Ablasser, A. *et al.* Cell intrinsic immunity spreads to bystander cells via the intercellular transfer of cGAMP. *Nature***503,** 530–4 (2013).

26. Kawai, T. & Akira, S. Toll-like receptors and their crosstalk with other innate receptors in infection and immunity. *Immunity***34,** 637–50 (2011).

27. Hodge, D. R., Hurt, E. M. & Farrar, W. L. The role of IL-6 and STAT3 in inflammation and cancer. *Eur. J. Cancer***41,** 2502–2512 (2005).

28. Luster, A. D., Alon, R. & von Andrian, U. H. Immune cell migration in inflammation: present and future therapeutic targets. *Nat. Immunol.***6,** 1182–90 (2005).

29. Serhan, C. N. & Savill, J. Resolution of inflammation: the beginning programs the end. *Nat. Immunol.***6,** 1191–1197 (2005).

30. Banchereau, J. & Steinman, R. M. Dendritic cells and the control of immunity. *Nature***392,** 245–252 (1998).

31. Bruel, T. *et al.* Plasmacytoid dendritic cell dynamics tune interferon-alfa production in SIV-infected cynomolgus macaques. *PLoS Pathog.***10,** e1003915 (2014).

32. Ketloy, C. *et al.* Expression and function of Toll-like receptors on dendritic cells and other antigen presenting cells from non-human primates. *Vet. Immunol. Immunopathol.***125,** 18–30 (2008).

33. Hume, D. a. Macrophages as APC and the dendritic cell myth. *J. Immunol.***181,** 5829–5835 (2008).

34. Falcone, M., Lee, J., Patstone, G., Yeung, B. & Sarvetnick, N. B lymphocytes are crucial antigen-presenting cells in the pathogenic autoimmune response to GAD65 antigen in nonobese

diabetic mice. *J. Immunol.***161,** 1163–1168 (1998).

35. Ahmed, R. & Gray, D. Immunological memory and protective immunity: understanding their relation. *Science (80-.).***272,** 54–60 (1996).

36. Itano, A. a & Jenkins, M. K. Antigen presentation to naive CD4 T cells in the lymph node. *Nat. Immunol.***4,** 733–9 (2003).

37. Idris-Khodja, N., Mian, M. O. R., Paradis, P. & Schiffrin, E. L. Dual opposing roles of adaptive immunity in hypertension. *Eur. Heart J.***35,** 1238–1244 (2014).

38. Diehl, S. & Rincón, M. The two faces of IL-6 on Th1/Th2 differentiation. *Mol. Immunol.***39,** 531–536 (2002).

39. Okada, R., Kondo, T., Matsuki, F., Takata, H. & Takiguchi, M. Phenotypic classification of human CD4+ T cell subsets and their differentiation. *Int. Immunol.***20,** 1189–1199 (2008).

40. Cher, D. J. & Mosmann, T. R. Two types of murine helper T cell clone. II. Delayed-type hypersensitivity is mediated by TH1 clones. *J. Imunol.***138,** 3688–94 (1987).

41. Coffman, R. L. *et al.* The role of helper T cell products in mouse B cell differentiation and isotype regulation. *Immunol. Rev.***102,** 5–28 (1988).

42. Schaerli, P. *et al.* CXC chemokine receptor 5 expression defines follicular homing T cells with B cell helper function. *J. Exp. Med.***192,** 1553–62 (2000).

43. Fazilleau, N., Mark, L., McHeyzer-Williams, L. & McHeyzer-Williams, M. Follicular Helper T Cells: Lineage and Location. *Immunity***30,** 324–335 (2009).

44. Crotty, S. Follicular Helper CD4 T Cells (T_{FH}). *Annu. Rev. Immunol.***29,** 621–663 (2011).

45. Petrovas, C. *et al.*CD4 T follicular helper cell dynamics during SIV infection. *J Clin Invest.***5,** 1–14 (2012).

46. Perreau, M. *et al.* Follicular helper T cells serve as the major CD4 T cell compartment for HIV-1 infection, replication, and production. *J. Exp. Med.***210,** 143–56 (2013).

47. Colineau, L. *et al.* HIV-infected spleens present altered follicular helper T cell (Tfh) subsets and skewed B cell maturation. *PLoS One***10,** 1–19 (2015).

48. Lowin, B., Hahne, M., Mattman, C. & Tchopp, J. Cytolytic T-cell cytotoxicity is mediated through perforin and Fas lytic pathway. *Lett. to Nat.***370,** (1994).

49. Liu, C., Walsh, C. M. & Young, J. D. Perforin : structure and function. *Immunol. Today***15,** 194–201 (1995).

50. Heusel, J. W., Wesselschmidt, R. L., Russell, J. H. & Ley, T. J. Cytotoxic Lymphocytes Require Granzyme B for the Rapid Induction of DNA Fragmentation and Apoptosis in Allogeneic Target Cells. *Cell***76,** 977–987 (1994).

51. Jenkins, M. K., Burrell, E. & Ashwell, J. D. Antigen presentation by resting B cells . Effectiveness at inducing T cell proliferation is determined by costimulatory signals , not T cell receptor occupancy. *J. Immunol.***144,** 1585–1590 (1990).

52. Abbas, A. K. *et al.* Activation and Functions of CD4 + T-Cell Subsets. *Immunol. Rev.* (1991).

53. Fey, T. M. *et al.* In the Absence of a CD40 Signal , B Cells Are Tolerogenic. *Immunity***2,** 645–653 (1995).

54. Fuchs, E. J. & Matzingert, P. B Cells Turn Off Virgin But Not Memory T Cells. *Science***2,** (1992).

55. Bonecchi, B. R. *et al.* Differential Expression of Chemokine Receptors and Chemotactic Responsiveness of Type 1 T Helper Cells. *J. Exp. Med.***187,** 129–134 (1998).

56. Imai, T. *et al.* Selective recruitment of CCR4-bearing T h 2 cells toward antigen-presenting cells by the CC chemokines thymus and activation-regulated chemokine and macrophage-derived chemokine. *Int. Immunol.***11,** 81–88 (1999).

57. Förster, R., Davalos-misslitz, A. C. & Rot, A. CCR7 and its ligands : balancing immunity and tolerance. *Nat. Rev. Immunol.***8,** (2008).

58. Fritsch, R. D. *et al.* Stepwise Differentiation of CD4 Memory T Cells Defined by Expression of CCR7 and CD27. *J. Immunol. (Baltimore, Md. 1950)***175,** 6489–6497 (2015).

59. Xu, H., Manivannan, A., Crane, I., Dawson, R. & Liversidge, J. Critical but divergent roles for CD62L and CD44 in directing blood monocyte trafficking in vivo during inflammation. *Blood***112,** 1166–1175 (2008).

60. Picker, L. J. *et al.* Control of lymphocyte recirculation in man. I. Differential regulation of the peripheral lymph node homing receptor L-selectin on T cells during the virgin to memory cell transition. *J. Immunol.* (1993).

61. Chaparas, S. D. L'immunite dans la tuberculose. *Bull. l'Organisation Mond. la Santé***60,** 827–844 (1982).

62. Wiendl, H., Hohlfeld, R. & Kieseier, B. C. Immunobiology of muscle: advances in understanding an immunological microenvironment. *Trends Immunol.***26,** 373–80 (2005).

63. Zehrung, D., Jarrahian, C. & Wales, A. Intradermal delivery for vaccine dose sparing: Overview of current issues. *Vaccine***31,** 3392–3395 (2013).

64. Zaric, M., Ibarzo Yus, B., Kalcheva, P. P. & Klavinskis, L. S. Microneedle-mediated delivery of viral vectored vaccines. *Expert Opin. Drug Deliv.***5247,** 17425247.2017.1230096 (2016).

65. Liang, F. *et al.* Dissociation of skeletal muscle for flow cytometric characterization of immune cells in macaques. *J. Immunol. Methods***425,** 69–78 (2015).

66. Abadie, V. *et al.* Original encounter with antigen determines antigen-presenting cell imprinting of the quality of the immune response in mice. *PLoS One***4,** e8159 (2009).

67. Calabro, S. *et al.* Vaccine adjuvants alum and MF59 induce rapid recruitment of neutrophils and monocytes that participate in antigen transport to draining lymph nodes. *Vaccine***29,** 1812–23 (2011).

68. Lu, F. & Hogenesch, H. Kinetics of the inflammatory response following intramuscular injection of aluminum adjuvant. *Vaccine***31,** 3979–86 (2013).

69. Caspar-Bauguil, S. *et al.* Adipose tissues as an ancestral immune organ: site-specific change in obesity. *FEBS Lett.***579,** 3487–92 (2005).

70. Pond, C. M. Adipose tissue and the immune system. *Prostaglandins Leukot. Essent. Fat. Acids***73,** 17–30 (2005).

71. Damouche, A. *et al.*Adipose Tissue Is a Neglected Viral Reservoir and an Inflammatory Site during Chronic HIV and SIV Infection. *PLoS Pathog.***11,** 1–28 (2015).

72. Mantoux, C. Intradermo-reaction de la tuberculine. *Comptes rendus l'Académie des Sci.***147,** 355–57 (1908).

73. Artenstein, A. W. Bifurcated vaccination needle. *Vaccine***32,** 895 (2014).

74. Roediger, B. *et al.*Cutaneous immunosurveillance and regulation of inflammation by group 2 innate lymphoid cells. *Nat. Immunol.***14,** 564–73 (2013).

75. Nestle, F. O., Di Meglio, P., Qin, J.-Z. & Nickoloff, B. J. Skin immune sentinels in health and disease. *Nat. Rev. Immunol.***9,** 679–691 (2009).

76. Zaid, A. *et al.* Persistence of skin-resident memory T cells within an epidermal niche. *Proc. Natl. Acad. Sci. U. S. A.***111,** 5307–12 (2014).

77. Malissen, B., Tamoutounour, S. & Henri, S. The origins and functions of dendritic cells and macrophages in the skin. *Nat. Rev. Immunol.***14,** 417–28 (2014).

78. Valladeau, J. & Saeland, S. Cutaneous dendritic cells. *Semin. Immunol.***17,** 273–83 (2005).

79. Kubo, A., Nagao, K., Yokouchi, M., Sasaki, H. & Amagai, M. External antigen uptake by Langerhans cells with reorganization of epidermal tight junction barriers. *J. Exp. Med.***206,** 2937–2946 (2009).

80. Shklovskaya, E. *et al.* Langerhans cells are precommitted to immune tolerance induction. *Proc. Natl. Acad. Sci. U. S. A.***108,** 18049–54 (2011).

81. Stoitzner, P. *et al.* Langerhans cells cross-present antigen derived from skin. *Proc. Natl. Acad. Sci. U. S. A.***103,** 7783–8 (2006).

82. Flacher, V. *et al.* Murine Langerin + dermal dendritic cells prime CD 8 + T cells while Langerhans cells induce cross-tolerance. 1–14 (2014).

83. Klechevsky, E. *et al.* Functional specializations of human epidermal Langerhans cells and CD14+ dermal dendritic cells. *Immunity***29,** 497–510 (2008).

84. Klechevsky, E. Human dendritic cells - stars in the skin. *Eur. J. Immunol.***43,** 3147–55 (2013).

85. Penel-Sotirakis, K., Simonazzi, E., Péguet-Navarro, J. & Rozières, A. Differential Capacity of Human Skin Dendritic Cells to Polarize CD4+T Cells into IL-17, IL-21 and IL-22 Producing Cells.

*PLoS One***7,** (2012).

86. Haniffa, M., Gunawan, M. & Jardine, L. Human skin dendritic cells in health and disease. *J. Dermatol. Sci.***77,** 85–92 (2015).

87. Haniffa, M. *et al.* Human Tissues Contain CD141 hi Cross-Presenting Dendritic Cells with Functional Homology to Mouse CD103 + Nonlymphoid Dendritic Cells. *Immunity***37,** 60–73 (2012).

88. Davis, M. M. A Prescription for Human Immunology. *Immunity***29,** 835–838 (2008).

89. Ostrand-Rosenberg, S. Animal models of tumor immunity, immunotherapy and cancer vaccines. *Curr. Opin. Immunol.***16,** 143–150 (2004).

90. von Herrath, M. G. & Nepom, G. T. Lost in translation: barriers to implementing clinical immunotherapeutics for autoimmunity. *J. Exp. Med.***202,** 1159–62 (2005).

91. Kennedy, R. C., Shearer, M. H. & Hildebrand, W. Nonhuman primate models to evaluate vaccine safety and immunogenicity. *Vaccine***15,** 903–908 (1997).

92. Quintana-Murci, L., Alcaïs, A., Abel, L. & Casanova, J.-L. Immunology in natura: clinical, epidemiological and evolutionary genetics of infectious diseases. *Nat. Immunol.***8,** 1165–71 (2007).

93. Mestas, J. & Hughes, C. C. W. Of mice and not men: differences between mouse and human immunology. *J. Immunol.***172,** 2731–2738 (2004).

94. Macchiarini, F., Manz, M. G., Palucka, a K. & Shultz, L. D. Humanized mice : are we there yet ? *Allergy***202,** 1307–11 (2005).

95. Ito, R., Takahashi, T., Katano, I. & Ito, M. Current advances in humanized mouse models. *Cell. Mol. Immunol.***9,** 208–14 (2012).

96. Hérodin, F., Thullier, P., Garin, D. & Drouet, M. Nonhuman primates are relevant models for research in hematology, immunology and virology. *Eur. Cytokine Netw.***16,** 104–116 (2005).

97. Merkel, T. J. & Halperin, S. A. Nonhuman primate and human challenge models of pertussis. *J. Infect. Dis.***209,** 20–23 (2014).

98. Geisbert, T. W., Strong, J. E. & Feldmann, H. Considerations in the Use of Nonhuman Primate Models of Ebola Virus and Marburg Virus Infection. *J. Infect. Dis.***212,** 91–97 (2015).

99. Flynn, J. L., Gideon, H. P., Mattila, J. T. & Lin, P. ling. Immunology studies in non-human primate models of tuberculosis. *Immunol. Rev.***264,** 60–73 (2015).

100. Gardner, M. B. & Luciw, P. a. Macaque models of human infectious disease. *ILAR J.***49,** 220–55 (2008).

101. Meurens, F., Summerfield, A., Nauwynck, H., Saif, L. & Gerdts, V. The pig: A model for human infectious diseases. *Trends Microbiol.***20,** 50–57 (2012).

102. Roberts, K. L. & Smith, G. L. Vaccinia virus morphogenesis and dissemination. *Trends Microbiol.***16,** 472–479 (2008).

103. Moss, B. Poxvirus entry and membrane fusion. *Virology***344,** 48–54 (2006).

104. Ichihashi, Y. Extracellular enveloped vaccinia virus escapes neutralization. *Virology***217,** 478–485 (1996).

105. Smith, G. L., Symons, J. A. & Vanderplasschen, A. Vaccinia virus immune evasion. *Immunol. Rev.***159,** 137–154 (1997).

106. Smith, G., Mackett, M. & Moss, B. Infectious vaccinia virus recombinants that express hepatitis B virus surface antigen. *Nature***302,** 490–495 (1983).

107. Meyer, H., Sutter, G. & Mayr, a. Mapping of deletions in the genome of the highly attenuated vaccinia virus MVA and their influence on virulence. *J. Gen. Virol.***72 (Pt 5),** 1031–8 (1991).

108. DiPerna, G. *et al.* Poxvirus Protein N1L Targets the I- B Kinase Complex, Inhibits Signaling to NF- B by the Tumor Necrosis Factor Superfamily of Receptors, and Inhibits NF- B and IRF3 Signaling by Toll-like Receptors. *J. Biol. Chem.***279,** 36570–36578 (2004).

109. Waibler, Z. *et al.* Vaccinia virus-mediated inhibition of type I interferon responses is a multifactorial process involving the soluble type I interferon receptor B18 and intracellular components. *J. Virol.***83,** 1563–1571 (2009).

110. Moss, B. *et al.* Host range restricted, non-replicating vaccinia virus vectors as vaccine

candidates. *Adv. Exp. Med. Biol.***397,** 7–13 (1996).

111. Sutter, G., Wyatt, L. S., Foley, P. L., Bennink, J. R. & Moss, B. A recombinant vector derived from the host range-restricted and highly attenuated MVA strain of vaccinia virus stimulates protective immunity in mice to influenza virus. *Vaccine***12,** 1032–1040 (1994).

112. Vollmar, J. *et al.* Safety and immunogenicity of IMVAMUNE, a promising candidate as a third generation smallpox vaccine. *Vaccine***24,** 2065–2070 (2006).

113. Sheehan, S. *et al.* A Phase I, Open-Label Trial, Evaluating the Safety and Immunogenicity of Candidate Tuberculosis Vaccines AERAS-402 and MVA85A, Administered by Prime-Boost Regime in BCG-Vaccinated Healthy Adults. *PLoS One***10,** e0141687 (2015).

114. Stickl, H. *et al.* MVA-Stufenimpfung gegen Pocken. *DMW - Dtsch. Medizinische Wochenschrift***99,** 2386–2392 (1974).

115. Altenburg, A. F. *et al.* Modified vaccinia virus ankara (MVA) as production platform for vaccines against influenza and other viral respiratory diseases. *Viruses***6,** 2735–61 (2014).

116. Zhou, Y. & Sullivan, N. J. Immunology and evolvement of the adenovirus prime, MVA boost Ebola virus vaccine. *Curr. Opin. Immunol.***35,** 131–136 (2015).

117. Gómez, C. E. *et al.* A Phase I Randomized Therapeutic MVA-B Vaccination Improves the Magnitude and Quality of the T Cell Immune Responses in HIV-1-Infected Subjects on HAART. *PLoS One***10,** e0141456 (2015).

118. Lelièvre, J.-D., Lacabaratz, C. & Richert, L. Essai de phase I/II sans insu, randomisé, multicentrique évaluant l'immunogénicite et la tolérance de 4 combinaisons « prime- boost » de candidats vaccins VIH (MVA HIV-B /LIPO-5; LIPO-5 / MVA HIV-B; GTU-MultiHIV B /LIPO-5; GTU-MultiHIV B / MVA HIV-B) chez. 33076 (2014). at <www.recherche-vaccinVIH.fr>

119. Richert, L. *et al.* Accelerating clinical development of HIV vaccine strategies: methodological challenges and considerations in constructing an optimised multi-arm phase I/II trial design. *Trials***15,** 68 (2014).

120. Kitano, H. Computatioal Systems Biology. *Nature***420,** 206–210 (2002).

121. Nakaya, H. I. & Pulendran, B. Vaccinology in the era of high-throughput biology. *Philos. Trans. R. Soc. Lond. B. Biol. Sci.***370,** (2015).

122. Querec, T. D. *et al.*Systems biology approach predicts immunogenicity of the yellow fever vaccine in humans. *Nat. Immunol.***10,** 116–125 (2009).

123. Obermoser, G. *et al.* Systems scale interactive exploration reveals quantitative and qualitative differences in response to influenza and pneumococcal vaccines. *Immunity***38,** 831–44 (2013).

124. Pulendran, B., Li, S. & Nakaya, H. I. Systems vaccinology. *Immunity***33,** 516–529 (2010).

125. Bécavin, C., Tchitchek, N., Mintsa-Eya, C., Lesne, A. & Benecke, A. Improving the efficiency of multidimensional scaling in the analysis of high-dimensional data using singular value decomposition. *Bioinformatics***27,** 1413–1421 (2011).

126. Schlitzer, A. & Ginhoux, F. Organization of the mouse and human DC network. *Curr. Opin. Immunol.***26,** 90–9 (2014).

127. Wille-Reece, U. *et al.* Toll-like receptor agonists influence the magnitude and quality of memory T cell responses after prime-boost immunization in nonhuman primates. *J. Exp. Med.***203,** 1249–58 (2006).

128. Nakaya, H. I. *et al.* Systems biology of vaccination for seasonal influenza in humans. *Nat. Immunol.***12,** 786–795 (2011).

129. Gannavaram, S. *et al.* Modulation of Innate Immune Mechanisms to Enhance Leishmania Vaccine-Induced Immunity: Role of Coinhibitory Molecules. *Front. Immunol.***7,** 1–10 (2016).

130. Hartman, Z. C., Appledorn, D. M. & Amalfitano, A. Adenovirus vector induced innate immune responses: Impact upon efficacy and toxicity in gene therapy and vaccine applications. *Virus Res.***132,** 1–14 (2008).

131. Coffman, R. L., Sher, A. & Seder, R. a. Vaccine adjuvants: putting innate immunity to work. *Immunity***33,** 492–503 (2010).

132. Iwasaki, A. & Medzhitov, R. Regulation of adaptive immunity by the innate immune system. *Science***327,** 291–295 (2010).

133. Maletto, B. a. *et al.* Presence of neutrophil-bearing antigen in lymphoid organs of immune mice. *Blood***108,** 3094–3102 (2006).

134. Pozzi, L. -a. M., Maciaszek, J. W. & Rock, K. L. Both Dendritic Cells and Macrophages Can Stimulate Naive CD8 T Cells In Vivo to Proliferate, Develop Effector Function, and Differentiate into Memory Cells. *J. Immunol.***175,** 2071–2081 (2005).

135. Kwissa, M., Nakaya, H. I., Oluoch, H., Pulendran, B. & Dc, W. Distinct TLR adjuvants differentially stimulate systemic and local innate immune responses in nonhuman primates Distinct TLR adjuvants differentially stimulate systemic and local innate immune responses in nonhuman primates. **119,** 2044–2055 (2012).

136. McMahon, J. M., Wells, K. E., Bamfo, J. E., Cartwright, M. a & Wells, D. J. Inflammatory responses following direct injection of plasmid DNA into skeletal muscle. *Gene Ther.***5,** 1283–90 (1998).

137. Cunningham, A. L., Carbone, F. & Geijtenbeek, T. B. H. Langerhans cells and viral immunity. *Eur. J. Immunol.***38,** 2377–85 (2008).

138. Liard, C. *et al.* Intradermal immunization triggers epidermal Langerhans cell mobilization required for CD8 T-cell immune responses. *J. Invest. Dermatol.***132,** 615–25 (2012).

139. Kenney, R. T. *et al.* Dose Sparing with Intradermal Injection of Influenza Vaccine. *J. Med.* 1–7 (2004).

140. Epaulard, O. *et al.* Macrophage- and Neutrophil-Derived TNF-α Instructs Skin Langerhans Cells To Prime Antiviral Immune Responses. *J. Immunol.***193,** 2416–2426 (2014).

141. Meyer, H., Sutter, G. & Mayr, A. Meyer, Sutter, Mayr - 1991 - Mapping of deletions in the genome of the highly attenuated vaccinia virus MVA and their influence on virul.pdf. **382,** 1031–1038 (1991).

142. Wilck, M. B. *et al.*Safety and immunogenicity of modified vaccinia Ankara (ACAM3000): effect of dose and route of administration. *J. Infect. Dis.***201,** 1361–1370 (2010).

143. Gómez, C. E., Perdiguero, B., García-Arriaza, J. & Esteban, M. Poxvirus vectors as HIV/AIDS

vaccines in humans. *Hum. Vaccines Immunother.***8,** 1192–1207 (2012).

144. Gómez, C. E. *et al.* High, broad, polyfunctional, and durable T cell immune responses induced in mice by a novel hepatitis C virus (HCV) vaccine candidate (MVA-HCV) based on modified vaccinia virus Ankara expressing the nearly full-length HCV genome. *J. Virol.***87,** 7282–300 (2013).

145. You, Q. *et al.* Subcutaneous administration of modified vaccinia virus Ankara expressing an Ag85B-ESAT6 fusion protein, but not an adenovirus-based vaccine, protects mice against intravenous challenge with Mycobacterium tuberculosis. *Scand. J. Immunol.***75,** 77–84 (2012).

146. Tapia, M. D. *et al.* Use of ChAd3-EBO-Z Ebola virus vaccine in Malian and US adults, and boosting of Malian adults with MVA-BN-Filo: a phase 1, single-blind, randomised trial, a phase 1b, open-label and double-blind, dose-escalation trial, and a nested, randomised, double-bli. *Lancet Infect. Dis.***3099,** 1–12 (2015).

147. Bontrop, R. E. Non-human primates: essential partners in biomedical research. *Immunol. Rev.***183,** 5–9 (2001).

148. Adam, L., Rosenbaum, P., Cosma, A., Le Grand, R. & Martinon, F. Identification of skin immune cells in non-human primates. *J. Immunol. Methods* 1–8 (2015). doi:10.1016/j.jim.2015.07.010

149. Ziegler-Heitbrock, L. The CD14+ CD16+ blood monocytes: their role in infection and inflammation. *J. Leukoc. Biol.***81,** 584–92 (2007).

150. Sui, Y. *et al.* Vaccine-induced myeloid cell population dampens protective immunity to SIV. 1–12 doi:10.1172/JCI73518DS1

151. Salabert, N. *et al.* Intradermal injection of an anti-Langerin-HIVGag fusion vaccine targets epidermal Langerhans cells in nonhuman primates and can be tracked in vivo. *Eur. J. Immunol.***46,** 689–700 (2016).

152. Abràmoff, M. D., Magalhães, P. J. & Ram, S. J. Image processing with imageJ. *Biophotonics Int.***11,** 36–41 (2004).

153. Kolesnikov, N. *et al.* ArrayExpress update-simplifying data submissions. *Nucleic Acids*

*Res.***43,**D1113–D1116 (2015).

154. Team, Rc. R: A language and environment for statistical computing. (2016). at <https://www.r-project.org/.>

155. Kruskal, J. B. & Wish, M. Multidimensional Scaling. *Sage Univ. Pap. Ser. Quant. Appl. Soc. Sci.* (1978).

156. Shannon, P. *et al.* Cytoscape: A software Environment for integrated models of biomolecular interaction networks. *Genome Res.***13,** 2498–2504 (2003).

157. Ramírez, J. C., Gherardi, M. M. & Esteban, M. Biology of attenuated modified vaccinia virus Ankara recombinant vector in mice: virus fate and activation of B- and T-cell immune responses in comparison with the Western Reserve strain and advantages as a vaccine. *J. Virol.***74,** 923–33 (2000).

158. McFadden, G. Poxvirus tropism. *Nat. Rev. Microbiol.***3,** 201–13 (2005).

159. Bronte, V. *et al.* Recommendations for myeloid-derived suppressor cell nomenclature and characterization standards. *Nat. Commun.***7,** 12150 (2016).

160. Newson, J. *et al.* Resolution of acute inflammation bridges the gap between innate and adaptive immunity. *Blood***124,** 1748–64 (2014).

161. Gilchrist, M. *et al.* Systems biology approaches identify ATF3 as a negative regulator of Toll-like receptor 4. *Nature***441,** 173–178 (2006).

162. MacLeod, D. T., Nakatsuji, T., Wang, Z., di Nardo, A. & Gallo, R. L. Vaccinia Virus Binds to the Scavenger Receptor MARCO on the Surface of Keratinocytes. *J. Invest. Dermatol.* (2014). doi:10.1038/jid.2014.330

163. Delaloye, J. *et al.* Innate immune sensing of modified vaccinia virus Ankara (MVA) is mediated by TLR2-TLR6, MDA-5 and the NALP3 inflammasome. *PLoS Pathog.***5,** (2009).

164. van Furth, R., Nibbering, P. H., van Dissel, J. T. & Diesselhoff-den Dulk, M. M. The characterization, origin, and kinetics of skin macrophages during inflammation. *J. Invest. Dermatol.***85,** 398–402 (1985).

165. Flechsig, C. *et al.* Uptake of antigens from modified vaccinia Ankara virus-infected leukocytes enhances the immunostimulatory capacity of dendritic cells. *Cytotherapy***13,** 739–52 (2011).

166. Dinarello, C. a. IL-18: A TH1 -inducing, proinflammatory cytokine and new member of the IL-1 family. *J. Allergy Clin. Immunol.***103,** 11–24 (1999).

167. Sagoo, P. *et al.* In vivo imaging of inflammasome activation reveals a subcapsular macrophage burst response that mobilizes innate and adaptive immunity. *Nat. Med.***22,** 64–71 (2016).

168. Ding, X. *et al.* TNF receptor 1 mediates dendritic cell maturation and CD8 T cell response through two distinct mechanisms. *J. Immunol.***187,** 1184–1191 (2011).

169. Talmadge, J. E. & Gabrilovich, D. I. History of myeloid-derived suppressor cells. *Nat. Rev. Cancer***13,** 739–52 (2013).

170. Nagaraj, S., Youn, J.-I. & Gabrilovich, D. I. Reciprocal Relationship between Myeloid-Derived Suppressor Cells and T Cells. *J. Immunol.***191,** 17–23 (2013).

171. Laurent, P. E. *et al.* Evaluation of the clinical performance of a new intradermal vaccine administration technique and associated delivery system. *Vaccine***25,** 8833–8842 (2007).

172. Igyártó, B. Z. & Kaplan, D. H. Antigen presentation by Langerhans cells. *Curr. Opin. Immunol.***25,** 115–119 (2013).

173. Montagne, J. R. La, Ph, D. & Fauci, A. S. Intradermal Influenza Vaccination — Can Less Be More ? *N. Engl. J. Med.***351,** 2330–2332 (2004).

174. Belshe, R. B. *et al.* Comparative immunogenicity of trivalent influenza vaccine administered by intradermal or intramuscular route in healthy adults. *Vaccine***25,** 6755–6763 (2007).

175. Roozbeh, J. *et al.* Low dose intradermal versus high dose intramuscular hepatitis B vaccination in patients on chronic hemodialysis. *Asaio J.***51,** 242–245 (2005).

176. Mohanan, D. *et al.* Administration routes affect the quality of immune responses: A cross-sectional evaluation of particulate antigen-delivery systems. *J. Control. Release***147,** 342–9 (2010).

177. Leung-Theung-Long, S. *et al.* A Novel MVA-Based Multiphasic Vaccine for Prevention or

Treatment of Tuberculosis Induces Broad and Multifunctional Cell-Mediated Immunity in Mice and Primates. *PLoS One***10,** e0143552 (2015).

178. Gómez, C. E. *et al.* Systems Analysis of MVA-C Induced Immune Response Reveals Its Significance as a Vaccine Candidate against HIV/AIDS of Clade C. *PLoS One***7,** e35485 (2012).

179. Pejoski, D. *et al.* Identification of vaccine-altered circulating B cell phenotypes using mass cytometry and a two-step clustering analysis. *J. Immunol.***in press,** (2016).

180. Tricot, S. *et al.* Evaluating the efficiency of isotope transmission for improved panel design and a comparison of the detection sensitivities of mass cytometer instruments. *Cytometry. A***87,** 357–68 (2015).

181. Finck, R. *et al.* Normalization of mass cytometry data with bead standards. *Cytom. Part A***83 A,** 483–494 (2013).

182. Kotecha, N., Krutzik, P. O. & Irish, J. M. Web-based analysis and publication of flow cytometry experiments. *Curr. Protoc. Cytom.***Chapter 10,** 1–24 (2010).

183. Linderman, M. D. *et al.* CytoSPADE: High-performance analysis and visualization of high-dimensional cytometry data. *Bioinformatics***28,** 2400–2401 (2012).

184. Newell, E. W., Sigal, N., Bendall, S. C., Nolan, G. P. & Davis, M. M. Cytometry by Time-of-Flight Shows Combinatorial Cytokine Expression and Virus-Specific Cell Niches within a Continuum of CD8 + T Cell Phenotypes. *Immunity***36,** 142–152 (2012).

185. Seubert, A., Monaci, E., Pizza, M., O'Hagan, D. T. & Wack, A. The adjuvants aluminum hydroxide and MF59 induce monocyte and granulocyte chemoattractants and enhance monocyte differentiation toward dendritic cells. *J. Immunol.***180,** 5402–5412 (2008).

186. Galli, S. J., Borregaard, N. & Wynn, T. a. Phenotypic and functional plasticity of cells of innate immunity: macrophages, mast cells and neutrophils. *Nat. Immunol.***12,** 1035–44 (2011).

187. Colonna, M. & Facchetti, F. TREM-1 (triggering receptor expressed on myeloid cells): a new player in acute inflammatory responses. *J Infect Dis***187 Suppl ,** S397–401 (2003).

188. Serhan, C. N. *et al.* Resolution of inflammation: state of the art, definitions and terms. *FASEB*

*J.***21,** 325–332 (2007).

189. Ibrahim, M. M. Subcutaneous and visceral adipose tissue: Structural and functional differences. *Obes. Rev.***11,** 11–18 (2010).

190. Hausman, G. J. & Richardson, R. L. Adipose tissue angiogenesis 1,2. *J Anim Sci* (2003). doi:10.1038/ijo.2010.180

191. Rasmussen, A. L. *et al.*Delayed inflammatory and cell death responses are associated with reduced pathogenicity in Lujo virus-infected cynomolgus macaques. *J. Virol.***89,** 2543–52 (2015).

192. Megiovanni, A. M., Gluckman, J. C., Boudaly, S. & Candida, D. Polymorphonuclear neutrophils deliver activation signals and antigenic molecules to dendritic cells : a new link between leukocytes upstream of T lymphocytes and mutually influence the two leukocyte popula- cesses occurring upstream of the interactions be. **79,** (2006).

193. Castillo, P. & Kolls, J. K. IL-10: A Paradigm for Counterregulatory Cytokines. *J. Immunol.***197,** 1529–1530 (2016).

194. Buggins, a G. *et al.* Effect of costimulation and the microenvironment on antigen presentation by leukemic cells. *Blood***94,** 3479–3490 (1999).

195. Kupper, T. & Fuhlbrigge, R. Immune surveillance in the skin: mechanisms and clinical consequences. *Nat. Rev. Immunol.***4,** 211–222 (2004).

196. Hansen, S. G. *et al.* Effector memory T cell responses are associated with protection of rhesus monkeys from mucosal simian immunodeficiency virus challenge. *Nat. Med.***15,** 293–299 (2009).

197. Kasturi, S., Skountzou, I. & Albrecht, R. Programming the magnitude and persistence of antibody responses with innate immunity. *Nature***470,** 543–547 (2011).

198. Li, S. *et al.* Molecular signatures of antibody responses derived from a systems biology study of five human vaccines. *Nat. Immunol.***15,** 195–204 (2014).

199. Palucka, K., Banchereau, J. & Mellman, I. Designing vaccines based on biology of human

dendritic cell subsets. *October***33,** 464–478 (2011).

200. Matthews, K. *et al.* Clinical Adjuvant Combinations Stimulate Potent B-Cell Responses In Vitro by Activating Dermal Dendritic Cells. *PLoS One***8,** e63785 (2013).

201. Kwissa, M. *et al.* Adjuvanting a DNA vaccine with a TLR9 ligand plus Flt3 ligand results in enhanced cellular immunity against the simian immunodeficiency virus. *J. Exp. Med.***204,** 2733–46 (2007).

202. Souza, J. De & Gottfried, C. Muscle injury: Review of experimental models. *J. Electromyogr. Kinesiol.***23,** 1253–1260 (2013).

203. Pillon, N. J., Bilan, P. J., Fink, L. N. & Klip, A. Cross-talk between skeletal muscle and immune cells: muscle-derived mediators and metabolic implications. *Am. J. Physiol. Endocrinol. Metab.***304,** E453–65 (2013).

204. Arnold, L. *et al.* Inflammatory monocytes recruited after skeletal muscle injury switch into antiinflammatory macrophages to support myogenesis. *J Exp Med***204,** 1057–1069 (2007).

205. Mosca, F. *et al.* Molecular and cellular signatures of human vaccine adjuvants. *Proc. Natl. Acad. Sci. U. S. A.***105,** 10501–6 (2008).

206. Samuvel, D. J., Sundararaj, K. P., Nareika, A., Lopes-Virella, M. F. & Huang, Y. Lactate boosts TLR4 signaling and NF-kappaB pathway-mediated gene transcription in macrophages via monocarboxylate transporters and MD-2 up-regulation. *J. Immunol. (Baltimore, Md. 1950)***182,** 2476–2484 (2009).

207. Carlsson, H. E., Schapiro, S. J., Farah, I. & Hau, J. Use of primates in research: A global overview. *Am. J. Primatol.***63,** 225–237 (2004).

208. Earl, P. L. *et al.* Immunogenicity of a highly attenuated MVA smallpox vaccine and protection against monkeypox. *Nature***428,** 182–185 (2004).

209. Pathan, A. a *et al.* Effect of vaccine dose on the safety and immunogenicity of a candidate TB vaccine, MVA85A, in BCG vaccinated UK adults. *Vaccine***30,** 5616–24 (2012).

210. Caskey, M. *et al.* Synthetic double-stranded RNA induces innate immune responses similar to

a live viral vaccine in humans. *J. Exp. Med.***208,** 2357–66 (2011).

211. Ammi, R. *et al.* Poly(I:C) as cancer vaccine adjuvant: Knocking on the door of medical breakthroughs. *Pharmacol. Ther.***146,** 120–131 (2015).

212. Tewari, K. *et al.* Poly(I:C) is an effective adjuvant for antibody and multi-functional CD4+ T cell responses to Plasmodium falciparum circumsporozoite protein (CSP) and ??DEC-CSP in non human primates. *Vaccine***28,** 7256–7266 (2010).

213. Rimaniol, A.-C., Gras, G. & Clayette, P. In vitro interactions between macrophages and aluminum-containing adjuvants. *Vaccine***25,** 6784–92 (2007).

214. Denning, T. L., Wang, Y., Patel, S. R., Williams, I. R. & Pulendran, B. Lamina propria macrophages and dendritic cells differentially induce regulatory and interleukin 17-producing T cell responses. *Nat. Immunol.***8,** 1086–94 (2007).

215. Nathan, C. Neutrophils and immunity: challenges and opportunities. *Nat. Rev. Immunol.***6,** 173–182 (2006).

216. Saclier, M., Cuvellier, S., Magnan, M., Mounier, R. & Chazaud, B. Monocyte/macrophage interactions with myogenic precursor cells during skeletal muscle regeneration. *FEBS J.***280,** 4118–4130 (2013).

217. Brigitte, M. *et al.* Muscle resident macrophages control the immune cell reaction in a mouse model of notexin-induced myoinjury. *Arthritis Rheum.***62,** 268–79 (2010).

218. Tidball, J. G. & Villalta, S. A. Regulatory interactions between muscle and the immune system during muscle regeneration. *Am. J. Physiol. Regul. Integr. Comp. Physiol.***298,** R1173–87 (2010).

219. Watson, N. B., Schneider, K. M. & Massa, P. T. SHP-1–Dependent Macrophage Differentiation Exacerbates Virus-Induced Myositis. (2016). doi:10.4049/jimmunol.1402210

220. Muzio, M. *et al.* Differential expression and regulation of toll-like receptors (TLR) in human leukocytes: selective expression of TLR3 in dendritic cells. *J. Immunol.***164,** 5998–6004 (2000).

221. Miller, L. S. Toll-Like Receptors in Skin. *Adv. Dermatol.***24,** 71–87 (2008).

222. Schreiner, B. *et al.*Expression of toll-like receptors by human muscle cells in vitro and in vivo: TLR3 is highly expressed in inflammatory and HIV myopathies, mediates IL-8 release and up-regulation of NKG2D-ligands. *FASEB J.***20,** 118–120 (2006).

223. Sugimoto, C. *et al.* Differentiation Kinetics of Blood Monocytes and Dendritic Cells in Macaques: Insights to Understanding Human Myeloid Cell Development. *J. Immunol.***195,** 1774–1781 (2015).

224. Autissier, P., Soulas, C., Burdo, T. H. & Williams, K. C. Immunophenotyping of lymphocyte, monocyte and dendritic cell subsets in normal rhesus macaques by 12-color flow cytometry: Clarification on DC heterogeneity. *J. Immunol. Methods***360,** 119–128 (2010).

225. Wang, Y., Lavender, P., Watson, J., Arno, M. & Lehner, T. Stress-activated dendritic cells (DC) induce dual interleukin (IL)-15- and IL1b-mediated pathways, which may elicit CD4+memory T cells and interferon (IFN)-stimulated genes. *J. Biol. Chem.***290,** 15595–15609 (2015).

226. Ovsyannikova, I. G. *et al.* Impact of cytokine and cytokine receptor gene polymorphisms on cellular immunity after smallpox vaccination. *Gene***510,** 59–65 (2012).

227. Bennouna, S., Bliss, S. K., Curiel, T. J. & Denkers, E. Y. Cross-Talk in the Innate Immune System: Neutrophils Instruct Recruitment and Activation of Dendritic Cells during Microbial Infection. *J. Immunol.***171,** 6052–6058 (2003).

228. Gómez, C. E. *et al.* Virus distribution of the attenuated MVA and NYVAC poxvirus strains in mice. *J. Gen. Virol.***88,** 2473–8 (2007).

229. Subramanian, A. *et al.* Gene set enrichment analysis: a knowledge-based approach for interpreting genome-wide expression profiles. *Proc. Natl. Acad. Sci. U. S. A.***102,** 15545–50 (2005).

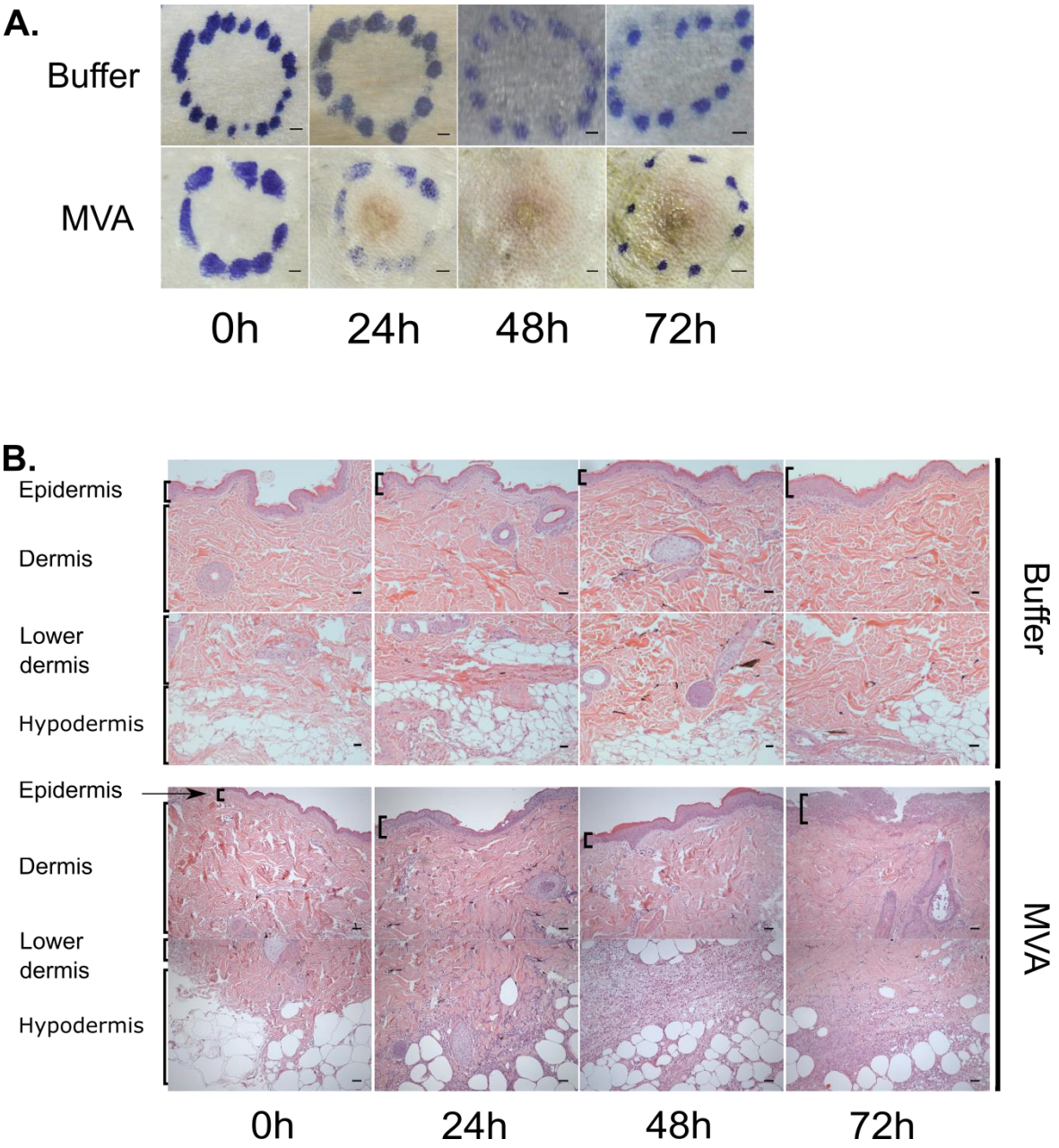

Figure 1.Skin reaction following rMVA i.d. injection

(A) Photography of the skin before and after rMVA/Buffer injection (24-48-72h). Crop of the zone of interest was performed and then resized. Felt pen delimits the area of injection. One representative experiment out of 3 is shown. Scale Bar equals 2 mm. (B) Skin biopsies of NHP were sampled using 8mm diameter punch at 0h, 24h, 48h and 72h post rMVA/Bufferinjection. Biopsy were fixed in paraformaldehyde 4% during 24h and then embedded in paraffin. Transversal sections were then performed and stained with HE coloration. Scale bar equals to 100µm. One representative experiment out of 2.

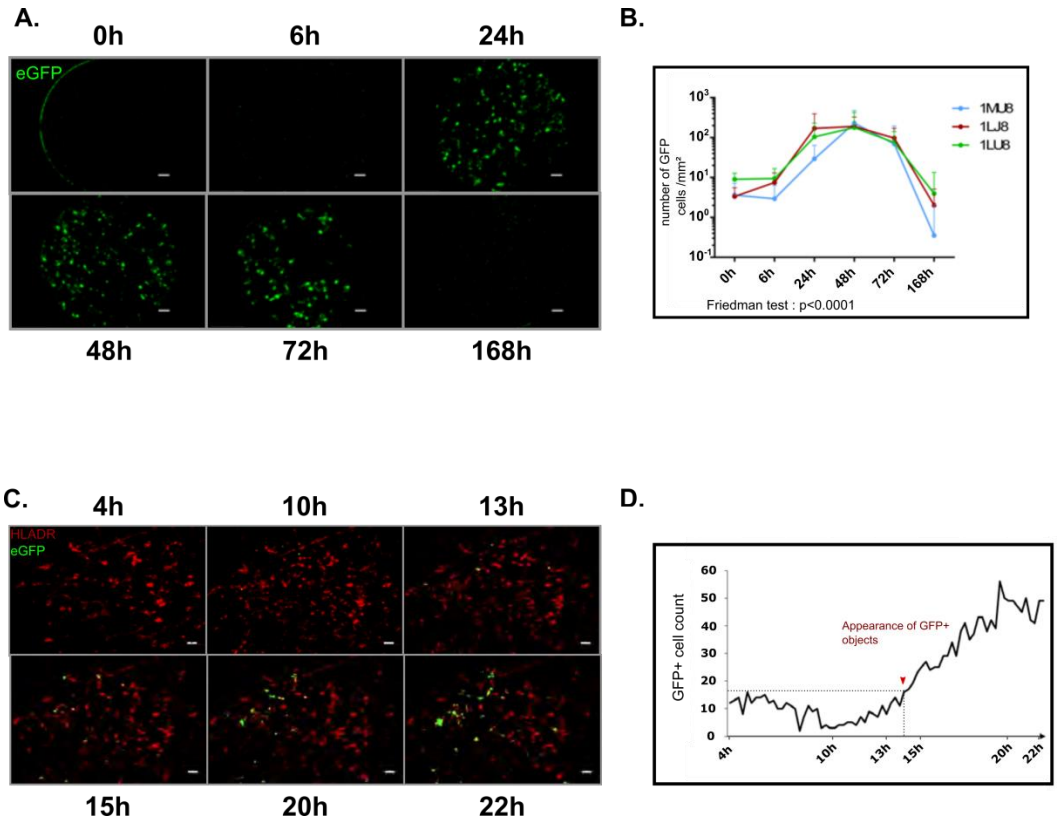

Figure 2 Dynamics of local rMVA infection following intradermal injection

(A) Representative images of 30 second videos recording local eGFP signal using*in vivo* confocal endomicroscopy. The site of injection was swept by a probe at around 150µm in depth in the skin (dermis). Scale bar equals 50µm. (B) The graphicindicates the number of GFP+ cells/mm² determined by counting GFP+ object >20µm² and selecting for each animals at each timepoints (with mean±SD) the 50 frames expressing the most important number of GFP+ cells. (C) Images of HLADR+ (in red) and GFP+ (in green) cells over time on skin. 4h post *in vivo* MVAeGFP and HLADR antibody injections, skin biopsies were gathered and then observed during 18h in time-lapse videoconfocal microscopy. The acquisition was performed from 50 to 150µm in depth in the skin (dermis) corresponding to a stack of 10 images. Visual representations correspond to a two dimension visualization of this stack at indicated timepoints, after a crop of the region of interest. Scale bar equals to 20µm. (D)The graphic indicates the number of GFP+ cells counted for each image (1 image per 15 minutes) during the 18h acquisition at the region of interest. Green objects between 200µm^3 and 4000µm^3 were counted as GFP+ cells. The approximate time of appearance of non-background GFP+ cells is indicated in red. The only successful experiment is shown.

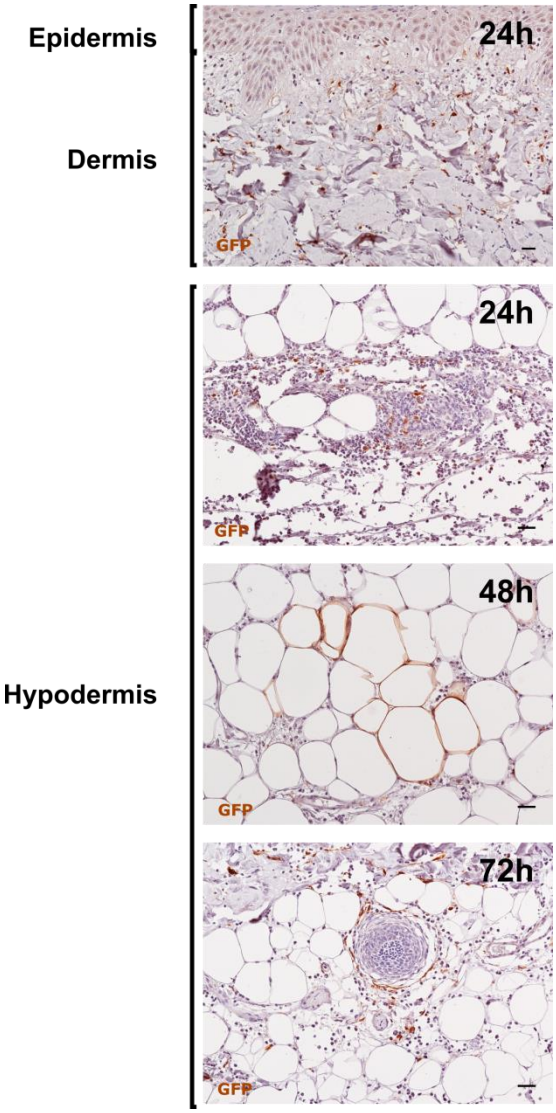

Figure 3.MVA infected cells localization and nature

Skin biopsies of NHP were sampled using 8mm diameter punch, fixed in paraformaldehyde 4% during 24h and then embedded in paraffin.Paraffin-embedded skin was stained using an anti-GFP antibody and then colored in HE. Transversal section of the skin biopsy was then performed. GFP+ cells are labeled in brown. Scale bar equals 100µm. One representative experiment of 2 is shown.

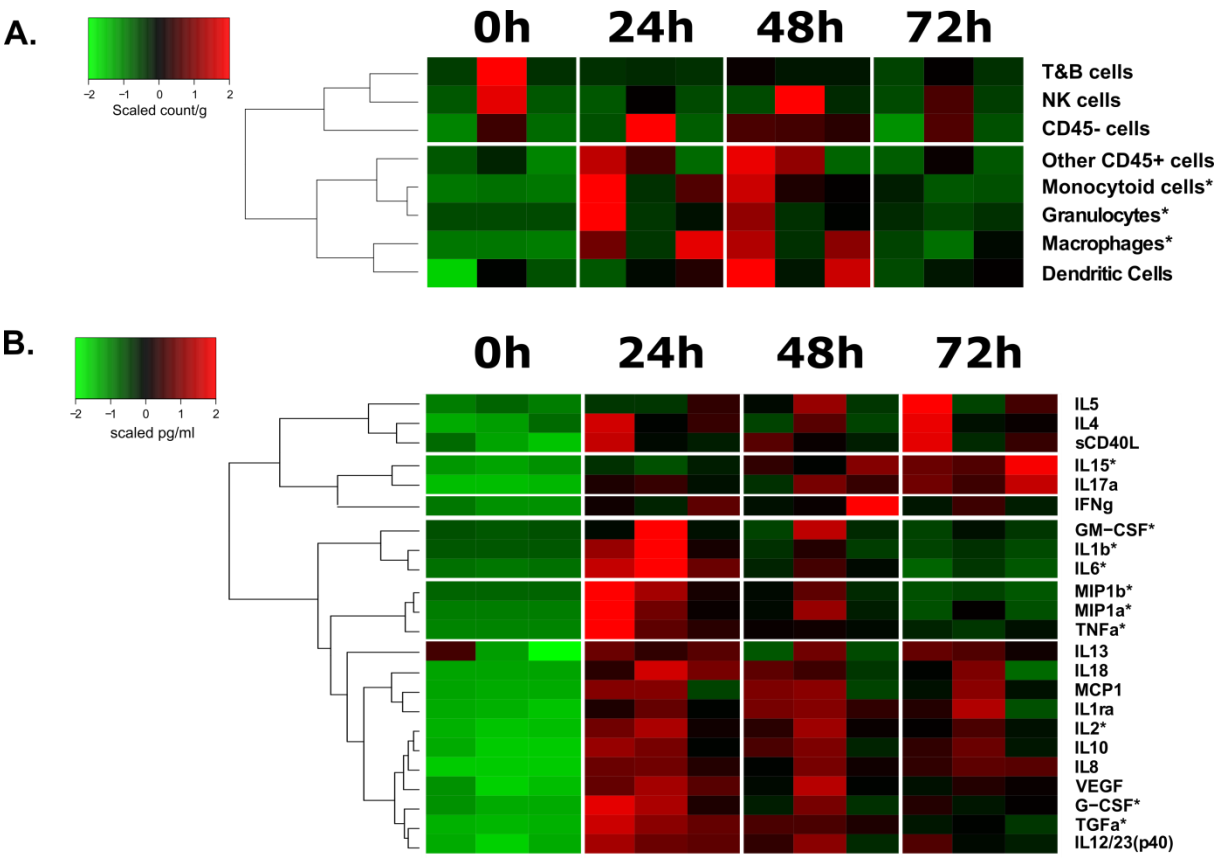

Figure 4.Local MVA induced cellular trafficking and cytokine releasing

(A) Heatmap representation of cell populations discriminated using flow cytometry in the skin. Cell populations were automatically based on their phenotypic proximity following a hierarchical clustering represented with dendrograms on the left. A single skin biopsy per condition was digested and then transformed in a cellular suspension. The number of cells was calculated dividing the number of events by the initial weight of the biopsy. In order to see correctly the kinetics, data for each cell population were normalized by subtracting the mean and dividing by the standard deviation .Proportionally low amount of cells corresponds to green coloration and high amounts of cells to a red coloration (n=3). Cell populations were discriminated by flow cytometry based on a gating strategy detailed in Figure S2A. (B)Heatmap representation of cytokine release on the skin over time post MVA injection. Cytokines releasing was automatically sorted following a hierarchical clustering represented with dendrograms on the left. Cytokine production on the skin was evaluated collecting medium collagenase supernatant used to extract cells from the biopsy. The concentration of cytokines was expressed in pg/ml.In order to see correctly the kinetics, data for each cytokine population were normalized by subtracting the mean and dividing by the standard deviation. Proportionallylow amount of cytokines corresponds to green coloration and high amounts of cells to a red coloration (n=3). Stars indicated on the right of the cell population/cytokines correspond to significance of a Friedman's test over time (*: 0.05>p-value>0.01).

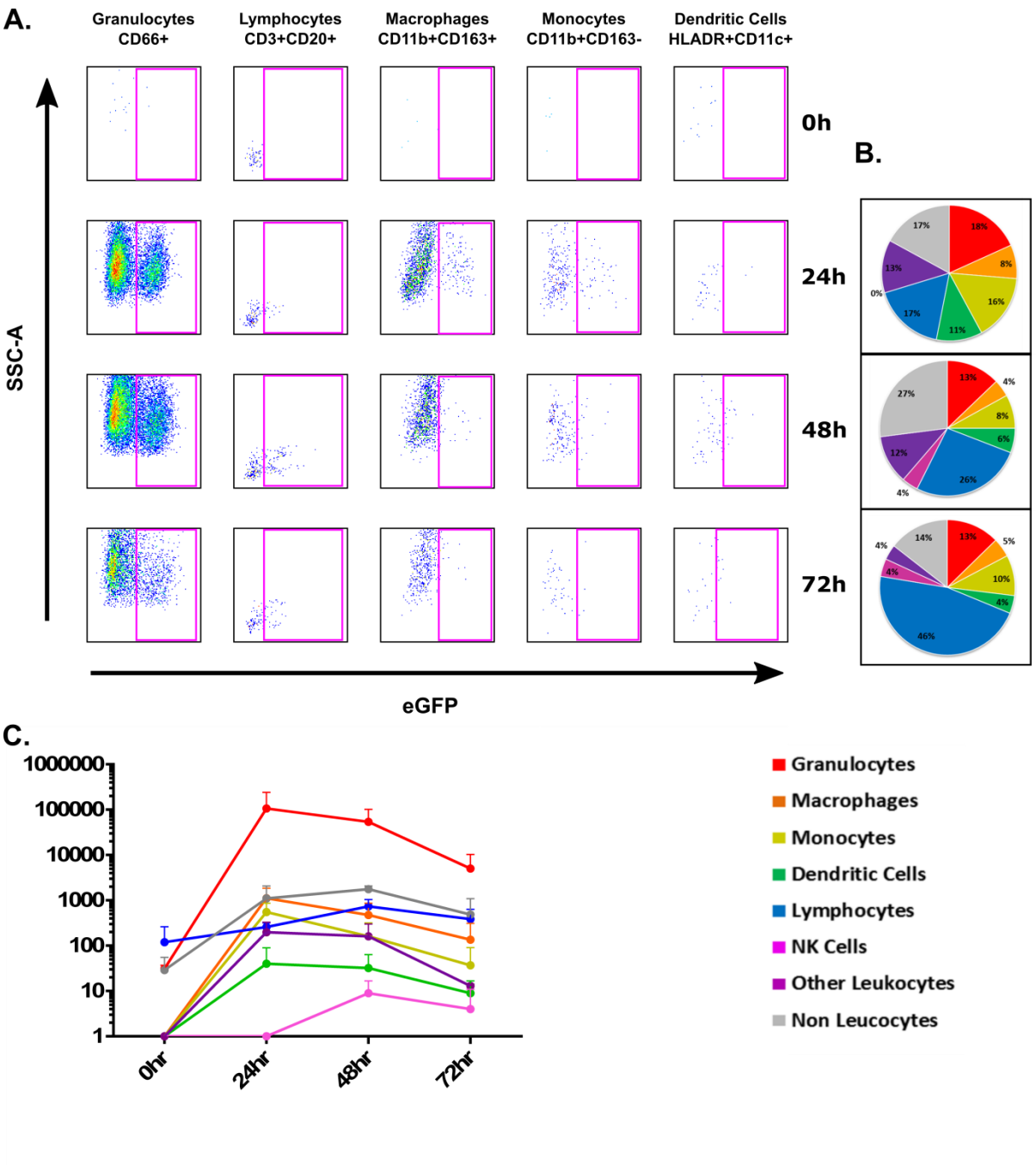

Figure 5. MVA infects a wide set of skin cells

(A) Dot plot representation of the percentage of MVA-infected cells of the main immune skin cell population. One representative experiment of three is shown. (B) Pie charts representation of the distribution of GFP+ cells among each cell population of the skin at 24h, 48h and 72h post-MVA injection (Mean; n=3). (C) Graphic indicating the number of GFP+ cells per gram of skin biopsy. Mean+SD is also indicated for each cell population (n=3).

One single skin biopsy per condition was gathered, digested, stained, and acquired in flow cytometry. Cell populations were discriminated by flow cytometry based on a gating strategy detailed in Figure S2A.

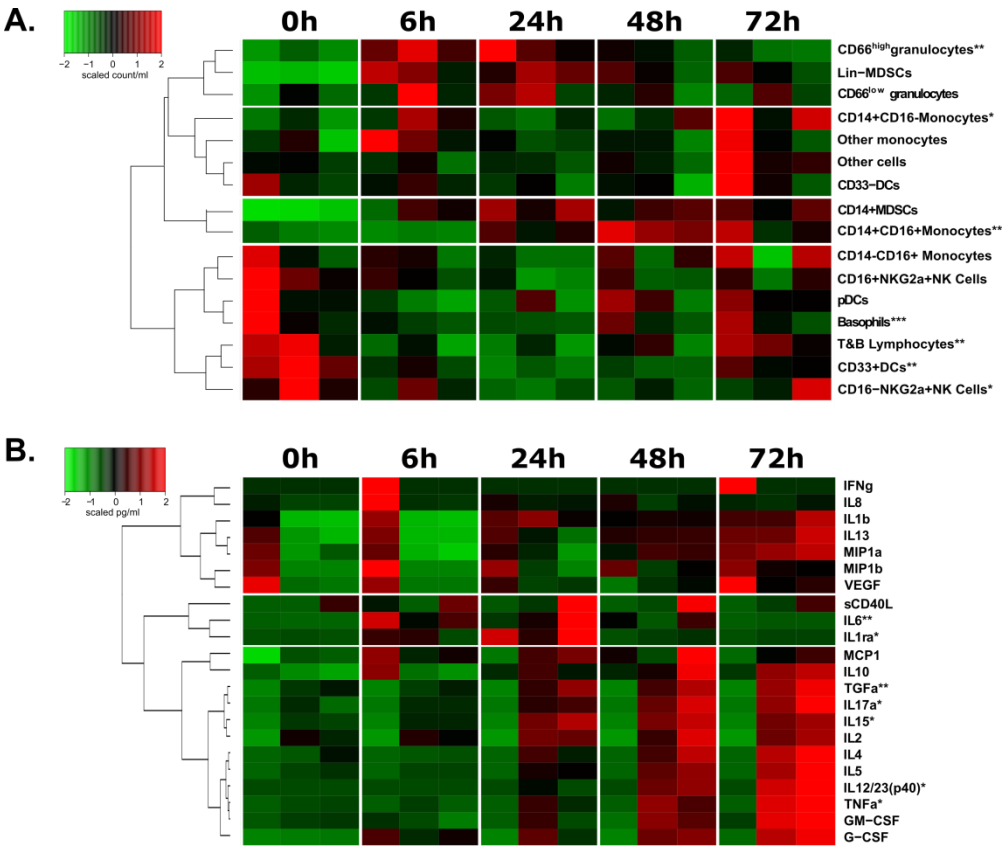

Figure6.Systemic MVA induced cellular trafficking and cytokine releasing. (A)Heatmap representation of cell populations discriminated using flow cytometry in the blood. Cell populations were automatically sorted following a hierarchical clustering represented with dendrograms on the left. 100µL of fresh blood was stained for a flow cytometry analysis. Absolute values were obtained multiplicating the cell count obtained in flow cytometry of a given cell population by the CBC number of leukocytes divided by the count of total blood cells obtained by flow cytometry. In order to see correctly the kinetics, data for each cell population were normalized by subtracting the mean and dividing by the standard deviation. Proportionally low amount of cells corresponds to green coloration and high amounts of cells to a red coloration (n=3). Cell populations were discriminated by flow cytometry based on a gating strategy detailed in Figure S2B. (B) Heatmap representation of cytokine release in the blood over time post MVA injection. Cytokines releasing was automatically sorted following a hierarchical clustering represented with dendrograms on the left. Cytokine production was evaluated collecting plasma from whole blood at each timepoint. The concentration of cytokines was expressed in pg/ml. In order to see correctly the kinetics, data for each cytokine population were normalized by subtracting the mean and dividing by the standard deviation. Proportionallylow amount of cytokines corresponds to green coloration and high amounts of cells to a red coloration (n=3). Stars indicated on the right of the cell population/cytokines correspond to significance of a Friedman's test over time(*: 0.05>p-value>0.01; **: 0.01>p-value> 0.001; ***: 0.001>p-value).

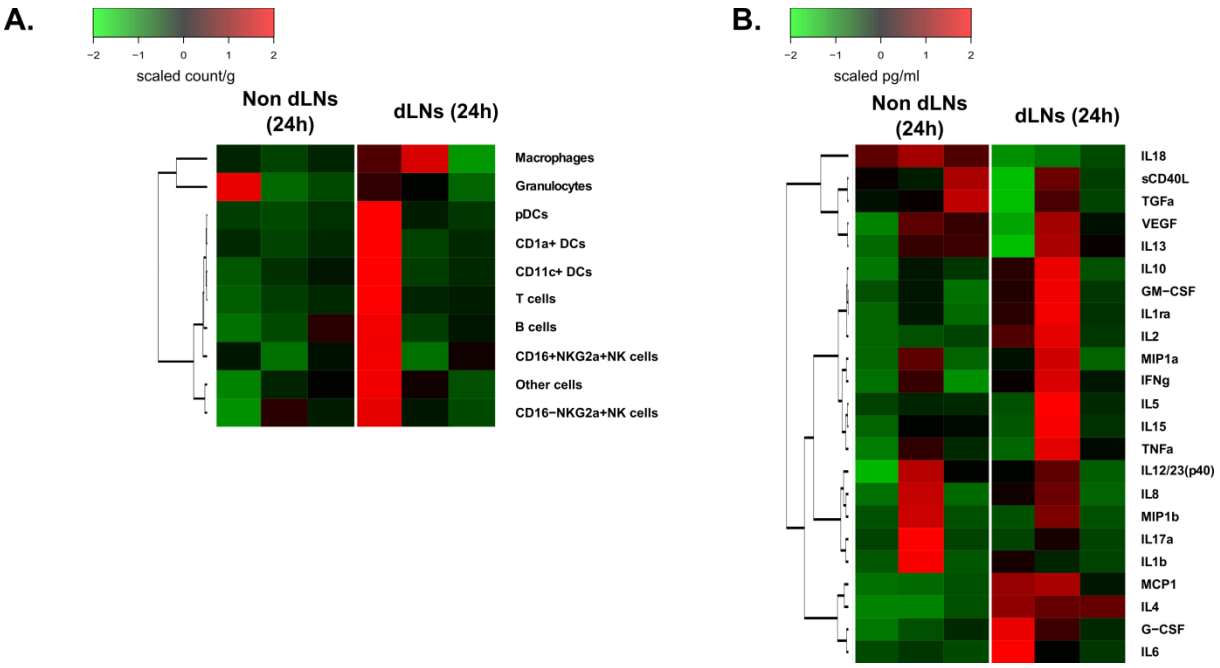

Figure 7.Lymph Node MVA induced cellular trafficking and cytokine releasing. (A)Heatmap representation of cell populations discriminated using flow cytometry in the opposite and draining lymph node 24h after MVA intradermal injection. Cell populations were automatically sorted following a hierarchical clustering represented with dendrograms on the left. A single lymph node was weighed and stained for a flow cytometry analysis. The number of cells was calculated dividing the number of events by the initial weight of the biopsy. In order to see correctly the kinetics, data for each cell population were normalized by subtracting the mean and dividing by the standard deviation. Proportionally low amount of cells corresponds to green coloration and high amounts of cells to a red coloration (n=3). Cell populations were discriminated by flow cytometry based on a gating strategy detailed in Figure S2C.

(B) Heatmap representation of cytokine release in the draining lymph node post MVA injection. Cytokines releasing was automatically sorted following a hierarchical clustering represented with dendrograms on the left. Cytokine production was evaluated collecting digestion medium of the lymph node. The concentration of cytokines was expressed in pg/ml. In order to see correctly the kinetics, data for each cytokine population were normalized by subtracting the mean and dividing by the standard deviation. Proportionallylow amount of cytokines corresponds to green coloration and high amounts of cells to a red coloration (n=3)

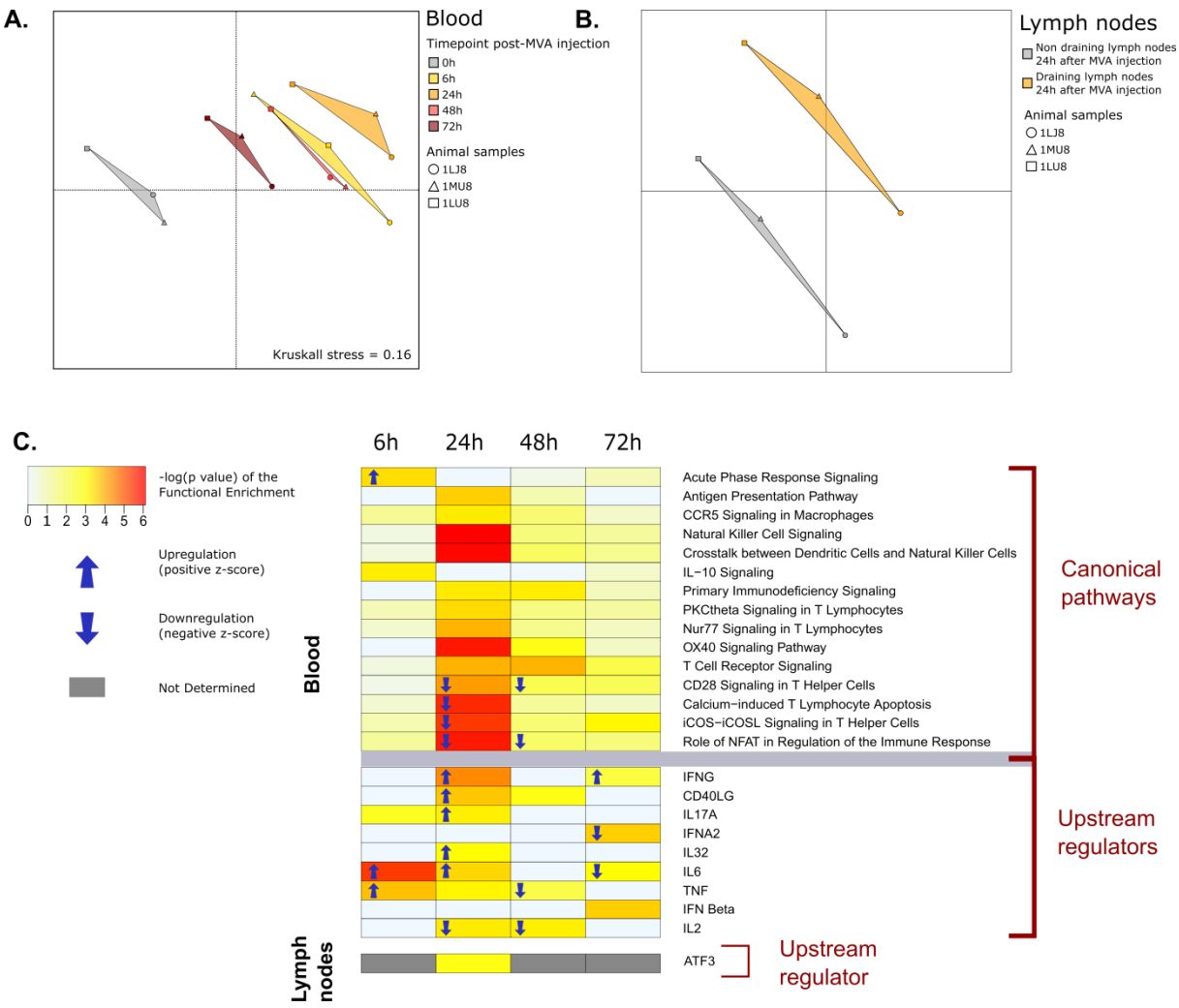

Figure 8.Transcriptomic analysis of blood and lymph nodes. (A) Multidimensional scaling representation (MDS) of transcriptomic signatures from blood µarray assay after 0h, 6h, 24h, 48h and 72h post-MVA injection. Biological samples were represented in a two dimension scale and correspond to geometric forms at the edge of the triangles. Differential gene expression between samples is translated into Euclidian distance between the samples (n=3). (B) Multidimensional scaling representation (MDS) of transcriptomic signatures from lymph node µarray assay between non-draining and draining inguinal lymph node 24h post-MVA injection. Biological samples were represented in a two dimension scale and correspond to the geometric forms at the edge of the triangles. Differential gene expression between samples is translated into Euclidian distance between the samples (n=3). (C) Heatmap representation of the functional enrichment (expressed in -log(p-value, cutoff –log(p-value)>3 for at least one timepoint)). Data extracted from lists of fold change of differentially expressed genes in comparison with baseline in the blood, and with non-draining lymph node for the lymph node condition. Only differentially expressed upstream regulators and canonical pathways linked to the immune response were represented. Arrows orientation correspond to the sign of the z-score, indicating if the pathway or the regulator is up- or down-regulation (n=3).

A.

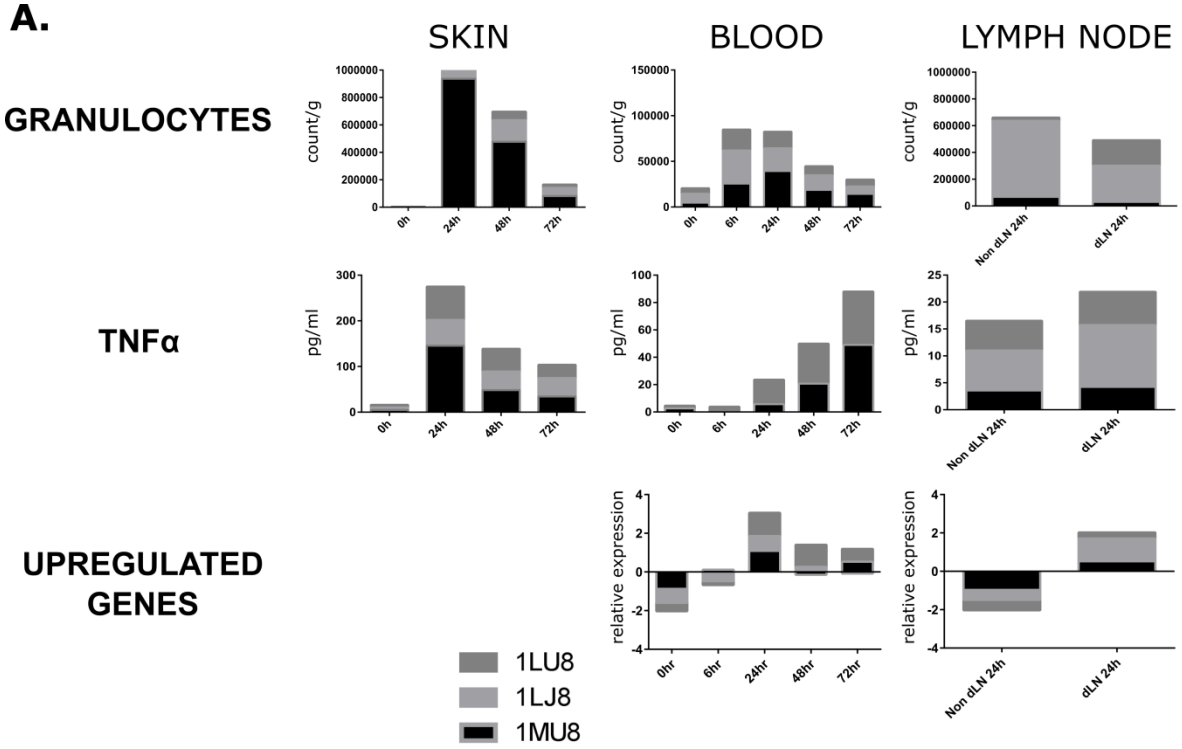

B.

	Parameters (q-value)	SKIN		BLOOD			LYMPH NODES		
		GRANULOCYTES	TNFα	GRANULOCYTES	TNFα	UPREGULATED GENES	GRANULOCYTES	TNFα	UPREGULATED GENES
SKIN	GRANULOCYTES		0,037	0,058	0,664	0,625	0,418	0,735	0,926
	TNFα			0,011	0,908	0,115	0,998	0,972	0,496
BLOOD	GRANULOCYTES				0,883	0,290	0,972	0,951	0,462
	TNFα					0,624			
	UPREGULATED GENES						0,836	0,675	0,120
LYMPH NODES	GRANULOCYTES							0,448	0,719
	TNFα								0,573
	UPREGULATED GENES								

significant correlation

not significant correlation

Figure 9. Histogram representation and correlation calculation of few biological variables

(A) Cumulated histogram representation of eight biological parameters over the time. Up-regulated genes refer to a cluster of differentially expressed genes being upregulated over the time. (B) Table of Pearsons correlation calculation results between the parameters. In green are shown significant correlations between two values (Pearson's correlation R>0.8 or R<0.8;q-value0.05 rounded down). In red are shown non- significant correlations between two values.

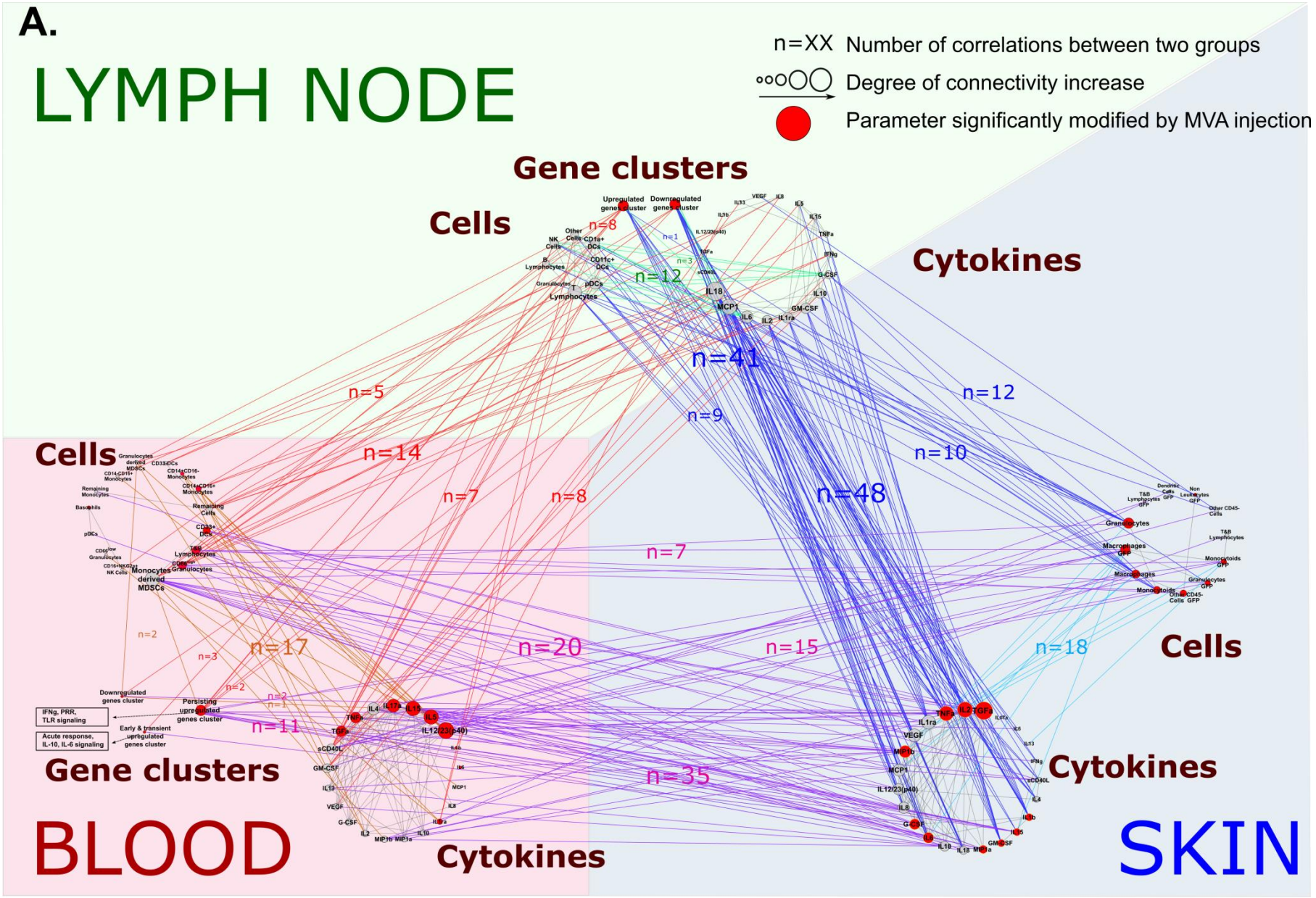
A.
LYMPH NODE
n=XX Number of correlations between two groups
Degree of connectivity increase
Parameter significantly modified by MVA injection
Gene clusters
Cells
Cytokines
n=8
n=1
n=3
n=12
n=41
n=5
n=9
n=12
n=14
n=7
n=8
n=10
n=48
n=7
Cells
n=2
n=3
n=17
n=20
n=15
n=18
Cells
n=2
n=2
n=1
n=11
n=35
Gene clusters
Cytokines
BLOOD
Cytokines
SKIN

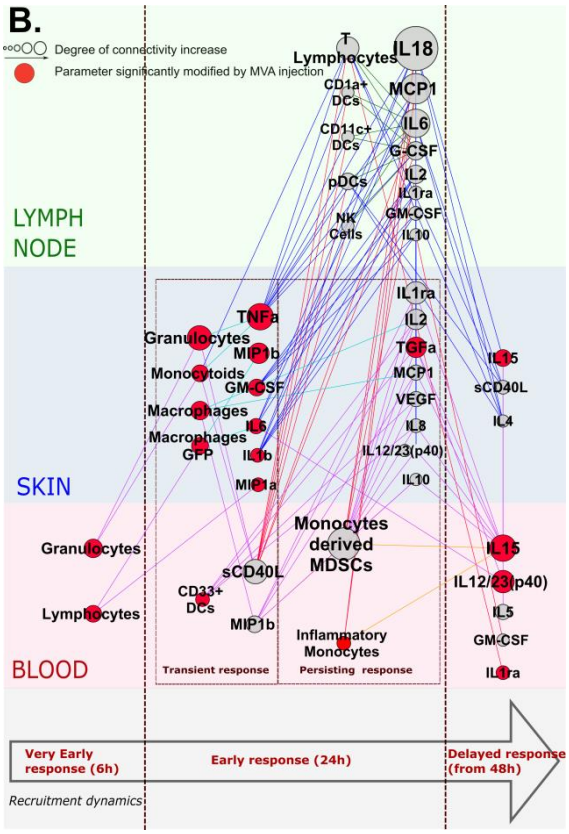

Figure 10.The magnitude of the inflammatory response in the blood and in the skin is correlated with dendritic cell recruitment and cytokine production in the lymph node.(A) Coexpression network showing the correlations between each biological variable evaluated. Data were sorted in groups depending on the compartment (blood, lymph node, or skin) and their type (cytokine, cell or gene cluster). Variables were then sorted depending on their size which is proportional with the number of significant correlation (degree of connectivity). All lines linking two parameters correspond to a significant correlation between those variables (R>0.8 or R<-0.8, q<0.05 rounded down). Circles filled by red surrounded by yellow correspond to variables significantly modified over time by MVA injection following Friedman's test. Values (n) indicated between two groups correspond to the number of correlation between groups. Each Circle represents a parameter analyzed in Luminex analysis, flow cytometry or µarray. For the transcriptomics, we separated in gene clusters differentially expressed markers having the same kinetic profile to obtain one single value to simplify the representation. Canonical pathways associated with the gene clusters were also represented. It additionally includes data gathered in draining lymph node in untreated and 24h post intradermal MVA injection. Details of all those raw data are available in supplementary table 1. (B)Sorted co-expression network based on the kinetic of recruitment andmost correlated variables (number of inter-group correlation > 5). Data were sorted depending on their compartment, their type, but also their kinetic and their peak of expression after MVA injection. Correlations between very different kinetic were also removed for a better understanding of the illustration.

Supplementary Figures

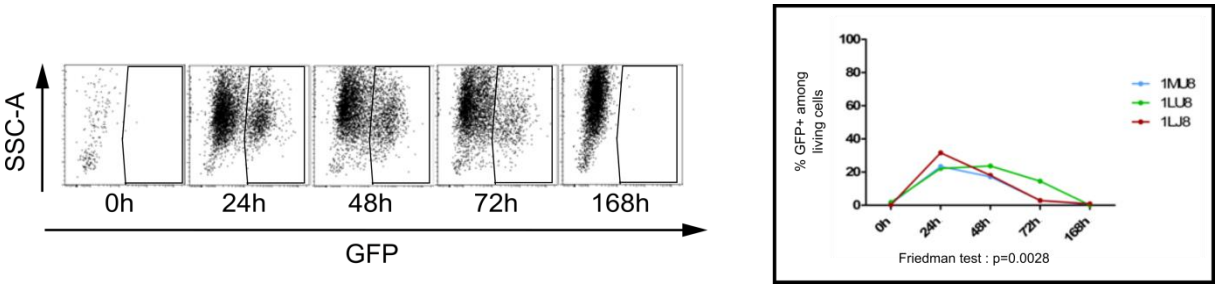

Supplementary Figure 1 Flow cytometry dot plots show the percentage of GFP+ cells expression over time among living cells from a digested skin biopsy (n=3). One representative experiment of 3 is shown.

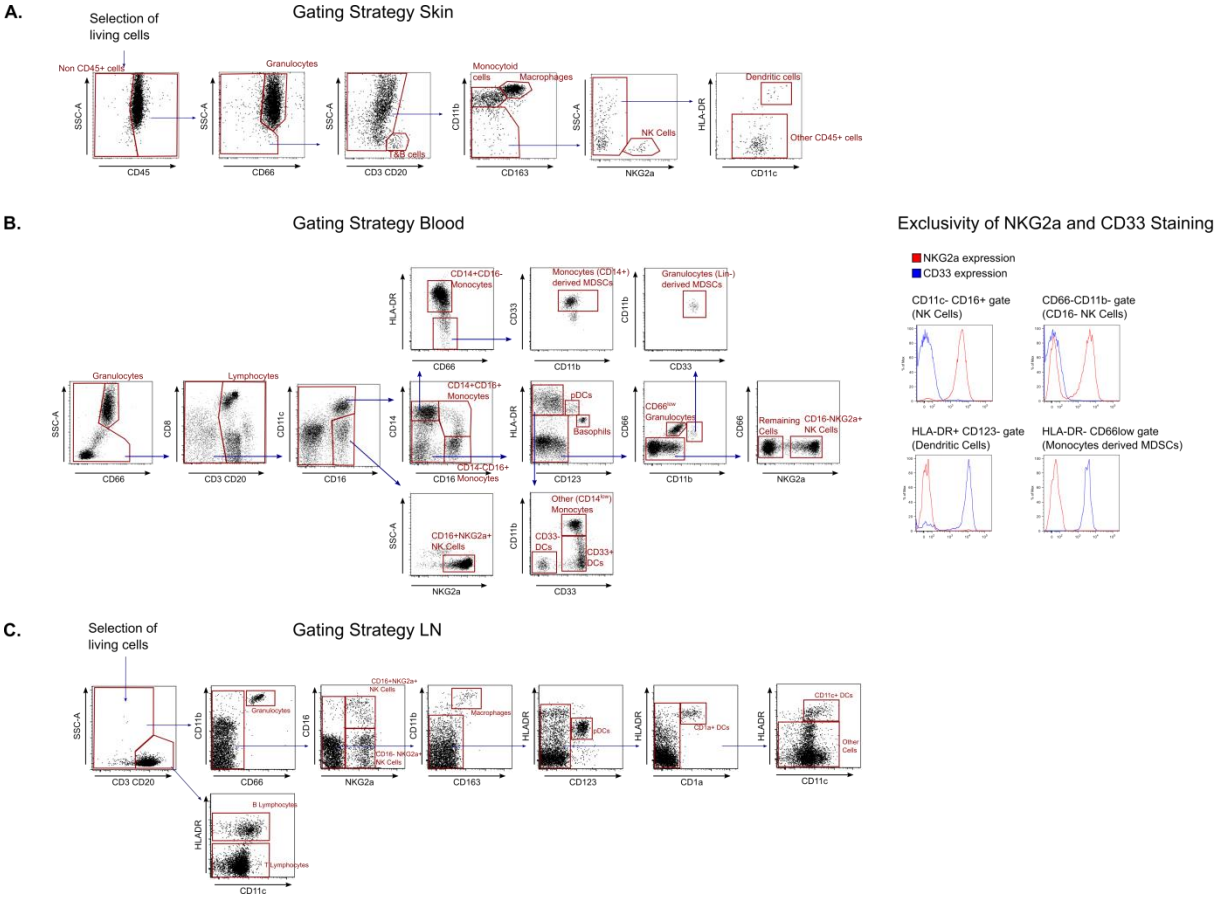

Supplementary Figure 2.Gating strategies for flow cytometry analysis (A) Dot plots showing the gating strategy of skin cells. 8mm skin biopsies were cut and digested in collagenase in order to obtain a cell suspension. Cells were then stained using a 12-color panel. Doublet and debris were removed based on FSH-H, FSC-A and SSC-A. Living cells were selected based on dead cell stain negative expression. (B) Characterization of immune cell populations on the blood using multiparameter flow cytometry. 100µL of blood were stained using an 11-color panel. Gating strategy with performed after doublet removal and debris removal based on FSH-H, FSC-A and SSC-A. Due to the use of one single channel for both CD33 and NKG2a, we show in the histograms that those markers are exclusive and those not expressed in the same populations. (C) Characterization of Immune cell populations on the lymph node using multiparameter flow cytometry. On single lymph node were cut and digested in collagenase in order to obtain a cell suspension. Cells were then stained using a 12-color panel. Gating strategy with performed after doublet removal and debris removal based on FSH-H, FSC-A and SSC-A. Living cells were selected based on blue dead cell stain negative expression.

Timepoint	0hr	0hr	0hr	24hr	24hr	24hr	48hr	48hr	48hr	72hr	72hr	72hr	p-value (Friedmann's test over time)	Significance (ps0,05)
Monkey	1MU8	1LU8	1LI8	1MU8	1LU8	1LI8	1MU8	1LU8	1LI8	1MU8	1LU8	1LI8		
Skin Cell populations Flow Cytometry (count/g)														
Granulocytes	2320,00	297,95	1353,38	936939,76	129397,59	55294,12	476913,04	158198,40	62046,29	81023,84	60282,89	23769,32	0,0174	Yes
Macrophages	464,00	93,11	526,32	15216,87	22518,07	4667,93	19043,48	16579,25	4847,75	3955,12	7623,76	1129,61	0,0174	Yes
Monocytoids	80,00	93,11	225,56	6891,57	3469,88	1328,27	5565,22	2120,87	2606,58	1626,93	693,07	606,42	0,0174	Yes
Dendritic cells	32,00	242,09	375,94	228,92	433,73	360,53	840,58	718,36	341,05	252,45	381,90	344,83	0,9097	No
Lymphocytes	736,00	1340,78	26340,85	1433,73	1530,12	1745,73	4507,25	2805,02	2911,08	336,61	1499,29	4185,49	0,7274	No
NK cells	0,00	0,00	325,81	0,00	12,05	94,88	14,49	45,61	377,59	14,03	28,29	166,47	0,0764	No
CD45- cells	1712,00	2513,97	7844,61	3228,92	2939,76	15445,92	8115,94	7217,79	8014,62	1276,30	3267,33	8466,11	0,3003	No
Other CD45+ cells	544,00	186,22	977,44	2771,08	433,73	1783,68	3144,93	444,70	2399,51	532,96	551,63	1319,86	0,2066	No
Skin Cytokines Luminex (pg/mL)														
G-CSF	4,22	0,00	0,00	58,32	50,08	29,12	20,32	42,05	18,08	29,90	21,97	25,46	0,0174	Yes
GM-CSF	0,53	0,46	0,54	2,57	12,54	2,45	0,95	8,31	1,66	0,97	2,36	1,33	0,0174	Yes
IFNg	2,22	0,78	1,01	9,32	6,74	13,52	7,64	9,19	26,24	7,26	11,94	7,00	0,1476	No
IL1b	1,02	1,88	0,41	1463,48	2618,53	640,02	240,11	738,21	147,10	105,92	239,54	48,68	0,0017	Yes
IL1ra	690,06	555,29	305,69	4382,54	5656,80	3764,00	6041,41	6305,43	4779,50	4495,01	7086,34	2349,98	0,0538	No
IL2	1,38	0,55	0,81	15,69	18,78	10,95	12,20	18,08	10,56	10,24	13,89	9,38	0,0170	Yes
IL4	0,78	1,23	2,76	12,85	6,22	7,94	4,06	9,01	4,06	13,70	5,79	6,65	0,1476	No
IL5	0,81	0,92	0,81	1,15	1,15	1,66	1,37	2,17	1,15	2,99	1,09	1,77	0,1476	No
IL6	4,76	3,18	4,89	505,49	600,65	363,84	129,28	298,47	178,91	29,75	104,37	51,47	0,0017	Yes
IL8	115,14	66,95	173,35	9384,23	9491,15	7260,88	6097,30	9642,91	6706,10	7526,79	8976,41	8732,36	0,1476	No
IL10	13,69	0,00	0,00	159,30	144,13	89,71	123,20	147,92	74,61	113,64	137,42	81,12	0,0538	No
IL12/23(p40)	4,46	1,29	4,06	28,09	23,98	23,15	19,87	26,44	13,34	22,33	15,79	14,15	0,0747	No
IL13	15,48	9,87	6,48	16,44	14,99	15,97	11,75	16,56	12,04	16,33	15,85	14,23	0,3003	No
IL15	3,30	2,20	3,84	11,35	8,91	12,43	18,73	14,78	25,06	23,00	20,86	33,86	0,0017	Yes
IL17a	0,00	0,00	0,01	1,94	2,19	1,56	1,22	2,76	2,17	2,68	2,22	3,45	0,0538	No
IL18	4,98	3,99	5,41	144,65	254,37	194,24	178,20	153,93	78,40	112,37	198,66	44,77	0,0538	No
MCP1	95,65	43,51	58,31	2549,06	2545,77	912,82	2520,87	2606,86	905,14	1342,34	2627,65	1328,01	0,1476	No
MIP1a	0,00	0,00	0,00	1636,41	940,16	525,74	444,16	1081,89	385,70	176,48	491,22	175,46	0,0174	Yes
MIP1b	0,00	0,00	0,00	823,37	534,88	246,24	182,84	395,20	118,73	35,55	71,61	22,44	0,0017	Yes
sCD40L	8,40	2,77	0,00	38,39	18,15	16,30	27,83	20,46	16,30	42,05	15,37	24,61	0,1354	No
TGFa	3,73	2,83	3,66	38,54	32,81	29,03	26,63	26,90	22,70	18,06	19,89	14,90	0,0017	Yes
TNFa	4,88	5,84	5,52	145,56	73,14	56,51	48,27	49,74	40,87	34,32	28,92	40,57	0,0017	Yes
VEGF	26,22	9,13	13,57	96,02	115,09	92,58	64,99	120,98	68,12	63,38	77,82	71,46	0,0538	No
Blood Cell populations Flow Cytometry (109/L)														
CD66^{high} Granulocytes	4771,94	5988,25	9777,78	39443,22	18105,11	24880,21	18755,79	9892,62	16016,76	14422,66	7578,50	8066,98	0,0028	Yes
CD66^{low} granulocytes	7,19	17,87	45,98	79,35	28,02	98,00	37,10	10,18	57,74	18,51	27,81	67,79	0,0743	No
Basophils	85,19	7,52	17,03	1,72	0,29	1,39	35,26	0,14	8,73	46,09	1,10	12,15	0,0004	Yes
Granulocytes derived MDSCs	2,22	1,10	2,87	31,22	39,20	46,79	36,68	13,89	27,90	36,36	16,29	26,17	0,0559	No
CD14+CD16- Monocytes	402,76	326,61	585,80	471,49	596,76	421,85	421,03	881,99	588,82	1333,28	1174,86	641,84	0,0284	Yes
CD14+CD16+ Monocytes	150,13	71,33	94,72	502,61	411,33	294,39	812,52	585,18	646,75	737,46	396,62	245,74	0,0028	Yes
CD14-CD16+ Monocytes	473,67	239,32	296,07	281,90	227,43	226,41	375,61	346,04	230,96	457,42	447,30	163,61	0,4927	No
Remaining Monocytes	33,35	9,56	46,91	41,16	32,14	29,26	38,40	20,29	37,67	81,46	28,03	41,13	0,0959	No
Monocytes derived MDSCs	20,42	50,38	27,27	492,72	507,44	322,43	266,41	410,40	373,25	407,13	418,06	295,34	0,1172	No
CD33-DCs	22,53	9,67	11,76	10,88	6,64	13,70	13,37	4,14	14,01	35,29	9,41	14,58	0,2164	No
CD33+DCs	27,89	22,20	41,64	2,75	4,05	6,66	9,07	5,97	5,97	20,82	13,65	13,09	0,0028	Yes
pDCs	25,25	9,00	8,68	5,18	1,97	14,46	18,03	2,99	13,26	17,16	9,96	10,10	0,3260	No
T&B Lymphocytes	4335,07	1981,08	4846,74	1017,24	739,65	1961,15	2194,39	952,26	2840,00	4108,53	2415,46	3493,35	0,0028	Yes
CD16+NKG2a+NK cells	719,59	247,75	381,02	212,45	64,40	38,49	321,85	126,90	113,12	303,20	293,61	80,46	0,0559	No
CD16-NKG2a+NK cells	41,40	39,01	89,56	17,95	21,76	14,83	20,41	17,88	30,03	23,20	69,64	30,05	0,0207	Yes
Remaining cells	124,89	74,97	132,74	104,16	55,06	98,57	153,19	32,39	110,95	551,01	181,64	157,07	0,0959	No
Blood Cytokines Luminex (pg/mL)														
G-CSF	4,33	2,77	74,36	30,13	79,62	0,00	93,64	84,34	0,00	133,93	111,84	10,45	0,0704	No
GM-CSF	1,50	1,40	1,51	1,25	2,68	1,01	3,11	3,65	0,79	5,35	4,67	1,43	0,4056	No
IFNg	0,00	0,00	0,59	0,00	0,00	0,00	0,00	0,00	0,00	0,00	0,00	0,43	0,1588	No
IL1b	0,00	0,09	2,75	1,59	2,60	2,22	1,65	1,71	1,53	2,97	2,06	2,05	0,3269	No
IL1ra	8,46	31,19	522,93	1736,63	488,64	1154,54	117,34	82,97	0,00	40,93	59,34	0,00	0,0200	Yes
IL2	6,43	9,45	0,00	14,09	14,80	0,00	20,93	11,48	0,00	17,73	14,48	0,00	0,1750	No
IL4	9,49	1,71	0,00	7,82	19,47	0,00	33,33	18,92	0,00	44,41	32,22	0,00	0,1500	No
IL5	0,89	0,52	0,00	1,76	2,14	0,00	4,16	3,34	0,00	7,39	4,55	0,00	0,0167	Yes
IL6	0,20	0,03	84,29	119,36	32,77	12,58	43,60	4,08	25,60	3,47	3,37	2,01	0,0053	Yes
IL8	17,87	18,82	856,67	92,82	81,10	167,65	99,98	33,57	172,67	87,94	54,51	66,42	0,2906	No
IL10	13,33	18,91	74,55	41,92	59,95	38,09	95,71	51,70	39,53	84,80	75,46	35,70	0,1626	No
IL12/23(p40)	0,00	0,00	0,00	0,00	7,77	0,00	24,84	20,40	0,00	43,64	32,52	0,00	0,0500	Yes
IL13	0,00	2,69	26,68	5,97	13,77	22,46	20,40	19,78	18,65	33,08	24,96	25,19	0,3172	No
IL15	1,69	2,04	0,00	7,84	6,20	0,00	8,33	6,36	0,00	7,42	6,32	0,00	0,0417	Yes
IL17a	0,08	0,42	0,00	1,04	0,88	0,00	1,86	1,24	0,00	2,08	1,49	0,00	0,0167	Yes
IL18	0,00	0,00	0,00	0,00	0,00	0,00	0,00	0,00	0,00	0,00	0,00	0,00	Not Detected	No
MCP1	133,89	146,43	320,51	298,11	259,99	113,38	444,03	148,71	217,84	256,77	203,59	122,58	0,2127	No
MIP1a	11,28	8,88	18,52	8,77	13,34	16,47	16,93	17,40	13,90	22,17	20,50	19,27	0,0959	No
MIP1b	0,00	0,00	16,36	0,00	3,05	11,93	5,68	2,95	9,77	5,85	6,19	11,46	0,4133	No
sCD40L	437,16	10,15	220,89	1139,40	111,27	25,01	1002,12	62,48	0,00	483,71	107,15	0,00	0,0954	No
TGFa	1,85	1,31	0,00	4,83	3,11	0,00	5,47	3,44	0,00	6,52	4,97	0,00	0,0083	Yes
TNFa	2,64	2,02	0,00	5,74	17,91	0,00	20,73	29,21	0,00	49,04	38,96	0,00	0,0417	Yes
VEGF	0,00	5,66	159,69	38,59	29,56	102,55	64,24	41,23	0,00	95,39	70,21	227,36	0,1222	No
Lymph Node Cell populations Flow Cytometry (count/g)														
Granulocytes	569183	68214	23975	271667	30694	189632	NA	NA	NA	NA	NA	NA	Not Determined	Not Determined
Macrophages	15769	15893	14416	20741	10735	26507	NA	NA	NA	NA	NA	NA	Not Determined	Not Determined
CD11c+ Dendritic cells	16875	37902	29338	127407	29796	23897	NA	NA	NA	NA	NA	NA	Not Determined	Not Determined
CD1a+ Dendritic cells	7981	9732	1136	102593	7878	1103	NA	NA	NA	NA	NA	NA	Not Determined	Not Determined
pDCs	35769	47321	21356	393333	41184	66176	NA	NA	NA	NA	NA	NA	Not Determined	Not Determined
TLymphocytes	20673077	58928571	46056782	303703704	72653061	66176471	NA	NA	NA	NA	NA	NA	Not Determined	Not Determined
BLymphocytes	3664567	28392857	9779180	60740741	18204082	11764706	NA	NA	NA	NA	NA	NA	Not Determined	Not Determined
NK cells	57692	61473	2019	219815	78776	1801	NA	NA	NA	NA	NA	NA	Not Determined	Not Determined
Other cells	372260	996384	851073	2196852	626531	1094596	NA	NA	NA	NA	NA	NA	Not Determined	Not Determined
Lymph Node Cytokines Luminex (pg/mL)														
G-CSF	0,00	2,65	4,96	22,78	11,59	4,96	NA	NA	NA	NA	NA	NA	Not Determined	Not Determined
GM-CSF	0,46	0,53	0,42	0,60	0,84	0,49	NA	NA	NA	NA	NA	NA	Not Determined	Not Determined
IFNg	0,32	1,61	0,10	1,25	2,83	1,01	NA	NA	NA	NA	NA	NA	Not Determined	Not Determined
IL1b	0,15	10,60	0,09	3,58	1,65	0,79	NA	NA	NA	NA	NA	NA	Not Determined	Not Determined
IL1ra	15,35	72,58	10,94	114,70	255,41	50,36	NA	NA	NA	NA	NA	NA	Not Determined	Not Determined
IL2	0,32	0,44	0,55	1,49	2,40	0,61	NA	NA	NA	NA	NA	NA	Not Determined	Not Determined
IL4	0,00	0,00	0,56	2,76	2,32	2,32	NA	NA	NA	NA	NA	NA	Not Determined	Not Determined
IL5	0,70	1,20	1,15	0,48	6,32	1,15	NA	NA	NA	NA	NA	NA	Not Determined	Not Determined
IL6	8,41	13,38	7,51	99,49	27,29	13,91	NA	NA	NA	NA	NA	NA	Not Determined	Not Determined
IL8	22,78	225,45	24,56	108,63	168,10	32,15	NA	NA	NA	NA	NA	NA	Not Determined	Not Determined
IL10	3,22	11,84	8,91	17,81	34,71	6,74	NA	NA	NA	NA	NA	NA	Not Determined	Not Determined
IL12/23(p40)	1,29	4,46	2,87	2,87	3,66	2,08	NA	NA	NA	NA	NA	NA	Not Determined	Not Determined
IL13	10,52	18,04	18,26	6,91	23,27	16,09	NA	NA	NA	NA	NA	NA	Not Determined	Not Determined
IL15	1,44	2,61	2,57	1,64	5,70	2,08	NA	NA	NA	NA	NA	NA	Not Determined	Not Determined
IL17a	0,00	0,21	0,00	0,00	0,06	0,00	NA	NA	NA	NA	NA	NA	Not Determined	Not Determined
IL18	198,20	243,80	189,99	34,33	52,83	80,81	NA	NA	NA	NA	NA	NA	Not Determined	Not Determined
MCP1	32,41	39,11	50,55	179,97	192,71	85,98	NA	NA	NA	NA	NA	NA	Not Determined	Not Determined
MIP1a	0,00	5,68	0,00	2,46	9,13	0,00	NA	NA	NA	NA	NA	NA	Not Determined	Not Determined
MIP1b	0,00	4,27	0,00	0,00	3,09	0,00	NA	NA	NA	NA	NA	NA	Not Determined	Not Determined
sCD40L	45,71	38,39	76,67	7,93	64,86	32,89	NA	NA	NA	NA	NA	NA	Not Determined	Not Determined
TGFa	7,28	7,89	12,07	3,10	9,30	6,02	NA	NA	NA	NA	NA	NA	Not Determined	Not Determined
TNFa	3,58	7,43	5,52	4,23	11,51	6,16	NA	NA	NA	NA	NA	NA	Not Determined	Not Determined
VEGF	13,57	48,88	42,32	7,75	59,06	31,34	NA	NA	NA	NA	NA	NA	Not Determined	Not Determined
Gene clusters (scaled expression)														
Migrating gene cluster_BD	-0,93	-0,19	-0,30	0,18	0,33	0,01	-0,53	-0,21	-0,31	-0,07	-0,14	-0,14	Not Determined	Not Determined
Early and transient upregulated gene clusters_BD	0,85	2,29	1,13	-0,69	-0,03	-0,88	-0,70	0,04	-0,57	0,40	0,73	-0,13	Not Determined	Not Determined
Persisting upregulated gene clusters_BD	-0,88	-0,43	-0,72	1,09	1,20	0,77	-0,15	1,14	0,26	0,53	0,66	-0,08	Not Determined	Not Determined
Upregulated genes cluster_LN	-0,97	-0,54	-0,52	0,25	0,89	0,89	NA	NA	NA	NA	NA	NA	Not Determined	Not Determined
Downregulated genes cluster_LN	0,52	0,31	1,19	-0,82	-0,94	-0,27	NA	NA	NA	NA	NA	NA	Not Determined	Not Determined

Supplementary Table 1. Biological variables used in the construction of the co-expression network.

Table showing all collected raw data for flow cytometry and Luminex in the blood, the skin and the lymph node.With the addition of gene clusters in the blood and lymph nodes. Some significance test were rated as “not determined” due to the nature of the data (mean of a selection of differentially expressed genes) or a lack of statistical power (lymph nodes)

Biological variable	50 highest Number of significant correlations (degree of connectivity)
Cytokine_LN_IL18	25
Cytokine_SK_TGFa	24
Transcriptomics_LN_Downregulated genes cluster	24
Transcriptomics_LN_Upregulated genes cluster	21
Cells_BD_Monocytes derived MDSCs	20
Cytokine_LN_MCP1	20
Cytokine_SK_IL2	20
Cytokine_SK_TNFa	19
Cytokine_BD_IL15	18
Cytokine_BD_IL5	18
Cytokine_BD_IL12/23(p40)	18
Cells_LN_T Lymphocytes	17
Cytokine_SK_VEGF	17
Cytokine_SK_IL1ra	17
Cytokine_BD_IL17a	16
Cytokine_SK_IL12/23(p40)	16
Cytokine_SK_IL8	16
Cytokine_SK_MCP1	16
Transcriptomics_BD_Persisting upregulated genes cluster	16
Cytokine_BD_IL4	15
Cytokine_LN_IL6	15
Cytokine_SK_G-CSF	15
Cells_LN_pDCs	14
Cytokine_SK_IL6	14
Cytokine_SK_MIP1b	14
Cells_SK_Granulocytes	13
Cytokine_BD_TGFa	13
Cytokine_SK_IL10	13
Cytokine_BD_sCD40L	12
Cytokine_BD_TNFa	12
Cytokine_LN_IL10	12
Cytokine_LN_IL2	12
Cytokine_LN_IL1ra	12
Cytokine_LN_GM-CSF	12
Cytokine_SK_IL18	12
Cells_LN_CD11c+ DCs	11
Cells_LN_CD1a+ DCs	11
Cells_SK_Macrophages GFP+	11
Cytokine_BD_GM-CSF	11
Cells_BD_T&B lymphocytes	10
Cells_BD_CD66high Granulocytes	10
Cells_LN_Other cells	10
Cells_LN_NK cells	10
Cells_SK_Macrophages	10
Cytokine_LN_G-CSF	10
Cytokine_SK_IL15	10
Cytokine_SK_IL1b	10
Cells_SK_Monocytoids	9
Cytokine_SK_MIP1a	9

Supplementary Table 2.Degree of connectivity top 50

Ranking of the fifty biological variable building the highest number of significant correlations.

B. Article 2 (manuscrit en préparation)

The devil is in the details: small local and systemic differences in the early immune response between SC, ID and IM administration routes can lead to different adaptive responses.

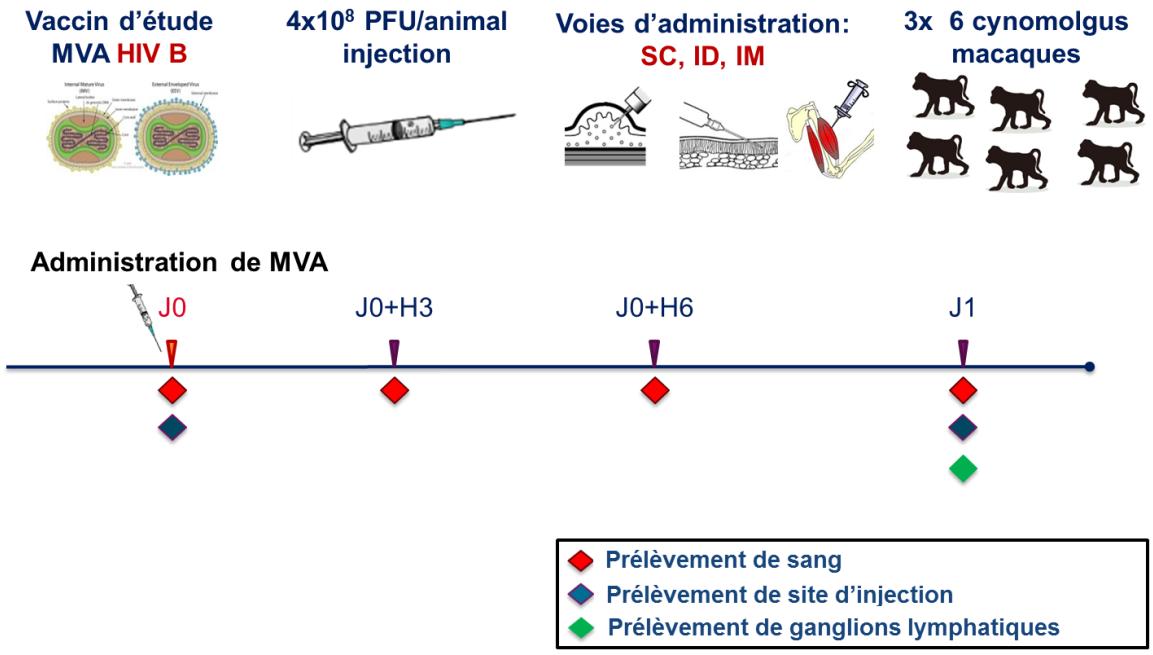

Figure 15 : Schéma expérimental de l'étude de la réponse innée précoce induite par le MVA par voie intradermique, sous cutanée, et intramusculaire

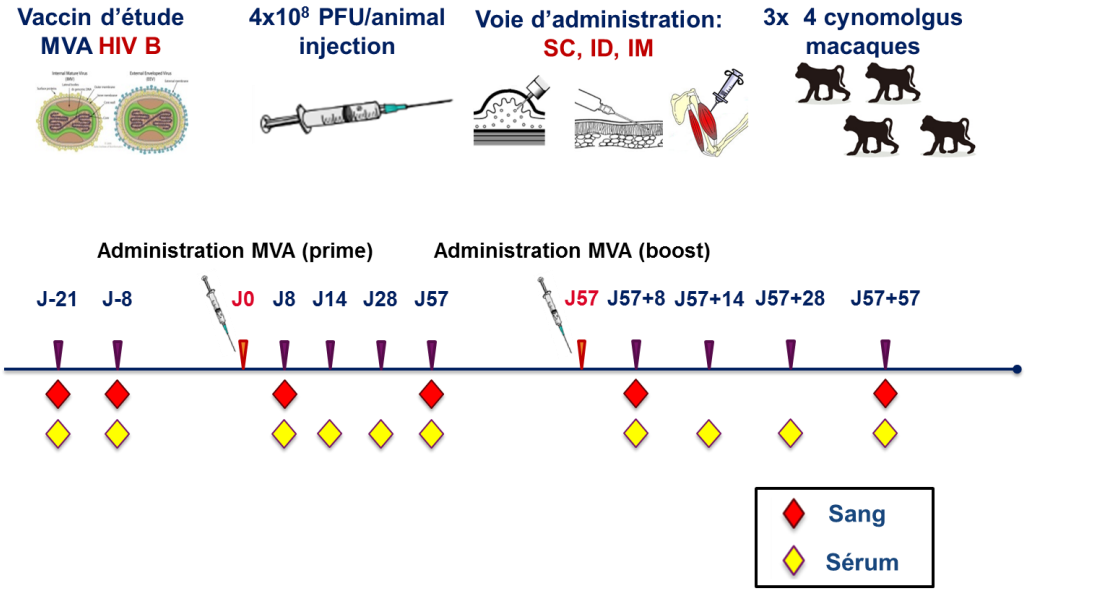

Figure 16 : Schéma expérimental de l'étude de la réponse acquise induite par le MVA par voie intradermique, sous cutanée, et intramusculaire

En nous basant sur les schémas expérimentaux indiqués en **figure 15 et 16**, nous avons comparé les réponses immunes innée et acquise induites par le MVA injecté par trois voies d'administration différentes. L'analyse de la réponse innée nous révèle une forte capacité de notre vaccin à induire une réponse inflammatoire quelle que soit la voie. En effet nous décrivons un recrutement massif de granulocytes (par voie SC et ID), et de macrophages (par voie SC, ID et IM) sur le site d'injection. Cette réponse inflammatoire se répercute également dans le compartiment sanguin, où un recrutement accru de sous populations de monocytes et de granulocytes est également observé. En parallèle les lymphocytes quittent le compartiment sanguin dans les premières heures après administration.et dans une moindre mesure au niveau des ganglions drainants. Ces recrutements cellulaires sont associés à une up-régulation des signatures moléculaires liées à l'inflammation (signalisation IL6 et interféron, maturation cellules dendritiques, phagocytose…) tant au niveau local que sanguin.

Une étude plus méticuleuse de cette réponse met cependant en évidence certaines différences entre les voies d'administration mettant souvent en opposition la voie SC d'une part et les voies ID et IM d'autre part. En effet, en plus de différences dans la localisation antigénique entre les voies SC et ID, la réaction inflammatoire locale semble plus importante après administration par voie SC (recrutement de cellules HLADR+ et de cellules monocytoides associées à une up-régulation accrue des voies de signalisation liées à l'activité macrophagique et inflammatoire). Au niveau sanguin également, la voie SC induit un recrutement plus abondant de pDCs après 24h, alors que les lymphocytes T CD8+ migrent moins. Cette dichotomie entre les voies SC et ID/IM est particulièrement visible lors de l'étude des signatures moléculaires au niveau sanguin, où les voies de signalisation liées à l'inflammation atteignent un pic 24h après administration par voie ID et IM, alors qu'il est beaucoup plus précoce après voie SC (3h). De plus les voies relatives aux lymphocytes T sont également plus réprimées après administration par les voies ID et IM en comparaison à la voie ID.

Ces subtiles différences sont possiblement à l'origine d'une réponse T et d'une réponse anticorps différente en fonction de la voie d'administration. Ainsi, on retrouve plus d'anticorps neutralisants après administration par voie SC, alors que la prolifération de cellules T CD4 et CD8 effectrices polyfonctionnelles est beaucoup plus marquée après administration par voie IM, bien qu'également présente par voie ID, alors que quasi inexistante par voie SC.

Ainsi, cette étude est l'une des rare à mettre en évidence que non seulement la voies d'administration est susceptible d'influencer l'amplitude de la réponse vaccinale, mais également sa qualité de manière importante. De plus, certaines subtiles modifications de la réponse innée observées à des temps très précoces pourraient en partie expliquer les différents profils de réponse acquise.

Par exemple, les flux de populations de lymphocytes TCD8 sanguin migrant précocement de manière plus importante possiblement vers les ganglions drainants après administration par voie ID et IM pourraient être à l'origine de la réponse effectrice accrue induites par ces voies. La composition en cellules présentatrices d'antigènes du site d'injection peut être également un facteur prépondérant, puisqu'il influera non seulement sur la réponse inflammatoire et la sécrétion de cytokines et chémokines, mais également sur la présentation antigénique.

D'autres paramètres peuvent également jouer un rôle important, comme les propriétés de vascularisation et de rétention de l'antigène au niveau du site d'injection.

The devil is in the details: small local and systemic differences in the early immune response between SC, ID and IM administration routes can lead to different adaptive response profiles.

Pierre Rosenbaum[1,4], Nicolas Tchitchek[1,4], Lev Stimmer[2,3], Hakim Hocini[4,5], Yves Levy[4,5], Anne-Sophie Beignon[1,4], Roger Le Grand[1,4], and Frédéric Martinon[1,4,†]

[1]CEA – Université Paris Sud 11 – INSERM U1184, Immunology of viral infections and autoimmune diseases, 92265 Fontenay-aux-Roses, France

[2]CEA – INSERM, MIRCen, UMS27, 92265 Fontenay-aux-Roses, France

[3]INSERM, U1169, 94270 Kremlin-Bicêtre, France

[4]Vaccine Research Institute, Henri Mondor Hospital, 94010 Créteil, France

[5]INSERM, U955, Team 16, Clinical and Infectious Diseases Department, Hospital Henri Mondor, University of Paris East, 94010 Créteil, France

[†]**Corresponding author**

Correspondence should be addressed to: Frédéric Martinon, CEA, 18 Route du Panorama, 92265 Fontenay-aux-Roses, France (frederic.martinon@cea.fr).

Abstract

A better understanding of immune mechanisms induced *in vivo* by vaccination processes could unlock new possibilities of vaccine therapeutics. We used a non-human primate (NHP) model vaccinated with a modified virus Ankara (MVA) to investigate in which measure the administration route could interfere with the profile of the immune response. For this study, we compared the effect of an intradermal (ID), subcutaneous (SC) and intramuscular (IM) administration. We analyzed in depth the very early response at the site of injection, the lymph node and the systemic compartment. We then measured the antibody and the CD4+ and CD8+ T cell response in the blood using CyTOF technology over the time in a homologous prime-boost. MVA has been shown to strongly induce the early immune system, with important amounts of granulocytes, macrophages and monocytes subsets mobilized at the site of injection and in the blood. Somemodest but present differences were however highlighted between the administrations routes tested in the nature of the immune cells migrations. We indeed observed differential lymphocytes recruitment in the skin in comparison with subcutaneous tissue, as well as slightly different amounts CD16+CD14+ monocytes and pDC recruited in the blood. We observed even more dissimilarities looking at transcriptomic analysis, notably in the magnitude and in the kinetic of the early immune effectors mobilized in the site of injection and in the blood. These heterogeneities may have an important impact on the vaccine profile since they appeared different depending on the administration route. In spite of similar MVA IgG titers, SC route lead to more neutralizing antibodies, but less IFNγ+ CD8+ and CD4+ T cells in comparison with ID and IM route. In addition, polyfunctional CD8+ and CD4+ T cells induced after IM administration over the time were more important, with more cells showing an effector profile expressing IFNγ, MIP1β, CD69 and TNFα. The proportion of cytotoxic cells (perforin+, granzymeB+) also differed depending on the administration route. Overall, we showed that administration route could do more than a dose sparing effect, and modulate in-depth the immune response profile of a same given vaccine in *an in vivo* NHP model. In addition, this vaccine response is

probably impacted by subtle modifications that could be observed in the blood, but also at the site of injection at the very first steps of the innate response.

Introduction

Vaccination is known as one of the best medical weapon to fight against infectious diseases. However, mechanisms leading to a suited immunity are still poorly known. A better understanding of all the immune process would allow the design of more efficient vaccines. On this topic, one important question is the influence of the administration route on the elaboration of the immune response. Indeed, it is known that the early immune response largely impacts the adaptive response profile, notably through antigen presenting cells (APCs) such as dendritic cells (DCs)[30]. As a result, this immune response is also supposed to be mediated by APCs present at the site of injection, which differs largely depending on the administration route. In vaccination, intramuscular (IM) route is the most commonly used administration route along with subcutaneous (SC) route due to its simplicity to access and its safety to use. Nevertheless, muscle tissue naturally lacks of immune cells[62] and thus is not expected to be an optimal vaccine immunization route[171]. At the opposite, the skin tissue is composed by a very broad type of immune cells including numerous dendritic cells (DCs) subsets able to present the antigen to the draining lymph nodes. Among them, Langerhans cells and dermal DCs are shown *in vitro* to prime efficiently CD4+ T cells into Th1 or Th2 depending on the stimulus or microenvironment[75,83,172].

It has been demonstrated that those immune properties can have a direct impact *in vivo* on the magnitude of the response. A dose-sparing effect has indeed been highlighted for some phase I/II clinical trials, allowing to inject up to ten times less vaccine through ID route to obtain a comparable rate of protection in comparison with classical SC or IM route[173]. It is notably well described in the case of influenza vaccine[174], but also referred in hepatitis B and malaria vaccine[113,174,175]. This kind of information is very valuable since it can have a very important economic impact. However, mechanisms related to this effect remain unclear since in most of the case, protection has been only determined looking at known correlates of protection such has antibody titers, and no other parameter of the response that may interfere with it and explain this results.

As a consequence, the impact of the administration route on the quality of the response remains unclear. Indeed, only few studies using murine models focused on the characterization of immune response depending on the administration route. Nevertheless, Mohanan *et al.* [176] showed that administration route appeared to strongly influence Th1 response with more IgG2a titers and IFNγ production in favor of ID and IM route in comparison with SC, but no major differences in IgG1 titers using antigen delivery systems. Another study using modified vaccinia virus Ankara (MVA) vaccine investigated earlier local responses and highlighted heterogeneity on immune cells migration in draining lymph node and T cell response profiles between ID and IM route[66].

In the present study, we investigated how ID, IM and SC administration routes could impact the magnitude and the quality of the vaccine response. To evaluate this, we chose a study model involving non-human primates (NHP) vaccinated with a recombinant MVA. NHP is indeed one of the most valuable model in immunology due to its phylogenic proximity with human[96,147], whereas MVA is a non-replicative (in mammals) living attenuated vaccinia virus. This vaccine was selected because it has already been used in administration route problematic[66,142], in addition to be highly immunogenic and safe. This makes MVA widely used in clinical trials as a promising viral vector for vaccines against Ebola, tuberculosis, or HIV[146,177,178]. The rMVA used in this study, which expresses genes coding HIV proteins is also involved in a phase I clinical trial[119].

We compared rMVA response induced after SC, IM, but also ID route. Inspired by system vaccinology approaches[121], this study was designed in order to characterize as completely as possible the early local and systemic innate immune reaction, but also the late vaccine response after prime and boost. In a first step, we aimed to perform an in-depth analysis of cell movements and transcriptomic signatures of the very early immune reaction. In a second time, we wanted put in perspective this early immune characterization with adaptive response induced in the blood, looking at anti-MVA antibody titers, neutralization, but also CD4+ and CD8+ T cells response profiles using CyTOF technology.

Materials and Methods

Experimental design

This work aimed to evaluate the immune responses induced by MVA, an approved vaccine, after SC, ID or IM administration route. This study is divided in two steps. The first step was focused on the very early local and systemic immune response. It involved three groups of six non-human primates - one for each administration route tested- having equivalent average weight and MHC profiles. For those animals, untreated biopsies of the site of injection and blood were sampled first. One month after, buffer injections were performed on the same animals. One month after, MVA immunizations were performed. Evaluation of the local response after intramuscular injection was not performed due difficulty to localize the site of injection with the impossibility to perform large muscle biopsies for ethical reasons. We evaluated local response 24h after MVA injection, supposedly corresponding to peak of inflammation and infection, whereas systemic response was evaluated 3h, 6h and 24h after injection. The second step of this study was allocated MVA-induced adaptive response, also comparing SC, ID and IM route. On this purpose twelve non-human primates were divided in three groups of four based on their weight and their MHC haplotypes. We chose to evaluate the T CD4 and CD8 response at day 8 post-prime and post boost, supposedly corresponding to the peak of response. We also selected day 57 post-prime has a baseline before boost and D28 post-boost to evaluate memory response. The experiments and analysis pipeline were performed following same protocols with previous in-house studies[179].

Ethical issues

Adult males cynomolgus macaques (*Macaca fascicularis*), each weighing between 4 to 6 kg, and imported from Mauritius, were housed in the animal facilities of the CEA (Fontenay-aux-Roses, France). Macaques were handled in accordance with national regulations (Commissariat à l'Energie Atomique et aux Energies – Alternatives Permit Number A 92-32-02), in compliance with Standards for Human Care and Use of Laboratory of the Office for Laboratory Animal Welfare under Office for

Laboratory Animal Welfare Assurance number A5826-01, and the European Directive (2010/63, recommendation N°9). This project received the authorization Number 12-013in accordance with the French Ethical policy.

A regular follow-up of the animals (clinical exam, temperature, weight) was performed during all the duration of the experiment. Interventions were handled by veterinarians and zootechnician staff of the "Animal Science and Welfare" core facility of IDMIT infrastructure. Injections, tissue biopsies and blood samples were performed after anesthesia with ketamin (10 mg/kg, Imalgen®, Rhone-Mérieux, Lyon, France).

Immunizations

Thesite of injection was shaved and cleaned with ethanol 70%. Sites of injection dedicated to imaging were tape stripped. For ID, SC and IM route group, animal received simultaneously respectively ten, two, and two injections containing a total of $4x10^8$ PFU in 2mL of a rMVA expressing HIV proteins Gag, Pol and Nef (MVA HIV-B MVATG17401 Transgene SA, Illkirch-Graffenstaden, France). The injections were equally divided into two areas: (i) 5 to 10 cm from the left inguinal lymph node area; and (ii) on the top left of the back. One month prior MVA injection, similar procedure was conducted on the same animals at the right side with MVA Buffer for each group. Prior buffer injection, untreated site of injection and blood were sampled. A dotted line was drawn around the site with a felt pen in order to later identify the site of injection at biopsy.

Tissue and blood samples

Prior to biopsies, the site of injection was cleaned with povidone iodate solution (Vetedine®, Vetoquinol SA, Lure, France). Skin biopsies sized 8mm in diameter. For the subcutaneous route, 5 x 1,5 cm (ellipse shape) deep skin biopsies were performed with a scalpel always following a same template. Blood was collected into K3-EDTA tubes (Greiner Bio-One, Frickenhausen, Germany) for CBC (HmX;Beckman Coulter), plasma collection and flow cytometry staining. For antibody titers, serum was collected from 2mL into serum clot activator tubes (Greiner Bio-One). Plasma and serum

werecollected after 10 minutes and 2000g centrifugation. A volume of 500µL of blood coming from lithium heparin tubes (Vacutainer BD) was mixed with 1mL tempus RNA tube (Thermofischer Scientific, Waltham,MA, USA), for transcriptomic analysis. For CyTOF staining purposes, 10mL of blood were collected in lithium heparin. Half parts of fresh subcutaneous or skin (dermis + epidermis) dedicated to transcriptomic analysis were conserved in 1 mL RNA later solution (Qiagen, Hilden, Germany) at 4°C overnight and then stored at -20°C.The overall number of major leukocyte subsets per milliliter of EDTA tube macaque blood was determined using an automated blood counter (HmX; Beckman Coulter).

Extraction of cells from tissue biopsies

In order to optimize cell extraction, the protocol used was inspired by several previous internal but also external works on tissue cell extraction[71,148]. After biopsies, tissues were cleaned again with 70% ethanol solution. For biopsies from ID group, subcutaneous tissue was removed to only obtain epidermis and dermis, which were not separated afterwards. For biopsies from SC group, subcutaneous tissue was entirely collected and the epidermis and dermis parts were removed. Biopsies were then washed with PBS, cut in small pieces, weighed and finally digested at 37°C under agitation during 60 minutes using 2mL of a solution containing RPMI (Thermofischer Scientific), 5% FCS (Lonza, Basel, Switzerland), 1% Penicillin Streptomycin Neomycin (Thermofischer Scientific), 10mM Hepes (Thermofischer Scientific), 2mg/mL collagenase D (Roche) and 0.02 mg/mL DNAse I (Roche, Basel, Switzerland). Tissue was then filtered using 70µm cell strainer and centrifuged. The supernatant was collected for the tissue cytokine analysis. Skin tissue leftover was shredded with GentleMACs® dissociator (Miltenyi Biotec, Paris, France). The cell suspension was then washed with PBS and then stained for flow cytometry analysis.Flow cytometry staining was performed from cell extraction coming from one single tissue biopsy.

Histology of local inflammation induced by MVA

Skin and subcutaneous for both SC and ID group were sampled and fixed at 4°C using 4% paraformaldehyde during 24h. Samples will be conserved in PBS condition at 4°C. Paraffin inclusion was made using an automaton successively replacing PBS with alcohol, xylene and paraffin. Tissue was cut afterward using microtome and set on slides. Hemalun Eosin coloration was then made using an automaton Microm HMS740 (Thermofischer Scientific), alternating xylene, alcohol, Hematoxylin (Labonord, Templemars, France), Eosin (VWR international, Fontenay-sous-Bois, France) baths.

Immunohistofluorescence

Briefly, skin biopsies were washed three times in PBS and then put in lysine and PFA solution (14,6 g/L-lysin(Sigma Aldrich); 4% PFA (Sigma Aldrich); 2 g/L Sodium(meta)periodate (Sigma Aldrich) in phosphate Buffer 0,05 mol/L (using in equal quantities 1 mol/L of monobasic and dibasic potassion phosphate solutions (Sigma Aldrich) at 4°C during 8H. Then skin was washed in PBS and tranferred in 30% sucrose (Sigma-Aldrich) solution overnight. Tissue was then frozen embedded in OCT in dry ice and aceton. Staining was performed processing successively (rincing with PBS between steps): a permeabilization step during 30' at 37°C using (PBS 0.3% triton (Sigma Aldrich)); a saturation step during 30' at 37°C using PBS 10% BSA (Sigma Aldrich) 10% Macaque serum (In-lab production); a primary antibody staining during 2h at 37°C using 1.5µL E3L (NIH Biodefense and Emerging Infections Research Resources Repository, NIAID, NIH: Monoclonal Anti-Vaccinia Virus E3L, Clone TW2.3 (produced *in vitro*), NR-4547.), 0.5µL CD66 (clone TET2, Miltenyi Biotec), 6µL CD163 (clone GHI/61, Biolegend) diluted in 100µL PBS 0.2% BSA; A secondary staining during 1h at 37°C using secondary antibodies (Thermofischer Scientific); A post-fixation step using PFA4% (15min) was then performed followed a DAPI staining (Thermofischer Scientific) and mounted. Stained slides were then conserved at 4°C.

Flow cytometry staining

Site of injection and Lymph node: All the steps of the staining were processed at 4°C. Cell suspensions were first stained with viability dye LiveDead® (Thermofischer Scientific) for 15 minutes, then washed with PBS. Fc receptors were blocked by using PBS supplemented with 5% macaque serum during 20 minutes. Tissue cell suspensions were stained during 30 minutes with 90µL of mix of antibodies diluted in BD Horizon Brilliant® Stain Buffer (BD) containing CD1a (DAKO, Glostrup, Denmark, Clone O10) extemporaneously coupled with Zenon IgG1 AF700 (Thermofischer Scientific), HLA-DR (BD Biosciences, Franklin Lakes, NJ, USA, clone G46-6), CD163 (BD, clone GHI/61), CD11c (Biolegend, San Diego CA, USA clone 3.9), CD45(BD, clone DO58-1283), CD66 (Miltenyi Biotec, clone TET2), CD3 (BD, clone SP34-2), CD20 (BD, clone 2H7), CD11b (Beckman Coulter, Brea, CA,USA, clone Bear 1), CD16 (Beckman Coulter, 3G8) and NKG2a (Beckman Coulter, clone Z199). Cells were then washed twice using PBS and fixed using 150µL BD Cellfix® (BD). Same antibodies were used for lymph node staining at the exception of CD45 replaced by CD123 (BD, Clone 7G3).

Blood: 100µL of blood were immediately stainedduring 30 minutes with 90µL of mix of antibodies diluted in BD Horizon® stained buffer (BD) containing CD123 (BD, Clone 7G3), HLA-DR (BD Biosciences,Franklin Lakes, NJ, USA, clone G46-6), CD163 (BD, clone GHI/61), CD11c (Biolegend, San Diego, CA, USA clone 3.9), CD45 (BD, clone DO58-1283), CD66 (Miltenyi Biotec, clone TET2), CD3 (BD, clone SP34-2),CD20 (BD, clone 2H7), CD8 (BD, clone RPA-T8), CD11b (Beckman Coulter, Brea, CA,USA, clone Bear 1),CD14(BD, Clone M5E2), CD33(Miltenyi, Clone AC104.3E3) CD16 (Beckman Coulter, 3G8) and NKG2a (Beckman Coulter, clone Z199) and then cell were fixed and red blood cells were removed with 1 mL of BD FACs Lysing® (BD) during 10 minutes at room temperature and washed twice using PBS. The design of cytometry panel and rational for gating strategies were mostly based upon previous work in the lab[148]. For the analysis of the site of injection, we divided the number of events obtained in each cell population by the initial weigh of the digested biopsy. This choice was done in order not to miss minor cell movement that could have been outshined by the massive inflammatory cell recruitments. Similarly, to keep absolute values in the blood, we

standardized our flow cytometry results based on complete blood count data, obtaining a number of cells per liter. To perform this, we applied the following formula: Number of cells of a given cell population multiplicated by CBC leukocytes divided by the total of blood cells obtained by flow cytometry.

Flow cytometry gating strategy for skin cells

The flow cytometry gating strategy of skincells is shown in Supplementary Figure 1.A. After doublet and debris exclusion, living cells were selected, and then CD45 discriminated leukocytes from non-leukocytes. Among CD45+ cells, granulocytes were first discriminated using CD66+ and SSC-A+. Among CD45+ CD66- cells, lymphocytes were regrouped as lin(CD3, CD20)+. Macrophages were identified as CD45+, Lin (CD3, CD20)-, CD66-, CD11b+ and CD163+ cells. CD45+, Lin (CD3, CD20)-, CD163-, CD66-, HLADR+, CD11b+ cells were considered as cells coming from blood monocytes due to their close phenotype and were thus called monocytoid cells. NK cells were defined as expressing the following phenotype: CD45+, CD66-, Lin (CD3, CD20)-, CD11b-, NKG2a+. Cells expressing CD45+, CD66-, Lin (CD3, CD20)-, CD11b-, NKG2a-, HLADR+ and CD11c+ were considered as dendritic cells. Cells showing no expression in our marker in the panel but CD45 were named “other leukocytes”.

Gating strategy of lymph node cells by flow cytometry

The flow cytometry gating strategy of lymph node cells is shown in Supplementary Figure 1.C. After excluding doublets, debris and selecting living cells, Lymphocytes were gated on their Lin (CD3, CD20)+ expression and then gated between B and T subtype using HLADR , being positive for B lymphocytes and negative for T lymphocytes. Then granulocytes were gated on Lin (CD3, CD20)-, CD11b+ and CD66+ expression; classical NK cells were identified as Lin (CD3, CD20)-, CD66-, CD16+ and NKG2a+, whereas another subpopulation considered as CD16- NK cells were identified as Lin (CD3, CD20)-, CD66-, CD16- and NKG2a+. Macrophages were distinguished with their expression of Lin (CD3, CD20)-, CD66-, NKG2a-, CD11b+ and CD163+. Three dendritic cell populations were then identified as follows: pDCs as lin(CD3, CD20)-, CD66-, NKG2a-,CD11b-, CD163- HLADR+ and CD123+;

CD1a+ dendritic cells as CD66-, NKG2a-, CD11b-, CD163-, HLADR+, CD123-, CD1a+; and finally CD11c+ dendritic cells as lin(CD3, CD20)-, NKG2a-, CD66-, CD11b-, CD163-, HLADR+, CD123-, CD1a- and CD11c+; Remaining cells expressing no markers in our panel were called “other cells”.

Gating strategy of blood cells by flow cytometry

The flow cytometry gating strategy of skincells is shown in Supplementary Figure 1.B. To optimize this panel, we used both NKG2a and CD33 markers on the same fluorochrome. We show on histograms that those markers are not staining the same cell populations and are thus exclusive (Fig). We confirm indeed that NKG2a but not CD33 is expressed on cells gated as NK cells and CD16- NK cells. Similarly, we show that CD33 but not NKG2a is expressed on cells defined as MDSC derived from monocyte and dendritic cell subsets. As a result, we discriminated cell populations described below accordingly. Likewise, the skin analysis, doublets and debris were excluded. Then, SSC-A+, CD66+, cells were considered as granulocytes. In spite of we highly suppose that most of them are neutrophils as their recruitment kinetic fits with neutrophil complete blood count, we cannot rule out the presence of subpar populations of eosinophils and basophils. Lymphocytes were gated as Lin (CD3, CD20)+ cells; NK cells as Lin (CD3, CD20)-, CD16+, NKG2a+. Three main subtypes of monocytes were discriminated using CD14 and CD16 markers[149] as follows: Non-conventional monocytes as Lin (CD3, CD20)-, CD14- and CD16+; Inflammatory monocytes as Lin (CD3, CD20)-, CD14+ and CD16+; Classical monocytes as Lin (CD3, CD20)-, CD14- and CD16+ and then HLADR+. pDCs were gated on their Lin (CD3, CD20)-, CD14-, CD16-, HLADR+ and CD123+ expression. Cells showing Lin (CD3, CD20)-, CD14-, CD16-, HLADR^{mid} and CD123+ expression were considered as remaining basophils. The use of the CD33 marker led us to discriminate other dendritic cell subsets as follows: Lin (CD3, CD20)-, CD14-, CD16-, HLADR+, CD123- and CD33- cells are showing unique phenotype and were thus considered as CD33- DCs; Lin (CD3, CD20)-, CD14-, CD16-, HLADR+, CD123- and CD33+ were identified as conventional CD33+ DCs; and Lin (CD3, CD20)-, CD14-, CD16-, HLADR+, CD123-, CD11b+ and CD33+ were identified as CD14low Monocytes as they show similar phenotypes as classical

monocytes with the only difference in the low expression of CD14. In accordance with literature[150], MDSCs were also identified as follows: Lin (CD3, CD20)-, CD14-, CD16-, HLADR-, CD123-, $CD66^{low}$, CD11b+, and most likely CD33+ for granulocytes derived MDSCs and Lin (CD3, CD20)-, CD14-, HLADR-, CD11b+, CD33+ for monocytes derived MDSCs. Other remaining HLADR- subpopulations were then discriminated as follows: Lin (CD3, CD20) -, CD14-, CD16-, HLADR-, CD123-, $CD11b^{low}$, $CD66^{low}$ as $CD66^{low}$ granulocytes escaping from the initial gating of granulocytes; Lin (CD3, CD20) -, CD14-, CD16-, HLADR-, CD123-, CD66-, (CD33, NKG2a)+, considered as CD16- NK cells; and cells expressing no markers in our panel were named "Remaining Cells".

RNA isolation and microarray sample preparation

Similar to a previous study[179]. Gene transcription in whole blood and biopsies was assessed. Biopsies were immediately immersed into RLT-beta-mercaptoethanol 1/100 lysis buffer (Qiagen, Courtaboeuf Cedex, France). Samples were then disrupted and homogenized using a TissueLyser LT (Qiagen, Courtaboeuf Cedex, France) and RNA purified on Qiagen RNeasy Micro Kit. Whole blood RNA was recovered in tempus tubes (ThermoFisher scientific) and RNA purified using *Tempus*™ Spin RNA Isolation*Kit* (ThermoFisher scientific). For both purifications, contaminant DNA was removed using RNA Cleanup step of RNeasy Micro Kit. Purified RNA was then quantified using a ND-8000 spectrophotometer (NanoDrop Technologies, Fisher Scientific, Illkirch Cedex, France) before being checked for integrity on a 2100 BioAnalyzer (Agilent Technologies, Massy Cedex, France). CDNA was synthesized and biotin-labelled using Ambion Illumina TotalPrep RNA Amplification Kits (Applied Biosystem/Ambion, Saint-Aubin, France). Labeled cRNA were hybridized on Illumina Human HT-12V4 BeadChips. All steps were done following the manufacturers' protocols. Raw and normalized microarray data have been deposited in the ArrayExpress database [153] under an accession number XXX (this number will be provided upon acceptance).

Measurement of total anti-MVA IgG and IgM in serum

Similar to a previous study[179].In brief, wild-type MVA (B. Verrier, Biologie tissulaire et ingénierie thérapeutique, Institute of Biology and Chemistry of Proteins, Lyon, France) was used to coat 96-wellMaxiSorp microplates (Nunc) at 105 PFU/well in coating buffer (200 mM NaHCO3,80mMNa2CO3, pH 9.5) overnight at 4˚C. Wells were washed five times with wash buffer (PBS, 0.1% Tween 20, 10 mM EDTA) and blocked for 1 h at RT with 3% w/v BSA (Sigma). Plates were washed five times and incubated with 2 -or 4-fold serial dilutions of macaque serum diluted in 1% w/v BSA in PBS for 2 h at RT, starting at 1:50 for IgG or 1:25 for IgM. Plates were then washed five times and 1:2500 or 1:1000 peroxidase- conjugated goat anti-monkey H+L chain IgG or IgM, respectively (AbD Serotec), in 1%BSA (w/v) PBS was added and incubated for 1 h at RT. Plates were washed five times and 100 ml3,39,5,59-tetramethylbenzidine (Thermo Scientific) was added and incubated for 30 min at RT in the dark. The reaction was stopped by adding 2NH2SO4.Absorbancewas measured at 450 nmusing a spectrophotometer (Multiskan FC, Thermo Scientific), and data were ana- lyzed using SoftMax Pro software (version 4.6; Molecular Devices). Ab titers were calculated by extrapolation from the OD as a function of a serum dilution

Ab neutralization assay

Similar to a previous study[179]. nAb titer was determined using a modified version of a standard plaque inhibition assay. In brief, wild-type MVA (1 PFU/cell) was mixed with an equal volume of 4-fold serial dilutions of serum in assay medium (DMEM, 2% FCS), starting at 1:20. After 60 min of incubation at 37˚C, 0.1 ml of the serum–virus mixture was transferred, in duplicate, to a 96-well plate containing subconfluent UMNSAH/DF-1 chicken fibroblasts (ATCC). After 48 h of incubation at 37˚C, cell viability was quantified using an MTS/PMS assay (CellTiter 96 AQueous Non-Radioactive Cell Proliferation Assay; Promega). Absorbance was measured at 492 nm using a spectrophotometer (Multiskan FC; Thermo Scientific), and data were analyzed using SoftMax Pro software (version 4.6; Molecular Devices). The sample dilution versus the percentage viability was plotted (fourparameter logistic curve) to calculate a neutralizing concentration, corresponding to the sample dilution

resulting in 50% neutralization of virus-mediated cell mortality. Cell viability in uninfected control cells and in infected cells incubated with undiluted vaccinia immune globulin i.v. (human polyclonal anti–vaccinia virus IgG; BEI Resources) was equivalent as expected.

Ab–element conjugation for CyTOF staining

Similar to a previous study[179]. Pure (carrier-protein–free) mAbs or polyclonal Abs from various manufacturers were coupled to elements using MAXPAR lanthanide labeling kits (Fluidigm, San Francisco, CA), as indicated in the manufacturer's preload method for 400 mg Ab, with the element–Ab combinations shown in **Supplementary Table I**. Element–Ab conjugates were adjusted to 1 mg/ml in Ab stabilizer buffer (Candor Bioscience, Wangen, Germany), supplemented with sodium azide (Santa Cruz Biotechnology) to a final concentration of 0.01%, and stored at 4˚C in sterile conditions throughout the study. Element–Abs were titrated on cells from healthy macaques to obtain optimal staining concentrations. Antibody specificity and batch modification an antibody background signal were closely monitored during the assay, leading us to analyze separately our 3 groups that were not all done at the same moment.

Intracellular cytokine staining of blood PBMCs and CyTOF staining

PBMC isolation was performed by overlaying a 1:1 (v/v) mixture of Li-heparin–collected whole blood and Dulbecco's PBS (Invitrogen) on a mixture of 95% Lymphocyte Separation Media 1077 (GE Healthcare, PAA, Austria) and 5% PBS, and centrifuging at 420 g for 45 min at room temperature (RT). PBMCs at the Separation Media–plasma interface were collected and washed twice in complete media (complete RPMI), which comprised RPMI 1640 media supplemented with 10% heat-inactivated FBS and 100 U/ml penicillin, strepto- mycin, and neomycin. If the pellet was red after lymphocytes separation, red blood cells were lysed during five minute with a hypotonic solution, and then washed with PBS. Fresh PBMCs (5.10^6 /well) were then stimulated *in vitro* using MVAwild type (MVA TGN33.1, Transgène) during four hours and then incubated overnight at 37°C with BFA. The day after, 1µL of rhodium (Fluidigm) was added in each well. Cells were then reincubated during

15min at 37°C. Cells were then washed twice in staining buffer (SB; BD Biosciences, Franklin Lakes, NJ) and then incubated for 45 min at 4°C with the element tagged surface-stain Abs detailed in Supplemental Table I in a total volume of 50 ml SB. Cells were washed twice with SB and then fixed in 2% paraformaldehyde (Electron Microscopy Sciences) in PBS for 45 min at 4°C. Cells were washed twice in SB and then three times in permeabilization buffer (eBioscience), and then stained with intracellular Abs (Supplemental Table I) in 50 ml permeabilization buffer on ice for 30 min. Cells were washed twice in SB and resuspended in 0.25 mM iridium DNAintercalator (Fluidigm) in 200 ml PBS + 2% paraformaldehyde overnight at 4˚C, before washing once in SB, once in PBS, and three times in ddH2O, and filtered through a 5 ml Polystyrene round-bottom tube with cell strainer cap (BD Biosciences). Fifty microliters of 4-Element EQ Beads (Fluidigm) was added to each sample, which were acquired as two replicates in mass cytometer (CyTOF; Fluidigm) following the standard procedure recommended by the manufacturer[180]. The CyTOF acquisition gave us standard flow cytometry standard files(fcs).

CytoF files preprocessing

Similar to a previous study[179]. Fcs files obtainedwere normalized separately for each administration routes but comprised all the kinetics with the MatLab Compiler software normalizer[181] using the signal from the 4-Element EQ beads (Fluidigm) as recommended by the software developers. The replicates of each sample were then concatenated using R software[10]. CD4 and CD8 T lymphocytes were manually gated as illustrated using Cytobank® software[182] in **Supplementary Fig.XX**.

Spanning-tree progression analysis of density-normalized event

Similar to a previous study[179]. The spanning-tree progression analysis of density-normalized events (SPADE) algorithm was then used to identify CD4 and CD8 T cell populations having similar marker intensities in cytometry datasets. SPADE was performed using the publicly available R/Bioconductor package[183].As a result, a total of 6 SPADE were performed for all our conditions: CD8 SC, CD8 ID, CD8 IM, CD4 SC, CD4 ID and CD4 IM. To reduce bias during the SPADE down-sampling step caused by

large variances between the numbers of cells events in each flow cytometry standard file, we first randomly selected the number of cells of the smallest sample uniformly for each sample for each SPADE analysis. We then performed the SPADE density-based down-sampling using a target 30% of those preselected cells. Individual SPADE trees were then generated using all CD4+ or CD8+ cells from each sample (up-sampling). For both CD4 and CD8 SPADE analyses algorithm sorted cells based on 13 clustering markers : Bcl2, GranzymeB, CD62L, CD69, CD154, CD197, IFNγ, IL2, IL17, Ki67, MIP1β, Perforin and TNFα. Those markers were selected due to their ability to define T cells functions and their signal reproducibility. The number of cluster (i.e number of group of cells) chosen was the best compromise we found between homogenic, but also not too empty clusters. We selected 50 clusters for CD8 T cells and 70 clusters for CD4 T cells.

Identification of differentially abundant clusters

Differentially abondant clusters (DACs) were identified based on the percentage of cells in individual SPADE clusters, relative to total CD8 or CD4 T cells. For each SPADE cluster at each time point, the mean percentage of CD8 or CD4 T cells were computed. A one-sample Student t test ($p< 0.05$) was used to determine whether clusters were abundant, and whether the proportion of each cluster was similar between the four macaques

Statistical analysis and graphical representations

Cytometry, Luminex and transcriptomic data were analyzed using R. Hierarchical clusterings were performed based on the Euclidean metric and using the Ward linkage method. Flow cytometry have been scaled in the heatmaps representations in order to have each the same minimal and maximal expression values. For transcriptomic, differentially expressed genes were identified using the paired Student t-test (q-value<0.01) and based on a fold-change threshold of 1.2. Multidimensional scaling representations were generated using the SVD-MDS algorithm [125]. Multidimensional scaling methods aim to represent the similarities between high-dimensional objects, generally in a 2- or 3-dimensions. The Kruskal Stress [155] indicated at the bottom of the representation quantifies the

quality of the MDS as the fraction of information lost during the dimensionality reduction process. Functional Enrichment analysis of the different lists of differentially expressed genes was performed using Ingenuity Pathway Analysis software (IPA®, Qiagen, http://www.qiagen.com/ingenuity). Upstream regulators having a q-value<10^{-3} and belonging to cytokine signaling, humoral immune response or pathogen influenced signaling categories were represented at the exception of FSH, LH and prolactin regulators. Canonical pathways having a q-value<10^{-3} and belonging to cellular immune response, cytokine signaling, humoral immune response and pathogen influenced signaling categories were represented. Statistical analysis for flow cytometry and Luminex data were performed using Prism 6.0® (Graphpad Software Inc., La Jolla, CA, USA). Two-sided Friedman tests followed by a Dunn's post-test comparing each timepoint with the baseline were performed. Significant correlations between Luminex, imaging, CBC, and cytometry variables were identified using the Pearson coefficient of correlation based on a correlation threshold of 0.80 and a q-value threshold of 0.05. Representation of the co-expression network was performed using Cytoscape® [156]. The phenotypic categorization of SPADE was calculated using the 5th and 95th percentile range for each marker intensity and then dividing this range into five uniform categories. The categorization was computed based on the means of the individual SPADE expression medians for each marker. The categories represented negative, low, medium, high, and very high marker expression using a color scale from white to dark red, which was used to produce a heat map. Hierarchical clustering for the clusters of the phenotypical heat map (Fig Dendro+Trees) was performed using the Euclidean metric and the complete linkage method

Results

Cellular changes at site of MVA injection and in draining lymphoid tissues

To characterize the local early immune response, we studied tissue structures, cell movements and molecular signatures 24h after MVA injection. MVA ID and SC injections induced local inflammation, whereas the tissues appeared unchanged after buffer injection (**Fig.1A**). Mantoux ID injection[72], results in a massive inflammation with dramatic polymorphonuclear neutrophils (PMN, or granulocytes) and macrophages recruitment, mainly localized in the dermis. By using an anti-E3L specific antibody - an MVA protein - we observed numerous MVA-infected cells mostly localized in the dermis. Response to SC injection is associated to a mild and focal granulocytic infiltration with necrosis, mainly localized at the dermis/hypodermis interface. A diffusemacrophage infiltrationis observed in the sub-epithelial area of the dermis (**Fig.1B**). By contrast to ID injection, no MVA-infected cells were observed in the dermis after SC administration. This could be explained by the fact that the MVA suspension injected in the subcutaneous tissue spreads out fast and thus is not massively retained by the tissue unlike after an ID administration, suggesting that most of the antigen presentation would likely be handled by resident skin cells after ID route, whereas passive diffusion to the draining lymph node (dLN) may predominate after SC route. We observed after both SC and ID route the presence of MVA-infected cells in dLNs, without however identifying any particular antigen presenting cells associated. Flow cytometry analysis on whole skin extracted cells confirmed the induction of inflammation by both routes (**Fig.2**). The magnitude of the local recruitment of inflammatory cells is also more diverse after SC including -in addition of granulocytes and macrophages- monocytes ($p=0.03$ after SC; $p=0.06$ after ID) and possibly other DR+ cells ($p=0.09$ after SC; $p=0.21$ after ID). Conversely, lymphocytes were recruited in higher proportions after ID injection ($p=0.31$ after SC; $p=0.03$ after ID). Altogether, this shows that MVA is highly active at inducing a strong local inflammation after both SC and ID route 24h after injection, with however some slight differences between the routes in the antigen localization, cell influx and the magnitude of the response. No particular trend has been highlighted in cell population movements in the dLNs

24h after MVA vaccine injection in comparison with buffer. This might be due to the fact that MVA-specific antigen presentation is not frequent enough to be distinguished from regular cell patrolling at the scale of an entire lymph node. In addition, we may not have selected the most activated lymph node of the inguinal chain. Indeed, no lymph node of the chain appeared particularly macroscopically singular 24h after MVA immunization.

Local immune reaction after MVA intramuscular (IM) administration was not evaluated in the same condition as ID and SC. Indeed, the use of more invasive biopsy sampling increased the difficulties to gather accurately the site of injection and increased the variability. Considering these technical issues, MVA also induced an important local reaction after IM route (**Fig.S1**). Lesions and cell subset recruitment appeared delayed to SC and ID routes, peaking at 48h rather than 24h post-MVA injection. In addition, macrophages but not granulocytes, lymphocytes or dendritic cells are significantly recruited at this timepoint. As a result, it appears that the local innate immune response following IM injection might also differ from ID and SC.

Local transcriptomic changes following MVA injection

Transcriptome analysis of the injection site after SC and ID MVA injection also highlighted an important local immune reaction (**Fig.3A**). We noted a comparable number of genes upregulated with both ID and SC routes, but more genes downregulated after ID route (4382 genes after ID; 599 genes after SC). Notably, we had more genes regulated in common (23.3%) after MVA ID and SC injections in comparison to buffer (2.9%) (**Fig.3B**). Almost no genes (20 for ID route, 24 for SC route) were regulated in dLN (**Fig.3A-B**). Multidimensional scaling (MDS) representation[125,155] depicted very different profiles of genes expressed in the epidermis plus dermis in comparison to subcutaneous tissues (**Fig.3C**). This method allows to rapidly and easily visualizing similarities and dissimilarities of the dataset. Each biological variable were represented in a two-dimension space with a dot. Differential gene expression between two variables was converted in to a Euclidian distance. An important distance between two variables indicates strong differences. Biological variable belonging

to a same group were then linked to form a colored polygon. As expected, differences are appeared between ID or SC route even at baseline and following buffer injection. MVA injections also exhibited a very different profile from control conditions. Confirming histology and flow cytometry analysis, extremely poor gene segregation between the different experimental conditions characterized dLN. Functional enrichment (**Fig.3D**) revealed an increase of inflammation-related effectors such as TREM1, interferon and acute phase response signaling. However, the number of upregulated pathways, including IL-6 and NfkB signaling as well as dendritic cell maturation was higher after SC than after ID injection. By contrast and in accordance with the previous analysis, no immune pathways in dLN were significantly induced. The molecular analysis of skin samples showed however, numerous transcripts decreased after MVA immunization, with more downregulations for ID when compared to SC (**Fig.3A, 3B** and **3C**). This difference may result from the massive inflammatory cells recruitment that could limit the detection of genes related to resident cells(more heterogenic in the skin) rather than true downregulationsfollowing MVA immunization. In addition, some rare cell populations such as dendritic cells could migrate from skin to dLNs. Cell migration could also explain the less important immune function activations following ID route such as dendritic cell maturation pathway. In addition, macrophages-related pathways such as reactive oxygen species production and Fc-gamma receptor phagocytosis appeared more regulated after SC route MVA injection. This suggests more important macrophage activation for SC route in comparison to ID route and also converges with the more important local inflammatory cell recruitment observed after SC route (**Fig.2**).

MVA-induced systemic inflammation echoes the innate response elicited at the injection sites.

We further analyzed the impact of injection site on MVA-induced early changes in blood compartment. We represented those changes in a log_2FC (fold change) scaled heatmap, allowing us to sort cell populations depending on their recruitment over the time. During the first hours following injection, the three routes of immunization induced an increase in the blood of CD14+ myeloid derived suppressive cells (MDSCs) (significance over the time: $p<0.0001$ for SC and ID; $p=0.005$ for IM) (**Fig.4A**). Similarly, we also noted significant recruitments over time of PMN and classical monocytes (CD14+CD16-). Early kinetics for those cell populations also appeared similar for the three conditions: PMN reached a peak 6h post MVA injection whereas CD14+ MDSCs and classical monocytes were more recruited 24h post MVA injection. At the opposite, lymphocytes left the blood compartment between 6h and 24h post MVA injection. However, 24h after MVA administration, CD14+CD16+ transitory monocytes ($p=0.015$), T CD8+ lymphocytes ($p=0.009$) and pDCs ($p=0.0022$) were significantly less recruited after ID route in comparison with SC route (**Fig.4B**). pDCs were also significantly more recruited in the blood after SC route in comparison with IM route ($p=0.026$ after 24h). In addition, differences in the recruitment of Lin-MDSCs at the advantage of IM route in comparison with ID were observed ($p=0.015$ after 24h).

Analysis of gene expression signatures highlighted some heterogeneity between administration routes (**Fig.5A**). More genes appeared to be downregulated after ID and IM route in comparison to SC route. In spite of a comparable magnitude (peak at around 800 genes), the number of upregulated genes over the time differed between each groups. Indeed, after SC route, the peak was reached at 6H and persisted at 24H whereas for ID route, the peak was transient, peaking at 6H and then rapidly decreasing at 24h. Following IM injection, the number of upregulated genes was already high at 3H and continued to increase until 24H. Venn's diagram showed that 22.4% of genes are common between the three conditions at 6H (**Fig.5B**). Notably, we observed more genes regulated in common between ID and IM route exclusively (37% at 3H, 17.6% at 6H and 17.7% at 24H) than between ID and SC route (8.7% at 3H, 2.9% at 6H and 2.9% at 24H genes regulated in common). MDS (performed

similarly than in Fig.3C) also depicted different gene expression profiles depending on the administration route (**Fig.5C**). After SC route, the shapes representing the timepoints are superimposed. It betrays similarities in the gene expression. They are slightly more clearly differentiated after ID route, with notably more distance between the untreated and the 24h post MVA administration condition. It was even more the case after IM route, especially 6H after MVA injection. Functional enrichment analysis revealed that the modulations of several immune related pathways are shared by all three conditions, in particular innate functions associated to lL-6 and TREM1-signaling (**Fig.5D**). This recapitulates changes observed at site of injection with however different kinetics and magnitude. Most of the significantly immune-related pathways were strongly upregulated very early, at 3H after IM and ID route. This upregulation occurred more lately after SC route, at 24H. The magnitude of this response was less important (for instance max Z-score TREM1 signaling: z=3.87 for SC, z=3.46 for IM; z=2.5 for ID) which is rather characterized by downregulated inflammatory related pathways at 24H such as LPS-stimulated MAPK signaling, dendritic cell maturation or IL-8 signaling. Also we observed several pathways related with lymphoid response (such as iCOS-iCOSL signaling in T helper cells, calcium-induced T Lymphocyte apoptosis, or CD28 signaling in T helper cells) downregulated after ID and IM route, but not SC route.

Overall, we observed important myeloid recruitment including Lin- and CD14+ MDSCs, but also granulocytes, classical monocytes and transitory monocytes arrival, whereas B and T lymphocytes left the blood circulation. Notably the cell movements were globally similar for each administration route, with however some exceptions such as T CD8+ lymphocytes, transitory monocytes and pDCs which decreased after 24h in ID route in comparison to SC route. These exceptions, in addition with different cell activation, could have a significant impact on the gene expression. We indeed highlighted different quantities of regulated genes depending on the administration route. More particularly, canonical pathways related with immune response were also following different kinetics and magnitude depending on the administration route. Notably, the kinetics of those pathways enrichment incite us to categorize the SC group (peak at 24h) from SC and ID group (peak at 3h).

Differences in early local and systemic responsesbetween SC, ID and IM administration routesresult in different adaptive response profiles.

The measure of MVA-specific IgG indicated a limited impact of the administration route on binding antibody responses with no significant titers observed after the boost(**Fig.6A**). However, IgG produced after SC route were found to be significantly more efficient to neutralize the MVA virus infection in comparison with ID (p=0.028 at day 8 post boost (D8PB); p=0.057 at D14PB) and IM route (p=0.028 at D8PB), at early time points following the boost (**Fig.6B**).

The CD8+ and CD4+ T lymphocyte responses were further characterized by intracellular production of cytokines following PBMCs *ex vivo* stimulation with MVA for 18h. Cells were than stained with antibodies coupled with metals and acquired by mass cytometry. A strong advantage of this recent technology is its ability to detect up to 40 parameters at a single cell level. In addition, mass cytometry was already found to be a valuable tool to evaluate B and T cell responses[179,184].The first mass cytometry analysis was focused on IFNγ production by CD8 and CD4 T cells. It was measured following a classical cytometry gating, like with a conventional flow cytometer (**Fig.S3**). Surprisingly, it showed important discrepancies according to the route. For the CD8+ T cells, we indeed observed a significantly lower IFNγ production after SC route in comparison with ID (p=0.029 at D8PB), and IM route (p=0.029 at D8PB), particularly after the boost. A similar but less clear trend was also observed for CD4+ T lymphocytes with significantly less productions in SC route vs IM at D8PB (p=0.015) (**Fig.6C**).

The second mass cytometry analysis aims to exploit most of the markers we used to evaluate CD8+ and CD4+ T cell response after MVA administration. To perform this, we first manually gated CD8+ and CD4+ T cell separately (**Fig.S3**). SPADE (spanning tree progression of density) algorithm was then used to sort out CD8+ and CD4+ T lymphocytes in clusters based on function and homing markers (Bcl2, Granzyme B, CD62L, CD69, CD154, CD197, IFNγ, IL-2, IL-17, Ki67, MIP-1β, perforin and TNFα). Each SPADE analysis was performed using one cell type (CD8+ or CD4+ T cell), one administration route (ID, IM, or SC), and the total of timepoints (Baseline, day 8 post prime (D8PP), D57PP, D8PB,

D28PB). The CD8+ T cells were divided in 3 SPADES (one for each administration route) of 50 clusters each, and the CD4+ T were divided in 3 SPADES (one for each administration route) of 70 clusters each. For each SPADE analysis, clusters were automatically sorted accordingly to their phenotype (**Fig.S4 & Fig.S5**). As a result we obtained six heatmaps where we can observe the marker expression of each cluster. We observed that for each condition, the phenotype profile of clusters is not uniform. Indeed, hierarchical clustering separated them in groups with distinct phenotypes, that are however different depending on the administration route and the cell type.

With the aim to identify MVA-specific cells and other singular profiles, we performed a MDS representing the clusters from the three CD8+ T cells SPADE analyses (**Fig.7**). Doing so, we identified eight clusters (two clusters from SC route, two from ID route, and four from IM route) that went very separated from the others (black circle) (**Fig.7A**). We then looked at the kinetics of the eight clusters, looking at the percentage of CD8+ T cells (**Fig.7B**). In the two clusters associated with the SC route (clusters SC 41 and 50), cells appeared to be recruited in only 50% of subjects after the prime and in very low quantities (313 cells in total for cluster 41; 415 cells for cluster 50). The two ID route clusters (clusters ID 44 and 50) were differentially enriched clusters (DEC) at D8PB and D57PB in comparison to the baseline. In the four IM route clusters (clusters IM 38, 48, 49 and 50), we observed more heterogeneity in the kinetics, with however overall more cell recruitment after the boost ($p<0.05$ at D8PB for cluster 38 and 50; $p<0.05$ at D28PB for cluster 48 and 50). We then performed a similar analysis for the CD4+ T cells (**Fig.8**). We identified only two very segregated clusters: one for SC route (cluster SC 70), one for the IM route (cluster IM 70), but none for ID route (**Fig.8A**). Looking at the kinetics, we found that the SC route cluster contained almost no cells (**Fig.8B**). However, the IM route cluster showed significantly more cells at D57PP, D8PB, and D57PB in comparison to the baseline.

The next task was to characterize the phenotypic profile of our CD8+ and CD4+ T cell clusters, with a particular attention for the very segregated clusters identified previously. The 50 CD8+ clusters were grouped into fiveblocks (**Fig.9**). Indeed, we could not obtain consistent and biologically coherent groups for the three administration route only using hierarchical clustering (**Fig.S3**). That is why we

reordered again few clusters after the hierarchical clustering process based on perforin, IFNγ, CD197 and Ki67 expression. Doing so we obtainedblocks delimitating groups sharing close biological functions that were found similar for each administration route. The polyfunctional group is characterized in this study by IFNγ, CD69, but also variable IL2, MIP1β and TNFα expression. The cytotoxic group is expressing perforin, but also variable levels of granzyme B. A proliferative group was producing Ki67. The migrating group express homing receptors to secondary lymphoid organs such as CD197, but also variable levels of CD62L, and the "various profiles" group contained someTNFα positive, MIP1β positive, and others heterogenic clusters.

Interestingly, the very segregated clusters harbored a polyfunctional phenotype. These polyfunctional clusters showed were pretty similar over the biological conditions. Indeed, in addition of the CD69, IFNγ, TNFα and IL2 backbone, we also observed some IL10 (expressed in IM route group) and CD278 (expressed in SC and IM route groups) expression. The cytotoxic CD8+ cells were not found to be particularly more enriched after SC or IM route, whereas two clusters were more enriched at D8PP after ID route. Proliferative CD8+ T cells group were induced at D8PP for each administration route. Migrating cells group showed more cluster differentially enriched after ID route.

We performed exactly similarly for CD4+ T cells. We split the 70 clusters resulting from each SPADE analysis into the same fiveblocks (**Fig.10**). Likewise CD8+ T cells,the very segregated clusters (SC cluster 70 and IM cluster 70) also harbored a polyfunctional phenotype. The two polyfunctional clusters (one in the IM group and one in the SC group) also express CD154 in addition to CD69, IFNγ, TNFα and IL-2. The polyfunctional cluster of the SC route exhibited however some level of IL-4 expression. The cytotoxic group was enriched after SC route with notably two DECs among three clusters at D57PP. This group of cells however decreased over the time after ID and IM route. Similarly to CD8+ T cells, MVA induced proliferative CD4+ T cells at D8PP for each administration route. The migrating group was found to include an important set of clusters, with however very few DECs observed in the SC group in comparison with ID or IM group.

In the “various profiles” blocks, we observed a different behavior over the time of TNFα positive clusters depending on the administration route for both TCD4 and TCD8, but it might be biased by the important TNFα production observed at H0 for ID and IM group.

Overall, study of adaptive response profiles in the blood showed important differences depending on the administration route. MVA administration through SC route gave a more effective Th2 oriented response with neutralizing antibodies production combined with limited quantities of polyfunctional CD4+ and CD8+ T cells. At the opposite, ID and IM administration were more associated with Th1 profiles, with less neutralizing antibodies but more IFNγ producing CD8+ T lymphocytes after the boost. More particularly, those cells produced more Th1 related cytokines such as TNFα, IFNγ, MIP1β or IL2. IM route appeared to be even more Th1 oriented, since it was the only administration route showing a CD4+ T cell polyfunctional cluster increased after the boost. T cells harboring a Th2 profile were less clearly detected in the blood. However, even if it was in very low quantities as well as not a DEC, CD4+ T cells polyfunctional cluster of SC route harbored some IL4 expression. That could be a sign of a strong Th2 activation in secondary lymphoid organs, explaining the best MVA neutralization efficiency after SC route.

Discussion

This exploratory study relied on four important strengths to evaluate the role of administration route in a vaccination process: 1) The relevance of the use of an *in vivo*non-human primate model to investigate complex biological process, associated with MVA 2) The system vaccinology approach, to study the immune responses in different key localizations (injection site, draining lympho node and blood) in its entirety. 3) The use of a wide set of multiparameter techniques allowing to analyze the immune response at a tissue scale (histology, immunohistofluorescence), cellular scale (flow cytometry, mass cytometry), and a molecular scale (microarrays) 4) Original data analysis tools from computational biology (MDS, SPADE analysis).

At a first sight, early local and systemic immune response gave comparable profiles between administration routes. MVA being very immunogenic, we observed strong local but also systemic inflammatory cells recruitment induced after SC, ID and IM route. We however did not observe any particular MVA-specific activation in the draining lymph node, even if some cells expressing a MVA protein were observed. However, looking in the details this early immune reaction made emerge important discrepancies between routes. At the site of injection, we indeed observed small differences in the quality of the innate immune response. After SC routes we observed a more diverse set of pro-inflammatory cells (including monocytes and other remaining HLADR+ cells) recruited in comparison with ID or IM routes. At the opposite, lymphocytes were more significantly recruited locally after ID route. We also had different antigen localization between SC and ID route, which was found after ID and not SC route. In addition, the acute immune response pathways were more intensively upregulated after SC route. Similarly to the injection site, the cellular response also differed in some aspects in the blood, with several cell populations more induced after SC route in comparison with IM/ID route such as CD16+CD14+ transitory monocytes, CD8+ T lymphocytes or pDCs. The transcriptomic immune signatures also gave different kinetic profiles, with however proximity between ID and IM route being very early induced (at 3H post injection), at the opposite of SC route being induced more lately (at 24H). This categorization between IM/ID group and SC group

remained at the analysis of the late vaccine response. In comparison with ID and IM route, we indeed found more neutralizing antibodies in favor of SC route, counterbalanced by a reduced induction of CD8+ and CD4+ T polyfunctional response. But interestingly, the few polyfunctional CD4+ T cell also expressed IL4. Overall, this study showed that SC route administration induced a more Th2 oriented profile in comparison with IM and ID route, which were more Th1 oriented.

The local and systemic acute inflammatory processes described after SC, ID, and IM route can be considered as an indicator of an important immunogenicity. Indeed, several studies focusing on local immune reaction characterized granulocytes and macrophages recruitments kinetics and functions after immunization, notably with vaccine adjuvants such as TLR ligands or oil-in water emulsion[131,140,185]. This rapid innate reaction appeared to be crucial to protect the organism against tissue lesions and infections. Granulocytes and macrophages were indeed able to release pro-inflammatory mediators and cytokines in addition to exert phagocytic activity to get rid of the threat[186]. This acute immune reaction was also logically mediated by several molecular pathways being upregulated such has IL6, nitric oxide production, or TREM1 (triggering receptor expressed on myeloid cells) [27,187].

The magnitude and the systemic kinetics of the inflammatory response were found to be slightly different depending on the route. SC route induced an overall stronger local inflammation than ID and IM route, which was in addition more persistent in the systemic compartment.In this study it also appeared that SC route gave a more Th2 oriented response. Two factors could explain how administration route could impact the inflammation profile.

The first one would be the nature of site of injection. Indeed, skin, as a barrier between body and environment, is an organ that has major immunosurveillance functions and thus hosts large quantities and variety cells dedicated to immune functions at steady state[75]. This intrinsic particularity might result to a better capacity to rapidly resolve the local acute inflammation induced by MVA[188]. On the other side, subcutaneous tissue is dedicated in triglycerides storage and metabolic functions, and is thus mostly composed by adipocytes, with however some macrophages and

lymphocytes[71,189]. In addition, unique microvascularization of adipose tissue, which could facilitate recruitment of cells from the blood, might amplify the magnitude and persistence of the inflammation[190]. Muscle tissue, which doesn't shine by any particular immune functions , also hosts some immune cells at steady state that might help to control the inflammation[65].

The second one is MVA diffusion in the tissue, which is only confined in a restricted zone after ID Mantoux immunization[171], whereas it spreads out way more importantly after subcutaneous injection. It would indeed allow MVA to infect and interact with large set of immune, but also non-immune cells, since it does not require any specific receptor. This might lead in the increase of the production of inflammatory mediators, inducing more inflammation and activation[158,163]. Muscle tissue, which has a fairly high density, would probably show an intermediate profile between subcutaneous tissue and skin.

This innate immune profile could also impact the adaptive response in many ways. The kinetic of inflammation is even crucial in the pathogenicity of particular viruses[191]. If macrophages are professional APCs[33], granulocytes can also potentially act as an antigen carrier, that may induce adaptive effectors of the draining lymph node, but can also produce cytokines that mediates dendritic cell activation[133,192]. Cytokines produced during inflammation process can also modulate the response[193,194]. The antigen presentating cells mobilized might differ as well depending on the administration route. If the persistence of the antigen in the skin after ID immunization suggests the possibility of an uptake by local DC subsets such as LCs or dermal DCs [75,195], we only observedtrends assessing a possible CD1a+ DCs migration from the skin. However this phenomenon might have been underestimated, and outshined by the massive changes of the skin cell composition due to the massive inflammatory cell recruitment. After SC route, due to the more important liquid spreading, MVA might be able to more diffuse passively to draining lymph node after SC route. This passive diffusion might lead to activation of subcapsular macrophages as shown in mice models[167] . It would be in accordance with the presence of MVA-infected cells around subcapsular sinus of draining lymph nodes observed at 24h after injection SC, but also ID route. In spite off we observed no major

difference at 24h, this cellular recruitment in lymph node could also occur at a different timepoint not investigated[66].

Otherwise, we provide a body of argument that T cell early mobilization is associated with the adaptive response profile. Indeed, after ID route more than SC route, lymphocytes are migrating from the blood to the skin tissue. Looking at the blood molecular signatures, after both ID and IM route functions related with T cells rapidly decrease in comparison with SC route. More particularly, blood CD8+ T cells –a key effector of Th1 response- were significantly less decreasing 24h after SC administration in comparison with ID route, IM route exhibiting an intermediate profile. This early polarization of T cells, particularly CD8+ T cells induced logically a more Th1 oriented response at later timepoints after ID and IM route in comparison with SC.

We also characterized in-depth CD4+ and CD8+ T lymphocyte profiles. Among several phenotypic profiles, we characterized finely –a "polyfunctional" profile characterized by IFNγ, but also TNFα, IL2 and MIP1β expression. This profile exactly matches with the T effector memory cells induced by a recombinant cytomegalovirus expressing SIV proteins described by Hansen *et al.*[196]. In this study, the presence of this particular phenotype, in addition of the absence of neutralizing antibodies induced a resistance of rhesus macaques of getting infected by SIV. We are in the same situation in this study after injecting MVA after ID route but not SC, IM showing intermediate titers of neutralizing antibodies. The only difference is that we measured the response induced against the viral vector but not the transgene. But if MVA behaves like rhCMV, MVA-HIV would be a promising vaccine using ID route, but might not be efficient enough after SC or even IM route, which are the classical routes of immunization. We however need to investigate further in the relationship between innate and adaptive effectors, to delineate why a given route would induce a more suitable immunity than the other. To reach this aim, computational biology could provide some answers. Indeed, this kind of dataset could be a precious resource to modelize immune processes and identify predictive biomarkers of the adaptive immunity.

Altogether, administration route appears to be critical to modulate vaccine induced immune response, and should be considered very wisely in vaccine trials as it could lead to strikingly different outcomes.

References

1. Rosenbaum, P. Etude de la réponse immunitaire induite par des adjuvants agonistes des TLR sur la peau de macaque. (These de pharmacie, Rennes, 2012). at <http://www.sudoc.fr/167282689>
2. van Panhuis, W. G. *et al.*Contagious Diseases in the United States from 1888 to the Present. *N. Engl. J. Med.***369,** 2152–2158 (2013).
3. Andersen, P. & Doherty, T. M. The success and failure of BCG - implications for a novel tuberculosis vaccine. *Nat. Rev. Microbiol.***3,** 656–662 (2005).
4. Mayr, A., Hochstein-Mintzel, V. & Stickl, H. Abstammung, Eigenschaften und Verwendung des attenuierten Vaccinia-Stammes MVA. *Infection***3,** 6–14 (1975).
5. Kim, J., Rerks-Ngarm, S. & Excler, J. HIV Vaccines-Lessons learned and the way forward. *Curr. Opin. HIV***5,** 428–434 (2010).
6. Ahmed, S. S., Plotkin, S. a, Black, S. & Coffman, R. L. Assessing the safety of adjuvanted vaccines. *Sci. Transl. Med.***3,** 93rv2 (2011).
7. Cristiani, C. *et al.* Safety of MF-59 adjuvanted vaccine for pandemic influenza: Results of the vaccination campaign in an Italian health district. *Vaccine***29,** 3443–3448 (2011).
8. Paavonen, J. *et al.* Efficacy of a prophylactic adjuvanted bivalent L1 virus-like-particle vaccine against infection with human papillomavirus types 16 and 18 in young women: an interim analysis of a phase III double-blind, randomised controlled trial. *Lancet***369,** 2161–2170 (2007).
9. Liko, J., Robison, S. G. & Cieslak, P. R. Priming with Whole-Cell versus Acellular Pertussis Vaccine. *N. Engl. J. Med.***368,** 581–2 (2013).
10. Warfel, J. M., Zimmerman, L. I. & Merkel, T. J. Acellular pertussis vaccines protect against disease but fail to prevent infection and transmission in a nonhuman primate model. *Proc. Natl. Acad. Sci. U. S. A.***111,** 787–92 (2014).
11. Buchbinder, S. P. *et al.* Efficacy assessment of a cell-mediated immunity HIV-1 vaccine (the Step Study): a double-blind, randomised, placebo-controlled, test-of-concept trial. *Lancet***372,** 1881–1893 (2008).
12. Rerks-Ngarm, S. *et al.* Vaccination with ALVAC and AIDSVAX to Prevent HIV-1 Infection in Thailand. *N. Engl. J. Med.***361,** 2209–2220 (2009).
13. Hewitt, E. W. The MHC class I antigen presentation pathway: Strategies for viral immune evasion. *Immunology***110,** 163–169 (2003).
14. Goulder, P. J. R. & Watkins, D. I. Impact of MHC class I diversity on immune control of immunodeficiency virus replication. *Nat. Rev. Immunol.***8,** 619–30 (2008).

15. Silzle, T., Randolph, G. J., Kreutz, M. & Kunz-Schughart, L. A. The fibroblast: Sentinel cell and local immune modulator in tumor tissue. *Int. J. Cancer***108,** 173–180 (2004).
16. Kupper, T. S. *et al.* Production of IL-6 by Keratinocytes. *Ann. N. Y. Acad. Sci.***557,** 454–465 (2008).
17. Saalbach, A. *et al.* Dermal fibroblasts induce maturation of dendritic cells. *J Immunol***178,** 4966–4974 (2007).
18. Tecle, T., Tripathi, S. & Hartshorn, K. L. Review: Defensins and cathelicidins in lung immunity. *Innate Immun.***16,** 151–159 (2010).
19. Danese, S., Dejana, E. & Fiocchi, C. Immune Regulation by Microvascular Endothelial Cells: Directing Innate and Adaptive Immunity, Coagulation, and Inflammation. *J. Immunol.***178,** 6017–6022 (2007).
20. Guilliams, M. *et al.* Dendritic cells, monocytes and macrophages: a unified nomenclature based on ontogeny TL - 14. *Nat. Rev. Immunol.***14 VN - r,** 571–578 (2014).
21. Epstein, F. H. & Luster, A. D. Chemokines — Chemotactic Cytokines That Mediate Inflammation. *N. Engl. J. Med.***338,** 436–445 (1998).
22. Biron, C. a. Role of early cytokines, including alpha and beta interferons (IFN-alpha/beta), in innate and adaptive immune responses to viral infections. *Semin. Immunol.***10,** 383–390 (1998).
23. Leroy, M. & Desmecht, D. Les interférons de type I et leur fonction antivirale. *Ann. médecine vétérinaire***150,** 73–107 (2006).
24. Dai, P. *et al.* Modified Vaccinia Virus Ankara Triggers Type I IFN Production in Murine Conventional Dendritic Cells via a cGAS/STING-Mediated Cytosolic DNA-Sensing Pathway. *PLoS Pathog.***10,** (2014).
25. Ablasser, A. *et al.* Cell intrinsic immunity spreads to bystander cells via the intercellular transfer of cGAMP. *Nature***503,** 530–4 (2013).
26. Kawai, T. & Akira, S. Toll-like receptors and their crosstalk with other innate receptors in infection and immunity. *Immunity***34,** 637–50 (2011).
27. Hodge, D. R., Hurt, E. M. & Farrar, W. L. The role of IL-6 and STAT3 in inflammation and cancer. *Eur. J. Cancer***41,** 2502–2512 (2005).
28. Luster, A. D., Alon, R. & von Andrian, U. H. Immune cell migration in inflammation: present and future therapeutic targets. *Nat. Immunol.***6,** 1182–90 (2005).
29. Serhan, C. N. & Savill, J. Resolution of inflammation: the beginning programs the end. *Nat. Immunol.***6,** 1191–1197 (2005).
30. Banchereau, J. & Steinman, R. M. Dendritic cells and the control of immunity. *Nature***392,** 245–252 (1998).

31. Bruel, T. *et al.* Plasmacytoid dendritic cell dynamics tune interferon-alfa production in SIV-infected cynomolgus macaques. *PLoS Pathog.***10,** e1003915 (2014).
32. Ketloy, C. *et al.* Expression and function of Toll-like receptors on dendritic cells and other antigen presenting cells from non-human primates. *Vet. Immunol. Immunopathol.***125,** 18–30 (2008).
33. Hume, D. a. Macrophages as APC and the dendritic cell myth. *J. Immunol.***181,** 5829–5835 (2008).
34. Falcone, M., Lee, J., Patstone, G., Yeung, B. & Sarvetnick, N. B lymphocytes are crucial antigen-presenting cells in the pathogenic autoimmune response to GAD65 antigen in nonobese diabetic mice. *J. Immunol.***161,** 1163–1168 (1998).
35. Ahmed, R. & Gray, D. Immunological memory and protective immunity: understanding their relation. *Science (80-.).***272,** 54–60 (1996).
36. Itano, A. a & Jenkins, M. K. Antigen presentation to naive CD4 T cells in the lymph node. *Nat. Immunol.***4,** 733–9 (2003).
37. Idris-Khodja, N., Mian, M. O. R., Paradis, P. & Schiffrin, E. L. Dual opposing roles of adaptive immunity in hypertension. *Eur. Heart J.***35,** 1238–1244 (2014).
38. Diehl, S. & Rincón, M. The two faces of IL-6 on Th1/Th2 differentiation. *Mol. Immunol.***39,** 531–536 (2002).
39. Okada, R., Kondo, T., Matsuki, F., Takata, H. & Takiguchi, M. Phenotypic classification of human CD4+ T cell subsets and their differentiation. *Int. Immunol.***20,** 1189–1199 (2008).
40. Cher, D. J. & Mosmann, T. R. Two types of murine helper T cell clone. II. Delayed-type hypersensitivity is mediated by TH1 clones. *J. Imunol.***138,** 3688–94 (1987).
41. Coffman, R. L. *et al.* The role of helper T cell products in mouse B cell differentiation and isotype regulation. *Immunol. Rev.***102,** 5–28 (1988).
42. Schaerli, P. *et al.* CXC chemokine receptor 5 expression defines follicular homing T cells with B cell helper function. *J. Exp. Med.***192,** 1553–62 (2000).
43. Fazilleau, N., Mark, L., McHeyzer-Williams, L. & McHeyzer-Williams, M. Follicular Helper T Cells: Lineage and Location. *Immunity***30,** 324–335 (2009).
44. Crotty, S. Follicular Helper CD4 T Cells (T_{FH}). *Annu. Rev. Immunol.***29,** 621–663 (2011).
45. Petrovas, C. *et al.*CD4 T follicular helper cell dynamics during SIV infection. *J Clin Invest.***5,** 1–14 (2012).
46. Perreau, M. *et al.* Follicular helper T cells serve as the major CD4 T cell compartment for HIV-1 infection, replication, and production. *J. Exp. Med.***210,** 143–56 (2013).
47. Colineau, L. *et al.* HIV-infected spleens present altered follicular helper T cell (Tfh) subsets and skewed B cell maturation. *PLoS One***10,** 1–19 (2015).

48. Lowin, B., Hahne, M., Mattman, C. & Tchopp, J. Cytolytic T-cell cytotoxicity is mediated through perforin and Fas lytic pathway. *Lett. to Nat.***370,** (1994).

49. Liu, C., Walsh, C. M. & Young, J. D. Perforin : structure and function. *Immunol. Today***15,** 194–201 (1995).

50. Heusel, J. W., Wesselschmidt, R. L., Russell, J. H. & Ley, T. J. Cytotoxic Lymphocytes Require Granzyme B for the Rapid Induction of DNA Fragmentation and Apoptosis in Allogeneic Target Cells. *Cell***76,** 977–987 (1994).

51. Jenkins, M. K., Burrell, E. & Ashwell, J. D. Antigen presentation by resting B cells . Effectiveness at inducing T cell proliferation is determined by costimulatory signals , not T cell receptor occupancy. *J. Immunol.***144,** 1585–1590 (1990).

52. Abbas, A. K. *et al.* Activation and Functions of CD4 + T-Cell Subsets. *Immunol. Rev.* (1991).

53. Fey, T. M. *et al.* In the Absence of a CD40 Signal , B Cells Are Tolerogenic. *Immunity***2,** 645–653 (1995).

54. Fuchs, E. J. & Matzingert, P. B Cells Turn Off Virgin But Not Memory T Cells. *Science***2,** (1992).

55. Bonecchi, B. R. *et al.* Differential Expression of Chemokine Receptors and Chemotactic Responsiveness of Type 1 T Helper Cells. *J. Exp. Med.***187,** 129–134 (1998).

56. Imai, T. *et al.* Selective recruitment of CCR4-bearing T h 2 cells toward antigen-presenting cells by the CC chemokines thymus and activation-regulated chemokine and macrophage-derived chemokine. *Int. Immunol.***11,** 81–88 (1999).

57. Förster, R., Davalos-misslitz, A. C. & Rot, A. CCR7 and its ligands : balancing immunity and tolerance. *Nat. Rev. Immunol.***8,** (2008).

58. Fritsch, R. D. *et al.* Stepwise Differentiation of CD4 Memory T Cells Defined by Expression of CCR7 and CD27. *J. Immunol. (Baltimore, Md. 1950)***175,** 6489–6497 (2015).

59. Xu, H., Manivannan, A., Crane, I., Dawson, R. & Liversidge, J. Critical but divergent roles for CD62L and CD44 in directing blood monocyte trafficking in vivo during inflammation. *Blood***112,** 1166–1175 (2008).

60. Picker, L. J. *et al.* Control of lymphocyte recirculation in man. I. Differential regulation of the peripheral lymph node homing receptor L-selectin on T cells during the virgin to memory cell transition. *J. Immunol.* (1993).

61. Chaparas, S. D. L'immunite dans la tuberculose. *Bull. l'Organisation Mond. la Santé***60,** 827–844 (1982).

62. Wiendl, H., Hohlfeld, R. & Kieseier, B. C. Immunobiology of muscle: advances in understanding an immunological microenvironment. *Trends Immunol.***26,** 373–80 (2005).

63. Zehrung, D., Jarrahian, C. & Wales, A. Intradermal delivery for vaccine dose sparing: Overview of current issues. *Vaccine***31,** 3392–3395 (2013).

64. Zaric, M., Ibarzo Yus, B., Kalcheva, P. P. & Klavinskis, L. S. Microneedle-mediated delivery of viral vectored vaccines. *Expert Opin. Drug Deliv.***5247,** 17425247.2017.1230096 (2016).
65. Liang, F. *et al.* Dissociation of skeletal muscle for flow cytometric characterization of immune cells in macaques. *J. Immunol. Methods***425,** 69–78 (2015).
66. Abadie, V. *et al.* Original encounter with antigen determines antigen-presenting cell imprinting of the quality of the immune response in mice. *PLoS One***4,** e8159 (2009).
67. Calabro, S. *et al.* Vaccine adjuvants alum and MF59 induce rapid recruitment of neutrophils and monocytes that participate in antigen transport to draining lymph nodes. *Vaccine***29,** 1812–23 (2011).
68. Lu, F. & Hogenesch, H. Kinetics of the inflammatory response following intramuscular injection of aluminum adjuvant. *Vaccine***31,** 3979–86 (2013).
69. Caspar-Bauguil, S. *et al.* Adipose tissues as an ancestral immune organ: site-specific change in obesity. *FEBS Lett.***579,** 3487–92 (2005).
70. Pond, C. M. Adipose tissue and the immune system. *Prostaglandins Leukot. Essent. Fat. Acids***73,** 17–30 (2005).
71. Damouche, A. *et al.*Adipose Tissue Is a Neglected Viral Reservoir and an Inflammatory Site during Chronic HIV and SIV Infection. *PLoS Pathog.***11,** 1–28 (2015).
72. Mantoux, C. Intradermo-reaction de la tuberculine. *Comptes rendus l'Académie des Sci.***147,** 355–57 (1908).
73. Artenstein, A. W. Bifurcated vaccination needle. *Vaccine***32,** 895 (2014).
74. Roediger, B. *et al.*Cutaneous immunosurveillance and regulation of inflammation by group 2 innate lymphoid cells. *Nat. Immunol.***14,** 564–73 (2013).
75. Nestle, F. O., Di Meglio, P., Qin, J.-Z. & Nickoloff, B. J. Skin immune sentinels in health and disease. *Nat. Rev. Immunol.***9,** 679–691 (2009).
76. Zaid, A. *et al.* Persistence of skin-resident memory T cells within an epidermal niche. *Proc. Natl. Acad. Sci. U. S. A.***111,** 5307–12 (2014).
77. Malissen, B., Tamoutounour, S. & Henri, S. The origins and functions of dendritic cells and macrophages in the skin. *Nat. Rev. Immunol.***14,** 417–28 (2014).
78. Valladeau, J. & Saeland, S. Cutaneous dendritic cells. *Semin. Immunol.***17,** 273–83 (2005).
79. Kubo, A., Nagao, K., Yokouchi, M., Sasaki, H. & Amagai, M. External antigen uptake by Langerhans cells with reorganization of epidermal tight junction barriers. *J. Exp. Med.***206,** 2937–2946 (2009).
80. Shklovskaya, E. *et al.* Langerhans cells are precommitted to immune tolerance induction. *Proc. Natl. Acad. Sci. U. S. A.***108,** 18049–54 (2011).
81. Stoitzner, P. *et al.* Langerhans cells cross-present antigen derived from skin. *Proc. Natl. Acad.*

*Sci. U. S. A.***103,** 7783–8 (2006).

82. Flacher, V. *et al.* Murine Langerin + dermal dendritic cells prime CD 8 + T cells while Langerhans cells induce cross-tolerance. 1–14 (2014).
83. Klechevsky, E. *et al.* Functional specializations of human epidermal Langerhans cells and CD14+ dermal dendritic cells. *Immunity***29,** 497–510 (2008).
84. Klechevsky, E. Human dendritic cells - stars in the skin. *Eur. J. Immunol.***43,** 3147–55 (2013).
85. Penel-Sotirakis, K., Simonazzi, E., Péguet-Navarro, J. & Rozières, A. Differential Capacity of Human Skin Dendritic Cells to Polarize CD4+T Cells into IL-17, IL-21 and IL-22 Producing Cells. *PLoS One***7,** (2012).
86. Haniffa, M., Gunawan, M. & Jardine, L. Human skin dendritic cells in health and disease. *J. Dermatol. Sci.***77,** 85–92 (2015).
87. Haniffa, M. *et al.* Human Tissues Contain CD141 hi Cross-Presenting Dendritic Cells with Functional Homology to Mouse CD103 + Nonlymphoid Dendritic Cells. *Immunity***37,** 60–73 (2012).
88. Davis, M. M. A Prescription for Human Immunology. *Immunity***29,** 835–838 (2008).
89. Ostrand-Rosenberg, S. Animal models of tumor immunity, immunotherapy and cancer vaccines. *Curr. Opin. Immunol.***16,** 143–150 (2004).
90. von Herrath, M. G. & Nepom, G. T. Lost in translation: barriers to implementing clinical immunotherapeutics for autoimmunity. *J. Exp. Med.***202,** 1159–62 (2005).
91. Kennedy, R. C., Shearer, M. H. & Hildebrand, W. Nonhuman primate models to evaluate vaccine safety and immunogenicity. *Vaccine***15,** 903–908 (1997).
92. Quintana-Murci, L., Alcaïs, A., Abel, L. & Casanova, J.-L. Immunology in natura: clinical, epidemiological and evolutionary genetics of infectious diseases. *Nat. Immunol.***8,** 1165–71 (2007).
93. Mestas, J. & Hughes, C. C. W. Of mice and not men: differences between mouse and human immunology. *J. Immunol.***172,** 2731–2738 (2004).
94. Macchiarini, F., Manz, M. G., Palucka, a K. & Shultz, L. D. Humanized mice : are we there yet ? *Allergy***202,** 1307–11 (2005).
95. Ito, R., Takahashi, T., Katano, I. & Ito, M. Current advances in humanized mouse models. *Cell. Mol. Immunol.***9,** 208–14 (2012).
96. Hérodin, F., Thullier, P., Garin, D. & Drouet, M. Nonhuman primates are relevant models for research in hematology, immunology and virology. *Eur. Cytokine Netw.***16,** 104–116 (2005).
97. Merkel, T. J. & Halperin, S. A. Nonhuman primate and human challenge models of pertussis. *J. Infect. Dis.***209,** 20–23 (2014).
98. Geisbert, T. W., Strong, J. E. & Feldmann, H. Considerations in the Use of Nonhuman Primate

Models of Ebola Virus and Marburg Virus Infection. *J. Infect. Dis.***212,** 91–97 (2015).

99. Flynn, J. L., Gideon, H. P., Mattila, J. T. & Lin, P. ling. Immunology studies in non-human primate models of tuberculosis. *Immunol. Rev.***264,** 60–73 (2015).
100. Gardner, M. B. & Luciw, P. a. Macaque models of human infectious disease. *ILAR J.***49,** 220–55 (2008).
101. Meurens, F., Summerfield, A., Nauwynck, H., Saif, L. & Gerdts, V. The pig: A model for human infectious diseases. *Trends Microbiol.***20,** 50–57 (2012).
102. Roberts, K. L. & Smith, G. L. Vaccinia virus morphogenesis and dissemination. *Trends Microbiol.***16,** 472–479 (2008).
103. Moss, B. Poxvirus entry and membrane fusion. *Virology***344,** 48–54 (2006).
104. Ichihashi, Y. Extracellular enveloped vaccinia virus escapes neutralization. *Virology***217,** 478–485 (1996).
105. Smith, G. L., Symons, J. A. & Vanderplasschen, A. Vaccinia virus immune evasion. *Immunol. Rev.***159,** 137–154 (1997).
106. Smith, G., Mackett, M. & Moss, B. Infectious vaccinia virus recombinants that express hepatitis B virus surface antigen. *Nature***302,** 490–495 (1983).
107. Meyer, H., Sutter, G. & Mayr, a. Mapping of deletions in the genome of the highly attenuated vaccinia virus MVA and their influence on virulence. *J. Gen. Virol.***72 (Pt 5),** 1031–8 (1991).
108. DiPerna, G. *et al.* Poxvirus Protein N1L Targets the I- B Kinase Complex, Inhibits Signaling to NF- B by the Tumor Necrosis Factor Superfamily of Receptors, and Inhibits NF- B and IRF3 Signaling by Toll-like Receptors. *J. Biol. Chem.***279,** 36570–36578 (2004).
109. Waibler, Z. *et al.* Vaccinia virus-mediated inhibition of type I interferon responses is a multifactorial process involving the soluble type I interferon receptor B18 and intracellular components. *J. Virol.***83,** 1563–1571 (2009).
110. Moss, B. *et al.* Host range restricted, non-replicating vaccinia virus vectors as vaccine candidates. *Adv. Exp. Med. Biol.***397,** 7–13 (1996).
111. Sutter, G., Wyatt, L. S., Foley, P. L., Bennink, J. R. & Moss, B. A recombinant vector derived from the host range-restricted and highly attenuated MVA strain of vaccinia virus stimulates protective immunity in mice to influenza virus. *Vaccine***12,** 1032–1040 (1994).
112. Vollmar, J. *et al.* Safety and immunogenicity of IMVAMUNE, a promising candidate as a third generation smallpox vaccine. *Vaccine***24,** 2065–2070 (2006).
113. Sheehan, S. *et al.* A Phase I, Open-Label Trial, Evaluating the Safety and Immunogenicity of Candidate Tuberculosis Vaccines AERAS-402 and MVA85A, Administered by Prime-Boost Regime in BCG-Vaccinated Healthy Adults. *PLoS One***10,** e0141687 (2015).
114. Stickl, H. *et al.* MVA-Stufenimpfung gegen Pocken. *DMW - Dtsch. Medizinische*

*Wochenschrift***99,** 2386–2392 (1974).

115. Altenburg, A. F. *et al.* Modified vaccinia virus ankara (MVA) as production platform for vaccines against influenza and other viral respiratory diseases. *Viruses***6,** 2735–61 (2014).
116. Zhou, Y. & Sullivan, N. J. Immunology and evolvement of the adenovirus prime, MVA boost Ebola virus vaccine. *Curr. Opin. Immunol.***35,** 131–136 (2015).
117. Gómez, C. E. *et al.* A Phase I Randomized Therapeutic MVA-B Vaccination Improves the Magnitude and Quality of the T Cell Immune Responses in HIV-1-Infected Subjects on HAART. *PLoS One***10,** e0141456 (2015).
118. Lelièvre, J.-D., Lacabaratz, C. & Richert, L. Essai de phase I/II sans insu, randomisé, multicentrique évaluant l'immunogénicite et la tolérance de 4 combinaisons « prime- boost » de candidats vaccins VIH (MVA HIV-B /LIPO-5; LIPO-5 / MVA HIV-B; GTU-MultiHIV B /LIPO-5; GTU-MultiHIV B / MVA HIV-B) chez. 33076 (2014). at <www.recherche-vaccinVIH.fr>
119. Richert, L. *et al.* Accelerating clinical development of HIV vaccine strategies: methodological challenges and considerations in constructing an optimised multi-arm phase I/II trial design. *Trials***15,** 68 (2014).
120. Kitano, H. Computatioal Systems Biology. *Nature***420,** 206–210 (2002).
121. Nakaya, H. I. & Pulendran, B. Vaccinology in the era of high-throughput biology. *Philos. Trans. R. Soc. Lond. B. Biol. Sci.***370,** (2015).
122. Querec, T. D. *et al.*Systems biology approach predicts immunogenicity of the yellow fever vaccine in humans. *Nat. Immunol.***10,** 116–125 (2009).
123. Obermoser, G. *et al.* Systems scale interactive exploration reveals quantitative and qualitative differences in response to influenza and pneumococcal vaccines. *Immunity***38,** 831–44 (2013).
124. Pulendran, B., Li, S. & Nakaya, H. I. Systems vaccinology. *Immunity***33,** 516–529 (2010).
125. Bécavin, C., Tchitchek, N., Mintsa-Eya, C., Lesne, A. & Benecke, A. Improving the efficiency of multidimensional scaling in the analysis of high-dimensional data using singular value decomposition. *Bioinformatics***27,** 1413–1421 (2011).
126. Schlitzer, A. & Ginhoux, F. Organization of the mouse and human DC network. *Curr. Opin. Immunol.***26,** 90–9 (2014).
127. Wille-Reece, U. *et al.* Toll-like receptor agonists influence the magnitude and quality of memory T cell responses after prime-boost immunization in nonhuman primates. *J. Exp. Med.***203,** 1249–58 (2006).
128. Nakaya, H. I. *et al.* Systems biology of vaccination for seasonal influenza in humans. *Nat. Immunol.***12,** 786–795 (2011).
129. Gannavaram, S. *et al.* Modulation of Innate Immune Mechanisms to Enhance Leishmania Vaccine-Induced Immunity: Role of Coinhibitory Molecules. *Front. Immunol.***7,** 1–10 (2016).

130. Hartman, Z. C., Appledorn, D. M. & Amalfitano, A. Adenovirus vector induced innate immune responses: Impact upon efficacy and toxicity in gene therapy and vaccine applications. *Virus Res.***132,** 1–14 (2008).
131. Coffman, R. L., Sher, A. & Seder, R. a. Vaccine adjuvants: putting innate immunity to work. *Immunity***33,** 492–503 (2010).
132. Iwasaki, A. & Medzhitov, R. Regulation of adaptive immunity by the innate immune system. *Science***327,** 291–295 (2010).
133. Maletto, B. a. *et al.* Presence of neutrophil-bearing antigen in lymphoid organs of immune mice. *Blood***108,** 3094–3102 (2006).
134. Pozzi, L. -a. M., Maciaszek, J. W. & Rock, K. L. Both Dendritic Cells and Macrophages Can Stimulate Naive CD8 T Cells In Vivo to Proliferate, Develop Effector Function, and Differentiate into Memory Cells. *J. Immunol.***175,** 2071–2081 (2005).
135. Kwissa, M., Nakaya, H. I., Oluoch, H., Pulendran, B. & Dc, W. Distinct TLR adjuvants differentially stimulate systemic and local innate immune responses in nonhuman primates Distinct TLR adjuvants differentially stimulate systemic and local innate immune responses in nonhuman primates. **119,** 2044–2055 (2012).
136. McMahon, J. M., Wells, K. E., Bamfo, J. E., Cartwright, M. a & Wells, D. J. Inflammatory responses following direct injection of plasmid DNA into skeletal muscle. *Gene Ther.***5,** 1283–90 (1998).
137. Cunningham, A. L., Carbone, F. & Geijtenbeek, T. B. H. Langerhans cells and viral immunity. *Eur. J. Immunol.***38,** 2377–85 (2008).
138. Liard, C. *et al.* Intradermal immunization triggers epidermal Langerhans cell mobilization required for CD8 T-cell immune responses. *J. Invest. Dermatol.***132,** 615–25 (2012).
139. Kenney, R. T. *et al.* Dose Sparing with Intradermal Injection of Influenza Vaccine. *J. Med.* 1–7 (2004).
140. Epaulard, O. *et al.* Macrophage- and Neutrophil-Derived TNF-α Instructs Skin Langerhans Cells To Prime Antiviral Immune Responses. *J. Immunol.***193,** 2416–2426 (2014).
141. Meyer, H., Sutter, G. & Mayr, A. Meyer, Sutter, Mayr - 1991 - Mapping of deletions in the genome of the highly attenuated vaccinia virus MVA and their influence on virul.pdf. **382,** 1031–1038 (1991).
142. Wilck, M. B. *et al.*Safety and immunogenicity of modified vaccinia Ankara (ACAM3000): effect of dose and route of administration. *J. Infect. Dis.***201,** 1361–1370 (2010).
143. Gómez, C. E., Perdiguero, B., García-Arriaza, J. & Esteban, M. Poxvirus vectors as HIV/AIDS vaccines in humans. *Hum. Vaccines Immunother.***8,** 1192–1207 (2012).
144. Gómez, C. E. *et al.* High, broad, polyfunctional, and durable T cell immune responses induced

in mice by a novel hepatitis C virus (HCV) vaccine candidate (MVA-HCV) based on modified vaccinia virus Ankara expressing the nearly full-length HCV genome. *J. Virol.***87,** 7282–300 (2013).

145. You, Q. *et al.* Subcutaneous administration of modified vaccinia virus Ankara expressing an Ag85B-ESAT6 fusion protein, but not an adenovirus-based vaccine, protects mice against intravenous challenge with Mycobacterium tuberculosis. *Scand. J. Immunol.***75,** 77–84 (2012).
146. Tapia, M. D. *et al.* Use of ChAd3-EBO-Z Ebola virus vaccine in Malian and US adults, and boosting of Malian adults with MVA-BN-Filo: a phase 1, single-blind, randomised trial, a phase 1b, open-label and double-blind, dose-escalation trial, and a nested, randomised, double-bli. *Lancet Infect. Dis.***3099,** 1–12 (2015).
147. Bontrop, R. E. Non-human primates: essential partners in biomedical research. *Immunol. Rev.***183,** 5–9 (2001).
148. Adam, L., Rosenbaum, P., Cosma, A., Le Grand, R. & Martinon, F. Identification of skin immune cells in non-human primates. *J. Immunol. Methods* 1–8 (2015). doi:10.1016/j.jim.2015.07.010
149. Ziegler-Heitbrock, L. The CD14+ CD16+ blood monocytes: their role in infection and inflammation. *J. Leukoc. Biol.***81,** 584–92 (2007).
150. Sui, Y. *et al.* Vaccine-induced myeloid cell population dampens protective immunity to SIV. 1–12 doi:10.1172/JCI73518DS1
151. Salabert, N. *et al.* Intradermal injection of an anti-Langerin-HIVGag fusion vaccine targets epidermal Langerhans cells in nonhuman primates and can be tracked in vivo. *Eur. J. Immunol.***46,** 689–700 (2016).
152. Abràmoff, M. D., Magalhães, P. J. & Ram, S. J. Image processing with imageJ. *Biophotonics Int.***11,** 36–41 (2004).
153. Kolesnikov, N. *et al.* ArrayExpress update-simplifying data submissions. *Nucleic Acids Res.***43,** D1113–D1116 (2015).
154. Team, Rc. R: A language and environment for statistical computing. (2016). at <https://www.r-project.org/.>
155. Kruskal, J. B. & Wish, M. Multidimensional Scaling. *Sage Univ. Pap. Ser. Quant. Appl. Soc. Sci.* (1978).
156. Shannon, P. *et al.* Cytoscape: A software Environment for integrated models of biomolecular interaction networks. *Genome Res.***13,** 2498–2504 (2003).
157. Ramírez, J. C., Gherardi, M. M. & Esteban, M. Biology of attenuated modified vaccinia virus Ankara recombinant vector in mice: virus fate and activation of B- and T-cell immune responses in comparison with the Western Reserve strain and advantages as a vaccine. *J. Virol.***74,** 923–33 (2000).

158. McFadden, G. Poxvirus tropism. *Nat. Rev. Microbiol.***3,** 201–13 (2005).
159. Bronte, V. *et al.* Recommendations for myeloid-derived suppressor cell nomenclature and characterization standards. *Nat. Commun.***7,** 12150 (2016).
160. Newson, J. *et al.* Resolution of acute inflammation bridges the gap between innate and adaptive immunity. *Blood***124,** 1748–64 (2014).
161. Gilchrist, M. *et al.* Systems biology approaches identify ATF3 as a negative regulator of Toll-like receptor 4. *Nature***441,** 173–178 (2006).
162. MacLeod, D. T., Nakatsuji, T., Wang, Z., di Nardo, A. & Gallo, R. L. Vaccinia Virus Binds to the Scavenger Receptor MARCO on the Surface of Keratinocytes. *J. Invest. Dermatol.* (2014). doi:10.1038/jid.2014.330
163. Delaloye, J. *et al.* Innate immune sensing of modified vaccinia virus Ankara (MVA) is mediated by TLR2-TLR6, MDA-5 and the NALP3 inflammasome. *PLoS Pathog.***5,** (2009).
164. van Furth, R., Nibbering, P. H., van Dissel, J. T. & Diesselhoff-den Dulk, M. M. The characterization, origin, and kinetics of skin macrophages during inflammation. *J. Invest. Dermatol.***85,** 398–402 (1985).
165. Flechsig, C. *et al.* Uptake of antigens from modified vaccinia Ankara virus-infected leukocytes enhances the immunostimulatory capacity of dendritic cells. *Cytotherapy***13,** 739–52 (2011).
166. Dinarello, C. a. IL-18: A TH1 -inducing, proinflammatory cytokine and new member of the IL-1 family. *J. Allergy Clin. Immunol.***103,** 11–24 (1999).
167. Sagoo, P. *et al.* In vivo imaging of inflammasome activation reveals a subcapsular macrophage burst response that mobilizes innate and adaptive immunity. *Nat. Med.***22,** 64–71 (2016).
168. Ding, X. *et al.* TNF receptor 1 mediates dendritic cell maturation and CD8 T cell response through two distinct mechanisms. *J. Immunol.***187,** 1184–1191 (2011).
169. Talmadge, J. E. & Gabrilovich, D. I. History of myeloid-derived suppressor cells. *Nat. Rev. Cancer***13,** 739–52 (2013).
170. Nagaraj, S., Youn, J.-I. & Gabrilovich, D. I. Reciprocal Relationship between Myeloid-Derived Suppressor Cells and T Cells. *J. Immunol.***191,** 17–23 (2013).
171. Laurent, P. E. *et al.* Evaluation of the clinical performance of a new intradermal vaccine administration technique and associated delivery system. *Vaccine***25,** 8833–8842 (2007).
172. Igyártó, B. Z. & Kaplan, D. H. Antigen presentation by Langerhans cells. *Curr. Opin. Immunol.***25,** 115–119 (2013).
173. Montagne, J. R. La, Ph, D. & Fauci, A. S. Intradermal Influenza Vaccination — Can Less Be More ? *N. Engl. J. Med.***351,** 2330–2332 (2004).
174. Belshe, R. B. *et al.* Comparative immunogenicity of trivalent influenza vaccine administered by intradermal or intramuscular route in healthy adults. *Vaccine***25,** 6755–6763 (2007).

175. Roozbeh, J. *et al.* Low dose intradermal versus high dose intramuscular hepatitis B vaccination in patients on chronic hemodialysis. *Asaio J.***51,** 242–245 (2005).

176. Mohanan, D. *et al.* Administration routes affect the quality of immune responses: A cross-sectional evaluation of particulate antigen-delivery systems. *J. Control. Release***147,** 342–9 (2010).

177. Leung-Theung-Long, S. *et al.* A Novel MVA-Based Multiphasic Vaccine for Prevention or Treatment of Tuberculosis Induces Broad and Multifunctional Cell-Mediated Immunity in Mice and Primates. *PLoS One***10,** e0143552 (2015).

178. Gómez, C. E. *et al.* Systems Analysis of MVA-C Induced Immune Response Reveals Its Significance as a Vaccine Candidate against HIV/AIDS of Clade C. *PLoS One***7,** e35485 (2012).

179. Pejoski, D. *et al.* Identification of vaccine-altered circulating B cell phenotypes using mass cytometry and a two-step clustering analysis. *J. Immunol.***in press,** (2016).

180. Tricot, S. *et al.* Evaluating the efficiency of isotope transmission for improved panel design and a comparison of the detection sensitivities of mass cytometer instruments. *Cytometry. A***87,** 357–68 (2015).

181. Finck, R. *et al.* Normalization of mass cytometry data with bead standards. *Cytom. Part A***83 A,** 483–494 (2013).

182. Kotecha, N., Krutzik, P. O. & Irish, J. M. Web-based analysis and publication of flow cytometry experiments. *Curr. Protoc. Cytom.***Chapter 10,** 1–24 (2010).

183. Linderman, M. D. *et al.* CytoSPADE: High-performance analysis and visualization of high-dimensional cytometry data. *Bioinformatics***28,** 2400–2401 (2012).

184. Newell, E. W., Sigal, N., Bendall, S. C., Nolan, G. P. & Davis, M. M. Cytometry by Time-of-Flight Shows Combinatorial Cytokine Expression and Virus-Specific Cell Niches within a Continuum of CD8 + T Cell Phenotypes. *Immunity***36,** 142–152 (2012).

185. Seubert, A., Monaci, E., Pizza, M., O'Hagan, D. T. & Wack, A. The adjuvants aluminum hydroxide and MF59 induce monocyte and granulocyte chemoattractants and enhance monocyte differentiation toward dendritic cells. *J. Immunol.***180,** 5402–5412 (2008).

186. Galli, S. J., Borregaard, N. & Wynn, T. a. Phenotypic and functional plasticity of cells of innate immunity: macrophages, mast cells and neutrophils. *Nat. Immunol.***12,** 1035–44 (2011).

187. Colonna, M. & Facchetti, F. TREM-1 (triggering receptor expressed on myeloid cells): a new player in acute inflammatory responses. *J Infect Dis***187 Suppl ,** S397–401 (2003).

188. Serhan, C. N. *et al.* Resolution of inflammation: state of the art, definitions and terms. *FASEB J.***21,** 325–332 (2007).

189. Ibrahim, M. M. Subcutaneous and visceral adipose tissue: Structural and functional differences. *Obes. Rev.***11,** 11–18 (2010).

190. Hausman, G. J. & Richardson, R. L. Adipose tissue angiogenesis 1,2. *J Anim Sci* (2003). doi:10.1038/ijo.2010.180

191. Rasmussen, A. L. *et al.*Delayed inflammatory and cell death responses are associated with reduced pathogenicity in Lujo virus-infected cynomolgus macaques. *J. Virol.***89,** 2543–52 (2015).

192. Megiovanni, A. M., Gluckman, J. C., Boudaly, S. & Candida, D. Polymorphonuclear neutrophils deliver activation signals and antigenic molecules to dendritic cells : a new link between leukocytes upstream of T lymphocytes and mutually influence the two leukocyte popula- cesses occurring upstream of the interactions be. **79,** (2006).

193. Castillo, P. & Kolls, J. K. IL-10: A Paradigm for Counterregulatory Cytokines. *J. Immunol.***197,** 1529–1530 (2016).

194. Buggins, a G. *et al.* Effect of costimulation and the microenvironment on antigen presentation by leukemic cells. *Blood***94,** 3479–3490 (1999).

195. Kupper, T. & Fuhlbrigge, R. Immune surveillance in the skin: mechanisms and clinical consequences. *Nat. Rev. Immunol.***4,** 211–222 (2004).

196. Hansen, S. G. *et al.* Effector memory T cell responses are associated with protection of rhesus monkeys from mucosal simian immunodeficiency virus challenge. *Nat. Med.***15,** 293–299 (2009).

197. Kasturi, S., Skountzou, I. & Albrecht, R. Programming the magnitude and persistence of antibody responses with innate immunity. *Nature***470,** 543–547 (2011).

198. Li, S. *et al.* Molecular signatures of antibody responses derived from a systems biology study of five human vaccines. *Nat. Immunol.***15,** 195–204 (2014).

199. Palucka, K., Banchereau, J. & Mellman, I. Designing vaccines based on biology of human dendritic cell subsets. *October***33,** 464–478 (2011).

200. Matthews, K. *et al.* Clinical Adjuvant Combinations Stimulate Potent B-Cell Responses In Vitro by Activating Dermal Dendritic Cells. *PLoS One***8,** e63785 (2013).

201. Kwissa, M. *et al.* Adjuvanting a DNA vaccine with a TLR9 ligand plus Flt3 ligand results in enhanced cellular immunity against the simian immunodeficiency virus. *J. Exp. Med.***204,** 2733–46 (2007).

202. Souza, J. De & Gottfried, C. Muscle injury: Review of experimental models. *J. Electromyogr. Kinesiol.***23,** 1253–1260 (2013).

203. Pillon, N. J., Bilan, P. J., Fink, L. N. & Klip, A. Cross-talk between skeletal muscle and immune cells: muscle-derived mediators and metabolic implications. *Am. J. Physiol. Endocrinol. Metab.***304,** E453–65 (2013).

204. Arnold, L. *et al.* Inflammatory monocytes recruited after skeletal muscle injury switch into

antiinflammatory macrophages to support myogenesis. *J Exp Med***204,** 1057–1069 (2007).

205. Mosca, F. *et al.* Molecular and cellular signatures of human vaccine adjuvants. *Proc. Natl. Acad. Sci. U. S. A.***105,** 10501–6 (2008).
206. Samuvel, D. J., Sundararaj, K. P., Nareika, A., Lopes-Virella, M. F. & Huang, Y. Lactate boosts TLR4 signaling and NF-kappaB pathway-mediated gene transcription in macrophages via monocarboxylate transporters and MD-2 up-regulation. *J. Immunol. (Baltimore, Md. 1950)***182,** 2476–2484 (2009).
207. Carlsson, H. E., Schapiro, S. J., Farah, I. & Hau, J. Use of primates in research: A global overview. *Am. J. Primatol.***63,** 225–237 (2004).
208. Earl, P. L. *et al.*Immunogenicity of a highly attenuated MVA smallpox vaccine and protection against monkeypox. *Nature***428,** 182–185 (2004).
209. Pathan, A. a *et al.* Effect of vaccine dose on the safety and immunogenicity of a candidate TB vaccine, MVA85A, in BCG vaccinated UK adults. *Vaccine***30,** 5616–24 (2012).
210. Caskey, M. *et al.* Synthetic double-stranded RNA induces innate immune responses similar to a live viral vaccine in humans. *J. Exp. Med.***208,** 2357–66 (2011).
211. Ammi, R. *et al.* Poly(I:C) as cancer vaccine adjuvant: Knocking on the door of medical breakthroughs. *Pharmacol. Ther.***146,** 120–131 (2015).
212. Tewari, K. *et al.* Poly(I:C) is an effective adjuvant for antibody and multi-functional CD4+ T cell responses to Plasmodium falciparum circumsporozoite protein (CSP) and ??DEC-CSP in non human primates. *Vaccine***28,** 7256–7266 (2010).
213. Rimaniol, A.-C., Gras, G. & Clayette, P. In vitro interactions between macrophages and aluminum-containing adjuvants. *Vaccine***25,** 6784–92 (2007).
214. Denning, T. L., Wang, Y., Patel, S. R., Williams, I. R. & Pulendran, B. Lamina propria macrophages and dendritic cells differentially induce regulatory and interleukin 17-producing T cell responses. *Nat. Immunol.***8,** 1086–94 (2007).
215. Nathan, C. Neutrophils and immunity: challenges and opportunities. *Nat. Rev. Immunol.***6,** 173–182 (2006).
216. Saclier, M., Cuvellier, S., Magnan, M., Mounier, R. & Chazaud, B. Monocyte/macrophage interactions with myogenic precursor cells during skeletal muscle regeneration. *FEBS J.***280,** 4118–4130 (2013).
217. Brigitte, M. *et al.* Muscle resident macrophages control the immune cell reaction in a mouse model of notexin-induced myoinjury. *Arthritis Rheum.***62,** 268–79 (2010).
218. Tidball, J. G. & Villalta, S. A. Regulatory interactions between muscle and the immune system during muscle regeneration. *Am. J. Physiol. Regul. Integr. Comp. Physiol.***298,** R1173–87 (2010).

219. Watson, N. B., Schneider, K. M. & Massa, P. T. SHP-1–Dependent Macrophage Differentiation Exacerbates Virus-Induced Myositis. (2016). doi:10.4049/jimmunol.1402210

220. Muzio, M. *et al.* Differential expression and regulation of toll-like receptors (TLR) in human leukocytes: selective expression of TLR3 in dendritic cells. *J. Immunol.***164,** 5998–6004 (2000).

221. Miller, L. S. Toll-Like Receptors in Skin. *Adv. Dermatol.***24,** 71–87 (2008).

222. Schreiner, B. *et al.*Expression of toll-like receptors by human muscle cells in vitro and in vivo: TLR3 is highly expressed in inflammatory and HIV myopathies, mediates IL-8 release and up-regulation of NKG2D-ligands. *FASEB J.***20,** 118–120 (2006).

223. Sugimoto, C. *et al.* Differentiation Kinetics of Blood Monocytes and Dendritic Cells in Macaques: Insights to Understanding Human Myeloid Cell Development. *J. Immunol.***195,** 1774–1781 (2015).

224. Autissier, P., Soulas, C., Burdo, T. H. & Williams, K. C. Immunophenotyping of lymphocyte, monocyte and dendritic cell subsets in normal rhesus macaques by 12-color flow cytometry: Clarification on DC heterogeneity. *J. Immunol. Methods***360,** 119–128 (2010).

225. Wang, Y., Lavender, P., Watson, J., Arno, M. & Lehner, T. Stress-activated dendritic cells (DC) induce dual interleukin (IL)-15- and IL1b-mediated pathways, which may elicit CD4+memory T cells and interferon (IFN)-stimulated genes. *J. Biol. Chem.***290,** 15595–15609 (2015).

226. Ovsyannikova, I. G. *et al.* Impact of cytokine and cytokine receptor gene polymorphisms on cellular immunity after smallpox vaccination. *Gene***510,** 59–65 (2012).

227. Bennouna, S., Bliss, S. K., Curiel, T. J. & Denkers, E. Y. Cross-Talk in the Innate Immune System: Neutrophils Instruct Recruitment and Activation of Dendritic Cells during Microbial Infection. *J. Immunol.***171,** 6052–6058 (2003).

228. Gómez, C. E. *et al.* Virus distribution of the attenuated MVA and NYVAC poxvirus strains in mice. *J. Gen. Virol.***88,** 2473–8 (2007).

229. Subramanian, A. *et al.* Gene set enrichment analysis: a knowledge-based approach for interpreting genome-wide expression profiles. *Proc. Natl. Acad. Sci. U. S. A.***102,** 15545–50 (2005).

Figures

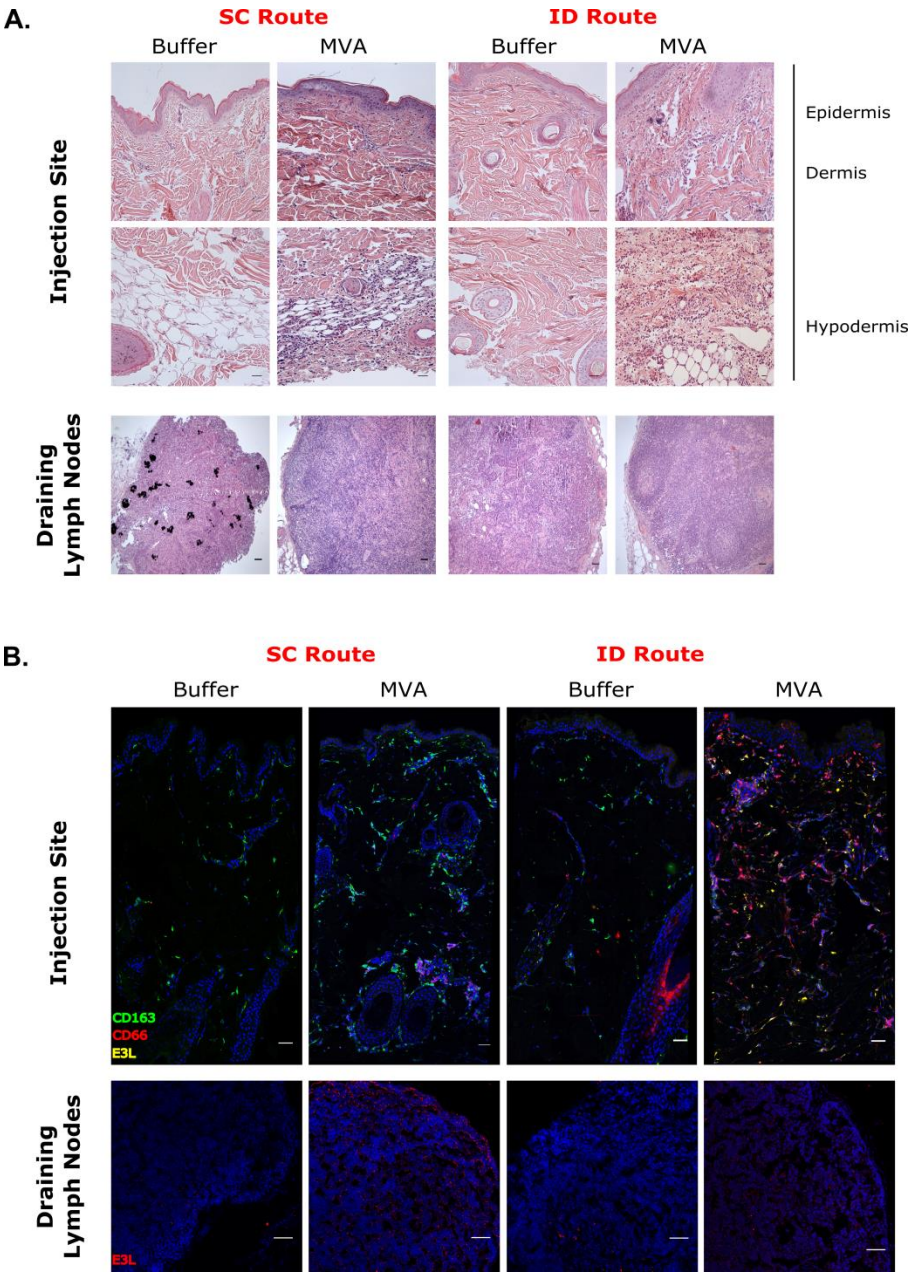

Figure 1: Skin and lymph node tissue after MVA immunization by SC or ID route

(A) HE staining of the site of injection (skin+subcutaneous tissue) and draining inguinal lymph node. Transversal sections of paraffin-embedded tissue cassettes 24h after buffer/ rMVA following intradermal/subcutaneous route. Scale bar equals to 50µm. One representative experiment out of 2 is shown. (B) Immunohistofluorescence of site of injection and draining inguinal lymph node.. Transversal sections of frozen cassettes 24h after buffer/ rMVA injection by ID or SC route. Scale bar equals to 50µm. For injections site: CD163 in green, CD66 in red, and E3L in yellow. For lymph nodes, E3L is in red. One representative experiment out of 2 is shown.

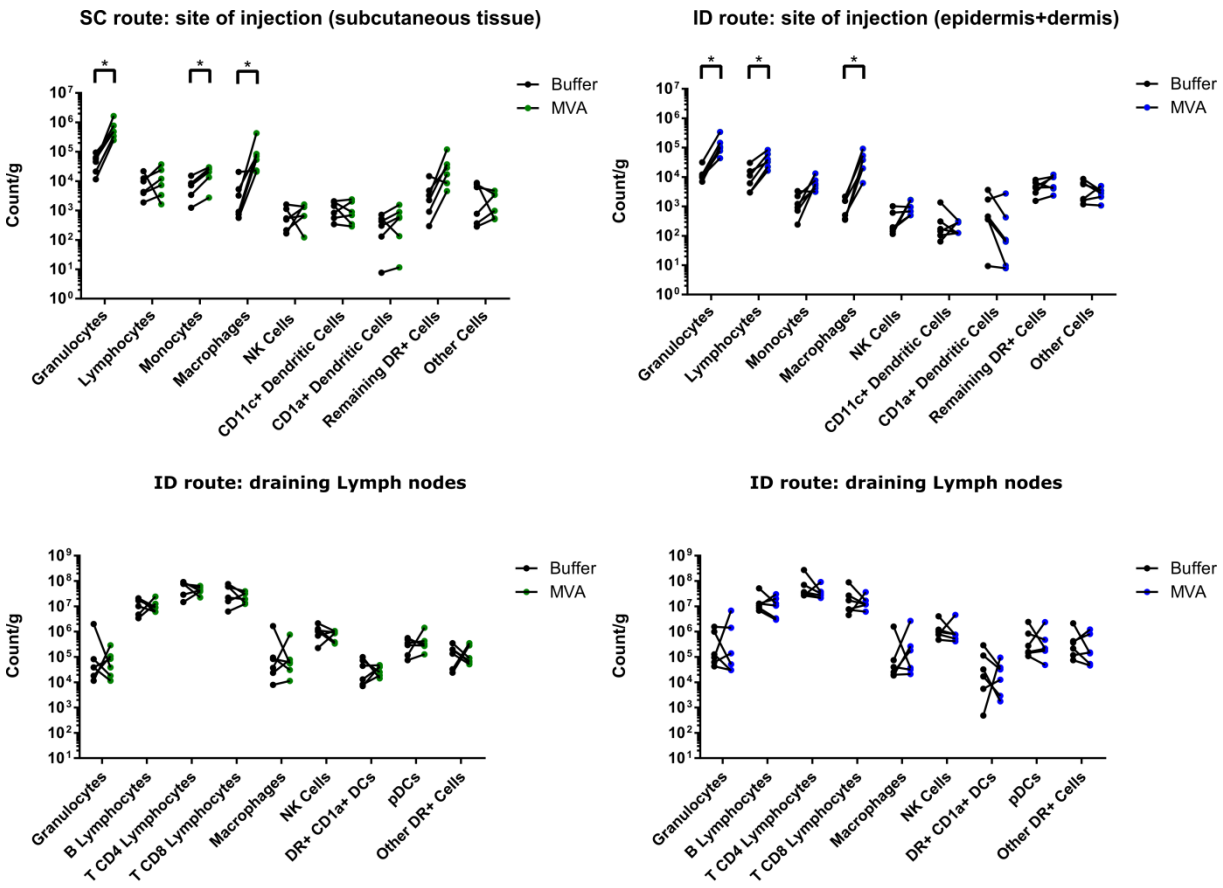

Figure 2:Local cellular recruitment after MVA immunization following SC/ID route

Scatter plot representation of local cellular movement at the site of injection and draining lymph nodes after buffer or rMVA injection by SC or ID route. All dots represented correspond to one biological sample (n=6 per group). Values expressed in count (ie number of event recorded conforming to the gating strategy in Supplementary figure 2) divided by the initial weight of the digested biopsy in grams. Statistical analysis performed by a Wilcoxon signed rank test. *: p-value<0.05

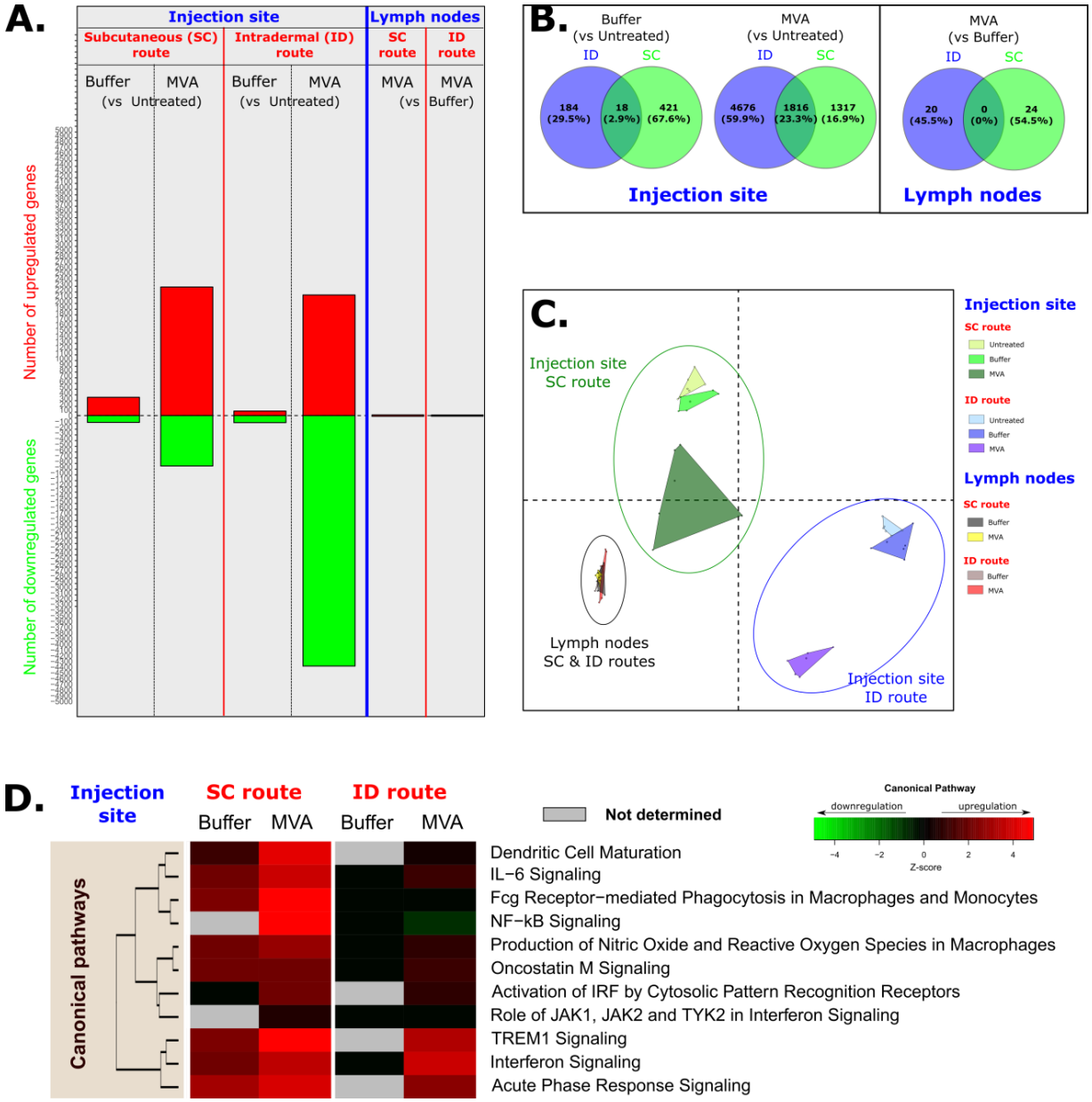

Figure 3. Transcriptomic analysis of early response locally induced by rMVA after SC or ID administration

Figure 3. Transcriptomic analysis of early response locally induced by rMVA after SC or ID administration

(A)Histogram of the number of significantly down-and up-regulated genes in comparison with untreated condition for injection site or 24h post-buffer injection for lymph nodes (paired t-test, p-value<0.05;n=6).(B) Venn diagram of the list of differentially expressed genes in comparison with untreated condition for injection site or 24h post-buffer injection for lymph nodes (paired t-test, p-value<0.05;n=6). It allows seeing differentially expressed genes shared between ID and SC route. (C) Multidimensional scaling representation (MDS) of transcriptomic signatures from injection site and lymph node microarray assay in untreated condition, 24h post-buffer and 24h post-MVA injection. Biological samples were represented in a two dimension scale and correspond to the colored and circled dots. Differential gene expression between samples is translated into Euclidian distance between the samples (n=6). (D) Heatmap representation after functional enrichment processing. Canonical pathways related to immune processing and cytokine signaling and having a p-value<10^{-3}in at least one condition were represented. Data extracted from lists of fold change of differentially expressed genes in comparison with untreated condition. Intensity of coloration corresponds to the Z-score, which is a coefficient directly related to the upregulation (in red) or the downregulation (in green) of the pathway (n=6). No canonical pathway related with lymph node dataset passed the cut-off used.

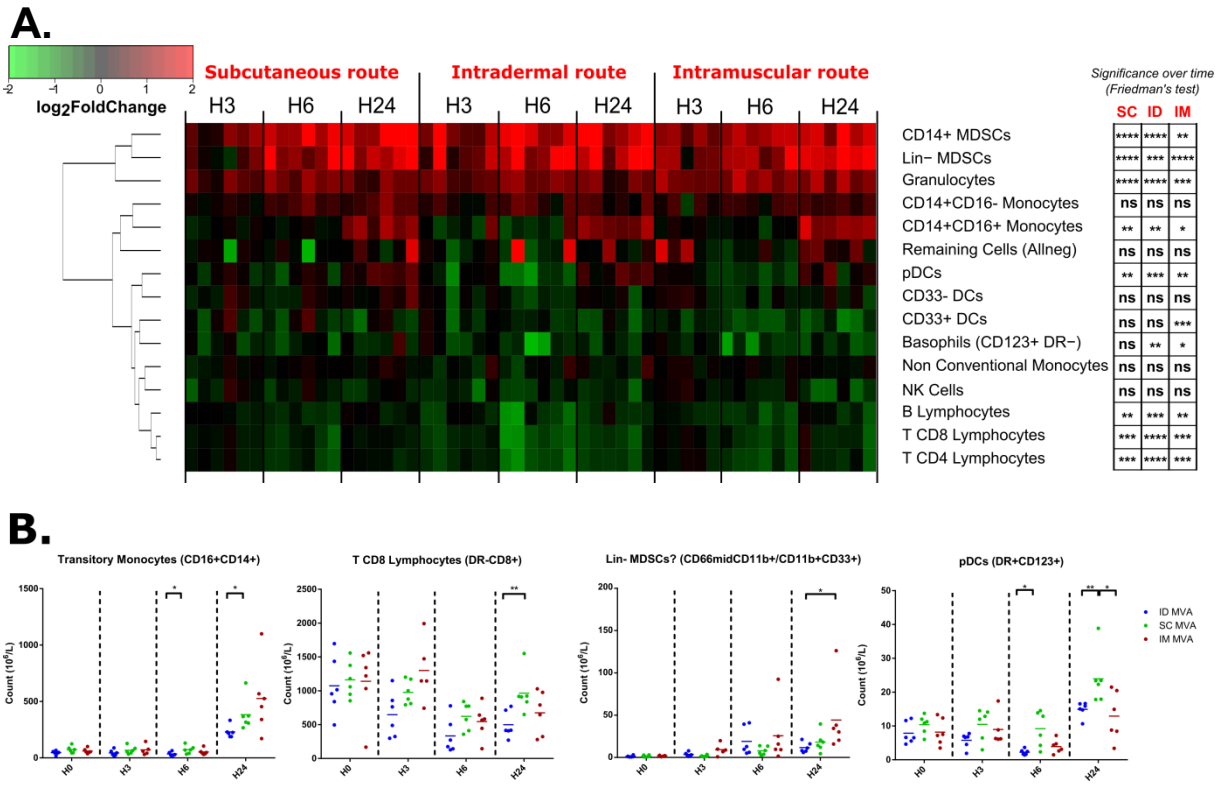

Figure 4.Systemic MVA induced cell recruitments

(A) Heatmap representation of cell populations discriminated using flow cytometry in the blood 3h, 6h and 24h after SC/ID/IM MVA injection. Cell populations were automatically sorted following a hierarchical clustering represented with dendrograms on the left. Data were normalized for each cell population, subtracting by the mean and dividing by the standard deviation. Low amounts correspond to green coloration and high amount to a red coloration. 100µL of fresh blood was stained for a flow cytometry analysis. CBC based amount of cells per liter used was calculated multiplying the cell count obtained in flow cytometry for a given population multiplied by CBC Number of leukocytes divided by the count of total blood cells obtained by flow cytometry (n=6). The values were then expressed in log_2FC relative to H0. On the right the significance over time for each administration route using Friedman test (SC route: n=6, ID route: n=6, IM route: n=5). (B) Scatter plot kinetic for cell population significantly different over time between routes (Mann Whitney test; n=6) expressed in CBC based amount of cell per liter. Each dot represents one single biological sample (*: 0.05>p-value>0.01; **: 0.01>p-value> 0.001; ***: 0.001>p-value).

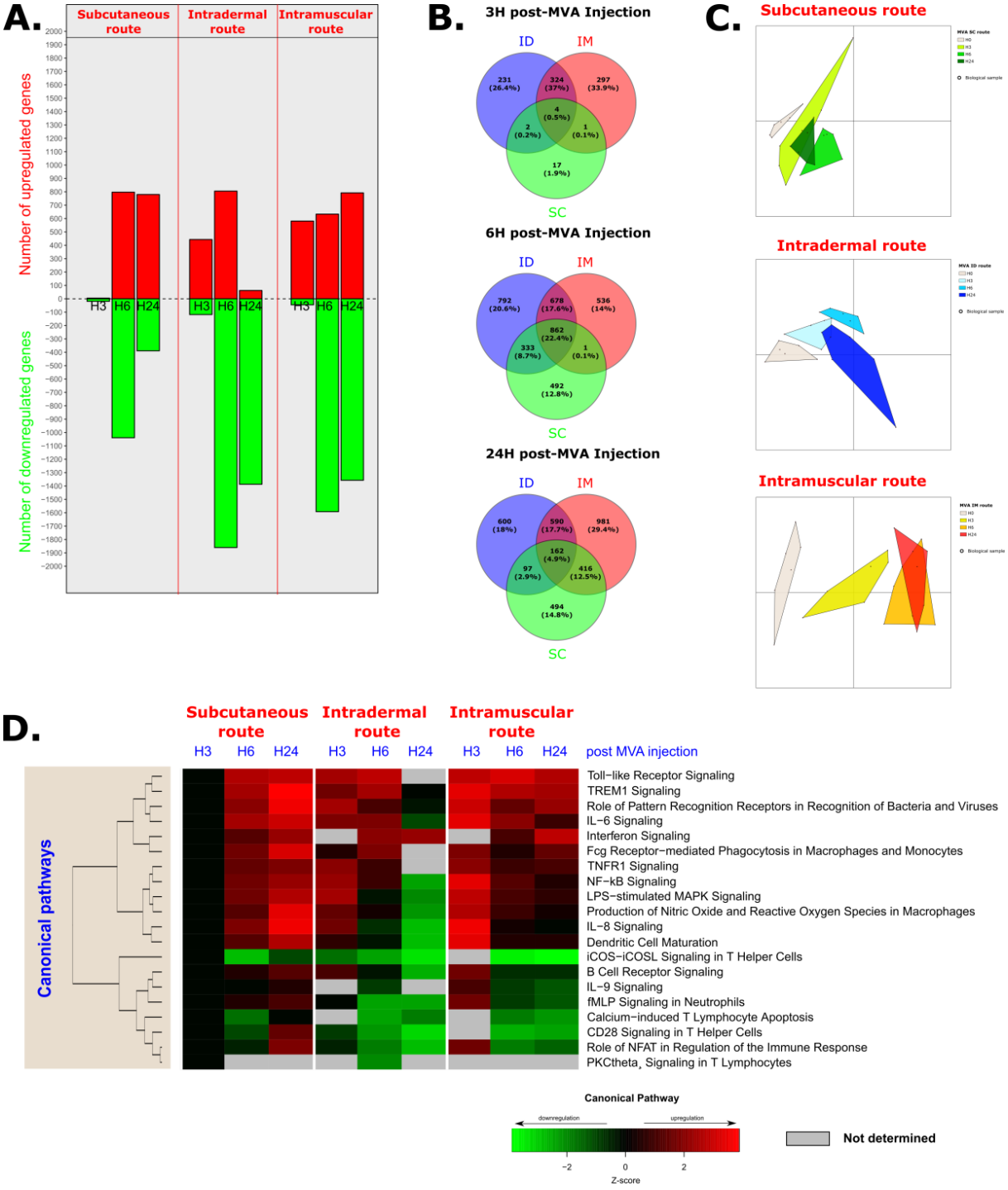

Figure 5. Transcriptomic analysis of systemic early response induced by SC/ID/IM injection of rMVA

Figure 5. Transcriptomic analysis of systemic early response induced by SC/ID/IM injection of rMVA

(A) Histogram of the number of significantly down-and up-regulated genes at 3h, 6h, and 24h after MVA injection in comparison with untreated condition (H0).(paired t-test, p-value<0.05;n=6).(B) Venn diagram of the list of differentially expressed genes at 3h, 6h, and 24h after MVA injection in comparison with untreated condition(paired t-test, p-value<0.05;n=6). It allows seeing differentially expressed genes shared between IM, ID and SC route. (C) Multidimensional scaling representation (MDS) of transcriptomic signatures in blood at 0h, 3h, 6h and 24h. Biological samples were represented in a two dimension scale and correspond to the colored and circled dots. Differential gene expression between samples is translated into Euclidian distance between the samples (n=6). (D) Heatmap representation after functional enrichment processing. Canonical pathways related to immune processing and cytokine signaling and having a p-value<10^{-3}over the time were represented. Data extracted from lists of fold change of differentially expressed genes in comparison with untreated condition (H0). Intensity of coloration corresponds to the Z-score, which is a coefficient directly related to the upregulation (in red) or the downregulation (in green) of the pathway (n=6).

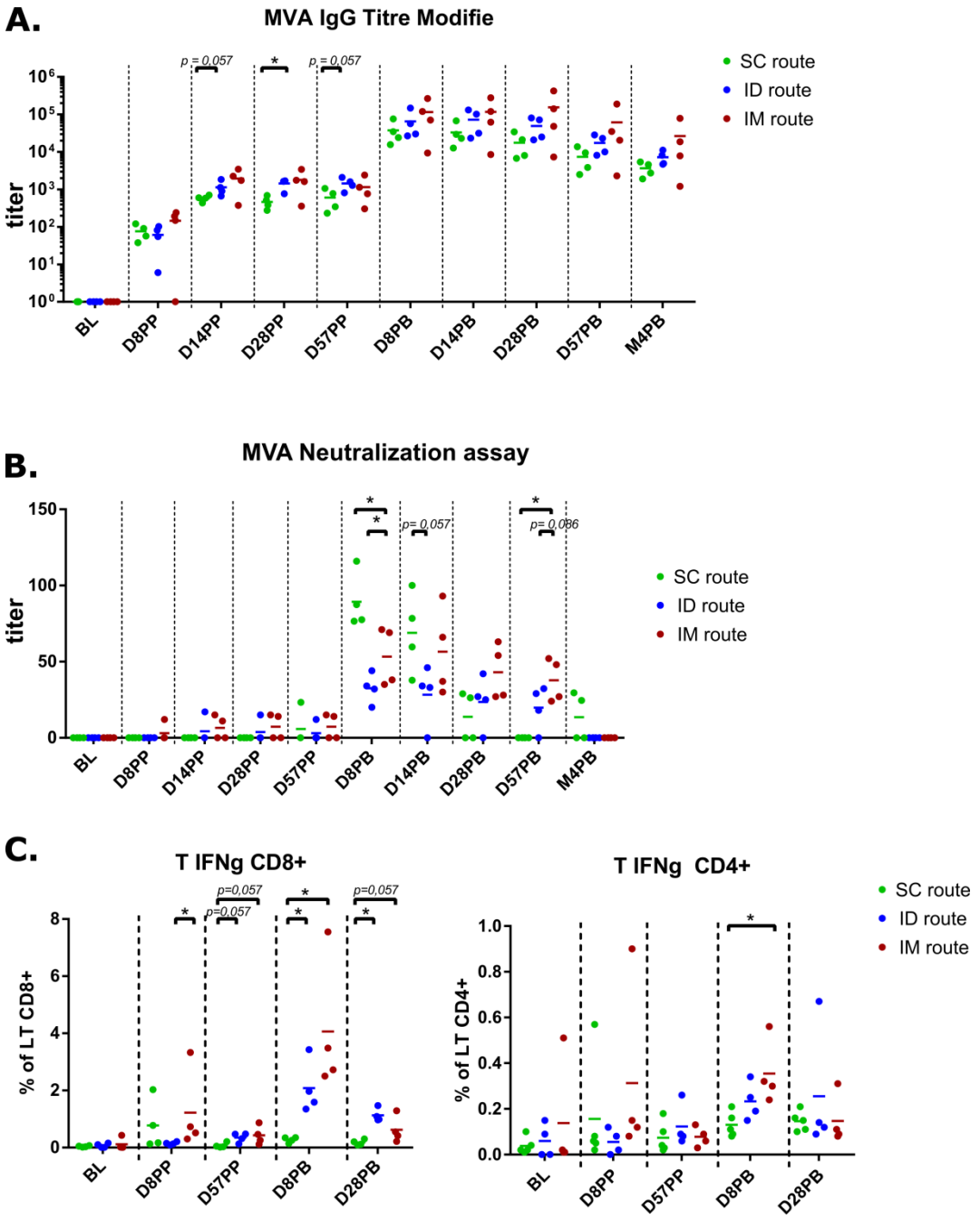

Figure 6.B and T cell responses induced by MVA homologous prime-boost administered by SC/ID/IM route.

(A) Scatter plot of MVA-specific IgG titers over the time using ELISA assay. Each plot corresponds to one single biological sample. (B) Scatter plot of MVA neutralization titers over the time using plaque reduction assay. Each plot corresponds to one single biological sample (C) Percentage of IFNγ positive CD4+ and CD8+ T cells. PBMC were gathered and stained for a CyTOF acquisition after *in vitro*stimulation with MVA. CD4+ and CD8+ T lymphocytes were gated based on CD3+, HLADR-, and CD14- expression as shown in supplementary figure3. Mann Whitney test was performed at each time point between ID, SC and IM group.*, p-value<0.05; BL, baseline; PP, post-prime; PB, post-boost.

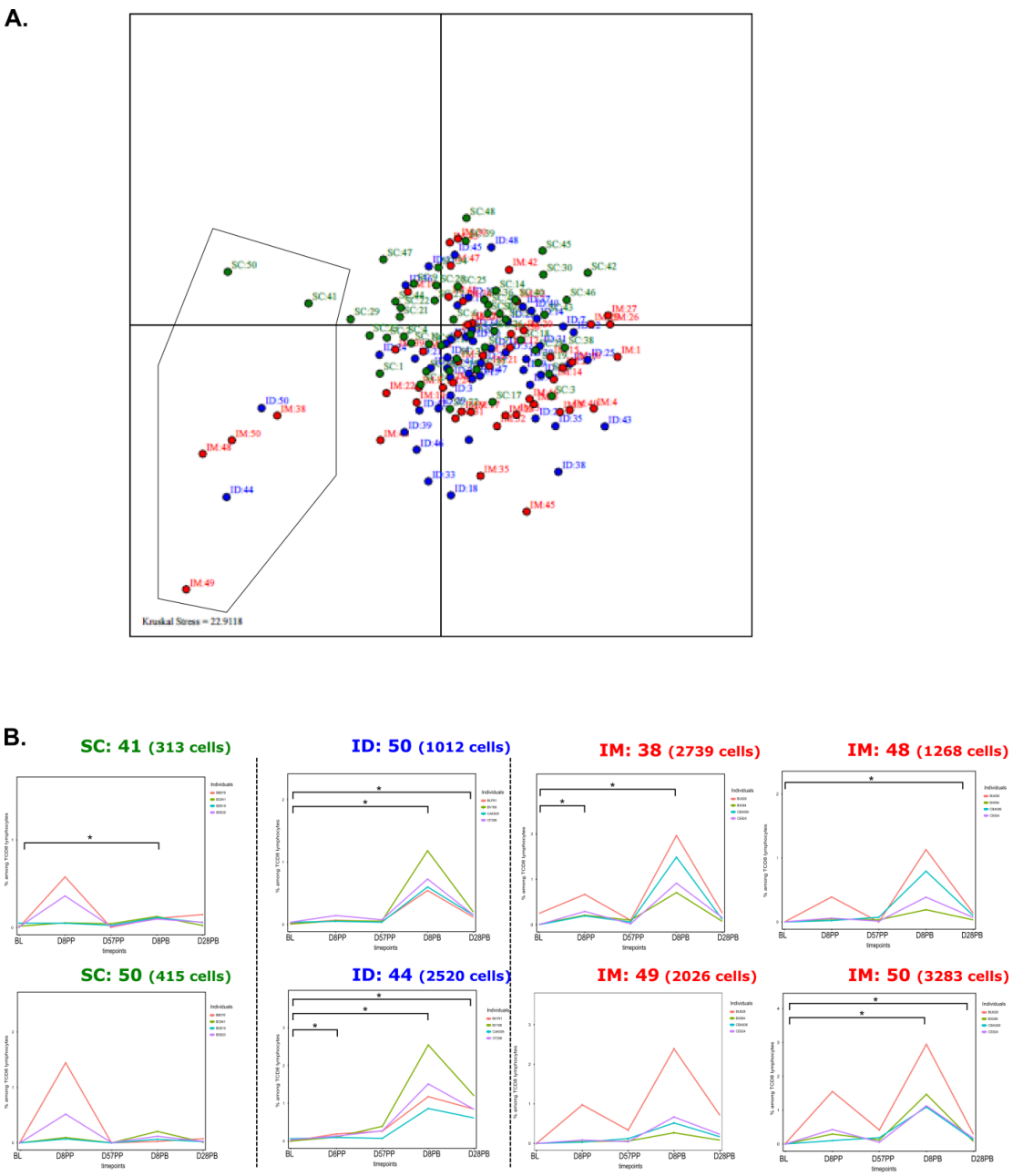

Figure 7.Identification of singular CD8+ T cells clusters induced by MVA homologous prime-boostby SC/ID/IM route

(A) MDS representation showing the similarities of the cluster phenotypes based on the MSI of the 13 SPADE clustering markers for all CD3+,CD14-,HLADR-, CD8+ events in the dataset. Each cell cluster contains cells from one administration route (4 macaques) and 5 time points. One SPADE analysis was performed for each administration route. Clusters were colored based on their administration route they belong to. Differential cluster phenotype between samples is translated into Euclidian distance between the samples. Circled cluster correspond to very singular ones. (B) Graphics of the percentage of CD8+ T cell over time in those segregated clusters. Differentially enriched cluster (DEC) for one given time point in comparison with the baseline was calculated using a paired t-test (n=4; *: p-value < 0.05). BL, baseline; PP, post-prime; PB, post-boost.

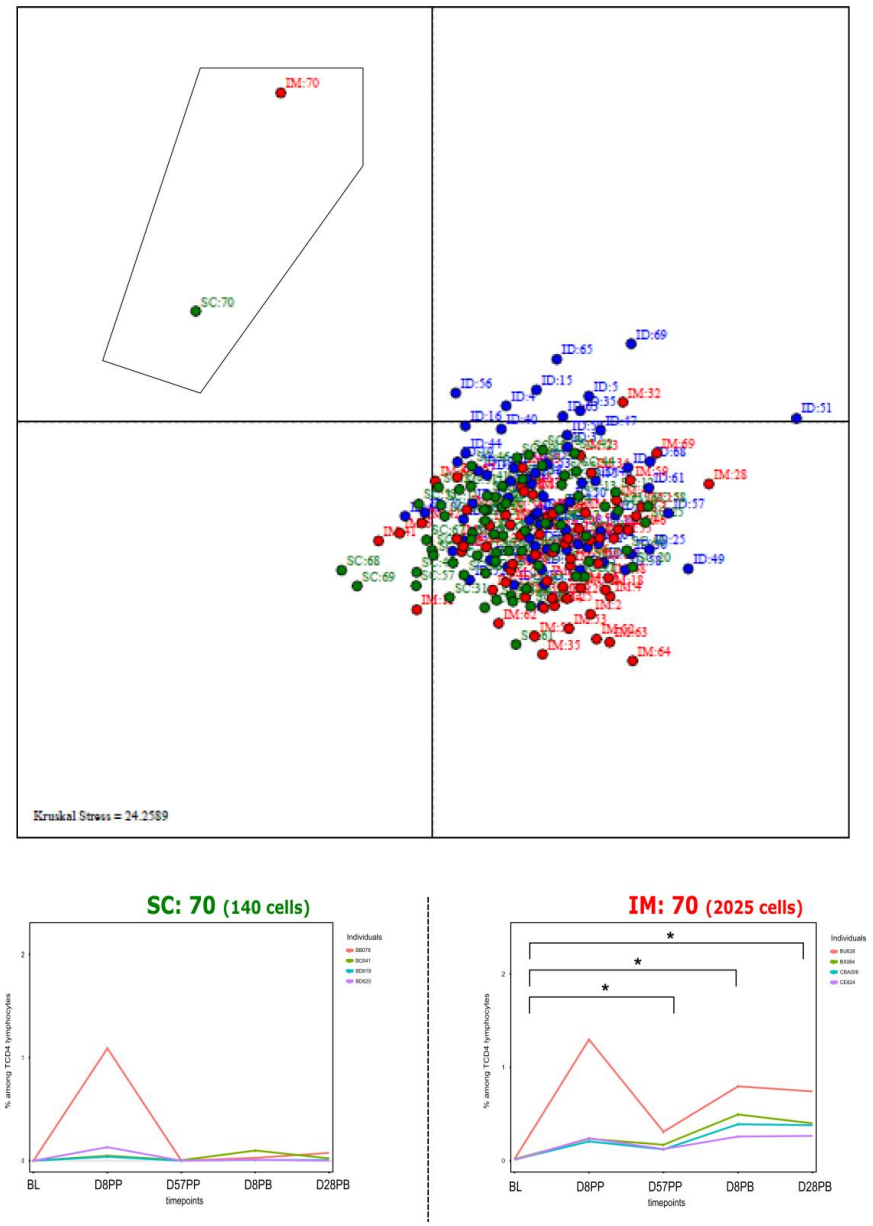

Figure 8.Identification of singular CD4+ T cells clusters induced by MVA homologous prime-boostby SC/ID/IM route

(A) MDS representation showing the similarities of the cluster phenotypes based on the MSI of the 13 SPADE clustering markers for all CD3+,CD14-,HLADR-, CD4+ events in the dataset Each cell cluster contains cells from one administration route (4 macaques) and 5 time points. One SPADE analysis was performed for each administration route. Clusters were colored based on their administration route they belong to. Differential cluster phenotype between samples is translated into Euclidian distance between the samples. Circled cluster correspond to very singular ones. (B) Graphics below show the percentage of CD8+ T cell over time in those segregated clusters. Differentially enriched cluster (DEC) for one given time point in comparison with the baseline was calculated using a paired t-test (n=4; *: p-value < 0.05 BL, baseline; PP, post-prime; PB, post-boost.

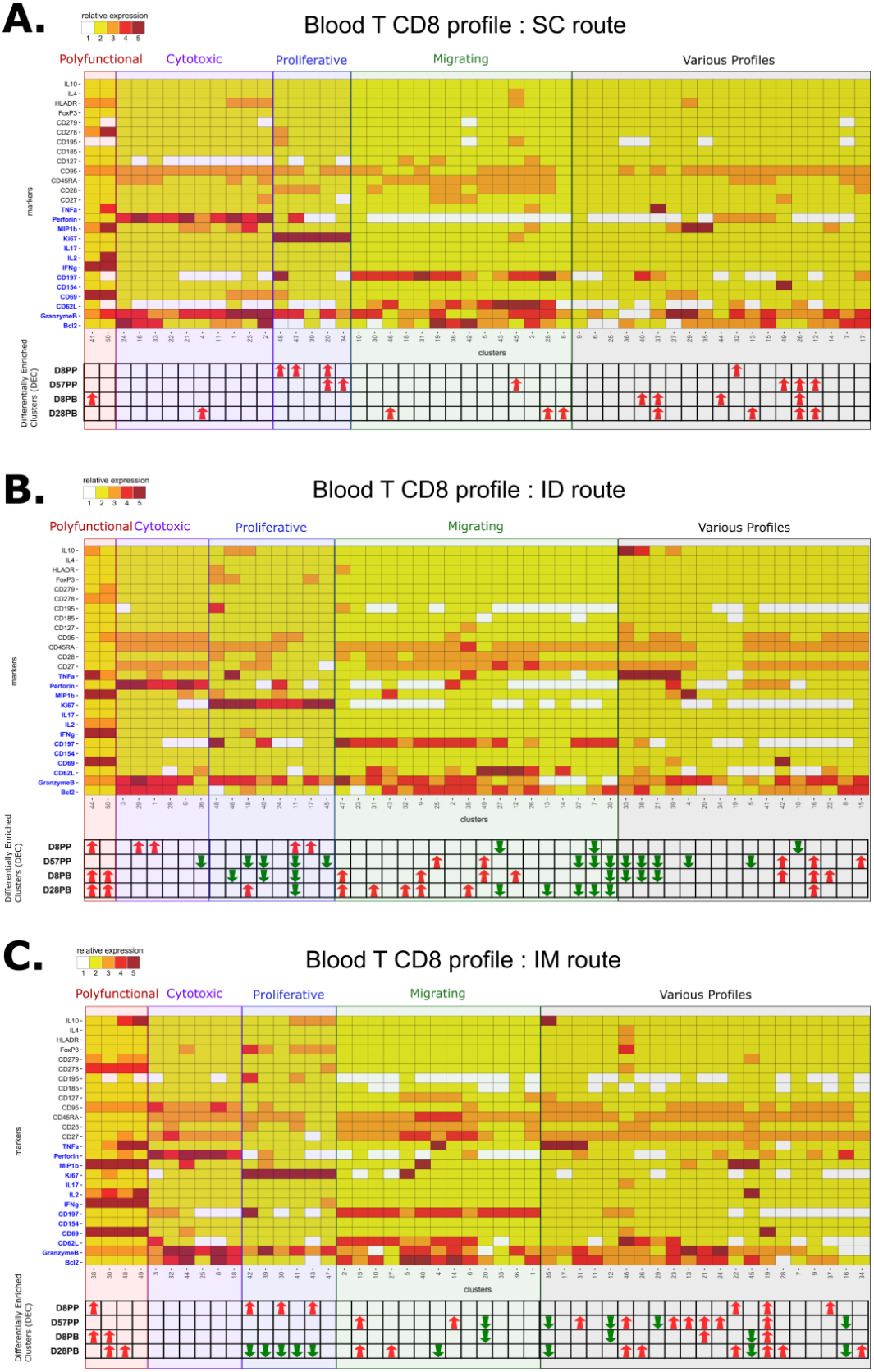

Figure 9.Comparison of CD8+ T cells clusters profiles induced by MVA homologous prime-boostby SC/ID/IM route

Figure 9.Comparison of CD8+ T cells clusters profiles induced by MVA homologous prime-boostby SC/ID/IM route

Heatmap representation of CD8+ T cells clusters gated as shown in supplementary figure 3. The numbers of clusters are reported on the X axis and the markers on the Y axis. Markers in blue have been used to sort cells through SPADE analysis. After a hierarchical clustering (step showed in Fig. S4), clusters have been sorted in blocks depending on their marker expression. The five-tiered color scale, from white to deep red, represents marker relative expression. Grid filled with arrows below the heatmap represents differentially enriched clusters over the time in comparison with baseline. Red arrow corresponds to a significantly more abundant cluster at the given time-point. Green arrow corresponds to a significantly less abundant cluster at the given time-point. (A) SC route (B) ID route (C) IM route. Differentially enriched cluster (DEC) for one given time-point in comparison with the baseline was calculated using a paired t-test (n=4; *: p-value < 0.05). BL, baseline; PP, post-prime; PB, post-boost.

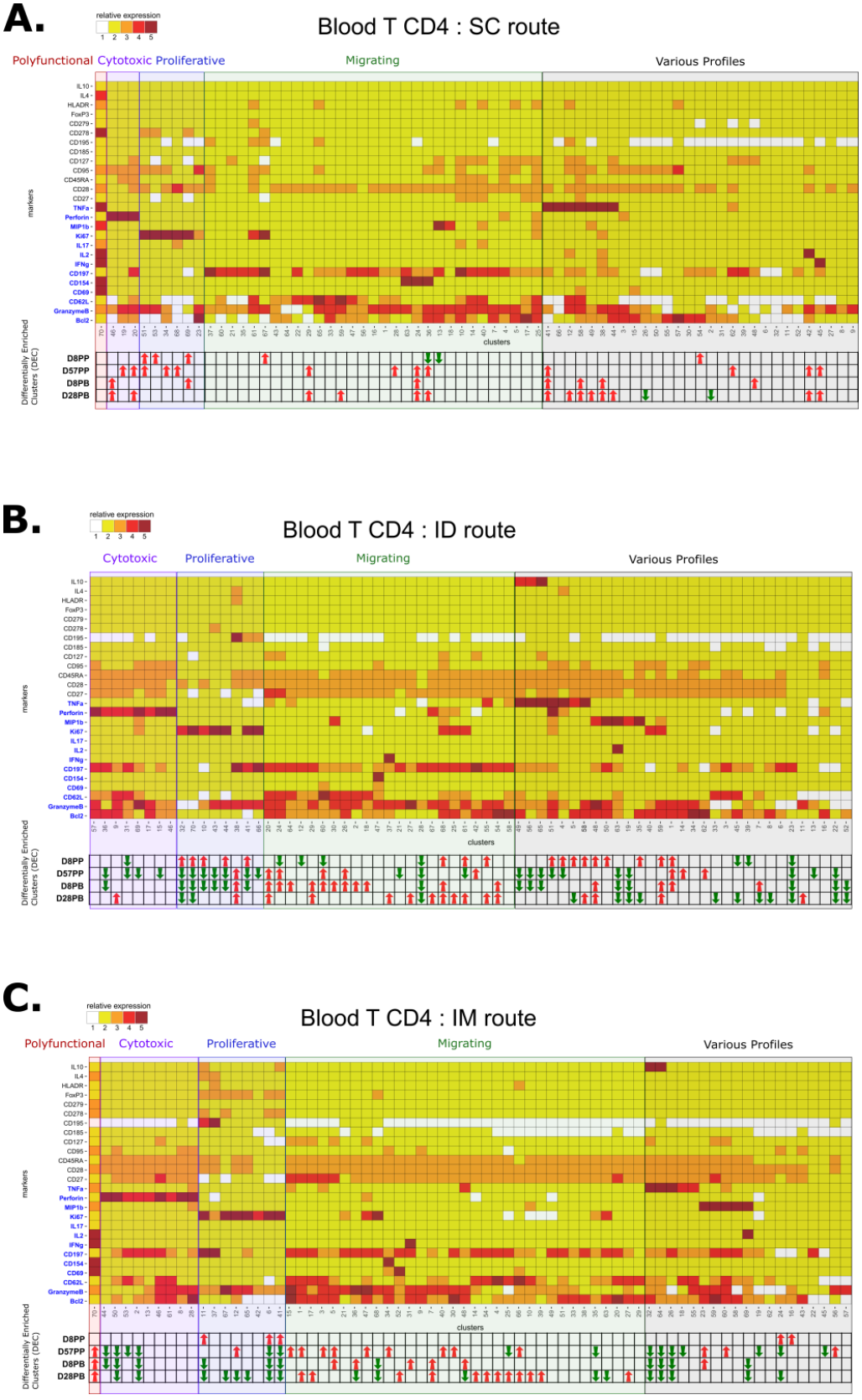

Figure 10.Comparison of CD4+ T cells clusters profiles induced by MVA homologous prime-boostby SC/ID/IM route

Figure 10.Comparison of CD4+ T cells clusters profiles induced by MVA homologous prime-boostby SC/ID/IM route

Heatmap representation of CD4+ T cells clusters gated as shown in supplementary figure 3. The numbers of clusters are reported on the X axis and the markers on the Y axis. Markers in blue have been used to sort cells through SPADE analysis. After a hierarchical clustering (step showed in Fig. S5), clusters have been sorted in blocks depending on their marker expression. The five-tiered color scale, from white to deep red, represents marker relative expression. Grid filled with arrows below the heatmap represents differentially enriched clusters over the time in comparison with baseline. Red arrow corresponds to a significantly more abundant cluster at the given time-point. Green arrow corresponds to a significantly less abundant cluster at the given time-point. (A) SC route (B) ID route (C) IM route. Differentially enriched cluster (DEC) for one given time-point in comparison with the baseline was calculated using a paired t-test (n=4; *: p-value < 0.05 BL, baseline; PP, post-prime; PB, post-boost.

Supplementary Figure

T Cytokine/Cytotoxicity Panel					
Metal	Antigen	Clone	Cytof optimal µl/well	Supplier(s)	Catalog
Nd(146)	HLA-DR	L243 (G46-6)	0,05	BD Biosciences	555810
Gd(156)	CD45RA	5H9	0,3	BD Biosciences	556625
Nd(150)	CD62L	SK11	0,3	BD Biosciences	559050
Dy(162)	CD279 (PD-1)	EH12.2H7	0,5	Biolegend	BLE329902
Yb(172)	CD95	DX2	1,3	BD Biosciences	555671
Er(168)	CD195 (CCR5)	3A9	1	BD Biosciences	556041
Nd(145)	CD197 (CCR7)	G043H7	1	Biolegend	BLE353202
Eu(151)	CD27	O323	1	Biolegend	BLE302802
Sm(147)	CD278 (ICOS)	C398.4A	2	Biolegend	BLE313502
Nd(144)	CD28	CD28.2	1,5	BD Biosciences	555726
Yb(174)	CD127 (IL-7R)	eBioRDR5	0,7	eBiosciences	16-1278-82
Sm(152)	CD185 (CXCR5)	710D82.1	0,7	NIH	710D82.1
Nd(148)	GranzymeB	GB11	0,05	Clinisciences	C112623
Lu(175)	TNF-α	MAb11	0,5	BD Biosciences	559071
Tm(169)	CD4	L200	0,2	BD Biosciences	550625
Sm(154)	CD8	RPA-T8	0,1	BD Biosciences	555364
Eu(153)	CD40L (CD154)	TRAP1	0,2	BD Biosciences	555698
Gd(158)	IFN-γ	B27	0,1	BD Biosciences	51-410-20661
Dy(164)	MIP-1β (CCL4)	D21-1351	0,1	BD Biosciences	51-410-23851
Ho(165)	IL-2	MQ1-17H12	0,1	BD Biosciences	51-410-18951
Yb(176)	IL-10	JES3-9D7	0,1	Miltenyi Biotec	130-096-041
Pr(141)	IL-17	eBio64DEC17	0,1	eBiosciences	14-7179-82
Gd(160)	Ki-67	B56	0,2	BD Biosciences	51-410-36521
Er(167)	IL-4	7A3-3	0,2	Miltenyi Biotec	120-000-031
Nd(143)	CD3	SP34-2	0,3	BD Biosciences	551916
Tb(159)	Bcl-2	Bcl-2/100	0,3	eBiosciences	14-1028-82
Yb(171)	Perforin	Pf-344	0,2	MabTech	3465-5-250
Nd(142)	CD69	FN50	0,1	BD Biosciences	5555529
Sm(149)	FoxP3	206D	0,3	Biolegend	320102
Ir(191/193)	DNA	N/A	1/500	DVS Sciences	201192A
Rh(103)	Viability-103	N/A	1/200	DVS Sciences	201103A

Intracellular staining

Supplementary table 1: Panel used for the CyTOF staining.

Recapitulation of markers used to identify CD4+ and CD8+ T cell profiles

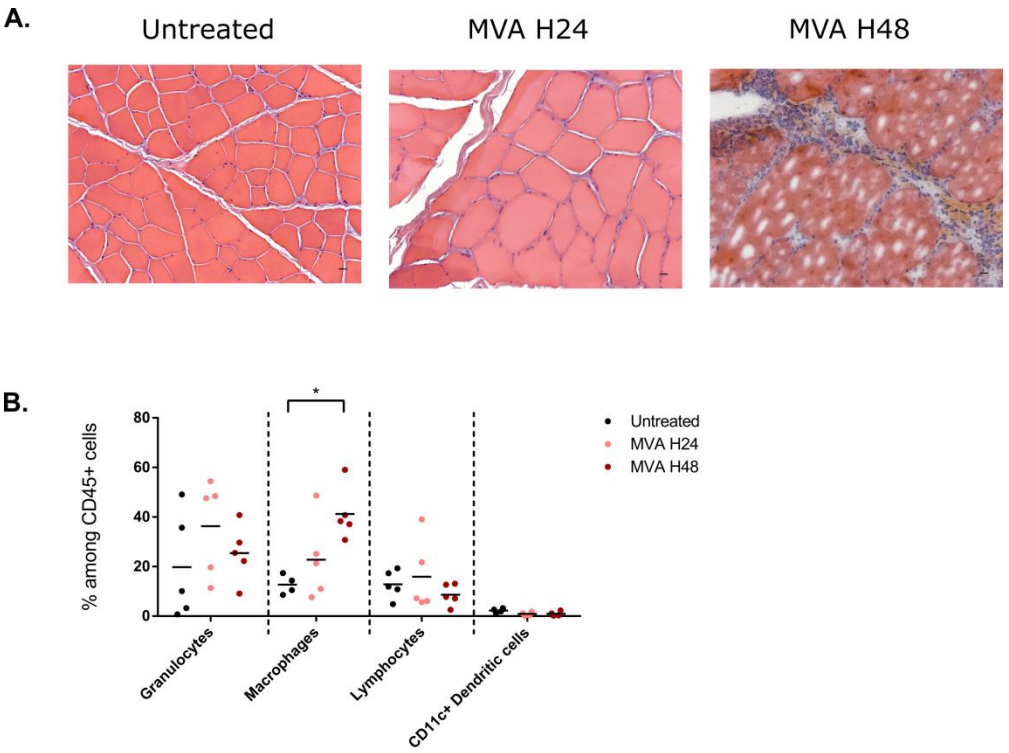

Supplementary figure 1: Local early innate response in the muscle tissue

(A) HE staining of muscle. Transversal sections of paraffin-embedded tissue cassettes at 0h, 24h and 48h after IM injection of MVA. Scale bar equals to 50µm. (B)Scatter plot for each cell population at 0h (untreated), 24h, and 48h after IM injectionof MVA,expressed in percentage among CD45+ cells, as shown in supplementary figure 2.Significance calculated using Mann Whitney test (n=5). Each dot represents one single biological sample (*: p-value<0.05).

Supplementary figure 2: Gating strategies used in flow cytometry for the study of the early innate response

(A) Strategy for skin and subcutaneous tissue. Dot-plot representation of one representative experiment (inflammatory condition). Similar gating strategy has been used for skin and subcutaneous tissue. (B) Strategy for muscle tissue. Dot-plot representation of one representative experiment (inflammatory condition) (C)Strategy for blood studies. Dot-plot representation of one representative experiment in inflamed condition. On the right graphics showing exclusivity of NKG2a and CD33 markers, justifying the choice to use the same fluorochrome for both these markers in the staining panel. (D) Strategy for lymph node. Dot-plot representation of one representative experiment. All the gating strategy combinations are developed in the materials and methods part.

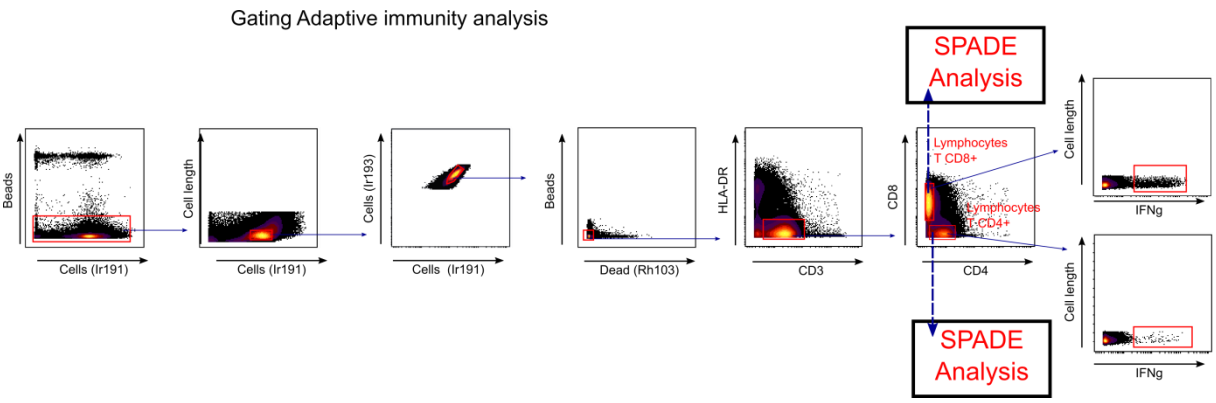

Supplementary figure 3: Gating strategies used in CyTOF for the study of the adaptive response

Dot plot representation of the gating strategy to gate CD4+ and CD8+ T cells. They were gated after selecting non beads, non doublets, non dead cells. And then based on HLADR-, CD3+, CD4+ or CD8+ expression. Those gated cells were used to perform SPADE analysis, but also to measure the percentage of IFNγ positive cells.

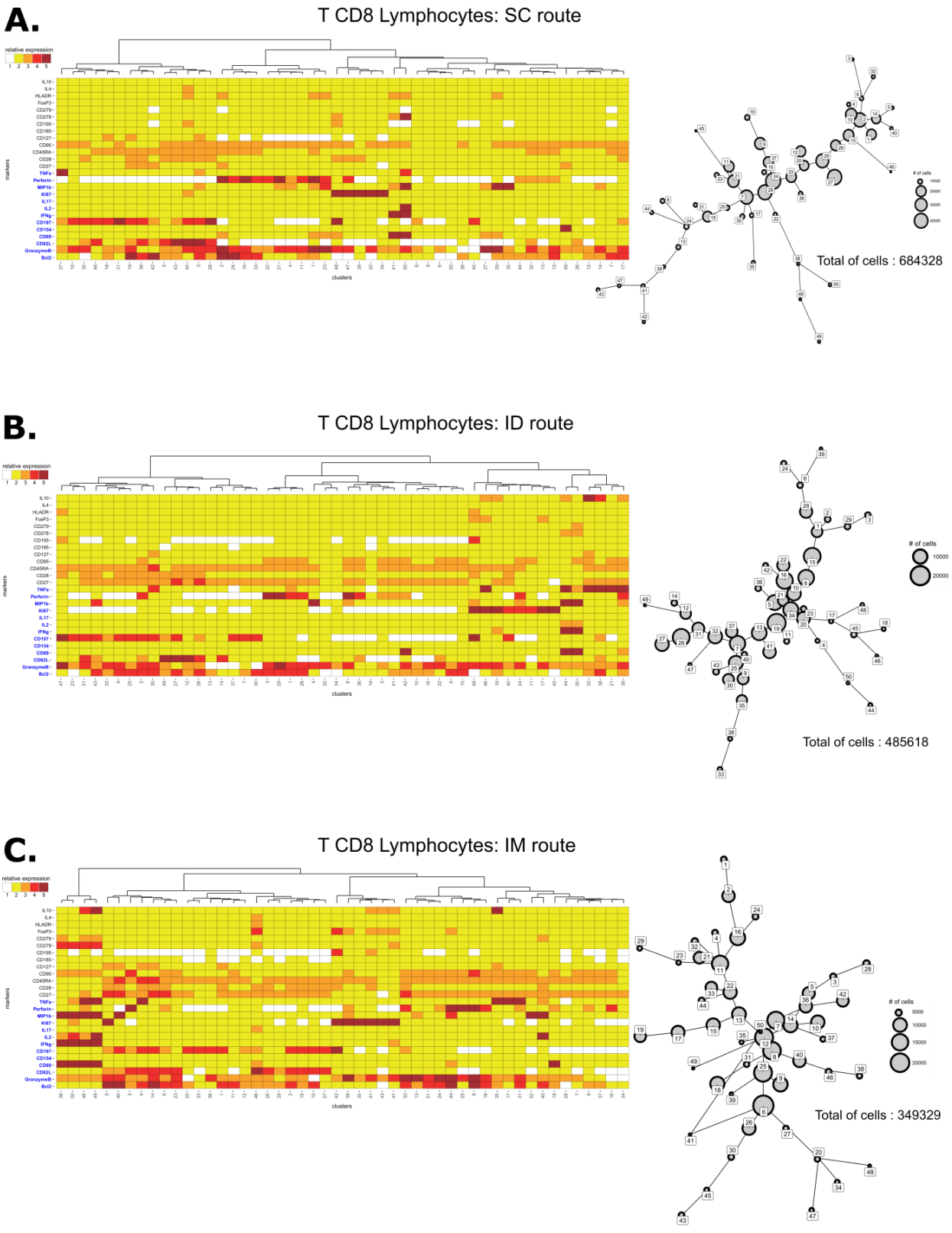

Supplementary figure 4: Heatmap and tree view generated from CD8+ T cell SPADE sorting

Supplementary figure 4: Heatmap and tree view generated from CD8+ T cell SPADE sorting

Heatmap representation of CD8+ T cells clusters gated as shown in supplementary figure 3. The numbers of clusters are reported on the X axis and the markers on the Y axis. CD8 T cells have been sorted through SPADE analysis based on their expression of clusterisation markers (in blue). Each column represents a cell clusters, which was automatically sorted following a hierarchical clustering represented by dendrograms on the top of the heatmaps. The five-tiered color scale, from white to deep red, represents marker relative expression. On the right of heatmap is associated a tree viewer. Clusters are represented in nodes, the size of each node depends on the number of cells in the cluster. Two node that are close to each other will have a phenotypic proximity. (A) SC route (B) ID route (C) IM route

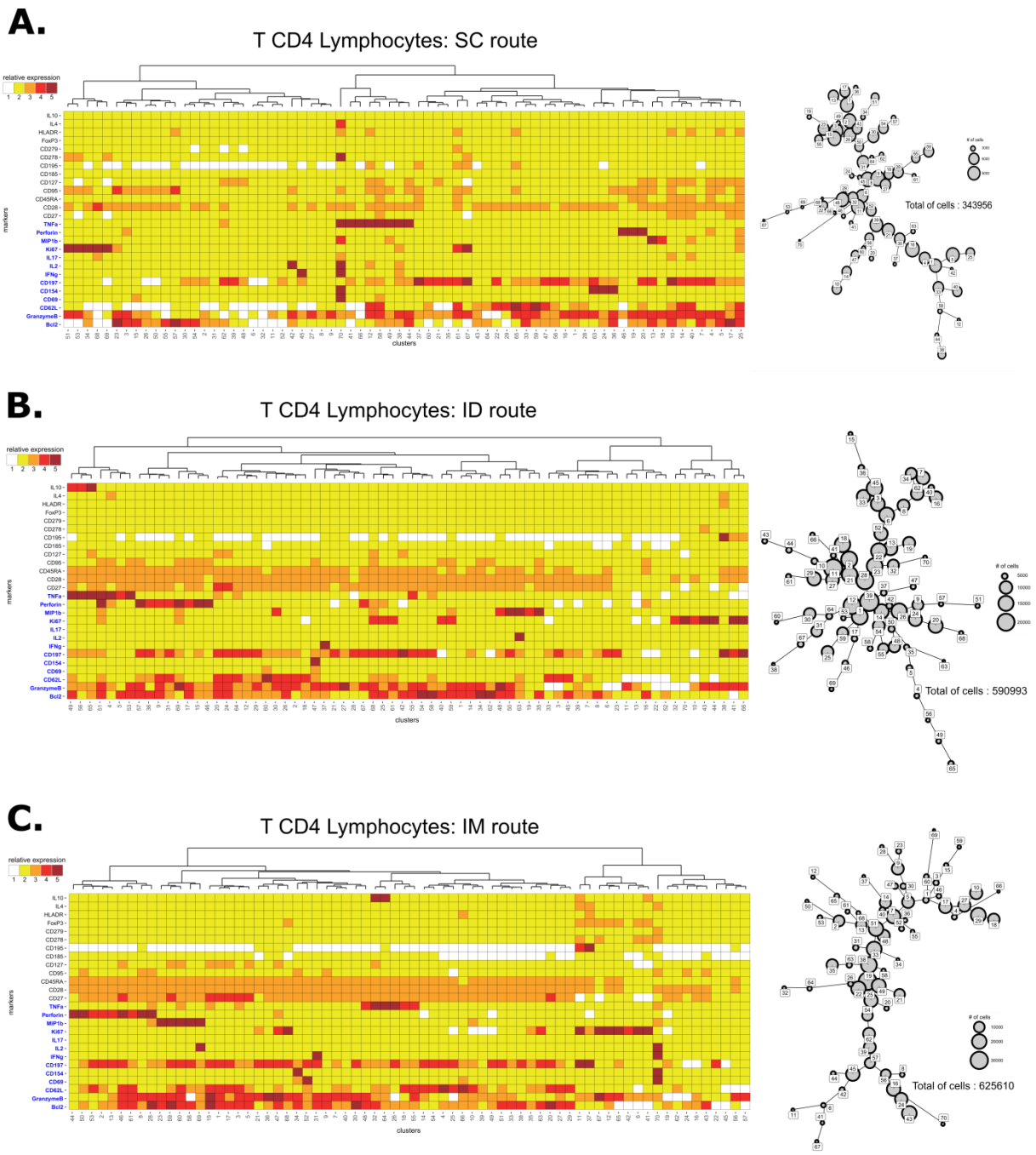

Supplementary figure 5: Heatmap and tree view generated from CD4+ T cell SPADE sorting

Heatmap representation of CD4+ T cells clusters gated as shown in supplementay figure 3. On the X axis is represented the number of cluster, on the Y axis is represented the markers. CD8 T cells have been sorted through SPADE analysis based on their expression of clusterisation markers (in blue). Each column represents a cell cluster, which was automatically sorted following a hierarchical clustering represented by dendrograms on the top of the heatmaps.The five-tiered color scale, from white to deep red, represent marker relative expression. The tree viewer on the right represent clusters in nodes, the size of each node depends on the number of cells in the cluster. Two node that are close to each other will have a phenotypic proximity. (A) SC route (B) ID route (C) IM route.

C. Article 3 (étude complémentaire)

Macrophages elicit the first steps of local innate immune response after MVA and Poly(I:C) IM administration in Non-Human primates

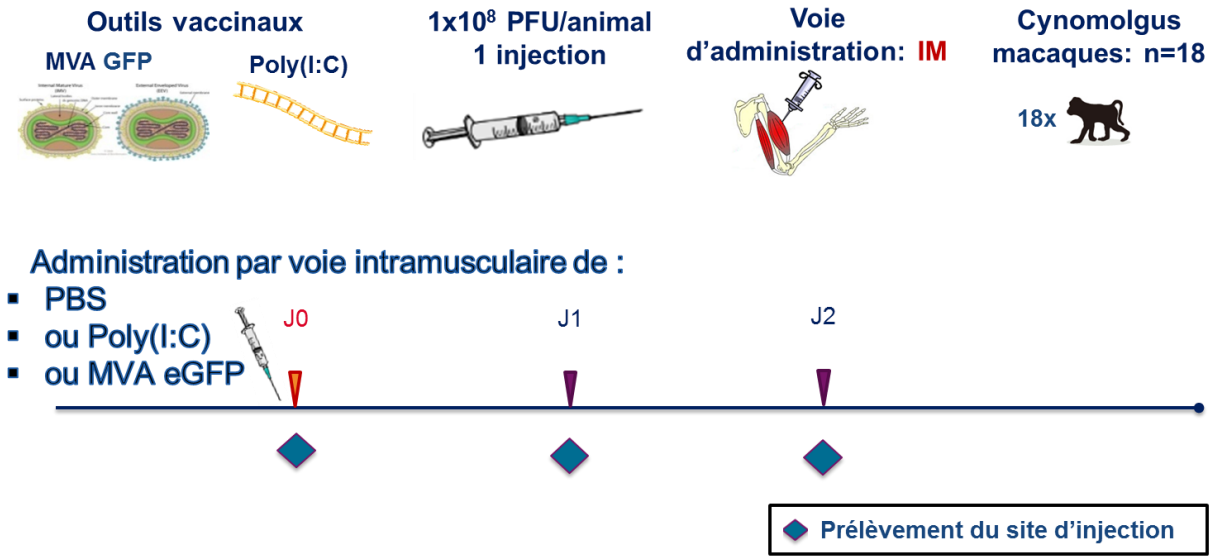

Figure 17 : Schéma expérimental de l'étude de la réponse innée locale induite par le MVA ou le Poly(I :C) par voie intramusculaire

Cet article est focalisé sur la réponse immunitaire locale induite 24h et 48h après injection intramusculaire de MVA ou de poly (I:C).

Nos observations mettent en évidence une dominance des macrophages, qui sont induits selon une cinétique différente en fonction du produit injecté. Ni les granulocytes –pourtant attendus- ni les cellules dendritiques n'ont particulièrement été mobilisés au niveau du site d'injection. Nous avons ensuite étudié l'activation de macrophages dérivés de PBMCs *in vitro* après stimulation par le MVA ou le poly (I:C). L'activation, caractérisée par une augmentation de l'expression de CD80 et CD86, s'accompagne d'une production importante de cytokines pro-inflammatoires (MIP1α, MIP1β, IL6, TNFα…).

Ces observations soulignent le rôle précoce et prépondérant des macrophages au niveau du muscle, notamment dans l'entretien de la réponse inflammatoire, première étape dans l'élaboration de la réponse immune aux vaccins.

Macrophages elicit the first steps of local innate immune response after MVA and Poly(I:C) intramuscular administration in Non-Human primates

Pierre Rosenbaum[1-2], Leslie Gosse[1-2], Lev Stimmer[??], Olivier Epaulard[5], Sébastien Langlois[1-2], Nathalie Dereuddre-Bosquet, Roger Le Grand[1], Frédéric Martinon[1-2]

(1) CEA-Univesité Paris Sud-Inserm U 1184, Immunology of viral infections and auto-immune diseases, IDMIT Infrastructure, iMETI, France

(2) Vaccine research institute, Crétéil, France

(3) CEA – INSERM, MIRCen, UMS27, 92265 Fontenay-aux-Roses, France

(4) INSERM, U1169, 94270 Kremlin-Bicêtre, France

(5) Infectious Diseases Unit; Grenoble University Hospital, Grenoble, 38043, France

Abstract

Better understanding the local early immune response is required for a rational design of future vaccines. More particularly the innate response induced at the site of injection is poorly described, especially in the muscle tissue, which is the most commonly used vaccine administration route. We have characterized *in vivo* the main immune cells recruited in muscles of cynomolgus macaques after either the modified attenuated vaccinia virus Ankara (MVA) or the Polyinosinic:polycytidylic acid (Poly(I:C)). Using flow cytometry and immunohistology, we were able to detect a local increase of macrophages recruitment. Dendritic cells, polymorphonuclear cells and lymphocytes were not significantly modified. Macrophages seem to be involved in the persistence of a local pro inflammatory environment that might be crucial for the elaboration of adaptive response.

Introduction

Innate immune system -which provides a first line of defense against microorganisms- plays a crucial role in the orientation and duration of the adaptive immune responses[197198].

Key players of the innate response – such as dendritic cells macrophages, polymorphonuclear cells or lymphocytes-can contribute to the inflammatory process.For instance, antigen presenting cells such has dendritic cells have the ability to capture the antigen, to cleave antigenic proteins into peptides that will be presented in association with class II molecules of the major histocompatibility complex (MHC II) and presence of co-stimulatory signals to antigen specific CD4+ T cells [199].

Those cells also express pattern recognition receptors (PRR) such as toll-like receptors (TLR) which are also strongly involved in innate immunity. Indeed, PRR are able to sense pattern expressed by pathogens such as microbial nucleic acids or lipopolysaccharides. Its activation trigger cytokines release and cellular maturation and migration of APCs to lymph nodes [127200201].

As a consequence, there is a major interest to deeply investigate the inflammatory process involved in vaccine responses in order to improve its efficiency. Several studies have investigated the local reaction in this tissue, most of them in rodent models mimicking muscle strain or contusion in human[202]. Among immune cells recruited in inflammatory muscle, a pivotal role is attributed to macrophages, which are able to change their pro-inflammatory into an anti-inflammatory phenotype.Doing so, they contribute tothe maintenance of the inflammatory response at the early steps, but also facilitates tissue reparation processes at later time points [203204]. However, only few studies have investigated the local effect after vaccination. Most of them focused on the local effects induced by adjuvants in mouse or *in vitro* models [67205206]. Those studies highlight the role of both neutrophils and macrophages at the first steps of the immune reaction combined with a high local pro-inflammatory signature[205206]. After MF59 adjuvant injection, these cells load the antigen and migrate to the draining lymph node where they are supposed to elicit lymphocytes activation [67]. Most of the related studies have been performed using mice models, and very little have reported in more relevant species for testing human vaccine candidates like non-human primates (NHP) [14796207].

Here we reported the characterization of the local innate immune response induced in cynomolgus macaques by an intramuscular injectionof a recombinant Modified Vaccinia virus Ankara (MVA), or the synthetic analog of double-stranded viral RNA Polyinosinic:polycytidylic acid (Poly(I:C)) as TLR-3 agonist.

MVA is an attenuated strain of vaccinia virus which is not replicative in most of the mammalian cells. It has been shown to induce a long lasting protective immunity with high cellular and humoral response against smallpox with a good safety profile [208112]. It also has the capacity to accept large inserts and is therefore considered as a potential vector recombinant antigen like HIV, *Mycobacterium tuberculosis*, HCV, Ebola and cancer antigens. Several clinical trials using rMVA are currently in progress [143209146].

We compared the inflammatory response induced by MVA to Poly(I:C),known to trigger innate immune response through MDA-5, also used by MVA [210140] and which is also used in several clinical studies[211212163].

In this work, we showed that the local inflammation induced by both Poly(I:C) or MVA in the muscle is mainly mediated by macrophages but not dendritic cells or neutrophils. Those macrophages seemed also to be involved in the persistence of a local pro inflammatory environment that might be crucial to the elaboration of adaptive response.

Materials and methods

Ethical issues

All experimental procedures on cynomolgus macaques were conducted accordingly to European guidelines for animal care (directive 63/2010, "Journal Officiel des Communautés Européennes", L276, September 22, 2010) and according to CEA institutional guidelines. Also in accordance to the French Ethical policy, this project received an authorization (number 0201501281731916 (APAF1S#170).02) from the research minister with a favorable evaluation of the ethic committee.

This includes also a regular following of the animal welfare (clinical exam, temperature, weight…) during all the duration of the experiment.

Intramuscular injections

Adult males cynomolgus macaques (*Macaca fascicularis*), each weighing 4 to 6 kg, imported from Mauritius, were housed within CEA facilities at Fontenay-Aux-Roses. Intramuscular injections were conducted after anaesthesia with ketamin (10 mg/kg, Imalgen®). Prior to injection, the skin was shaved, cleaned with ethanol 70%. Intramuscular immunization with 200µL of Phosphate Buffer Saline (PBS, Gibco®), polyinosinic-polycytidylic acid (PolyI:C, 200µg, Invivogen®) or GFP recombining Modified Vaccinia virus Ankara (MVA 1.10^8 PFU, Dr Bernard Verrier, UMR5086 CNRS) was performed in biceps, triceps, or quadriceps muscle. The 1.10^8 PFU MVA dose corresponds to an amount able to induce at least vaccinal response to the Dryvax®, a calf lymph smallpox vaccine leading to smallpox eradication[208], whereas 200µg of poly(I:C) was shown to be enough to induce inflammation in cynomolgus macaques[140].

In order to ensure to gather the good localization of the site of injection, PBS, MVA, or Poly(I:C) were injected in two half doses with 3cm interval. We therefore formed a 45° angle between the syringe and the injection surface to have a large and identified muscle region that has received the compound. Each animal received up to six injections and biopsies, with a maximum of three at a same time.

Muscular biopsies

Muscular biopsies were conducted after anaesthesia of the animal with tiletamin/zolazepam (Zolétil®, 5 mg/kg). Prior to biopsies, the skin was cleaned with povidone iodate solution (Vetedine®). Targeted muscles were triceps, biceps, and quadriceps. An incision was made between the two injections zone to perform the biopsies. Biopsies were processed 24h or 48h after the injections. A part of the muscle biopsy was fixed with paraformaldehyde and then frozen for histology and the other part was used for cell phenotyping in flow cytometry. Some muscular biopsies were also performed during necropsies.

Extraction of cells from muscular biopsies.

Muscle biopsies were washed, cut in small pieces and digested up to three times during ten minutes at 37°C using an enzymatic solution containing RPMI (Life Technologies®), 10% FCS (Lonza®), 1% Penicillin Streptomycin Neomycin (Life Technologies®), 10mM Hepes (Thermo Fischer®), 2mg/mL collagenase D (Roche) and 0,02 mg/mL DNAse I (Roche®). After each digestion, tissue was filtered using 70µm cell strainer and washed afterwards in 50 mL of PBS solution.

Cell Phenotyping in flow cytometry

All the steps of the staining were processed at 4°C. Cell suspension were first stained using viability dye LiveDead® (Thermofischer) during 15 minutes, then washed. Fc receptors were satured using in house producted PBS 5% macaque serum during 20 minutes. Muscle cells suspension were then stained during 30 minutes with 100µL of mix of antibodies diluted in PBS containing HLA DR (BD, clone G46-6), CD163 (BD, clone GHI/61), CD11c (BD, clone S-HCL-3), CD45(BD, clone DO58-1283), CD66 (Miltenyi Biotec, clone TET2), CD3 (BD, clone SP34-2), CD8 (BD; clone RPA-T8); CD20 (BD, clone 2H7), CD11b (Beckman Coulter, clone Bear 1). In vitro cultured PBMCs derived macrophages were stained during 30 minutes with 100µL of mix of antibodies diluted in PBS containing HLA DR (BD, clone G46-6), CD163 (BD, clone GHI/61), CD14 (BD, clone M5E2), CD206 (BD, clone 19.2), CD80 (BD,

clone L307.4), CD86 (BD, clone 2331(Fun-1)), CCR7(R&D; clone 150503), CD11b (Beckman Coulter, clone Bear 1),and CD45 (BD, clone DO58-1283). Cells were then fixed in 150µL of Cellfix (BD) and acquired in Fortessa® flow cytometer (BD).

Histology

Muscle was then frozen in OCT in isopentan in nitrogen liquid. The tissue was then cut in 8µm slices on superfrost slides ®. Hematoxylin Eosin Saffron coloration was performed using an automaton Microm HMS740. Briefly slides were stained and washed with different solutions corresponding to hemalun, HCl, Lithium Carbonate, Eosin, Alcohol 100°, Saffron, Alcool 100° again and Xylene.

PBMC derived macrophage differentiation

PBMCs were first separated from plasma and granulocytes using BD vacutainer® mononuclear cell preparation tube. PBMCs were then centrifugated up to three times at low speed rate to remove platelets.Monocytes were then separated from PBMC by adherence and *in vitro* differentiated in macrophages during 7 days as described in previous works[213], but using 10 ng/mL of M-CSF and 2 ng/mL GM-CSF (R&D Systems). Differentiated macrophages were then harvested, counted and separated in order to obtain 3×10^5 cells /cm². 24h later, cells were incubated with 1 to 20µg/mL of Poly(I:C), or 0,01 to 1 MOI of MVA.

Cytokine analysis

24h and 48h after macrophage stimulation, a fraction of supernatant was harvested and then stored at -80°C. These samples were used to run a 16 cytokine analyses using 16-plex MAP Non-Human Primates Immunoassay kit (Millipore®) according to supplier's instruction.

Statistical analysis

Data were analyzed with Prism 6.0 (Graphpad Software Inc. ®). Cellular recruitment on the muscle tissue was evaluated using two-sided Mann-Whitney test. In order to respect the independence hypothesis, some data gathered in a same animal were randomly removed for this test. Macrophage activation was evaluated with two-sided Wilcoxon signed matched rank test. Cytokine production was first analyzed with Friedman test. In case of relevant significances, cytokines release was afterwards evaluated with two-sided Wilcoxon signed matched rank test. Because of the constraints of the study model and the fundamental purpose of this work, the sample size provided was limited. This induces a low statistical power, which means that only clear-cut results can have been evaluated as significant.

Test results were represented as follows: NS : p-value> 0.05 ; * : 0.05>p-value>0.01 ; ** : 0.01>p-value> 0.001 ;*** : 0.001>p-value>0.0001 ; ****: 0.0001>p-value

Results

To evaluate the local immune response on the skeletal muscle tissue of cynomolgus macaques, we injected either PBS, rMVA or Poly(I:C) and performed muscular biopsies after 24h and 48h.

Poly(I:C) and MVA induce moderate inflammation profile at the injection site.

The skeletal muscle, which main function is motor activity, is not particularly exposed to pathogens. As a consequence, skeletal muscles logically lack of immune cells[62]. When sterile PBS was injected in animal muscle, no tissue modification or inflammation was observed.Only low amounts of immune cells were observed in histological sections(**Fig.1A**). However, IM injection of Poly(I:C) or rMVA induced multifocal cellular infiltrations through the perimysium and the endomysium, with an increased thickness of those conjunctive layers (**Fig.1B** and **Fig.1C**). Recruited cells were macrophages in majority, however small numbers of polymorphonuclear (PMN) cells are also observed. No severe tissue necrosis or fiber degeneration could be also noticed. No similar infiltration could be observed in the muscle in sites distant to injection.

Poly(I:C) and MVA induce muscular macrophage recruitment with different kinetics.

We digested freshly biopsied muscle previously treated withPBS, Poly(I:C) or rMVA in order to better characterize the recruited immune cells using flow cytometry as we previously reported for the skin[148] [F.Liang *et al.]* [65]**(Fig.2A)**. After excluding doublets, dead cells and CD45- cells, we gated HLA-DR+, CD3-, CD8-, CD20- and CD163+ cells as macrophages; HLA-DRmid, CD3-, CD8-, CD20- , CD163- and CD11c+ as dendritic cells (DC); HLADR-, Lin (CD3, CD8, CD20)+ as lymphocytes and HLADR-, Lin (CD3, CD8, CD20)- , CD66+ as polymorphonuclear neutrophil (PMN) cells. Alternatively, we used side scatter(SSC) to gate lymphocytes and CD11b instead of CD66 to isolate granulocytes. Among CD45+ cells,we showed a significant correlation ($p<0.0001$) between the proportion of CD11b+ and CD66+ PMN **(Fig.2B)**. More generally, we found a very important proximity between our two gating strategies for macrophages ($p<0.0001$), lymphocytes ($p<0.0001$) and granulocytes **(Fig.2C)**, using

Pearson's correlations with slopes of the linear equation varying between 0.90±SD for lymphocytes to 1.20±SD for PMN.

Altogether, those results indicate that, refining cytometry panels allow discrimination of main immune cells using a minimal number of markers. In our case, lineage CD3, CD8, CD20 and CD66 appear to not be as crucial as expected and let the possibility to use other pan-myeloid markers like CD11b, or activating markers, or even reduce the number of channels used.

Using both gating strategies described above, we aimed to more deeply analyze the nature of the cellular recruitment. Immune cell subsets proportions in the muscle tissue are mainly depending on the treatment and the time after injection **(Fig.3)**. In accordance to **Fig.1**, we confirmed by flow cytometry the limited amount of immune cells at the steady state. After injection of Poly(I:C), rMVA or even PBS, macrophages become predominant, particularly at 48h. Interestingly, lymphocytes, granulocytes and dendritic cells proportions do not significantly change between 24hand 48h after MVA or Poly(I:C) injection in the muscle. However, macrophage recruitment peaked at 24h and 48h after injection of poly(I:C) and rMVA respectively.

Interestingly, at those time points, macrophages is the only recruited cell population, whereas we would also have expected an increase of granulocytes and dendritic cells as reported in mouse models [67]. Macrophages may certainly play a key role at the elaboration of the vaccine immune response after an intramuscular inoculation. Those cells are indeed able to act as antigen presenting cells[134214], but could also have an impact on the local microenvironment.

In vitro cultured PBMC derived macrophages show similar activated and pro-inflammatory profile after Poly(I:C) or MVA stimulation.

To better understand the role of recruited macrophages in the muscle tissue, *in vitro* monkey PBMC derived macrophages were produced. The phenotype of these macrophages are close to the muscle tissue macrophages, characterized by a high expression of CD14 and CD163 markers, with however a difference for the CD206 **(Fig 4A)**. In the presence of MVA or Poly(I:C), in vitro derived macrophages significantly increase the expression of CD80 and CD86 activation markers within 48h of incubation **(Fig. 4B)**. By contrast, CCR7 is slightly upregulated only in rMVA stimulated cells. These cells release **(Fig.S1)**. pro-inflammatory cytokines (**Fig. 4C)** and includes IL1Ra, IL1b, IL6 and MIP1β in Poly(I:C) and MVA condition. Interestingly, 24h after Poly(I:C) stimulation, IL1ra, IL1b and TNFα have already reached a peak or a plateau whereas the same cytokine production by macrophages after rMVA stimulation seems to be delayed. These observations are in accordance with the kinetic of recruitment of macrophages in the muscle **(Fig.3)** and suggests that although Poly(I:C) and MVA are induced in similar proportions, the innate immune response with MVA may persist longer. This could lead to a more sustained antigen presentation in presence of MVA and have an impact on the adaptive immune response. Those results also suggest that inflammatory macrophages are widely involved on the maintenance of an inflammation in the muscle tissue.

Discussion

Our data converge to suggest a critical role of macrophages after MVA or Poly(I:C) i.m vaccination, in contrast with other main immune cells like dendritic cells, neutrophils or lymphocytes. It is illustrated with multifocal infiltrations and with a robust DR+CD163+ cell local recruitment. A small magnitude and kinetic differences were reported between the live attenuated vaccine and the synthetic TLR3 ligand. These observations on early local innate immune events raise several interrogationson the role and mechanisms of activation of inflammatory cells recruited after intramuscular vaccination in NHP.

Previous studies [67140] revealed a rapid and massive local neutrophilic recruitment after vaccine adjuvant injections. Hence, by producing a wide set of compounds, including peroxidases, metalloproteins, or lactoferrin, those cells are vital for microorganism sterilization and wound healing. However, they are able to attract macrophages and can also interact with other immune cells like lymphocytes or dendritic cells through, IFNγ, TNFα or chemokine releases [215]. As a major effector of the early steps of the inflammation process, the most probable hypothesis is that neutrophils might have been recruited within the first 24 h post injection.

Macrophages constitute another known effector of the skeletal muscle physiopathology. Thanks to their important cellular plasticity which allow them to produce a wide range of cytokines and chemokines in addition to their high phagocytic activity[216], they can massively infiltrate the muscle where they can wear a key role in tissue reparation after different type of lesions, such as toxin administration, exercise, or infection[217–219]. The fact that we observe a similar phenomenon short time after i.m Poly(I:C) or MVA confirm their local and not MVA or Poly(I:C) specific immunogenicity.

Different inflammation profiles depending on the administration route can be noted : by comparison with the injection of a same dose of Poly(I:C) by intradermal route[140], much more neutrophils are observed in the skin up to three days after i.d vaccination whereas macrophage population is recruited similarly both in skin and skeletal muscle tissues. Some local modifications have also been reported after MVA injection in mouse, with more macrophages but less neutrophil recruitment in

the muscle tissue in comparison with the skin [66]. These variations can be due to the different nature of the tissue resident cells.The skin is indeed naturally composed by a large range of specific resident DC, including Langerhans cells and subtypes of dermal DC[84], but also macrophages, mast cells, lymphocytes and non-immune cells like keratinocytes and fibroblasts, by contrast to the skeletal muscle which houses a limited number of cell populations. For instance, after Poly(I:C) administration, the first signal of danger is triggered by cells expressing TLR-3 or MDA5, which correspond mostly to keratinocytes and dendritic cells in the skin[220221] and myocytes in the muscle[222]. As a consequence, the local micro-environment will be modified differently according to the type of cell population stimulated, leading to a different cellular recruitment, maturation and activation. Those differences in the innate immunity may lead to the dose sparing effect observed in favor of intradermal in several vaccine trials when measuring systemic immune response signatures to various vaccines [63139], including MVA [142]. Despite this dose sparing effect, the quality of the response remains generally nearly similar between i.d and i.m administration.

Unlike skin, skeletal muscle also provides very low quantities of immune cells due to the fact that it is not an organ particularly exposed to pathogen and has no particular immune functions. As a consequence there is a lack of dendritic cells or other APC at the steady state in the skeletal muscle [62]. So the immune response driven after vaccination is probably elicited either by a passive diffusion of the vaccine through draining lymph node, but also by the intervention of freshly recruited APC from the blood. The presence of blood dendritic cells is well described in NHP models [223]. If we cannot exclude the fact that some DCs subsets that are expressing low levels of CD11c[224] could have not been detected for technical reasons in this study, another possibility could be that macrophages observed in the tissue derive from blood monocytes and were selectively recruited to the detriment of other APCs due to the particular cocktail of chemoattractant, including MIP1β which is known to attract this cell population in particular. In this study, we indeed showed that monocyte derived macrophages produce a particular set of pro-inflammatory cytokines in vitro. We anticipate that muscular macrophages would produce similar pro-inflammatory cytokines on the site of injection.

One function of those cytokines is probably to maintain the inflammation process in the skeletal muscle, keeping attracting macrophages at the lesion : As a result, those recruited inflammatory cells could substitute to DC in the muscle in the elaboration of the vaccine response, including antigen capture, migration to draining lymph nodes and antigen presentation to T cells [214].

Those cytokines could also act at a larger extent on the orientation of the adaptive response. Indeed, evidence has been shown that IL1b influences CD4 T cell upregulation and proliferation [225] and participates to the Th1 response in smallpox vaccination[226]. TNFα can also induce DC activation and maturation under certain circumstances [227].

Altogether, we demonstrated that macrophages are a key component of the innate immune response after either intramuscular MVA or Poly(I:C) vaccination. They are more recruited at the site of injection than any other immune cell population. Due to their ability to release cytokines and exert phagocytosis of vaccine infected apoptotic cells, those cells are deeply involved to the muscle reparation process after the lesion induced by our vaccine compounds. Macrophages are also able to act as antigen presenting cells, orientating the immune response profile. As a consequence, even the slight timing differences observed on the use Poly(I:C) and MVA for a potential vaccine could have large repercussions on correlates of protection of a potential vaccine. In this case, macrophages could be crucial to decide of the fate of the vaccine responses after intramuscular immunization.

References

1. Rosenbaum, P. Etude de la réponse immunitaire induite par des adjuvants agonistes des TLR sur la peau de macaque. (These de pharmacie, Rennes, 2012). at <http://www.sudoc.fr/167282689>
2. van Panhuis, W. G. *et al.*Contagious Diseases in the United States from 1888 to the Present. *N. Engl. J. Med.***369,** 2152–2158 (2013).
3. Andersen, P. & Doherty, T. M. The success and failure of BCG - implications for a novel tuberculosis vaccine. *Nat. Rev. Microbiol.***3,** 656–662 (2005).
4. Mayr, A., Hochstein-Mintzel, V. & Stickl, H. Abstammung, Eigenschaften und Verwendung des attenuierten Vaccinia-Stammes MVA. *Infection***3,** 6–14 (1975).
5. Kim, J., Rerks-Ngarm, S. & Excler, J. HIV Vaccines-Lessons learned and the way forward. *Curr. Opin. HIV***5,** 428–434 (2010).
6. Ahmed, S. S., Plotkin, S. a, Black, S. & Coffman, R. L. Assessing the safety of adjuvanted vaccines. *Sci. Transl. Med.***3,** 93rv2 (2011).
7. Cristiani, C. *et al.* Safety of MF-59 adjuvanted vaccine for pandemic influenza: Results of the vaccination campaign in an Italian health district. *Vaccine***29,** 3443–3448 (2011).
8. Paavonen, J. *et al.* Efficacy of a prophylactic adjuvanted bivalent L1 virus-like-particle vaccine against infection with human papillomavirus types 16 and 18 in young women: an interim analysis of a phase III double-blind, randomised controlled trial. *Lancet***369,** 2161–2170 (2007).
9. Liko, J., Robison, S. G. & Cieslak, P. R. Priming with Whole-Cell versus Acellular Pertussis Vaccine. *N. Engl. J. Med.***368,** 581–2 (2013).
10. Warfel, J. M., Zimmerman, L. I. & Merkel, T. J. Acellular pertussis vaccines protect against disease but fail to prevent infection and transmission in a nonhuman primate model. *Proc. Natl. Acad. Sci. U. S. A.***111,** 787–92 (2014).
11. Buchbinder, S. P. *et al.* Efficacy assessment of a cell-mediated immunity HIV-1 vaccine (the Step Study): a double-blind, randomised, placebo-controlled, test-of-concept trial. *Lancet***372,** 1881–1893 (2008).
12. Rerks-Ngarm, S. *et al.* Vaccination with ALVAC and AIDSVAX to Prevent HIV-1 Infection in Thailand. *N. Engl. J. Med.***361,** 2209–2220 (2009).
13. Hewitt, E. W. The MHC class I antigen presentation pathway: Strategies for viral immune evasion. *Immunology***110,** 163–169 (2003).
14. Goulder, P. J. R. & Watkins, D. I. Impact of MHC class I diversity on immune control of immunodeficiency virus replication. *Nat. Rev. Immunol.***8,** 619–30 (2008).

15. Silzle, T., Randolph, G. J., Kreutz, M. & Kunz-Schughart, L. A. The fibroblast: Sentinel cell and local immune modulator in tumor tissue. *Int. J. Cancer***108,** 173–180 (2004).
16. Kupper, T. S. *et al.* Production of IL-6 by Keratinocytes. *Ann. N. Y. Acad. Sci.***557,** 454–465 (2008).
17. Saalbach, A. *et al.* Dermal fibroblasts induce maturation of dendritic cells. *J Immunol***178,** 4966–4974 (2007).
18. Tecle, T., Tripathi, S. & Hartshorn, K. L. Review: Defensins and cathelicidins in lung immunity. *Innate Immun.***16,** 151–159 (2010).
19. Danese, S., Dejana, E. & Fiocchi, C. Immune Regulation by Microvascular Endothelial Cells: Directing Innate and Adaptive Immunity, Coagulation, and Inflammation. *J. Immunol.***178,** 6017–6022 (2007).
20. Guilliams, M. *et al.* Dendritic cells, monocytes and macrophages: a unified nomenclature based on ontogeny TL - 14. *Nat. Rev. Immunol.***14 VN - r,** 571–578 (2014).
21. Epstein, F. H. & Luster, A. D. Chemokines — Chemotactic Cytokines That Mediate Inflammation. *N. Engl. J. Med.***338,** 436–445 (1998).
22. Biron, C. a. Role of early cytokines, including alpha and beta interferons (IFN-alpha/beta), in innate and adaptive immune responses to viral infections. *Semin. Immunol.***10,** 383–390 (1998).
23. Leroy, M. & Desmecht, D. Les interférons de type I et leur fonction antivirale. *Ann. médecine vétérinaire***150,** 73–107 (2006).
24. Dai, P. *et al.* Modified Vaccinia Virus Ankara Triggers Type I IFN Production in Murine Conventional Dendritic Cells via a cGAS/STING-Mediated Cytosolic DNA-Sensing Pathway. *PLoS Pathog.***10,** (2014).
25. Ablasser, A. *et al.* Cell intrinsic immunity spreads to bystander cells via the intercellular transfer of cGAMP. *Nature***503,** 530–4 (2013).
26. Kawai, T. & Akira, S. Toll-like receptors and their crosstalk with other innate receptors in infection and immunity. *Immunity***34,** 637–50 (2011).
27. Hodge, D. R., Hurt, E. M. & Farrar, W. L. The role of IL-6 and STAT3 in inflammation and cancer. *Eur. J. Cancer***41,** 2502–2512 (2005).
28. Luster, A. D., Alon, R. & von Andrian, U. H. Immune cell migration in inflammation: present and future therapeutic targets. *Nat. Immunol.***6,** 1182–90 (2005).
29. Serhan, C. N. & Savill, J. Resolution of inflammation: the beginning programs the end. *Nat. Immunol.***6,** 1191–1197 (2005).
30. Banchereau, J. & Steinman, R. M. Dendritic cells and the control of immunity. *Nature***392,** 245–252 (1998).

31. Bruel, T. *et al.* Plasmacytoid dendritic cell dynamics tune interferon-alfa production in SIV-infected cynomolgus macaques. *PLoS Pathog.***10,** e1003915 (2014).
32. Ketloy, C. *et al.* Expression and function of Toll-like receptors on dendritic cells and other antigen presenting cells from non-human primates. *Vet. Immunol. Immunopathol.***125,** 18–30 (2008).
33. Hume, D. a. Macrophages as APC and the dendritic cell myth. *J. Immunol.***181,** 5829–5835 (2008).
34. Falcone, M., Lee, J., Patstone, G., Yeung, B. & Sarvetnick, N. B lymphocytes are crucial antigen-presenting cells in the pathogenic autoimmune response to GAD65 antigen in nonobese diabetic mice. *J. Immunol.***161,** 1163–1168 (1998).
35. Ahmed, R. & Gray, D. Immunological memory and protective immunity: understanding their relation. *Science (80-.).***272,** 54–60 (1996).
36. Itano, A. a & Jenkins, M. K. Antigen presentation to naive CD4 T cells in the lymph node. *Nat. Immunol.***4,** 733–9 (2003).
37. Idris-Khodja, N., Mian, M. O. R., Paradis, P. & Schiffrin, E. L. Dual opposing roles of adaptive immunity in hypertension. *Eur. Heart J.***35,** 1238–1244 (2014).
38. Diehl, S. & Rincón, M. The two faces of IL-6 on Th1/Th2 differentiation. *Mol. Immunol.***39,** 531–536 (2002).
39. Okada, R., Kondo, T., Matsuki, F., Takata, H. & Takiguchi, M. Phenotypic classification of human CD4+ T cell subsets and their differentiation. *Int. Immunol.***20,** 1189–1199 (2008).
40. Cher, D. J. & Mosmann, T. R. Two types of murine helper T cell clone. II. Delayed-type hypersensitivity is mediated by TH1 clones. *J. Imunol.***138,** 3688–94 (1987).
41. Coffman, R. L. *et al.* The role of helper T cell products in mouse B cell differentiation and isotype regulation. *Immunol. Rev.***102,** 5–28 (1988).
42. Schaerli, P. *et al.* CXC chemokine receptor 5 expression defines follicular homing T cells with B cell helper function. *J. Exp. Med.***192,** 1553–62 (2000).
43. Fazilleau, N., Mark, L., McHeyzer-Williams, L. & McHeyzer-Williams, M. Follicular Helper T Cells: Lineage and Location. *Immunity***30,** 324–335 (2009).
44. Crotty, S. Follicular Helper CD4 T Cells (T_{FH}). *Annu. Rev. Immunol.***29,** 621–663 (2011).
45. Petrovas, C. *et al.*CD4 T follicular helper cell dynamics during SIV infection. *J Clin Invest.***5,** 1–14 (2012).
46. Perreau, M. *et al.* Follicular helper T cells serve as the major CD4 T cell compartment for HIV-1 infection, replication, and production. *J. Exp. Med.***210,** 143–56 (2013).
47. Colineau, L. *et al.* HIV-infected spleens present altered follicular helper T cell (Tfh) subsets and skewed B cell maturation. *PLoS One***10,** 1–19 (2015).

48. Lowin, B., Hahne, M., Mattman, C. & Tchopp, J. Cytolytic T-cell cytotoxicity is mediated through perforin and Fas lytic pathway. *Lett. to Nat.***370,** (1994).

49. Liu, C., Walsh, C. M. & Young, J. D. Perforin : structure and function. *Immunol. Today***15,** 194–201 (1995).

50. Heusel, J. W., Wesselschmidt, R. L., Russell, J. H. & Ley, T. J. Cytotoxic Lymphocytes Require Granzyme B for the Rapid Induction of DNA Fragmentation and Apoptosis in Allogeneic Target Cells. *Cell***76,** 977–987 (1994).

51. Jenkins, M. K., Burrell, E. & Ashwell, J. D. Antigen presentation by resting B cells . Effectiveness at inducing T cell proliferation is determined by costimulatory signals , not T cell receptor occupancy. *J. Immunol.***144,** 1585–1590 (1990).

52. Abbas, A. K. *et al.* Activation and Functions of CD4 + T-Cell Subsets. *Immunol. Rev.* (1991).

53. Fey, T. M. *et al.* In the Absence of a CD40 Signal , B Cells Are Tolerogenic. *Immunity***2,** 645–653 (1995).

54. Fuchs, E. J. & Matzingert, P. B Cells Turn Off Virgin But Not Memory T Cells. *Science***2,** (1992).

55. Bonecchi, B. R. *et al.* Differential Expression of Chemokine Receptors and Chemotactic Responsiveness of Type 1 T Helper Cells. *J. Exp. Med.***187,** 129–134 (1998).

56. Imai, T. *et al.* Selective recruitment of CCR4-bearing T h 2 cells toward antigen-presenting cells by the CC chemokines thymus and activation-regulated chemokine and macrophage-derived chemokine. *Int. Immunol.***11,** 81–88 (1999).

57. Förster, R., Davalos-misslitz, A. C. & Rot, A. CCR7 and its ligands : balancing immunity and tolerance. *Nat. Rev. Immunol.***8,** (2008).

58. Fritsch, R. D. *et al.* Stepwise Differentiation of CD4 Memory T Cells Defined by Expression of CCR7 and CD27. *J. Immunol. (Baltimore, Md. 1950)***175,** 6489–6497 (2015).

59. Xu, H., Manivannan, A., Crane, I., Dawson, R. & Liversidge, J. Critical but divergent roles for CD62L and CD44 in directing blood monocyte trafficking in vivo during inflammation. *Blood***112,** 1166–1175 (2008).

60. Picker, L. J. *et al.* Control of lymphocyte recirculation in man. I. Differential regulation of the peripheral lymph node homing receptor L-selectin on T cells during the virgin to memory cell transition. *J. Immunol.* (1993).

61. Chaparas, S. D. L'immunite dans la tuberculose. *Bull. l'Organisation Mond. la Santé***60,** 827–844 (1982).

62. Wiendl, H., Hohlfeld, R. & Kieseier, B. C. Immunobiology of muscle: advances in understanding an immunological microenvironment. *Trends Immunol.***26,** 373–80 (2005).

63. Zehrung, D., Jarrahian, C. & Wales, A. Intradermal delivery for vaccine dose sparing: Overview of current issues. *Vaccine***31,** 3392–3395 (2013).

64. Zaric, M., Ibarzo Yus, B., Kalcheva, P. P. & Klavinskis, L. S. Microneedle-mediated delivery of viral vectored vaccines. *Expert Opin. Drug Deliv.***5247,** 17425247.2017.1230096 (2016).
65. Liang, F. *et al.* Dissociation of skeletal muscle for flow cytometric characterization of immune cells in macaques. *J. Immunol. Methods***425,** 69–78 (2015).
66. Abadie, V. *et al.* Original encounter with antigen determines antigen-presenting cell imprinting of the quality of the immune response in mice. *PLoS One***4,** e8159 (2009).
67. Calabro, S. *et al.* Vaccine adjuvants alum and MF59 induce rapid recruitment of neutrophils and monocytes that participate in antigen transport to draining lymph nodes. *Vaccine***29,** 1812–23 (2011).
68. Lu, F. & Hogenesch, H. Kinetics of the inflammatory response following intramuscular injection of aluminum adjuvant. *Vaccine***31,** 3979–86 (2013).
69. Caspar-Bauguil, S. *et al.* Adipose tissues as an ancestral immune organ: site-specific change in obesity. *FEBS Lett.***579,** 3487–92 (2005).
70. Pond, C. M. Adipose tissue and the immune system. *Prostaglandins Leukot. Essent. Fat. Acids***73,** 17–30 (2005).
71. Damouche, A. *et al.*Adipose Tissue Is a Neglected Viral Reservoir and an Inflammatory Site during Chronic HIV and SIV Infection. *PLoS Pathog.***11,** 1–28 (2015).
72. Mantoux, C. Intradermo-reaction de la tuberculine. *Comptes rendus l'Académie des Sci.***147,** 355–57 (1908).
73. Artenstein, A. W. Bifurcated vaccination needle. *Vaccine***32,** 895 (2014).
74. Roediger, B. *et al.*Cutaneous immunosurveillance and regulation of inflammation by group 2 innate lymphoid cells. *Nat. Immunol.***14,** 564–73 (2013).
75. Nestle, F. O., Di Meglio, P., Qin, J.-Z. & Nickoloff, B. J. Skin immune sentinels in health and disease. *Nat. Rev. Immunol.***9,** 679–691 (2009).
76. Zaid, A. *et al.* Persistence of skin-resident memory T cells within an epidermal niche. *Proc. Natl. Acad. Sci. U. S. A.***111,** 5307–12 (2014).
77. Malissen, B., Tamoutounour, S. & Henri, S. The origins and functions of dendritic cells and macrophages in the skin. *Nat. Rev. Immunol.***14,** 417–28 (2014).
78. Valladeau, J. & Saeland, S. Cutaneous dendritic cells. *Semin. Immunol.***17,** 273–83 (2005).
79. Kubo, A., Nagao, K., Yokouchi, M., Sasaki, H. & Amagai, M. External antigen uptake by Langerhans cells with reorganization of epidermal tight junction barriers. *J. Exp. Med.***206,** 2937–2946 (2009).
80. Shklovskaya, E. *et al.* Langerhans cells are precommitted to immune tolerance induction. *Proc. Natl. Acad. Sci. U. S. A.***108,** 18049–54 (2011).
81. Stoitzner, P. *et al.* Langerhans cells cross-present antigen derived from skin. *Proc. Natl. Acad.*

*Sci. U. S. A.***103,** 7783–8 (2006).

82. Flacher, V. *et al.* Murine Langerin + dermal dendritic cells prime CD 8 + T cells while Langerhans cells induce cross-tolerance. 1–14 (2014).
83. Klechevsky, E. *et al.* Functional specializations of human epidermal Langerhans cells and CD14+ dermal dendritic cells. *Immunity***29,** 497–510 (2008).
84. Klechevsky, E. Human dendritic cells - stars in the skin. *Eur. J. Immunol.***43,** 3147–55 (2013).
85. Penel-Sotirakis, K., Simonazzi, E., Péguet-Navarro, J. & Rozières, A. Differential Capacity of Human Skin Dendritic Cells to Polarize CD4+T Cells into IL-17, IL-21 and IL-22 Producing Cells. *PLoS One***7,** (2012).
86. Haniffa, M., Gunawan, M. & Jardine, L. Human skin dendritic cells in health and disease. *J. Dermatol. Sci.***77,** 85–92 (2015).
87. Haniffa, M. *et al.* Human Tissues Contain CD141 hi Cross-Presenting Dendritic Cells with Functional Homology to Mouse CD103 + Nonlymphoid Dendritic Cells. *Immunity***37,** 60–73 (2012).
88. Davis, M. M. A Prescription for Human Immunology. *Immunity***29,** 835–838 (2008).
89. Ostrand-Rosenberg, S. Animal models of tumor immunity, immunotherapy and cancer vaccines. *Curr. Opin. Immunol.***16,** 143–150 (2004).
90. von Herrath, M. G. & Nepom, G. T. Lost in translation: barriers to implementing clinical immunotherapeutics for autoimmunity. *J. Exp. Med.***202,** 1159–62 (2005).
91. Kennedy, R. C., Shearer, M. H. & Hildebrand, W. Nonhuman primate models to evaluate vaccine safety and immunogenicity. *Vaccine***15,** 903–908 (1997).
92. Quintana-Murci, L., Alcaïs, A., Abel, L. & Casanova, J.-L. Immunology in natura: clinical, epidemiological and evolutionary genetics of infectious diseases. *Nat. Immunol.***8,** 1165–71 (2007).
93. Mestas, J. & Hughes, C. C. W. Of mice and not men: differences between mouse and human immunology. *J. Immunol.***172,** 2731–2738 (2004).
94. Macchiarini, F., Manz, M. G., Palucka, a K. & Shultz, L. D. Humanized mice : are we there yet ? *Allergy***202,** 1307–11 (2005).
95. Ito, R., Takahashi, T., Katano, I. & Ito, M. Current advances in humanized mouse models. *Cell. Mol. Immunol.***9,** 208–14 (2012).
96. Hérodin, F., Thullier, P., Garin, D. & Drouet, M. Nonhuman primates are relevant models for research in hematology, immunology and virology. *Eur. Cytokine Netw.***16,** 104–116 (2005).
97. Merkel, T. J. & Halperin, S. A. Nonhuman primate and human challenge models of pertussis. *J. Infect. Dis.***209,** 20–23 (2014).
98. Geisbert, T. W., Strong, J. E. & Feldmann, H. Considerations in the Use of Nonhuman Primate

Models of Ebola Virus and Marburg Virus Infection. *J. Infect. Dis.***212,** 91–97 (2015).

99. Flynn, J. L., Gideon, H. P., Mattila, J. T. & Lin, P. ling. Immunology studies in non-human primate models of tuberculosis. *Immunol. Rev.***264,** 60–73 (2015).
100. Gardner, M. B. & Luciw, P. a. Macaque models of human infectious disease. *ILAR J.***49,** 220–55 (2008).
101. Meurens, F., Summerfield, A., Nauwynck, H., Saif, L. & Gerdts, V. The pig: A model for human infectious diseases. *Trends Microbiol.***20,** 50–57 (2012).
102. Roberts, K. L. & Smith, G. L. Vaccinia virus morphogenesis and dissemination. *Trends Microbiol.***16,** 472–479 (2008).
103. Moss, B. Poxvirus entry and membrane fusion. *Virology***344,** 48–54 (2006).
104. Ichihashi, Y. Extracellular enveloped vaccinia virus escapes neutralization. *Virology***217,** 478–485 (1996).
105. Smith, G. L., Symons, J. A. & Vanderplasschen, A. Vaccinia virus immune evasion. *Immunol. Rev.***159,** 137–154 (1997).
106. Smith, G., Mackett, M. & Moss, B. Infectious vaccinia virus recombinants that express hepatitis B virus surface antigen. *Nature***302,** 490–495 (1983).
107. Meyer, H., Sutter, G. & Mayr, a. Mapping of deletions in the genome of the highly attenuated vaccinia virus MVA and their influence on virulence. *J. Gen. Virol.***72 (Pt 5),** 1031–8 (1991).
108. DiPerna, G. *et al.* Poxvirus Protein N1L Targets the I- B Kinase Complex, Inhibits Signaling to NF- B by the Tumor Necrosis Factor Superfamily of Receptors, and Inhibits NF- B and IRF3 Signaling by Toll-like Receptors. *J. Biol. Chem.***279,** 36570–36578 (2004).
109. Waibler, Z. *et al.* Vaccinia virus-mediated inhibition of type I interferon responses is a multifactorial process involving the soluble type I interferon receptor B18 and intracellular components. *J. Virol.***83,** 1563–1571 (2009).
110. Moss, B. *et al.* Host range restricted, non-replicating vaccinia virus vectors as vaccine candidates. *Adv. Exp. Med. Biol.***397,** 7–13 (1996).
111. Sutter, G., Wyatt, L. S., Foley, P. L., Bennink, J. R. & Moss, B. A recombinant vector derived from the host range-restricted and highly attenuated MVA strain of vaccinia virus stimulates protective immunity in mice to influenza virus. *Vaccine***12,** 1032–1040 (1994).
112. Vollmar, J. *et al.* Safety and immunogenicity of IMVAMUNE, a promising candidate as a third generation smallpox vaccine. *Vaccine***24,** 2065–2070 (2006).
113. Sheehan, S. *et al.* A Phase I, Open-Label Trial, Evaluating the Safety and Immunogenicity of Candidate Tuberculosis Vaccines AERAS-402 and MVA85A, Administered by Prime-Boost Regime in BCG-Vaccinated Healthy Adults. *PLoS One***10,** e0141687 (2015).
114. Stickl, H. *et al.* MVA-Stufenimpfung gegen Pocken. *DMW - Dtsch. Medizinische*

*Wochenschrift***99,** 2386–2392 (1974).

115. Altenburg, A. F. *et al.* Modified vaccinia virus ankara (MVA) as production platform for vaccines against influenza and other viral respiratory diseases. *Viruses***6,** 2735–61 (2014).
116. Zhou, Y. & Sullivan, N. J. Immunology and evolvement of the adenovirus prime, MVA boost Ebola virus vaccine. *Curr. Opin. Immunol.***35,** 131–136 (2015).
117. Gómez, C. E. *et al.* A Phase I Randomized Therapeutic MVA-B Vaccination Improves the Magnitude and Quality of the T Cell Immune Responses in HIV-1-Infected Subjects on HAART. *PLoS One***10,** e0141456 (2015).
118. Lelièvre, J.-D., Lacabaratz, C. & Richert, L. Essai de phase I/II sans insu, randomisé, multicentrique évaluant l'immunogénicite et la tolérance de 4 combinaisons « prime- boost » de candidats vaccins VIH (MVA HIV-B /LIPO-5; LIPO-5 / MVA HIV-B; GTU-MultiHIV B /LIPO-5; GTU-MultiHIV B / MVA HIV-B) chez. 33076 (2014). at <www.recherche-vaccinVIH.fr>
119. Richert, L. *et al.* Accelerating clinical development of HIV vaccine strategies: methodological challenges and considerations in constructing an optimised multi-arm phase I/II trial design. *Trials***15,** 68 (2014).
120. Kitano, H. Computatioal Systems Biology. *Nature***420,** 206–210 (2002).
121. Nakaya, H. I. & Pulendran, B. Vaccinology in the era of high-throughput biology. *Philos. Trans. R. Soc. Lond. B. Biol. Sci.***370,** (2015).
122. Querec, T. D. *et al.*Systems biology approach predicts immunogenicity of the yellow fever vaccine in humans. *Nat. Immunol.***10,** 116–125 (2009).
123. Obermoser, G. *et al.* Systems scale interactive exploration reveals quantitative and qualitative differences in response to influenza and pneumococcal vaccines. *Immunity***38,** 831–44 (2013).
124. Pulendran, B., Li, S. & Nakaya, H. I. Systems vaccinology. *Immunity***33,** 516–529 (2010).
125. Bécavin, C., Tchitchek, N., Mintsa-Eya, C., Lesne, A. & Benecke, A. Improving the efficiency of multidimensional scaling in the analysis of high-dimensional data using singular value decomposition. *Bioinformatics***27,** 1413–1421 (2011).
126. Schlitzer, A. & Ginhoux, F. Organization of the mouse and human DC network. *Curr. Opin. Immunol.***26,** 90–9 (2014).
127. Wille-Reece, U. *et al.* Toll-like receptor agonists influence the magnitude and quality of memory T cell responses after prime-boost immunization in nonhuman primates. *J. Exp. Med.***203,** 1249–58 (2006).
128. Nakaya, H. I. *et al.* Systems biology of vaccination for seasonal influenza in humans. *Nat. Immunol.***12,** 786–795 (2011).
129. Gannavaram, S. *et al.* Modulation of Innate Immune Mechanisms to Enhance Leishmania Vaccine-Induced Immunity: Role of Coinhibitory Molecules. *Front. Immunol.***7,** 1–10 (2016).

130. Hartman, Z. C., Appledorn, D. M. & Amalfitano, A. Adenovirus vector induced innate immune responses: Impact upon efficacy and toxicity in gene therapy and vaccine applications. *Virus Res.***132,** 1–14 (2008).
131. Coffman, R. L., Sher, A. & Seder, R. a. Vaccine adjuvants: putting innate immunity to work. *Immunity***33,** 492–503 (2010).
132. Iwasaki, A. & Medzhitov, R. Regulation of adaptive immunity by the innate immune system. *Science***327,** 291–295 (2010).
133. Maletto, B. a. *et al.* Presence of neutrophil-bearing antigen in lymphoid organs of immune mice. *Blood***108,** 3094–3102 (2006).
134. Pozzi, L. -a. M., Maciaszek, J. W. & Rock, K. L. Both Dendritic Cells and Macrophages Can Stimulate Naive CD8 T Cells In Vivo to Proliferate, Develop Effector Function, and Differentiate into Memory Cells. *J. Immunol.***175,** 2071–2081 (2005).
135. Kwissa, M., Nakaya, H. I., Oluoch, H., Pulendran, B. & Dc, W. Distinct TLR adjuvants differentially stimulate systemic and local innate immune responses in nonhuman primates Distinct TLR adjuvants differentially stimulate systemic and local innate immune responses in nonhuman primates. **119,** 2044–2055 (2012).
136. McMahon, J. M., Wells, K. E., Bamfo, J. E., Cartwright, M. a & Wells, D. J. Inflammatory responses following direct injection of plasmid DNA into skeletal muscle. *Gene Ther.***5,** 1283–90 (1998).
137. Cunningham, A. L., Carbone, F. & Geijtenbeek, T. B. H. Langerhans cells and viral immunity. *Eur. J. Immunol.***38,** 2377–85 (2008).
138. Liard, C. *et al.* Intradermal immunization triggers epidermal Langerhans cell mobilization required for CD8 T-cell immune responses. *J. Invest. Dermatol.***132,** 615–25 (2012).
139. Kenney, R. T. *et al.* Dose Sparing with Intradermal Injection of Influenza Vaccine. *J. Med.* 1–7 (2004).
140. Epaulard, O. *et al.* Macrophage- and Neutrophil-Derived TNF-α Instructs Skin Langerhans Cells To Prime Antiviral Immune Responses. *J. Immunol.***193,** 2416–2426 (2014).
141. Meyer, H., Sutter, G. & Mayr, A. Meyer, Sutter, Mayr - 1991 - Mapping of deletions in the genome of the highly attenuated vaccinia virus MVA and their influence on virul.pdf. **382,** 1031–1038 (1991).
142. Wilck, M. B. *et al.*Safety and immunogenicity of modified vaccinia Ankara (ACAM3000): effect of dose and route of administration. *J. Infect. Dis.***201,** 1361–1370 (2010).
143. Gómez, C. E., Perdiguero, B., García-Arriaza, J. & Esteban, M. Poxvirus vectors as HIV/AIDS vaccines in humans. *Hum. Vaccines Immunother.***8,** 1192–1207 (2012).
144. Gómez, C. E. *et al.* High, broad, polyfunctional, and durable T cell immune responses induced

in mice by a novel hepatitis C virus (HCV) vaccine candidate (MVA-HCV) based on modified vaccinia virus Ankara expressing the nearly full-length HCV genome. *J. Virol.***87,** 7282–300 (2013).

145. You, Q. *et al.* Subcutaneous administration of modified vaccinia virus Ankara expressing an Ag85B-ESAT6 fusion protein, but not an adenovirus-based vaccine, protects mice against intravenous challenge with Mycobacterium tuberculosis. *Scand. J. Immunol.***75,** 77–84 (2012).
146. Tapia, M. D. *et al.* Use of ChAd3-EBO-Z Ebola virus vaccine in Malian and US adults, and boosting of Malian adults with MVA-BN-Filo: a phase 1, single-blind, randomised trial, a phase 1b, open-label and double-blind, dose-escalation trial, and a nested, randomised, double-bli. *Lancet Infect. Dis.***3099,** 1–12 (2015).
147. Bontrop, R. E. Non-human primates: essential partners in biomedical research. *Immunol. Rev.***183,** 5–9 (2001).
148. Adam, L., Rosenbaum, P., Cosma, A., Le Grand, R. & Martinon, F. Identification of skin immune cells in non-human primates. *J. Immunol. Methods* 1–8 (2015). doi:10.1016/j.jim.2015.07.010
149. Ziegler-Heitbrock, L. The CD14+ CD16+ blood monocytes: their role in infection and inflammation. *J. Leukoc. Biol.***81,** 584–92 (2007).
150. Sui, Y. *et al.* Vaccine-induced myeloid cell population dampens protective immunity to SIV. 1–12 doi:10.1172/JCI73518DS1
151. Salabert, N. *et al.* Intradermal injection of an anti-Langerin-HIVGag fusion vaccine targets epidermal Langerhans cells in nonhuman primates and can be tracked in vivo. *Eur. J. Immunol.***46,** 689–700 (2016).
152. Abràmoff, M. D., Magalhães, P. J. & Ram, S. J. Image processing with imageJ. *Biophotonics Int.***11,** 36–41 (2004).
153. Kolesnikov, N. *et al.* ArrayExpress update-simplifying data submissions. *Nucleic Acids Res.***43,** D1113–D1116 (2015).
154. Team, Rc. R: A language and environment for statistical computing. (2016). at <https://www.r-project.org/.>
155. Kruskal, J. B. & Wish, M. Multidimensional Scaling. *Sage Univ. Pap. Ser. Quant. Appl. Soc. Sci.* (1978).
156. Shannon, P. *et al.* Cytoscape: A software Environment for integrated models of biomolecular interaction networks. *Genome Res.***13,** 2498–2504 (2003).
157. Ramírez, J. C., Gherardi, M. M. & Esteban, M. Biology of attenuated modified vaccinia virus Ankara recombinant vector in mice: virus fate and activation of B- and T-cell immune responses in comparison with the Western Reserve strain and advantages as a vaccine. *J. Virol.***74,** 923–33 (2000).

158. McFadden, G. Poxvirus tropism. *Nat. Rev. Microbiol.***3,** 201–13 (2005).

159. Bronte, V. *et al.* Recommendations for myeloid-derived suppressor cell nomenclature and characterization standards. *Nat. Commun.***7,** 12150 (2016).

160. Newson, J. *et al.* Resolution of acute inflammation bridges the gap between innate and adaptive immunity. *Blood***124,** 1748–64 (2014).

161. Gilchrist, M. *et al.* Systems biology approaches identify ATF3 as a negative regulator of Toll-like receptor 4. *Nature***441,** 173–178 (2006).

162. MacLeod, D. T., Nakatsuji, T., Wang, Z., di Nardo, A. & Gallo, R. L. Vaccinia Virus Binds to the Scavenger Receptor MARCO on the Surface of Keratinocytes. *J. Invest. Dermatol.* (2014). doi:10.1038/jid.2014.330

163. Delaloye, J. *et al.* Innate immune sensing of modified vaccinia virus Ankara (MVA) is mediated by TLR2-TLR6, MDA-5 and the NALP3 inflammasome. *PLoS Pathog.***5,** (2009).

164. van Furth, R., Nibbering, P. H., van Dissel, J. T. & Diesselhoff-den Dulk, M. M. The characterization, origin, and kinetics of skin macrophages during inflammation. *J. Invest. Dermatol.***85,** 398–402 (1985).

165. Flechsig, C. *et al.* Uptake of antigens from modified vaccinia Ankara virus-infected leukocytes enhances the immunostimulatory capacity of dendritic cells. *Cytotherapy***13,** 739–52 (2011).

166. Dinarello, C. a. IL-18: A TH1 -inducing, proinflammatory cytokine and new member of the IL-1 family. *J. Allergy Clin. Immunol.***103,** 11–24 (1999).

167. Sagoo, P. *et al.* In vivo imaging of inflammasome activation reveals a subcapsular macrophage burst response that mobilizes innate and adaptive immunity. *Nat. Med.***22,** 64–71 (2016).

168. Ding, X. *et al.* TNF receptor 1 mediates dendritic cell maturation and CD8 T cell response through two distinct mechanisms. *J. Immunol.***187,** 1184–1191 (2011).

169. Talmadge, J. E. & Gabrilovich, D. I. History of myeloid-derived suppressor cells. *Nat. Rev. Cancer***13,** 739–52 (2013).

170. Nagaraj, S., Youn, J.-I. & Gabrilovich, D. I. Reciprocal Relationship between Myeloid-Derived Suppressor Cells and T Cells. *J. Immunol.***191,** 17–23 (2013).

171. Laurent, P. E. *et al.* Evaluation of the clinical performance of a new intradermal vaccine administration technique and associated delivery system. *Vaccine***25,** 8833–8842 (2007).

172. Igyártó, B. Z. & Kaplan, D. H. Antigen presentation by Langerhans cells. *Curr. Opin. Immunol.***25,** 115–119 (2013).

173. Montagne, J. R. La, Ph, D. & Fauci, A. S. Intradermal Influenza Vaccination — Can Less Be More ? *N. Engl. J. Med.***351,** 2330–2332 (2004).

174. Belshe, R. B. *et al.* Comparative immunogenicity of trivalent influenza vaccine administered by intradermal or intramuscular route in healthy adults. *Vaccine***25,** 6755–6763 (2007).

175. Roozbeh, J. *et al.* Low dose intradermal versus high dose intramuscular hepatitis B vaccination in patients on chronic hemodialysis. *Asaio J.***51,** 242–245 (2005).

176. Mohanan, D. *et al.* Administration routes affect the quality of immune responses: A cross-sectional evaluation of particulate antigen-delivery systems. *J. Control. Release***147,** 342–9 (2010).

177. Leung-Theung-Long, S. *et al.* A Novel MVA-Based Multiphasic Vaccine for Prevention or Treatment of Tuberculosis Induces Broad and Multifunctional Cell-Mediated Immunity in Mice and Primates. *PLoS One***10,** e0143552 (2015).

178. Gómez, C. E. *et al.* Systems Analysis of MVA-C Induced Immune Response Reveals Its Significance as a Vaccine Candidate against HIV/AIDS of Clade C. *PLoS One***7,** e35485 (2012).

179. Pejoski, D. *et al.* Identification of vaccine-altered circulating B cell phenotypes using mass cytometry and a two-step clustering analysis. *J. Immunol.***in press,** (2016).

180. Tricot, S. *et al.* Evaluating the efficiency of isotope transmission for improved panel design and a comparison of the detection sensitivities of mass cytometer instruments. *Cytometry. A***87,** 357–68 (2015).

181. Finck, R. *et al.* Normalization of mass cytometry data with bead standards. *Cytom. Part A***83 A,** 483–494 (2013).

182. Kotecha, N., Krutzik, P. O. & Irish, J. M. Web-based analysis and publication of flow cytometry experiments. *Curr. Protoc. Cytom.***Chapter 10,** 1–24 (2010).

183. Linderman, M. D. *et al.* CytoSPADE: High-performance analysis and visualization of high-dimensional cytometry data. *Bioinformatics***28,** 2400–2401 (2012).

184. Newell, E. W., Sigal, N., Bendall, S. C., Nolan, G. P. & Davis, M. M. Cytometry by Time-of-Flight Shows Combinatorial Cytokine Expression and Virus-Specific Cell Niches within a Continuum of CD8 + T Cell Phenotypes. *Immunity***36,** 142–152 (2012).

185. Seubert, A., Monaci, E., Pizza, M., O'Hagan, D. T. & Wack, A. The adjuvants aluminum hydroxide and MF59 induce monocyte and granulocyte chemoattractants and enhance monocyte differentiation toward dendritic cells. *J. Immunol.***180,** 5402–5412 (2008).

186. Galli, S. J., Borregaard, N. & Wynn, T. a. Phenotypic and functional plasticity of cells of innate immunity: macrophages, mast cells and neutrophils. *Nat. Immunol.***12,** 1035–44 (2011).

187. Colonna, M. & Facchetti, F. TREM-1 (triggering receptor expressed on myeloid cells): a new player in acute inflammatory responses. *J Infect Dis***187 Suppl ,** S397–401 (2003).

188. Serhan, C. N. *et al.*Resolution of inflammation: state of the art, definitions and terms. *FASEB J.***21,** 325–332 (2007).

189. Ibrahim, M. M. Subcutaneous and visceral adipose tissue: Structural and functional differences. *Obes. Rev.***11,** 11–18 (2010).

190. Hausman, G. J. & Richardson, R. L. Adipose tissue angiogenesis 1,2. *J Anim Sci* (2003). doi:10.1038/ijo.2010.180

191. Rasmussen, A. L. *et al.*Delayed inflammatory and cell death responses are associated with reduced pathogenicity in Lujo virus-infected cynomolgus macaques. *J. Virol.***89,** 2543–52 (2015).

192. Megiovanni, A. M., Gluckman, J. C., Boudaly, S. & Candida, D. Polymorphonuclear neutrophils deliver activation signals and antigenic molecules to dendritic cells : a new link between leukocytes upstream of T lymphocytes and mutually influence the two leukocyte popula- cesses occurring upstream of the interactions be. **79,** (2006).

193. Castillo, P. & Kolls, J. K. IL-10: A Paradigm for Counterregulatory Cytokines. *J. Immunol.***197,** 1529–1530 (2016).

194. Buggins, a G. *et al.* Effect of costimulation and the microenvironment on antigen presentation by leukemic cells. *Blood***94,** 3479–3490 (1999).

195. Kupper, T. & Fuhlbrigge, R. Immune surveillance in the skin: mechanisms and clinical consequences. *Nat. Rev. Immunol.***4,** 211–222 (2004).

196. Hansen, S. G. *et al.* Effector memory T cell responses are associated with protection of rhesus monkeys from mucosal simian immunodeficiency virus challenge. *Nat. Med.***15,** 293–299 (2009).

197. Kasturi, S., Skountzou, I. & Albrecht, R. Programming the magnitude and persistence of antibody responses with innate immunity. *Nature***470,** 543–547 (2011).

198. Li, S. *et al.* Molecular signatures of antibody responses derived from a systems biology study of five human vaccines. *Nat. Immunol.***15,** 195–204 (2014).

199. Palucka, K., Banchereau, J. & Mellman, I. Designing vaccines based on biology of human dendritic cell subsets. *October***33,** 464–478 (2011).

200. Matthews, K. *et al.* Clinical Adjuvant Combinations Stimulate Potent B-Cell Responses In Vitro by Activating Dermal Dendritic Cells. *PLoS One***8,** e63785 (2013).

201. Kwissa, M. *et al.* Adjuvanting a DNA vaccine with a TLR9 ligand plus Flt3 ligand results in enhanced cellular immunity against the simian immunodeficiency virus. *J. Exp. Med.***204,** 2733–46 (2007).

202. Souza, J. De & Gottfried, C. Muscle injury: Review of experimental models. *J. Electromyogr. Kinesiol.***23,** 1253–1260 (2013).

203. Pillon, N. J., Bilan, P. J., Fink, L. N. & Klip, A. Cross-talk between skeletal muscle and immune cells: muscle-derived mediators and metabolic implications. *Am. J. Physiol. Endocrinol. Metab.***304,** E453–65 (2013).

204. Arnold, L. *et al.* Inflammatory monocytes recruited after skeletal muscle injury switch into

antiinflammatory macrophages to support myogenesis. *J Exp Med***204,** 1057–1069 (2007).

205. Mosca, F. *et al.* Molecular and cellular signatures of human vaccine adjuvants. *Proc. Natl. Acad. Sci. U. S. A.***105,** 10501–6 (2008).
206. Samuvel, D. J., Sundararaj, K. P., Nareika, A., Lopes-Virella, M. F. & Huang, Y. Lactate boosts TLR4 signaling and NF-kappaB pathway-mediated gene transcription in macrophages via monocarboxylate transporters and MD-2 up-regulation. *J. Immunol. (Baltimore, Md. 1950)***182,** 2476–2484 (2009).
207. Carlsson, H. E., Schapiro, S. J., Farah, I. & Hau, J. Use of primates in research: A global overview. *Am. J. Primatol.***63,** 225–237 (2004).
208. Earl, P. L. *et al.* Immunogenicity of a highly attenuated MVA smallpox vaccine and protection against monkeypox. *Nature***428,** 182–185 (2004).
209. Pathan, A. a *et al.* Effect of vaccine dose on the safety and immunogenicity of a candidate TB vaccine, MVA85A, in BCG vaccinated UK adults. *Vaccine***30,** 5616–24 (2012).
210. Caskey, M. *et al.* Synthetic double-stranded RNA induces innate immune responses similar to a live viral vaccine in humans. *J. Exp. Med.***208,** 2357–66 (2011).
211. Ammi, R. *et al.* Poly(I:C) as cancer vaccine adjuvant: Knocking on the door of medical breakthroughs. *Pharmacol. Ther.***146,** 120–131 (2015).
212. Tewari, K. *et al.* Poly(I:C) is an effective adjuvant for antibody and multi-functional CD4+ T cell responses to Plasmodium falciparum circumsporozoite protein (CSP) and ??DEC-CSP in non human primates. *Vaccine***28,** 7256–7266 (2010).
213. Rimaniol, A.-C., Gras, G. & Clayette, P. In vitro interactions between macrophages and aluminum-containing adjuvants. *Vaccine***25,** 6784–92 (2007).
214. Denning, T. L., Wang, Y., Patel, S. R., Williams, I. R. & Pulendran, B. Lamina propria macrophages and dendritic cells differentially induce regulatory and interleukin 17-producing T cell responses. *Nat. Immunol.***8,** 1086–94 (2007).
215. Nathan, C. Neutrophils and immunity: challenges and opportunities. *Nat. Rev. Immunol.***6,** 173–182 (2006).
216. Saclier, M., Cuvellier, S., Magnan, M., Mounier, R. & Chazaud, B. Monocyte/macrophage interactions with myogenic precursor cells during skeletal muscle regeneration. *FEBS J.***280,** 4118–4130 (2013).
217. Brigitte, M. *et al.* Muscle resident macrophages control the immune cell reaction in a mouse model of notexin-induced myoinjury. *Arthritis Rheum.***62,** 268–79 (2010).
218. Tidball, J. G. & Villalta, S. A. Regulatory interactions between muscle and the immune system during muscle regeneration. *Am. J. Physiol. Regul. Integr. Comp. Physiol.***298,** R1173–87 (2010).

219. Watson, N. B., Schneider, K. M. & Massa, P. T. SHP-1–Dependent Macrophage Differentiation Exacerbates Virus-Induced Myositis. (2016). doi:10.4049/jimmunol.1402210

220. Muzio, M. *et al.* Differential expression and regulation of toll-like receptors (TLR) in human leukocytes: selective expression of TLR3 in dendritic cells. *J. Immunol.***164,** 5998–6004 (2000).

221. Miller, L. S. Toll-Like Receptors in Skin. *Adv. Dermatol.***24,** 71–87 (2008).

222. Schreiner, B. *et al.*Expression of toll-like receptors by human muscle cells in vitro and in vivo: TLR3 is highly expressed in inflammatory and HIV myopathies, mediates IL-8 release and up-regulation of NKG2D-ligands. *FASEB J.***20,** 118–120 (2006).

223. Sugimoto, C. *et al.* Differentiation Kinetics of Blood Monocytes and Dendritic Cells in Macaques: Insights to Understanding Human Myeloid Cell Development. *J. Immunol.***195,** 1774–1781 (2015).

224. Autissier, P., Soulas, C., Burdo, T. H. & Williams, K. C. Immunophenotyping of lymphocyte, monocyte and dendritic cell subsets in normal rhesus macaques by 12-color flow cytometry: Clarification on DC heterogeneity. *J. Immunol. Methods***360,** 119–128 (2010).

225. Wang, Y., Lavender, P., Watson, J., Arno, M. & Lehner, T. Stress-activated dendritic cells (DC) induce dual interleukin (IL)-15- and IL1b-mediated pathways, which may elicit CD4+memory T cells and interferon (IFN)-stimulated genes. *J. Biol. Chem.***290,** 15595–15609 (2015).

226. Ovsyannikova, I. G. *et al.*Impact of cytokine and cytokine receptor gene polymorphisms on cellular immunity after smallpox vaccination. *Gene***510,** 59–65 (2012).

227. Bennouna, S., Bliss, S. K., Curiel, T. J. & Denkers, E. Y. Cross-Talk in the Innate Immune System: Neutrophils Instruct Recruitment and Activation of Dendritic Cells during Microbial Infection. *J. Immunol.***171,** 6052–6058 (2003).

228. Gómez, C. E. *et al.* Virus distribution of the attenuated MVA and NYVAC poxvirus strains in mice. *J. Gen. Virol.***88,** 2473–8 (2007).

229. Subramanian, A. *et al.* Gene set enrichment analysis: a knowledge-based approach for interpreting genome-wide expression profiles. *Proc. Natl. Acad. Sci. U. S. A.***102,** 15545–50 (2005).

Figures

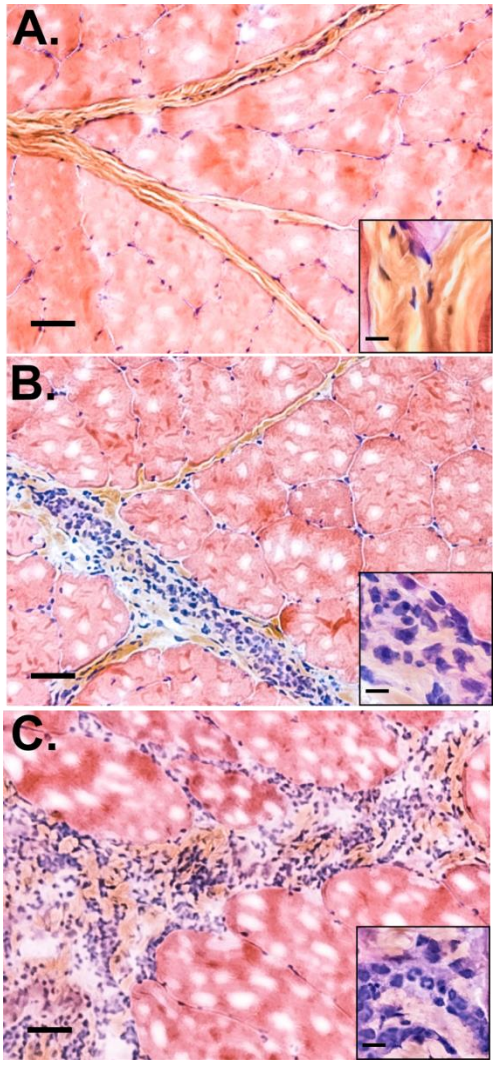

Figure 1

Structural modifications of the NHP injection site after PBS (**FigA.**), Poly(I:C) (**FigB.**), or MVA (**FigC.**) intramuscular administration

6nm Transversal sections of skeletal muscle from triceps or quadriceps after Hematoxylin-Eosin-Saffron staining (X100). Blue arrow represent area that has been oversized (x400). Muscles where previously either treated using PBS, 200µg Poly(I:C), or 1.10^8 PFU MVA. Injection sites where gathered 24h or 48h after injection. PBS treated site show a similar structure as an untreated muscle (**a.**). Local cellular recruitment after Poly(I:C) or MVA treatment with an increase of the flux of cells in the perymisium **(b.)** containing inflammatory cells, mostly macrophagic-round cells with eccentric nucleus **(c.)**, but also polymorphonuclearcells**(e.)**.Those cell types have been determined by histological assessments based on the shape and the nucleus localization.Some cases of cellular infiltration through the endomysium **(d.)** and also oedema are also reported.

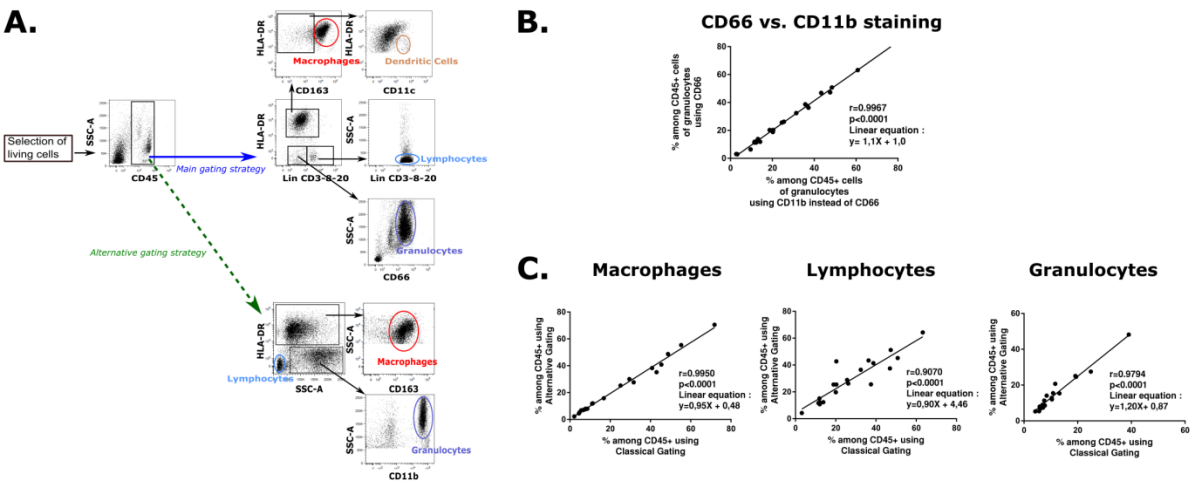

Figure 2

Classical gating strategy used to discriminate the main immune cells of the NHP muscle tissue. This illustration shown corresponds to cells of a muscle tissue that were previously treated in vivo with MVA. FACs Dot plot were obtained after enzymatic digestion of the muscle tissue. Considering the low amount of immune cells in untreated muscle tissue, the gating strategy is shown from a stimulated tissue. We selected living cells using a live/dead fixable cell staining in a 9-color flow cytometry panel. (A) Gating strategies. FACs Dot plot were obtained after enzymatic digestion of the muscle tissue. (B) Comparison between CD66 or CD11b marker to identify granulocytes. Living cells, then DR- and SSC-A+ cells were previously selected to compare the markers. Each plot corresponds to a couple of data on one given non-human primate granulocyte treated with using either CD66 or CD11b. Correlation test was performed, giving indicated r value and p-value. Linear regression line is also represented. (C) Comparison of the cell populations discriminated using classic strategy vs alternative gating strategy. Each plot corresponds to a couple of data on one given non-human primate granulocyte treated with using either CD66 or CD11b. Correlation test was performed, giving indicated r value and p-value. Linear regression line is also represented.

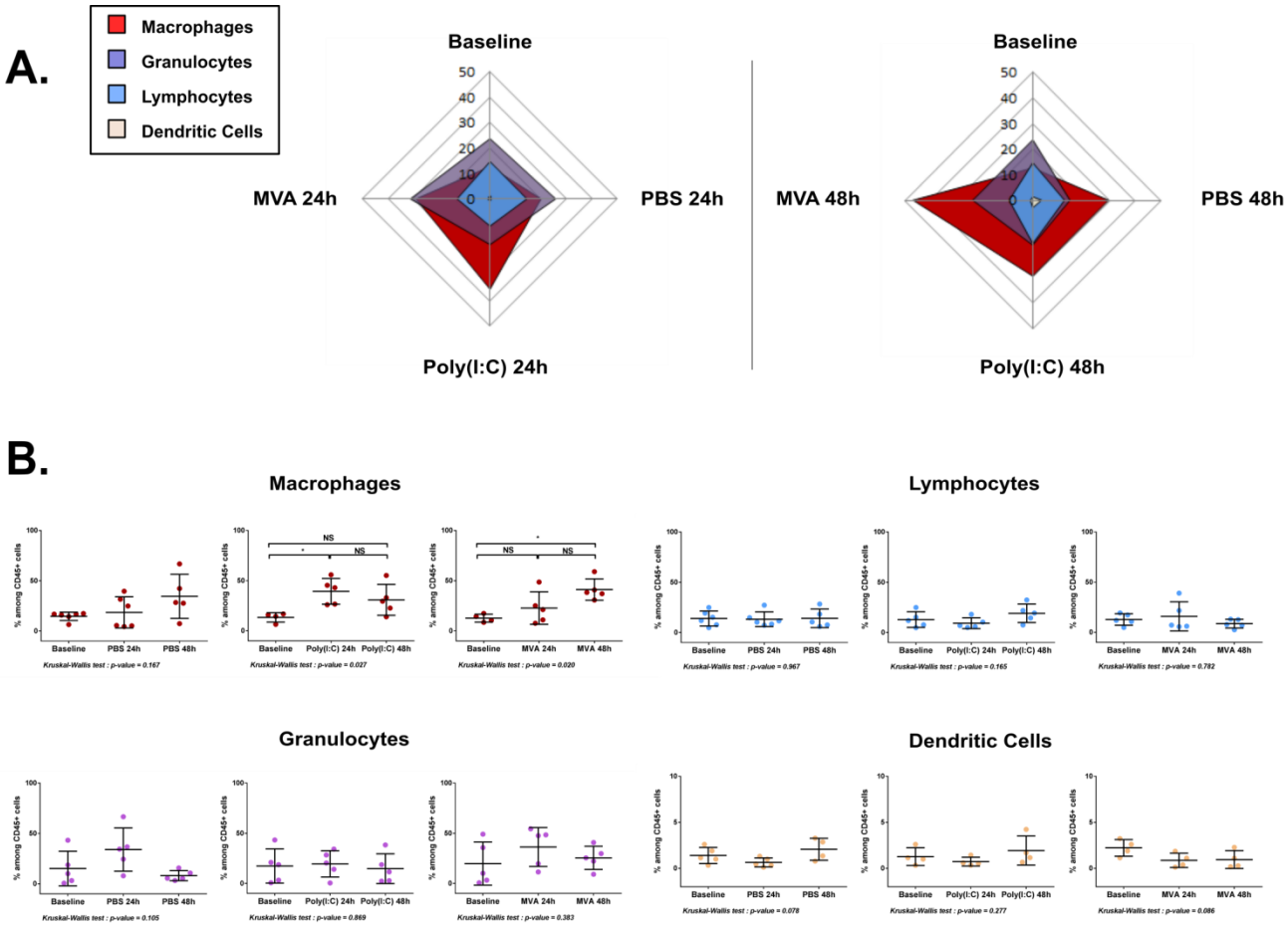

Figure 3

Macrophage is the main cell population recruited in the tissue after Poly(I:C)or MVA stimulation, following different kinetics.

Muscles were previously either untreated or treated using PBS, 200µg Poly(I:C), or 1.10^8 PFU MVA. Injection sites where sampled 24h to 48h after stimulation. FACs datas were obtained after enzymatic digestion of the muscle tissue. Percentage among CD45+ cells values for each cell population were obtained using gating strategies previously described. (A) Radar-like visualization of muscle tissue characterized immune cells. Each polygon represents a cell population. The corner of the polygon corresponds at the arithmetical mean (n=5 to 10) of the percentage of the cell population among CD45+ cells.(B)Scatter-plot charts of granulocytes, macrophages, lymphocytes and dendritic cells. Arithmetical mean ± SD (n=4 to 6). Statistical analyses were performed using Kruskal-Walis test. In case of positive Kruskal-Walis test, double tailed Mann-Whitney test were conducted to compare separately each groups. Non-significant p-values (p>0.05) were calculated but not represented. * : 0.05>p-value>0.01 ;** : 0.01>p-value> 0.001 ; *** : 0.001>p-value

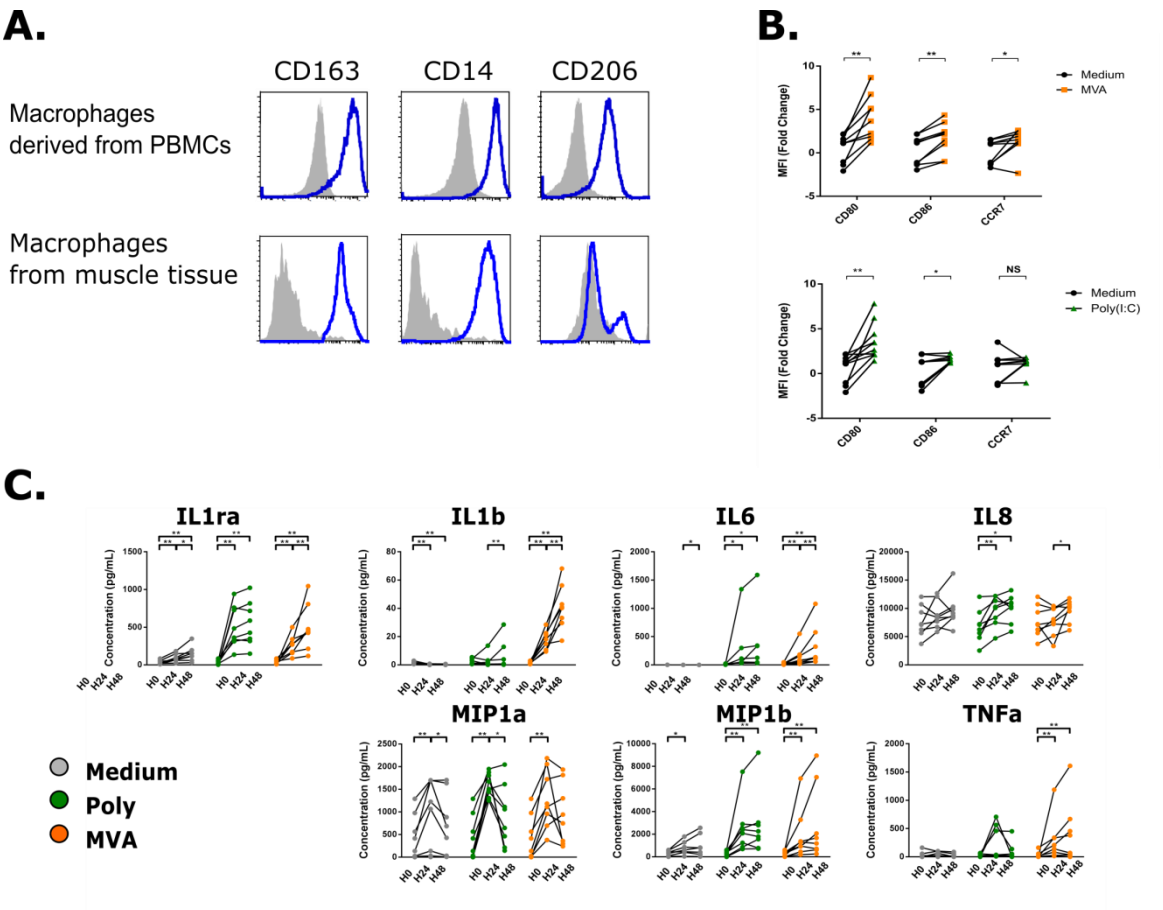

Figure 4

In vitro PBMC derived macrophages are activated and release mainly pro-inflammatory cytokines after Poly(I:C) or MVA stimulation. PBMC derived macrophages were gathered directly after their differentiation (H0) or 48h (H48) after stimulation. Macrophages supernatant used to perform luminex analysis were gathered before stimulation (H0), 24h or 48h after stimulation. Stimulations of macrophages were performed using either medium, 20µg/mL Poly(I:C) or 0.1 MOI MVA. (A)Comparison of phenotypic profile using CD14, CD163 and CD206 markers between *in vitro* PBMC derived macrophages and *in vivo* muscular tissue macrophages. Isotype control and macrophage fluorescence intensities mean are respectively represented in filled grey and in a blue line. (B) Analysis of the activation markers CD80, CD86 and CCR7 of PBMC derived Poly(I:C) or MVA stimulation. Each linked plot represents macrophage population from a same non-human primate. Measures were established making the Fold change ratio between the fluorescence intensity mean of either CD80, CD86 and CCR7 in Medium, Poly(I:C) or MVA treated macrophages during 48h and the fluorescence intensity mean of untreated macrophages. Arithmetical mean ± SD (n= 8 to 11). Statistical analysis was conducted using paired Wilcoxon test. Non-significant p-values (p>0.05) were calculated but not represented. (C) Scatter-plot of released cytokines after macrophages stimulation. Only cytokines whom Poly(I:C) or MVA stimulated macrophages gave significant results using Friedman are shown (see Supplementary Data Fig. 1B for data not shown). Wilcoxon paired test were performed to compare each column separately. Non-significant p-values (p>0.05) were calculated but not represented.

Supplementary figures

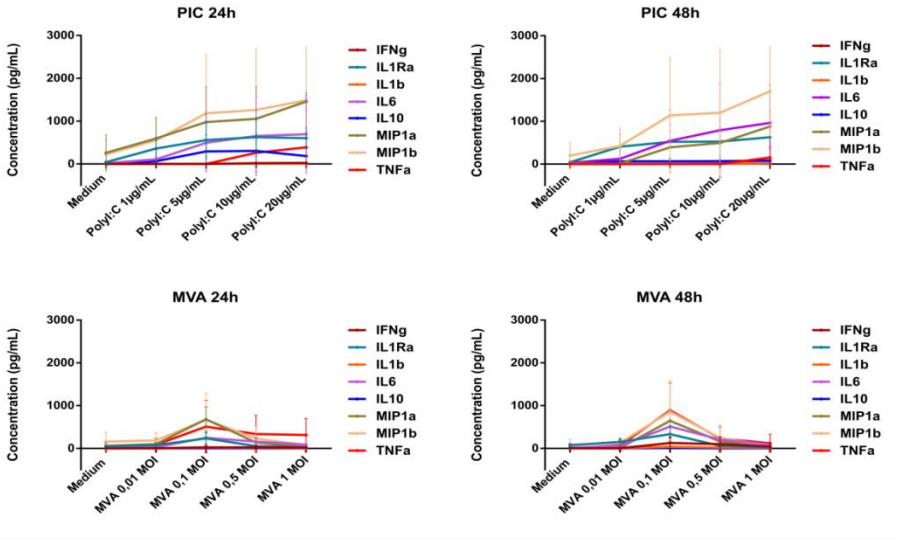

Cytokines Tested	Medium stimulated Macrophages dosed at H0, H24 and H48		Poly:C stimulated Macrophages dosed at H0, H24 and H48		MVAstimulated Macrophages dosed at H0, H24 and H48	
	Friedman's test p-value	*Significance*	*Friedman's test p-value*	*Significance*	*Friedman's test p-value*	*Significance*
GM-CSF	0.1197	NS	0.7943	NS	0.6543	NS
IFNg	0.0556	NS	0.6523	NS	0.1147	NS
IL1ra	<0.0001	****	0.0003	***	<0.0001	****
IL1b	0.0004	**	0.0303	*	<0.0001	****
IL2	0.0029	**	0.1066	NS	0.6543	NS
IL4	0.6667	NS	0.5000	NS	>0.9999	NS
IL5	>0.9999	NS	0.4074	NS	0.2088	NS
IL6	0.2851	NS	0.0003	***	<0.0001	****
IL8	0.3553	NS	0.0080	**	0.0789	NS
IL10	>0.9999	NS	0.1667	NS	0.1111	NS
IL12/23	0.0521	NS	0.4742	NS	0.0515	NS
IL13	0.5833	NS	0.1574	NS	0.2778	NS
IL17a	0.3611	NS	0.2130	NS	0.1481	NS
MIP1a	0.0025	**	0.0099	**	0.0048	**
MIP1b	0.1495	NS	0.0011	**	0.0003	***
TNFa	0.0907	NS	0.0289	*	0.0009	***

Supplementary Figure 1

Selection of optimal Poly(I:C) and MVA concentration to stimulate in vitro PBMC derived macrophages. (A)The cytokine concentration of macrophage supernatants were measured using luminex assay. For each concentration, experiments were conducted three times. The arithmetical mean (± SD, n=3) is represented for cytokine released after stimulation. (B) Sum up table of cytokines released by PBMC derived macrophages after Poly(I:C) or MVA stimulation. The cytokine concentration of macrophage supernatants were measured using luminex assay. Stimulation of macrophages were performed using either medium, 20µg/mL Poly(I:C) or 0.1 MOI MVA.

Discussion

A. Analyse rétrospective

I. Analyse rétrospective liées modèle d'étude

a. Le choix du macaque cynomolgus

Cette étude des mécanismes immuns s'est appuyée sur un modèle *in vivo*de primates non-humains (NHP). Cela a été rendu possible grâce à la présence d'infrastructures adéquates pour effectuer des expérimentations sur ces grands animaux dans de bonnes conditions. Par ailleurs, l'équipe « Animal Science and Welfare » dispose d'un savoir-faire technique permettant de tirer au maximum parti de ce modèle.

Malgré de nombreux points forts, ce modèle comprend certaines limites. Ainsi, la taille des effectifs utilisés pour nos études est minimale, même si elle est restée suffisante pour mettre en évidence des différences significatives. Ainsi, on manque de puissance statistique pour trouver des différences significatives entre certains de nos paramètres évalués. Cette remarque est valable pour la plupart des études effectuées sur NHP, et est une conséquence de son coût financier important.

L'animal ne dispose également pas de ressources illimitées, et oblige donc à faire des choix. Ainsi, nous avons par exemple décidé d'évaluer la réponse précoce au niveau du site d'injection et des ganglions drainants (qui nécessitent d'être prélevés), au détriment d'un suivi longitudinal au niveau du compartiment systémique uniquement, qui nous aurait permis de corréler marqueurs de la réponse innée et réponse adaptative. En effet, retirer le site d'injection ainsi que les ganglions drainant à des temps précoces a pour conséquence de tronquer l'élaboration de la réponse adaptative. Nous avons par exemple montré dans l'article 1 que l'antigène persistait au niveau local au-delà de 24h après injection par voie ID. Prélever le site d'injection après 24h a donc pour conséquence de diminuer à la fois l'expression, mais aussi la réponse antigénique.

b. *Le choix du MVA*

A postériori, le MVA s'est avéré être un bon modèle d'étude dans la mesure où il a induit des réponses immunitaires de forte amplitude avec une bonne reproductibilité. Comme prévu, ce vaccin a de plus été très bien toléré par les animaux, ce qui nous a permis des analyses poussées. Il ne faut cependant pas oublier que le MVA est un virus vivant atténué. Bien qu'il ne se réplique pas dans la plupart des cellules de mammifères, il possède une capacité à disséminer (relativement faiblement[132]) dans l'organisme, tout en infectant un panel large et hétérogène de cellules. Cela peut donc avoir une incidence sur notre étude du site d'injection, où l'on retrouve différentes populations cellulaires résidentes. De plus, l'étude de la réponse immunitaire induite par ce virus en devient plus complexe. En effet, on ne peut pas distinguer les éléments de la réponse innée induits par le virus pour échapper au système immunitaire (évoqués en Introduction partie B.II.b.3.) de ceux qui ont une efficacité directe. De même, on s'interroge également sur l'état des cellules –notamment des granulocytes et macrophages- exprimant la GFP ou le E3L. S'agit-il bel et bien de cellules infectées par le virus, où bien d'une phagocytose d'une cellule elle-même infectée ?

II. Analyse rétrospective liée aux techniques utilisées

a. *Sur les biopsies*

La quasi-totalité des prélèvements se sont déroulés dans d'excellentes conditions du fait de l'expertise de l'équipe technique. Cependant, la réalisation des biopsies musculaires au niveau du site d'injection se sont avérées plus compliquées que prévu. En effet, cette dernière ne s'étend que sur une faible surface par rapport au muscle entier, pour ne pas entraver la mobilité de l'animal. De plus, cette biopsie est relativement invasive, et se situe en profondeur. De ce fait, contrairement à la peau, nous avons manqué de repères fiables ou d'indicateur garantissant que la biopsie soit bel et bien pratiquée sur le site précis de l'injection. Dans le même registre, le liquide injecté diffuse probablement beaucoup plus après injection par voie sous cutanée et intramusculaire que par voie intradermique. L'apparition d'une papule post-injection nous indique clairement où prélever après injection par voie ID, en plus de nous donner une idée de la zone de diffusion du liquide. De surcroit,

bien que cette papule disparaisse quelque minute après l'injection, elle est succédée par l'apparition d'une zone d'inflammation aisément identifiable macroscopiquement (article 1). Nous ne disposons pas de cet élément après administration par voie SC et IM, mais des expérimentations effectuées avec un colorant, l'encre de Chine nous ont indiqué que le liquide s'étale sur une très large surface et peut rapidement atteindre le fascia et les ganglions drainants, particulièrement après voie SC. Ainsi, il n'a pas été possible de prélever l'ensemble de ce site pour des raisons éthique évidentes. Les zones d'inflammation, quant à elles ne sont également pas identifiables après examen macroscopique au niveau des tissus sous cutané et musculaires du fait que ces tissus sont situés plus en profondeur dans l'organisme.

b. *Sur les techniques d'analyse*

Outre l'histologie et la cytométrie en flux, des techniques innovantes ont pu ajouter une vraie plus-value à cette étude. Ainsi, l'endomicroscopie *in vivo* non invasive nous a permis de précisément apprécier la persistance virale dans la peau. Aussi, l'utilisation d'un cymomètre de masse rendu possible le développement de panels de 35 marqueurs permettant d'analyser simultanément les cytokines, les marqueurs d'activation, de maturation et de différenciation des lymphocytes T. Il faut ajouter à cela le support bioinformatique de grande qualité pour analyser et intégrer ces données. Une des forces de cette étude réside également dans ses collaborations. En effet, pour mener à bien ce projet interdisciplinaire, le laboratoire s'est associé avec des équipes expertes en microarrays (Plateforme Immuno-monitoring Hôpital Henri Mondor), en test de neutralisation et dosage d'anticorps par (Bertin Pharma®), et en analyse anatomo-pathologique (MirCen, CEA). Cette étude a beaucoup bénéficié de collaborations en interne, notamment avec les équipes Flowcytech, IMmemory et d'imagerie.Tous ces ingrédients ont été autant d'éléments d'une importance inestimable dans le bon déroulement de ce projet.

Malgré cette aide, la détection des APCs au niveau des ganglions drainant a présenté certaines limitations. Si les ganglions drainants ont bien été identifiés par la détection de cellules infectées, le drainage permanent des populations cellulaires innées et provenant de diverses régions a compliqué

l'analyse plus poussée des cellules d'intérêt. De surcroit, le prélèvement d'un unique ganglion de la chaîne inguinale a pu aboutir à la récupération d'un ganglion faiblement activé. Enfin, l'importante densité de cellules lymphocytaires peut également brouiller certaines informations, notamment lorsqu'il s'agit d'évaluer le profil transcriptomique du tissu entier.

B. Intérêts scientifiques

Les résultats présentés dans cette thèse ont été obtenus grâce à une combinaison de compétences dans le domaine de l'expérimentation animale, des biotechnologies de pointe et de la bioinformatique. Il a ainsi été possible de décrire la réaction inflammatoire précoce induite par le rMVA à la fois au niveau tissulaire, cellulaire, et moléculaire, et de surcroit au niveau du site d'injection, des ganglions drainants et du sang. L'intégration de ces données nous a amené à proposer une approche inédite pour visualiser l'interaction entre les effecteurs de la réponse innée au travers d'un réseau de coexpression en fonction du temps (article 1). Cette approche, qui présente l'intérêt d'être effectuée sans à priori, a permis de mettre en évidence la précocité de la mise en place de la réponse adaptative dans les ganglions drainants. De plus elle a mené à l'identification de certains biomarqueurs comme les cellules MDSCs et le TNFα, qui, à défaut d'être prédictifs de la réponse (nous ne disposons pas d'éléments pour l'affirmer) jouent de toute évidence un rôle clé dans l'élaboration de la réponse immunitaire adaptative. Ce type d'approche précurseur peut offrir de nouvelles perspectives sur la compréhension de la complexité de la machinerie immunitaire.

La multiplicité des données a également permis de mettre en évidence des différences notables dans la réaction précoce au MVA induite par les différentes voies d'administration. Ces différences ont été associées à une réponse cellulaire T et anticorps singulièrement différente en fonction des voies. Ainsi, ces nouveaux outils ont également mis en évidence l'importance de la voie d'administration dans la vaccination, dont l'influence est à ce jour encore mal connue.

Conclusion et perspectives

Au cours de cette étude, nous sommes parvenus à finement caractériser le profil de réponse immunitaire innée induite par un MVA recombinant après administration par voie intradermique, mais aussi sous cutanée et intra musculaire.

Après administration par voie intradermique, nous avons également pu déterminer une cinétique d'infection locale et déterminer la nature des cellules infectées.

Nous avons également pu évaluer la réponse adaptative en effectuant à la fois une étude poussée cinétique de la réponse T dans le sang, mais aussi un titrage d'immunoglobulines spécifiques du MVA au cours d'un prime boost homologue. Nous sommes également parvenus, dans une certaine mesure à relier les événements de la réponse innée à ceux de la réponse adaptative, que ce soit dans l'article 1 en regardant une réponse précoce cependant au niveau des ganglions drainants, ou dans l'article 2 sur des cinétiques plus longues sans toutefois pouvoir les corréler (Cf limites du modèle).

Ainsi une bonne partie des objectifs prévus dans le cadre de la thèse ont été remplis. Cependant, il reste également beaucoup à accomplir.

I. Exploiter au maximum les données

Les techniques d'analyse de données se sont révélées extrêmement complexes étant donné le nombre de paramètres évalués. Ainsi, nous avons développé certaines approches, que ce soit en étudiant les corrélations entre les effecteurs (dans l'article 1) ou en nous concentrant sur une technique d'enrichissement fonctionnel particulière pour les données de transcriptomique (articles 1 et 2). Le choix de ces méthodes d'analyse, bien qu'appropriées, peut être discuté du fait qu'il existe des alternatives que nous n'avons pas exploitées. L'idéal serait peut-être de confronter les données en utilisant ces autres méthodes d'analyse. Par exemple :

- Utiliser un autre algorithme que SPADE (comme viSNE, ACCENSE…) pour exploiter les données de cytométrie de masse,

- Avoir recours a d'autre méthodes d'enrichissement fonctionnel pour l'étude du transcriptome (GeneATLAS, Gene Set Enrichment Analysis[133]…).

II. Exploiter l'intégralité des données des données produites

L'analyse des données, notamment de cytométrie de masse s'est avérée très chronophage. Ainsi, certains échantillons destinés à l'analyse de la réponse immunitaire innée précoce dans le sang par cytométrie de masse attendent encore d'être analysés. L'évaluation de la réponse B par cytométrie de masse –dont l'acquisition des échantillons a été effectuée avec succès- pourra également nous apporter des informations supplémentaires précieuses.

Par ailleurs, évaluer si la réponse contre le transgène varie en fonction de la voie d'administration semble pertinent. Comparer cette réponse à celle induite contre le vecteur viral pourra nous donner en outre des indications sur le fonctionnement du MVA-HIV utilisé dans l'article 2. Des échantillons ont de ce fait été prélevés dans cet objectif.

III. Compléter par des approches in vitro

Les modèles d'interactions, ainsi que les hypothèses proposées au cours de cette étude sont uniquement basées sur notre caractérisation des événements cellulaires et moléculaires sur un modèle d'étude *in vivo* bien défini. De ce fait, nous il faut fractionner les mécanismes immunitaires supposés et confirmer les résultats obtenus avec des expérimentations *in vitro*. Ces études nous permettront de :

a. Soigneusement évaluer la fonction des effecteurs cellulaires

Exemple (Article 1) : Les cellules présentant un phénotype de MDSC exercent elles vraiment des fonctions immunosuppressives sur la réponse inflammatoire et sur la réponse T CD8 ?

b. *Valider les hypothèses de travail*

Exemple (Article 1) : Le TNFα permet-il à lui seul d'entrainer une production d'IL18 ou d'IL2 dans le ganglion ? Quelles cellules en sont à l'origine ? Quelles combinaisons de cellules/cytokine fonctionnent le mieux ?

Exemple (Article Complémentaire) : Les macrophages recrutés dans le muscle après administration de poly(I :C) ou MVA présentent ils des capacités à présentation de l'antigène au lymphocytes T ? Quel profil de réponse induisent-ils ?

IV. Modéliser la réponse

Le but ultime de ces analyses est la modélisation des réponses contre les vaccins. On cherche en effet à long terme à intégrer les paramètres du vaccin (voie d'administration, mais également vecteur, adjuvant, populations ciblée…) dans une approche *in silico* permettant de prédire la réponse immunitaire induite par ce dernier. Il s'agit donc d'une procédure complexe nécessitant de nombreuses expertises et collaborations. Cette dernière peut mener à une meilleure connaissance des mécanismes de vaccination, qui pourra s'avérer précieuse dans le développement de futurs vaccins. Cette tâche sera prise en charge par l'équipe SISTM (Statistics In Systems biology and Translational Medicine) spécialisée dans la biologie computationelle.

Si cette étude a été réalisée dans l'objectif d'être intégrée dans une telle approche, il reste ici aussi beaucoup de chemin à parcourir. En effet, on ne peut bien évidemment pas prétendre que les réponses immunitaires de tous les vaccins s'effectueront de la même manière que le MVA chez le macaque cynomolgus. Ainsi si la voie d'administration a pu être évaluée dans ce contexte, de nombreux autres paramètres clés nécessitent d'être analysés de manière extensive. Ainsi, plus le nombre de paramètres intégrés dans le processus de modélisation sera important, plus il sera pertinent.

a. *Le choix du vaccin*

Le type de vaccin ou d'adjuvant influence largement le profil de la réponse immunitaire. Nous avons utilisé dans cette étude un vaccin vivant atténué. Il faudrait étendre les expérimentations de ce type sur d'autres vaccins susceptibles d'orienter la réponse immunitaire différemment. Il pourra s'agir de vecteurs viraux ou de virus tués, mais également des protéines de fusion ciblant des sous population de cellules dendritiques particulières ou des adjuvants particuliers comme les ligands de TLR. Le choix de l'antigène est également déterminant dans ce type d'approche. Cela nous permettrait par exemple de voir si les mêmes effecteurs immunitaires sont engagés dans l'élaboration de la réponse immunitaire.

b. *La cinétique et la localisation de la réponse*

Cette étude a montré que beaucoup d'événements ont lieu à des temps très précoces après l'injection du vaccin. Cependant, la mise en place de cette réponse perdure également dans le temps. Ainsi, il reste très difficile, voire impossible, de déterminer une cinétique « parfaite » au cours de laquelle on pourrait répertorier toute les étapes clé de la réponse. En effet, l'étude de la réponse dans un compartiment donné soulève des interrogations sur l'influence des prélèvements sur la réponse plus tardive. Il n'existe probablement pas de solution pour pallier totalement à cette limitation. Cependant, l'intégration progressive d'études analysant différentes cinétiques dans un processus de modélisation pourrait permettre de dégager des moments ainsi que des lieux clés de la réponse

c. *Autres paramètres à prendre en compte*

En plus de ceux déjà abordés, énormément de paramètres entrent en jeu lorsque l'on évalue un processus aussi complexe que la réponse immunitaire. Le modèle (murin, humain…), l'âge, le sexe, le poids, le CMH, les gènes, les cytokines, les cellules immunitaires en font par exemple partie. De ce fait, même dans un objectif d'intégration de nombreuses données dans une approche de

modélisation en biologie computationnelle, il faudra probablement veiller à très soigneusement sélectionner les paramètres évalués.

Mais malgré toutes les complexités que cela représente, c'est peut-être dans ce genre d'approche que réside l'une de nos meilleures chances de parvenir à développer les vaccins efficaces qui nous font aujourd'hui encore terriblement défaut.

Bibliographie

1. Rosenbaum, P. Etude de la réponse immunitaire induite par des adjuvants agonistes des TLR sur la peau de macaque. (These de pharmacie, Rennes, 2012). at <http://www.sudoc.fr/167282689>
2. van Panhuis, W. G. *et al.*Contagious Diseases in the United States from 1888 to the Present. *N. Engl. J. Med.***369,** 2152–2158 (2013).
3. Andersen, P. & Doherty, T. M. The success and failure of BCG - implications for a novel tuberculosis vaccine. *Nat. Rev. Microbiol.***3,** 656–662 (2005).
4. Mayr, A., Hochstein-Mintzel, V. & Stickl, H. Abstammung, Eigenschaften und Verwendung des attenuierten Vaccinia-Stammes MVA. *Infection***3,** 6–14 (1975).
5. Kim, J., Rerks-Ngarm, S. & Excler, J. HIV Vaccines-Lessons learned and the way forward. *Curr. Opin. HIV***5,** 428–434 (2010).
6. Ahmed, S. S., Plotkin, S. a, Black, S. & Coffman, R. L. Assessing the safety of adjuvanted vaccines. *Sci. Transl. Med.***3,** 93rv2 (2011).
7. Cristiani, C. *et al.* Safety of MF-59 adjuvanted vaccine for pandemic influenza: Results of the vaccination campaign in an Italian health district. *Vaccine***29,** 3443–3448 (2011).
8. Paavonen, J. *et al.* Efficacy of a prophylactic adjuvanted bivalent L1 virus-like-particle vaccine against infection with human papillomavirus types 16 and 18 in young women: an interim analysis of a phase III double-blind, randomised controlled trial. *Lancet***369,** 2161–2170 (2007).
9. Liko, J., Robison, S. G. & Cieslak, P. R. Priming with Whole-Cell versus Acellular Pertussis Vaccine. *N. Engl. J. Med.***368,** 581–2 (2013).
10. Warfel, J. M., Zimmerman, L. I. & Merkel, T. J. Acellular pertussis vaccines protect against disease but fail to prevent infection and transmission in a nonhuman primate model. *Proc. Natl. Acad. Sci. U. S. A.***111,** 787–92 (2014).
11. Buchbinder, S. P. *et al.* Efficacy assessment of a cell-mediated immunity HIV-1 vaccine (the Step Study): a double-blind, randomised, placebo-controlled, test-of-concept trial. *Lancet***372,** 1881–1893 (2008).
12. Rerks-Ngarm, S. *et al.* Vaccination with ALVAC and AIDSVAX to Prevent HIV-1 Infection in Thailand. *N. Engl. J. Med.***361,** 2209–2220 (2009).
13. Hewitt, E. W. The MHC class I antigen presentation pathway: Strategies for viral immune evasion. *Immunology***110,** 163–169 (2003).
14. Goulder, P. J. R. & Watkins, D. I. Impact of MHC class I diversity on immune control of immunodeficiency virus replication. *Nat. Rev. Immunol.***8,** 619–30 (2008).
15. Silzle, T., Randolph, G. J., Kreutz, M. & Kunz-Schughart, L. A. The fibroblast: Sentinel cell and local immune modulator in tumor tissue. *Int. J. Cancer***108,** 173–180 (2004).
16. Kupper, T. S. *et al.* Production of IL-6 by Keratinocytes. *Ann. N. Y. Acad. Sci.***557,** 454–465 (2008).
17. Saalbach, A. *et al.* Dermal fibroblasts induce maturation of dendritic cells. *J Immunol***178,** 4966–4974 (2007).
18. Tecle, T., Tripathi, S. & Hartshorn, K. L. Review: Defensins and cathelicidins in lung immunity. *Innate Immun.***16,** 151–159 (2010).
19. Danese, S., Dejana, E. & Fiocchi, C. Immune Regulation by Microvascular Endothelial Cells: Directing Innate and Adaptive Immunity, Coagulation, and Inflammation. *J. Immunol.***178,** 6017–6022 (2007).
20. Guilliams, M. *et al.* Dendritic cells, monocytes and macrophages: a unified nomenclature based on ontogeny TL - 14. *Nat. Rev. Immunol.***14 VN - r,** 571–578 (2014).
21. Epstein, F. H. & Luster, A. D. Chemokines — Chemotactic Cytokines That Mediate Inflammation. *N. Engl. J. Med.***338,** 436–445 (1998).

22. Biron, C. a. Role of early cytokines, including alpha and beta interferons (IFN-alpha/beta), in innate and adaptive immune responses to viral infections. *Semin. Immunol.***10,** 383–390 (1998).
23. Leroy, M. & Desmecht, D. Les interférons de type I et leur fonction antivirale. *Ann. médecine vétérinaire***150,** 73–107 (2006).
24. Dai, P. *et al.* Modified Vaccinia Virus Ankara Triggers Type I IFN Production in Murine Conventional Dendritic Cells via a cGAS/STING-Mediated Cytosolic DNA-Sensing Pathway. *PLoS Pathog.***10,** (2014).
25. Ablasser, A. *et al.* Cell intrinsic immunity spreads to bystander cells via the intercellular transfer of cGAMP. *Nature***503,** 530–4 (2013).
26. Kawai, T. & Akira, S. Toll-like receptors and their crosstalk with other innate receptors in infection and immunity. *Immunity***34,** 637–50 (2011).
27. Hodge, D. R., Hurt, E. M. & Farrar, W. L. The role of IL-6 and STAT3 in inflammation and cancer. *Eur. J. Cancer***41,** 2502–2512 (2005).
28. Luster, A. D., Alon, R. & von Andrian, U. H. Immune cell migration in inflammation: present and future therapeutic targets. *Nat. Immunol.***6,** 1182–90 (2005).
29. Serhan, C. N. & Savill, J. Resolution of inflammation: the beginning programs the end. *Nat. Immunol.***6,** 1191–1197 (2005).
30. Banchereau, J. & Steinman, R. M. Dendritic cells and the control of immunity. *Nature***392,** 245–252 (1998).
31. Bruel, T. *et al.* Plasmacytoid dendritic cell dynamics tune interferon-alfa production in SIV-infected cynomolgus macaques. *PLoS Pathog.***10,** e1003915 (2014).
32. Ketloy, C. *et al.* Expression and function of Toll-like receptors on dendritic cells and other antigen presenting cells from non-human primates. *Vet. Immunol. Immunopathol.***125,** 18–30 (2008).
33. Hume, D. a. Macrophages as APC and the dendritic cell myth. *J. Immunol.***181,** 5829–5835 (2008).
34. Falcone, M., Lee, J., Patstone, G., Yeung, B. & Sarvetnick, N. B lymphocytes are crucial antigen-presenting cells in the pathogenic autoimmune response to GAD65 antigen in nonobese diabetic mice. *J. Immunol.***161,** 1163–1168 (1998).
35. Ahmed, R. & Gray, D. Immunological memory and protective immunity: understanding their relation. *Science (80-.).***272,** 54–60 (1996).
36. Itano, A. a & Jenkins, M. K. Antigen presentation to naive CD4 T cells in the lymph node. *Nat. Immunol.***4,** 733–9 (2003).
37. Idris-Khodja, N., Mian, M. O. R., Paradis, P. & Schiffrin, E. L. Dual opposing roles of adaptive immunity in hypertension. *Eur. Heart J.***35,** 1238–1244 (2014).
38. Diehl, S. & Rincón, M. The two faces of IL-6 on Th1/Th2 differentiation. *Mol. Immunol.***39,** 531–536 (2002).
39. Okada, R., Kondo, T., Matsuki, F., Takata, H. & Takiguchi, M. Phenotypic classification of human CD4+ T cell subsets and their differentiation. *Int. Immunol.***20,** 1189–1199 (2008).
40. Cher, D. J. & Mosmann, T. R. Two types of murine helper T cell clone. II. Delayed-type hypersensitivity is mediated by TH1 clones. *J. Imunol.***138,** 3688–94 (1987).
41. Coffman, R. L. *et al.* The role of helper T cell products in mouse B cell differentiation and isotype regulation. *Immunol. Rev.***102,** 5–28 (1988).
42. Schaerli, P. *et al.* CXC chemokine receptor 5 expression defines follicular homing T cells with B cell helper function. *J. Exp. Med.***192,** 1553–62 (2000).
43. Fazilleau, N., Mark, L., McHeyzer-Williams, L. & McHeyzer-Williams, M. Follicular Helper T Cells: Lineage and Location. *Immunity***30,** 324–335 (2009).
44. Linterman, M. a *et al.* IL-21 acts directly on B cells to regulate Bcl-6 expression and germinal center responses. *J. Exp. Med.***207,** 353–63 (2010).
45. Shapiro-Shelef, M. & Calame, K. Regulation of plasma-cell development. *Nat. Rev. Immunol.***5,** 230–42 (2005).

46. Malefyt, W. *et al.* IgA by Human Naive B Cells Is Differentially IL-21-Induced Isotype Switching to IgG and IL-21-Induced Isotype Switching to IgG and IgA by Human Naive B Cells Is Differentially Regulated by IL-4 1. *J Immunol Ref.***181,** 1767–1779 (2008).
47. Wurster, A. L., Rodgers, V. L., White, M. F., Rothstein, T. L. & Grusby, M. J. Interleukin-4-mediated protection of primary B cells from apoptosis through Stat6-dependent up-regulation of Bcl-xL. *J. Biol. Chem.***277,** 27169–27175 (2002).
48. Yusuf, I. *et al.* Germinal center T follicular helper cell IL-4 production is dependent on signaling lymphocytic activation molecule receptor (CD150). *J. Immunol.***185,** 190–202 (2010).
49. Crotty, S. Follicular Helper CD4 T Cells (T_{FH}). *Annu. Rev. Immunol.***29,** 621–663 (2011).
50. Leong, Y. A. *et al.*CXCR5(+) follicular cytotoxic T cells control viral infection in B cell follicles. *Nat. Immunol.* (2016). doi:10.1038/ni.3543
51. Petrovas, C. *et al.* CD4 T follicular helper cell dynamics during SIV infection. *J Clin Invest.***5,** 1–14 (2012).
52. Perreau, M. *et al.* Follicular helper T cells serve as the major CD4 T cell compartment for HIV-1 infection, replication, and production. *J. Exp. Med.***210,** 143–56 (2013).
53. Colineau, L. *et al.* HIV-infected spleens present altered follicular helper T cell (Tfh) subsets and skewed B cell maturation. *PLoS One***10,** 1–19 (2015).
54. Lowin, B., Hahne, M., Mattman, C. & Tchopp, J. Cytolytic T-cell cytotoxicity is mediated through perforin and Fas lytic pathway. *Lett. to Nat.***370,** (1994).
55. Liu, C., Walsh, C. M. & Young, J. D. Perforin : structure and function. *Immunol. Today***15,** 194–201 (1995).
56. Heusel, J. W., Wesselschmidt, R. L., Russell, J. H. & Ley, T. J. Cytotoxic Lymphocytes Require Granzyme B for the Rapid Induction of DNA Fragmentation and Apoptosis in Allogeneic Target Cells. *Cell***76,** 977–987 (1994).
57. Jenkins, M. K., Burrell, E. & Ashwell, J. D. Antigen presentation by resting B cells . Effectiveness at inducing T cell proliferation is determined by costimulatory signals , not T cell receptor occupancy. *J. Immunol.***144,** 1585–1590 (1990).
58. Abbas, A. K. *et al.* Activation and Functions of CD4 + T-Cell Subsets. *Immunol. Rev.* (1991).
59. Fey, T. M. *et al.* In the Absence of a CD40 Signal , B Cells Are Tolerogenic. *Immunity***2,** 645–653 (1995).
60. Fuchs, E. J. & Matzingert, P. B Cells Turn Off Virgin But Not Memory T Cells. *Science***2,** (1992).
61. Bonecchi, B. R. *et al.* Differential Expression of Chemokine Receptors and Chemotactic Responsiveness of Type 1 T Helper Cells. *J. Exp. Med.***187,** 129–134 (1998).
62. Imai, T. *et al.* Selective recruitment of CCR4-bearing T h 2 cells toward antigen-presenting cells by the CC chemokines thymus and activation-regulated chemokine and macrophage-derived chemokine. *Int. Immunol.***11,** 81–88 (1999).
63. Förster, R., Davalos-misslitz, A. C. & Rot, A. CCR7 and its ligands : balancing immunity and tolerance. *Nat. Rev. Immunol.***8,** (2008).
64. Fritsch, R. D. *et al.* Stepwise Differentiation of CD4 Memory T Cells Defined by Expression of CCR7 and CD27. *J. Immunol. (Baltimore, Md. 1950)***175,** 6489–6497 (2015).
65. Xu, H., Manivannan, A., Crane, I., Dawson, R. & Liversidge, J. Critical but divergent roles for CD62L and CD44 in directing blood monocyte trafficking in vivo during inflammation. *Blood***112,** 1166–1175 (2008).
66. Picker, L. J. *et al.* Control of lymphocyte recirculation in man. I. Differential regulation of the peripheral lymph node homing receptor L-selectin on T cells during the virgin to memory cell transition. *J. Immunol.* (1993).
67. Chaparas, S. D. L'immunite dans la tuberculose. *Bull. l'Organisation Mond. la Santé***60,** 827–844 (1982).
68. Wiendl, H., Hohlfeld, R. & Kieseier, B. C. Immunobiology of muscle: advances in understanding an immunological microenvironment. *Trends Immunol.***26,** 373–80 (2005).
69. Zehrung, D., Jarrahian, C. & Wales, A. Intradermal delivery for vaccine dose sparing: Overview of current issues. *Vaccine***31,** 3392–3395 (2013).

70. Zaric, M., Ibarzo Yus, B., Kalcheva, P. P. & Klavinskis, L. S. Microneedle-mediated delivery of viral vectored vaccines. *Expert Opin. Drug Deliv.***5247,** 17425247.2017.1230096 (2016).
71. Liang, F. *et al.* Dissociation of skeletal muscle for flow cytometric characterization of immune cells in macaques. *J. Immunol. Methods***425,** 69–78 (2015).
72. Abadie, V. *et al.* Original encounter with antigen determines antigen-presenting cell imprinting of the quality of the immune response in mice. *PLoS One***4,** e8159 (2009).
73. Calabro, S. *et al.* Vaccine adjuvants alum and MF59 induce rapid recruitment of neutrophils and monocytes that participate in antigen transport to draining lymph nodes. *Vaccine***29,** 1812–23 (2011).
74. Lu, F. & Hogenesch, H. Kinetics of the inflammatory response following intramuscular injection of aluminum adjuvant. *Vaccine***31,** 3979–86 (2013).
75. Caspar-Bauguil, S. *et al.* Adipose tissues as an ancestral immune organ: site-specific change in obesity. *FEBS Lett.***579,** 3487–92 (2005).
76. Pond, C. M. Adipose tissue and the immune system. *Prostaglandins Leukot. Essent. Fat. Acids***73,** 17–30 (2005).
77. Damouche, A. *et al.*Adipose Tissue Is a Neglected Viral Reservoir and an Inflammatory Site during Chronic HIV and SIV Infection. *PLoS Pathog.***11,** 1–28 (2015).
78. Mantoux, C. Intradermo-reaction de la tuberculine. *Comptes rendus l'Académie des Sci.***147,** 355–57 (1908).
79. Artenstein, A. W. Bifurcated vaccination needle. *Vaccine***32,** 895 (2014).
80. Roediger, B. *et al.*Cutaneous immunosurveillance and regulation of inflammation by group 2 innate lymphoid cells. *Nat. Immunol.***14,** 564–73 (2013).
81. Nestle, F. O., Di Meglio, P., Qin, J.-Z. & Nickoloff, B. J. Skin immune sentinels in health and disease. *Nat. Rev. Immunol.***9,** 679–691 (2009).
82. Zaid, A. *et al.* Persistence of skin-resident memory T cells within an epidermal niche. *Proc. Natl. Acad. Sci. U. S. A.***111,** 5307–12 (2014).
83. Malissen, B., Tamoutounour, S. & Henri, S. The origins and functions of dendritic cells and macrophages in the skin. *Nat. Rev. Immunol.***14,** 417–28 (2014).
84. Valladeau, J. & Saeland, S. Cutaneous dendritic cells. *Semin. Immunol.***17,** 273–83 (2005).
85. Kubo, A., Nagao, K., Yokouchi, M., Sasaki, H. & Amagai, M. External antigen uptake by Langerhans cells with reorganization of epidermal tight junction barriers. *J. Exp. Med.***206,** 2937–2946 (2009).
86. Shklovskaya, E. *et al.* Langerhans cells are precommitted to immune tolerance induction. *Proc. Natl. Acad. Sci. U. S. A.***108,** 18049–54 (2011).
87. Stoitzner, P. *et al.* Langerhans cells cross-present antigen derived from skin. *Proc. Natl. Acad. Sci. U. S. A.***103,** 7783–8 (2006).
88. Flacher, V. *et al.* Murine Langerin + dermal dendritic cells prime CD 8 + T cells while Langerhans cells induce cross-tolerance. 1–14 (2014).
89. Klechevsky, E. *et al.* Functional specializations of human epidermal Langerhans cells and CD14+ dermal dendritic cells. *Immunity***29,** 497–510 (2008).
90. Klechevsky, E. Human dendritic cells - stars in the skin. *Eur. J. Immunol.***43,** 3147–55 (2013).
91. Penel-Sotirakis, K., Simonazzi, E., Péguet-Navarro, J. & Rozières, A. Differential Capacity of Human Skin Dendritic Cells to Polarize CD4+T Cells into IL-17, IL-21 and IL-22 Producing Cells. *PLoS One***7,** (2012).
92. Haniffa, M., Gunawan, M. & Jardine, L. Human skin dendritic cells in health and disease. *J. Dermatol. Sci.***77,** 85–92 (2015).
93. Haniffa, M. *et al.* Human Tissues Contain CD141 hi Cross-Presenting Dendritic Cells with Functional Homology to Mouse CD103 + Nonlymphoid Dendritic Cells. *Immunity***37,** 60–73 (2012).
94. Davis, M. M. A Prescription for Human Immunology. *Immunity***29,** 835–838 (2008).
95. Ostrand-Rosenberg, S. Animal models of tumor immunity, immunotherapy and cancer vaccines. *Curr. Opin. Immunol.***16,** 143–150 (2004).

96. von Herrath, M. G. & Nepom, G. T. Lost in translation: barriers to implementing clinical immunotherapeutics for autoimmunity. *J. Exp. Med.***202,** 1159–62 (2005).
97. Kennedy, R. C., Shearer, M. H. & Hildebrand, W. Nonhuman primate models to evaluate vaccine safety and immunogenicity. *Vaccine***15,** 903–908 (1997).
98. Quintana-Murci, L., Alcaïs, A., Abel, L. & Casanova, J.-L. Immunology in natura: clinical, epidemiological and evolutionary genetics of infectious diseases. *Nat. Immunol.***8,** 1165–71 (2007).
99. Mestas, J. & Hughes, C. C. W. Of mice and not men: differences between mouse and human immunology. *J. Immunol.***172,** 2731–2738 (2004).
100. Macchiarini, F., Manz, M. G., Palucka, a K. & Shultz, L. D. Humanized mice : are we there yet ? *Allergy***202,** 1307–11 (2005).
101. Ito, R., Takahashi, T., Katano, I. & Ito, M. Current advances in humanized mouse models. *Cell. Mol. Immunol.***9,** 208–14 (2012).
102. Hérodin, F., Thullier, P., Garin, D. & Drouet, M. Nonhuman primates are relevant models for research in hematology, immunology and virology. *Eur. Cytokine Netw.***16,** 104–116 (2005).
103. Merkel, T. J. & Halperin, S. A. Nonhuman primate and human challenge models of pertussis. *J. Infect. Dis.***209,** 20–23 (2014).
104. Geisbert, T. W., Strong, J. E. & Feldmann, H. Considerations in the Use of Nonhuman Primate Models of Ebola Virus and Marburg Virus Infection. *J. Infect. Dis.***212,** 91–97 (2015).
105. Flynn, J. L., Gideon, H. P., Mattila, J. T. & Lin, P. ling. Immunology studies in non-human primate models of tuberculosis. *Immunol. Rev.***264,** 60–73 (2015).
106. Gardner, M. B. & Luciw, P. a. Macaque models of human infectious disease. *ILAR J.***49,** 220–55 (2008).
107. Meurens, F., Summerfield, A., Nauwynck, H., Saif, L. & Gerdts, V. The pig: A model for human infectious diseases. *Trends Microbiol.***20,** 50–57 (2012).
108. Roberts, K. L. & Smith, G. L. Vaccinia virus morphogenesis and dissemination. *Trends Microbiol.***16,** 472–479 (2008).
109. Moss, B. Poxvirus entry and membrane fusion. *Virology***344,** 48–54 (2006).
110. Ichihashi, Y. Extracellular enveloped vaccinia virus escapes neutralization. *Virology***217,** 478–485 (1996).
111. Smith, G. L., Symons, J. A. & Vanderplasschen, A. Vaccinia virus immune evasion. *Immunol. Rev.***159,** 137–154 (1997).
112. Smith, G., Mackett, M. & Moss, B. Infectious vaccinia virus recombinants that express hepatitis B virus surface antigen. *Nature***302,** 490–495 (1983).
113. Meyer, H., Sutter, G. & Mayr, a. Mapping of deletions in the genome of the highly attenuated vaccinia virus MVA and their influence on virulence. *J. Gen. Virol.***72 (Pt 5),** 1031–8 (1991).
114. DiPerna, G. *et al.* Poxvirus Protein N1L Targets the I- B Kinase Complex, Inhibits Signaling to NF- B by the Tumor Necrosis Factor Superfamily of Receptors, and Inhibits NF- B and IRF3 Signaling by Toll-like Receptors. *J. Biol. Chem.***279,** 36570–36578 (2004).
115. Waibler, Z. *et al.* Vaccinia virus-mediated inhibition of type I interferon responses is a multifactorial process involving the soluble type I interferon receptor B18 and intracellular components. *J. Virol.***83,** 1563–1571 (2009).
116. Moss, B. *et al.* Host range restricted, non-replicating vaccinia virus vectors as vaccine candidates. *Adv. Exp. Med. Biol.***397,** 7–13 (1996).
117. Sutter, G., Wyatt, L. S., Foley, P. L., Bennink, J. R. & Moss, B. A recombinant vector derived from the host range-restricted and highly attenuated MVA strain of vaccinia virus stimulates protective immunity in mice to influenza virus. *Vaccine***12,** 1032–1040 (1994).
118. Vollmar, J. *et al.* Safety and immunogenicity of IMVAMUNE, a promising candidate as a third generation smallpox vaccine. *Vaccine***24,** 2065–2070 (2006).
119. Sheehan, S. *et al.* A Phase I, Open-Label Trial, Evaluating the Safety and Immunogenicity of Candidate Tuberculosis Vaccines AERAS-402 and MVA85A, Administered by Prime-Boost Regime in BCG-Vaccinated Healthy Adults. *PLoS One***10,** e0141687 (2015).

120. Stickl, H. *et al.* MVA-Stufenimpfung gegen Pocken. *DMW - Dtsch. Medizinische Wochenschrift***99,** 2386–2392 (1974).
121. Altenburg, A. F. *et al.* Modified vaccinia virus ankara (MVA) as production platform for vaccines against influenza and other viral respiratory diseases. *Viruses***6,** 2735–61 (2014).
122. Zhou, Y. & Sullivan, N. J. Immunology and evolvement of the adenovirus prime, MVA boost Ebola virus vaccine. *Curr. Opin. Immunol.***35,** 131–136 (2015).
123. Gómez, C. E. *et al.* A Phase I Randomized Therapeutic MVA-B Vaccination Improves the Magnitude and Quality of the T Cell Immune Responses in HIV-1-Infected Subjects on HAART. *PLoS One***10,** e0141456 (2015).
124. Lelièvre, J.-D., Lacabaratz, C. & Richert, L. Essai de phase I/II sans insu, randomisé, multicentrique évaluant l'immunogénicite et la tolérance de 4 combinaisons « prime- boost » de candidats vaccins VIH (MVA HIV-B /LIPO-5; LIPO-5 / MVA HIV-B; GTU-MultiHIV B /LIPO-5; GTU-MultiHIV B / MVA HIV-B) chez. 33076 (2014). at <www.recherche-vaccinVIH.fr>
125. Richert, L. *et al.* Accelerating clinical development of HIV vaccine strategies: methodological challenges and considerations in constructing an optimised multi-arm phase I/II trial design. *Trials***15,** 68 (2014).
126. Kitano, H. Computatioal Systems Biology. *Nature***420,** 206–210 (2002).
127. Nakaya, H. I. & Pulendran, B. Vaccinology in the era of high-throughput biology. *Philos. Trans. R. Soc. Lond. B. Biol. Sci.***370,** (2015).
128. Querec, T. D. *et al.*Systems biology approach predicts immunogenicity of the yellow fever vaccine in humans. *Nat. Immunol.***10,** 116–125 (2009).
129. Obermoser, G. *et al.* Systems scale interactive exploration reveals quantitative and qualitative differences in response to influenza and pneumococcal vaccines. *Immunity***38,** 831–44 (2013).
130. Pulendran, B., Li, S. & Nakaya, H. I. Systems vaccinology. *Immunity***33,** 516–529 (2010).
131. Bécavin, C., Tchitchek, N., Mintsa-Eya, C., Lesne, A. & Benecke, A. Improving the efficiency of multidimensional scaling in the analysis of high-dimensional data using singular value decomposition. *Bioinformatics***27,** 1413–1421 (2011).
132. Gómez, C. E. *et al.* Virus distribution of the attenuated MVA and NYVAC poxvirus strains in mice. *J. Gen. Virol.***88,** 2473–8 (2007).
133. Subramanian, A. *et al.* Gene set enrichment analysis: a knowledge-based approach for interpreting genome-wide expression profiles. *Proc. Natl. Acad. Sci. U. S. A.***102,** 15545–50 (2005).

université PARIS-SACLAY | ÉCOLE DOCTORALE Innovation thérapeutique : du fondamental à l'appliqué

Titre : Changements cellulaires et moléculaires précoces au site d'injection des vaccins : Caractérisation de la réponse innée et adaptative à l'injection d'un MVArecombinant

Mots clés : MVA, réponse immunitaire innée, vaccin, voie d'administration, primate non-humain, biologie des systemes

Résumé : La vaccination est considérée aujourd'hui comme l'une des méthodes les plus efficaces de se prémunir des maladies infectieuses. Cependant notre incapacité à produire un vaccin protégeant contre certaines maladies comme le SIDA ou l'hépatite C trahissent notre manque de compréhension des processus immuns.
Cette thèse s'appuie sur une modèle primate non-humain associé à un vaccin vivant attenué dérivé du virus de la vaccine, le MVA (Modified Vaccinia virus Ankara) pour y décortiquer en détails la réponse immunitaire innée, mais aussi acquise.
Le MVA induit une importante réaction inflammatoire au niveau du site d'injection et dans le compartiment systémique par voie intramusculaire, sous-cutanée, et intradermique. Pourtant, l'amplitude de cette réaction immunitaire ainsi que les effecteurs cellulaires et moléculaires engagés varie selon la voie d'administration. Les conséquences en sont importantes, puisque cela est à l'origine d'une réponse acquiseproduisant plus d'anticorps neutralisants après voie sous cutanée, et plutôt une réponse T effectrice après voies intramusculaire et intradermique. Ainsi, nous mettons en évidence certaines signatures cellulaires et moléculaires susceptible d'orienter la réponse immunitaire dans notre modèle.

Title : Early cellular and molecular changings and the injection site of vaccines : Characterization of the innate and adaptive immune response after a recombining MVA injection

Keywords : MVA, innate immune response, vaccine, administration route, non-human primate, systems biology

Abstract : Vaccination is considered as one of the best therapeutic intervention to fight against infectious diseases. However, we still fail to develop protective vaccines for diseases such as AIDS or B hepatitis, which highlights our lack of knowledge of immune processes.
For this thesis, we relied on a non-human primate model associated wih a vaccinia virus living attenuated vaccine derived called MVA (Modified Vaccinia virus Ankara). We deciphered innate, but also adaptive immune response using this model. MVA induces an important inflammatory reaction at the injection site and in the blood after intramuscular, subcutaneous, and intradermal administration.
However, the magnitude of this immune reaction, as well as cellular and molecular effectorsin varies depending on the administration route. The consequences are important and lead to different adaptive immune profiles, with neutralizing antibodies production after subcutaneous route, and more T effector oriented response after intramuscular and intradermal route. It allowed us to highlight several cellular and molecular signatures that might modulate immune response in our model.